Institut für Biochemie und Biologie

Max-Planck-Institut für Molekulare Pflanzenphysiologie
Arbeitsgruppe Metabolomic Analysis

Comprehensive metabolite analysis in *Chlamydomonas reinhardtii*

Method development and application to the study of environmental and genetic perturbations

Dissertation zur Erlangung des akademischen Grades

doctor rerum naturalium (Dr. rer. nat.)

in der Wissenschaftsdisziplin Biochemie der Pflanzen

eingereicht an der

Mathematisch-Naturwissenschaftlichen Fakultät der Universität Potsdam

von

Christian Bölling

Potsdam, den 01.09.2006

Summary

This study introduces a method for multiparallel analysis of small organic compounds in the unicellular green alga *Chlamydomonas reinhardtii*, one of the premier model organisms in cell biology. With the recent completion of the Chlamydomonas genome project, a systems biology perspective to develop an understanding of how the numerous components in a living system interact to comprise a functioning whole comes into focus for this model organism too. The comprehensive study of the changes of metabolite composition, or metabolomics, in response to environmental, genetic or developmental signals is an important complement of other functional genomic techniques in the effort to develop an understanding of how genes, proteins and metabolites are all integrated into a seamless and dynamic network to sustain cellular functions.

The sample preparation protocol was tailored for the application to suspension cultures and optimized to quickly inactivate enzymatic activity, achieve maximum extraction capacity and process large sample quantities. As a result of the rapid sampling, extraction and analysis by gas chromatography coupled to time-of-flight mass spectrometry (GC-TOF) more than 800 analytes from a single sample can be measured, of which over a 100 could be positively identified. As part of the analysis of GC-TOF raw data, aliquot ratio analysis to systematically remove artifact signals and tools for the use of principal component analysis (PCA) on metabolomic datasets are proposed.

Cells subjected to nitrogen (N), phosphorus (P), sulfur (S) or iron (Fe) depleted growth conditions develop highly distinctive metabolite profiles with metabolites implicated in many different processes being affected in their concentration during adaptation to nutrient deprivation. All treatments could be clearly discriminated by PCA which also indicated that P depleted conditions induce a deficiency syndrome quite different from the response to N, S or Fe starvation, possibly due to the availability of internal P reserves in Chlamydomonas cells.

Metabolite profiling allowed characterization of both specific and general responses to nutrient deprivation at the metabolite level. Modulation of the substrates for N-assimilation and the oxidative pentose phosphate pathway, including glutamate, glutamine, glucose-6-phosphate, and 6-phosphogluconate, indicated a priority for maintaining the capability for immediate activation of N assimilation even under conditions of decreased metabolic activity and arrested growth. Fe-deprivation led to an increase of the organic acids citrate and succinate, which could well be related to their iron-chelating properties, while the rise in 4-hydroxyproline in S deprived cells could be related to enhanced degradation of proteins of the cell wall, which has been shown to be rearranged under S limitation. A number of analytes linking important circuits of primary metabolism such as pyruvate and 2-oxoglutarate were similarly affected in the different nutrient deplete conditions and could be related to the adjustment of metabolic activity in cells exposed to unfavourable growth conditions to match their potential to grow and divide.

In a metabolomics approach that used both identified and unidentified metabolite signals, the adaptation to sulfur deficiency was analyzed with greater temporal resolution and responses of wild-

type cells were compared with mutant cells deficient in *SAC1*, an important regulator of the sulfur deficiency response. Multivariate data analysis techniques revealed five main types of response patterns of metabolite pools under sulfur deprivation, of which the most prominent is the gradual decline of metabolite pools as S depletion continues. Whereas concurrent metabolite depletion and accumulation occurs during adaptation to S deficiency in wild-type cells, the *sac1* mutant strain is characterized by a massive incapability to sustain many processes that normally lead to transient or permanent accumulation of the levels of certain metabolites or recovery of metabolite levels after initial down-regulation. Modulation of individual metabolites confirmed the inability of *sac1* cells to enhance sulfur uptake and scavenging activity and to adjust metabolic activity in response to S deprivation.

For most of the steps in arginine biosynthesis in Chlamydomonas mutants have been isolated that are deficient in the respective enzyme activities. This presents the unique opportunity to probe the potential of metabolite analysis for elucidating regulation of amino acid biosynthesis in a photosynthetic eukaryote by analyzing the effects of the introduction of selective breakpoints in a well-defined biochemical module through the specific loss of enzymatic activity. Three strains deficient in the activities of *N*-acetylglutamate-5-phosphate reductase (*arg1*), N^2-acetylornithine-aminotransferase (*arg9*), and argininosuccinate lyase (*arg2*), respectively, were analyzed with regard to activation of endogenous arginine biosynthesis after withdrawal of externally supplied arginine. Enzymatic blocks in the arginine biosynthetic pathway could be characterized by precursor accumulation, like the amassment of argininosuccinate in *arg2* cells, and depletion of intermediates occurring downstream of the enzymatic block, e.g. N^2-acetylornithine, ornithine, and argininosuccinate depletion in *arg9* cells. The unexpected finding of substantial levels of the arginine pathway intermediates *N*-acetylornithine, citrulline, and argininosuccinate downstream the enzymatic block in *arg1* cells provided an explanation for the residual growth capacity of these cells in the absence of external arginine sources. The presence of these compounds, together with the unusual accumulation of N-Acetylglutamate, the first intermediate that commits the glutamate backbone to ornithine and arginine biosynthesis, in *arg1* cells suggests that alternative pathways, possibly involving the activity of ornithine aminotransferase, may be active when the default reaction sequence to produce ornithine via acetylation of glutamate is disabled.

The results of this study suggest that Chlamydomonas may be highly suitable as a model for metabolomic research, especially in the context of photosynthetic processes. The possibility to control growth conditions precisely and to obtain large amounts of homogeneous sample material is a clear advantage in the attempt to study complex metabolic changes in fine-scaled gradients of conditions or with high temporal resolution.

Zusammenfassung

Entwicklung und Anwendung von Methoden zur multiparallelen Analyse von Metaboliten in der einzelligen Grünalge *Chlamydomonas reinhardtii*, einem der wichtigsten Modellorganismen der Zellbiologie, sind Gegenstand dieser Arbeit. Insbesondere seit der Verfügbarkeit des Chlamydomonas-Genoms ist eine systembiologische Perspektive, wie eine Vielzahl an Komponenten im lebenden System zusammenwirkt und ein funktionierendes Ganzes bildet, auch für diesen Modellorganismus ins Blickfeld der Forschung gerückt. Metabolomanalyse, die umfassende Analyse von Veränderungen der Konzentrationen von Stoffwechselprodukten durch Umweltreize oder genetische und entwicklungsbedingte Signale, ist ein wichtiges Komplement anderer Genomanalysemethoden, um die Integration von Genen, Proteinen und Metaboliten in ein nahtloses und dynamisches Netzwerk zur Aufrechterhaltung der Lebensfunktionen eines Organismus zu verstehen.

Die Methode wurde für die Metabolitenanalyse von Material aus Suspensionskulturen entwickelt und im Hinblick auf schnelle Inaktivierung enzymatischer Aktivität, Maximierung der Extraktionskapazität und Behandlung großer Probenmengen optimiert. Im Ergebnis der Probenaufarbeitung, Extraktion und Analyse mittels Gaschromatographie und Time-Of-Flight-Massenspektrometrie konnten mehr als 800 analytische Signale in Einzelproben dargestellt werden, von denen über 100 identifiziert werden konnten. Die Arbeit stellt methodische Innovationen zur systematischen Erkennung von Artefakten in GC-MS Chromatogrammen und Werkzeuge zur Anwendung der Hauptkomponentenanalyse auf Metabolom-Daten vor.

Zellen unter Stickstoff- (N), Phosphor- (P), Schwefel- (S), oder Eisen- (Fe) Mangel zeigen deutliche Unterschiede in ihrer Metabolitenausstattung. Die einzelnen Mangelsituationen konnten durch Anwendung der Hauptkomponentenanalyse auf die Metabolitenprofile deutlich unterschieden werden. Die Ergebnisse der Hauptkomponentenanalyse deuten außerdem darauf hin, dass Phosphat-Mangel, möglicherweise durch die Verfügbarkeit intrazellulärer P-Reserven, durch ein deutlich anderes Mangelsyndrom gekennzeichnet ist als N-, S- und Fe-Mangel. Die Anpassung an die einzelnen Nährstoffmangelsituationen ist durch spezifische Änderungen einer Reihe von Metaboliten zentraler Prozesse des Primärstoffwechsels gekennzeichnet. Die Konzentrationsänderungen von Substraten für die Stickstoffassimilation und den oxidativen Pentosephosphatweg, wie z.B. Glutamat, Glutamin, Glukose-6-phosphat und 6-Phosphogluconat, deuten darauf hin, dass die Fähigkeit zur schnellen Aktivierung der N-Assimilation auch unter Bedingungen herabgesetzter Stoffwechsel- und Wachstumsaktivität aufrecht erhalten wird. Eisenmangel führte zu einer Zunahme organischer Säuren wie Citrat und Succinat, die im Zusammenhang mit den Eisen-komplexierenden Eigenschaften dieser Stoffe stehen könnte. Die Akkumulation von 4-Hydroxyprolin unter Schwefelmangel könnte im Zusammenhang stehen mit der Degradation von Proteinen der Chlamydomonas-Zellwand, deren wesentlicher Bestandteil hydroxyprolinreiche Glykoproteine sind und die unter Schwefelmangel aktiv umgebaut wird. Die Anpassung an Schwefelmangel wurde mit größerer zeitlicher Auflösung und unter Einbeziehung sowohl von identifizierten wie nicht identifizierten Metaboliten in Wildtyp-Zellen und Zellen des *sac1*-Stammes untersucht. *SAC1* ist ein zentraler Regulator der

Schwefelmangelantwort in Chlamydomonas. Durch Anwendung multivariater Analysemethoden wie Cluster- und Hauptkomponentenanalyse konnten fünf Haupttypen der Regulation von Metaboliten bei der Anpassung an Schwefelmangel identifiziert werden. Der quantitativ bedeutsamste Prozess in Bezug auf Anzahl der beteiligten Metabolite und Stärke der Änderungen ist die allmähliche Abnahme der Konzentration mit zunehmender Dauer des Schwefelmangels. Zeitgleiche Ab- und Zunahme von Metaboliten ist ein charakteristisches Element der Anpassung an Schwefelmangel in Wildtypzellen. Die Reaktion von *SAC1*-Mutanten auf Schwefelmangel ist durch weit reichenden Verlust zur Steuerung von Prozessen gekennzeichnet, die normalerweise zur vorübergehenden oder dauerhaften Anreicherung bestimmter Metabolite führen. Des Weiteren konnte die Unfähigkeit von *sac1*-Zellen zur Aktivierung verstärkter Sulfat-Assimilation und zur Drosselung der Stoffwechselaktivität als Reaktion auf Schwefel-Entzug bestätigt werden.

Die Verfügbarkeit von Chlamydomonas-Stämmen mit fehlender Enzymaktivität für fast jeden der Schritte der Argininbiosynthese eröffnet die Möglichkeit, das Potential der Metabolitenanalyse zur Untersuchung der Regulation der Aminosäurebiosynthese in photosynthetischen Eukaryoten zur Anwendung zu bringen und die Effekte zu untersuchen, die das Einfügen spezifischer Stopppunkte in einem wohldefinierten biochemischen Modul zur Folge hat. Drei Stämme, mit fehlender Aktivität für *N*-Acetylglutamat-5-phosphat Reduktase (*arg1*), N^2-Acetylornithin-Aminotransferase (*arg9*) beziehungsweise Argininosuccinat Lyase (*arg2*) wurden in Bezug auf die Aktivierung ihrer endogenen Argininbiosynthese nach Entzug externer Argininquellen analysiert. Die einzelnen enzymatischen Blocks konnten durch Precursor-Anreicherung, wie die Anhäufung von Argininosuccinat in *arg2*-Zellen, und Erschöpfung von Intermediaten nachgelagerter Reaktionen, beispielweise die deutliche Abnahme von N^2-Acetylornithin, Ornithine und Argininosuccinat in *arg9*-Zellen charakterisiert werden. Das unerwartete Vorhandensein von zum Teil das Wildtyp-Niveau überschreitender Mengen von N^2-Acetylornithin, Citrullin und Argininosuccinat, die Produkte bzw. Substrate dem enzymatischen Block nachgelagerter Reaktionen in *arg1*-Zellen sind, bot eine Erklärung für eine noch vorhandene Restkapazität zum Wachstum des *arg1*-Stamms auch ohne äußere Arginingabe. Der Nachweis dieser Verbindungen sowie die ungewöhnliche Anreicherung von *N*-Acetylglutamat, der ersten Verbindung, die das Glutamat-Gerüst für die Ornithin- und Argininsynthese bindet, in *arg1*-Zellen könnte auf alternative Reaktionen, möglicherweise unter Beteiligung von Ornithin-Aminotransferase, zur Synthese von Ornithin hindeuten, die in Erscheinung treten, wenn die Synthesekette nach Acetylierung von Glutamat blockiert ist.

Die Ergebnisse kennzeichnen Chlamydomonas als ein überaus geeignetes Modell für Metabolomanalysen, das insbesondere für die Untersuchung von Prozessen der Photosynthese und nachgelagerter Stoffwechselaktivitäten von großem Interesse sein dürfte. Die Möglichkeit zur präzisen Einstellung von Wachstumsbedingungen und zur Gewinnung großer Mengen homogenen Probenmaterials erweist sich als bedeutender Vorzug, wenn Veränderungen des Stoffwechsels auf komplexer Ebene und in eng abgestuften Gradienten äußerer Parameter oder hoher zeitlicher Auflösung untersucht werden sollen.

Abbreviations

Compounds

2OG	2-oxoglutarate
3PGA	3-phosphoglycerate
AMP	adenosine monophosphate
APS	adenosine phosphosulfate
ArgSuc	argininosuccinate
ATP	adenosine triphosphate
BSA	*N,O*-bistrimethylsilylacetamide
BSTFA	*N,O*-bistrimethylsilyltrifluoroacetamide
CIT	citrate
DMF	dimethylformamide
DNA	desoxyribonucleic acid
F6P	fructose-6-phosphate
FBP	fructose-1,6-bisphosphate
G1P	glucose-1-phosphate
G6P	glucose-6-phosphate
GAP	glyceraldehyde-3-phosphate
Glu-γ-P	glutamyl-γ-phosphate
GlyP	sn-glycerol-3-phosphate
GSA	glutamate-5-semialdehyde
GSH	glutathione (reduced form)
Hyp	4-hydroxyproline
IbGAL	inositol-β-galactoside
MCW	Methanol-Chloroform-Water
MI	myo-inositol
MSTFA	*N*-methyl-*N*-trimethylsilyltrifluoroacetamide
NAD	nicotinamide-Adenine Dinucleotid (NADH: reduced form)
NADP	nicotinamide-Adenine Dinucleotid Phosphate (NADPH: reduced form)
NAG	*N*-Acetylglutamate
NAG5P	*N*-Acetylglutamate-5-phosphate
NAGSA	*N*-Acetylglutamate-5-semialdehyde
NAO	N^2-Acetylornithine
OA	oxaloacetate
OAS	*O*-Acetylserine
P2C	Δ^1-pyrroline-2-carboxylate
P5C	Δ^1-pyrroline-5-carboxylate
PAPS	3'-phosphoadenosine-phosphosulfate
PEP	phosphoenolpyruvate
P_i	orthophosphate
PP_i	pyrophosphate
PYR	pyruvate
S17P	sedoheptulose 1,7-bisphosphate
SUC	succinate
TAP	TRIS-Acetate-Phosphate
THRa	threonate
TMBS	trimethylbromosilane
TMCS	trimethylchlorosilane
TMS	trimethylsilyl group
TRIS	2-Amino-2-(hydroxymethyl)-1,3-propanediol

Proteinogenic amino acids are abbreviated by their three-letter code.

Enzymes

APR	adenosine phosphosulfate reductase
ARS	aryl sulfatase

ASL	argininosuccinate lyase
ASS	argininosuccinate synthase
ATS	ATP sulfurylase
CM	chorismate mutase
GOGAT	glutamine-2-oxoglutarate aminotransferase
GS	glutamine synthetase
NAGK	*N*-Acetylglutamate kinase
NAGPR	*N*-Acetylglutamate-5-P reductase
NAGS	*N*-Acetylglutamate synthase
NAOAT	N^2-Acetylornithine aminotransferase
NAOGAcT	N^2-acetylornithine:N-acetylglutamate acetyltransferase
NR	nitrate reductase
OAS-TL	*O*-Acetylserine (thiol) lyase
OTC	ornithine transcarbamoylase
PEPc	phosphoenolpyruvate carboxylase
PK	pyruvate kinase
SAT	serine acetyltransferase

Miscellaneous

CSC	cysteine synthase complex
DTD	Direct Thermal Desorption
FT-MS	Fourier Transform mass spectrometry
GC	Gas Chromatography
GC-MS	Gas Chromatography [coupled to] Mass Spectrometry
HCA	Hierarchical Cluster Analysis
HPLC	high performance liquid chromatography
LC-MS	Liquid Chromatography [coupled to] Mass Spectrometry
LHCI	Light Harvesting Complex I
LOD	Limit Of Detection
MS	Mass Spectrometry
NMR	Nuclear Magnetic Resonance
OPPP	Oxidative Pentose Phosphate Pathway
PC	Principal Component
PCA	Principal Component Analysis
PSI	Photosystem I
RT	Room Temperature
TCA	TriCarboxylic Acid
TOF	Time Of Flight

Chlamydomonas strain characterization

arg	arginine requiring
cw	cell-wall deficient
mt	mating type
shf	short flagella
wt	wild-type

Genetic nomenclature

Type/ *Origin*	*Chlamydomonas and plants*	*Prokaryotes*	*S. cerevisiae*	*Animals*
Gene (DNA), wild-type allele	*ABC1*	*abc/ abcA*	*ABC1*	*ABC1*
Gene (DNA), mutant allele	*abc1*	*abc1/ abcA1*	*abc1*	*abc1*
Gene product (protein)	Abc1	*abc* gene product	Abc1p	Abc1

Contents

1 Introduction

The unicellular green alga *Chlamydomonas reinhardtii* is one of the premier model organisms in cell biology. With the recent completion of the Chlamydomonas[i] genome project, a systems biology perspective to develop an understanding of how the numerous components in a living system interact to comprise a functioning whole comes into focus for this model organism too. To this end, investigation of the world beyond mRNA abundance will be essential: genes, proteins and metabolites are all integrated into a seamless and dynamic network to sustain cellular functions[1, 2].

Metabolomic analysis aims at the unbiased representation and quantitative determination of the suite of metabolites in a biological sample[3]. It complements transcript profiling and proteomic approaches in functional genomics[4, 5].

Metabolic profiles reflect the dynamic response of the network of biochemical reactions to environmental, genetic or developmental signals. As such, they are a valuable integrated measure of how a living system adjusts to a changing environment. This property has led to the successful application of large scale analysis of metabolites in distinguishing between silent plant phenotypes[6], or characterization of freezing tolerance in plants[7]. It is also of considerable interest in biomarker recovery[8], biotechnological engineering[9, 10] or disease profiling[11].

1.1 Chlamydomonas as Model Organism

Chlamydomonas reinhardtii was established as a laboratory model organism in the 1940s and 50s. *C. reinhardtii* laboratory strains were the subject of pioneering studies on sexual differentiation, cell motility and regulation of the cell cycle[12]. The possibility to obtain viable non-photosynthetic mutants made *Chlamydomonas reinhardtii* early on an excellent system to study synthesis and assembly of the photosynthetic machinery and to dissect photosynthetic electron transport. The cells have the capacity to grow with light as a sole energy source (photoautotrophic growth) or on acetate in the dark (heterotrophically), facilitating detailed examination of genes and proteins critical for photosynthetic or respiratory function. Flagellar structure and function, genetics of basal bodies (centrioles), light perception, cell-cell recognition and cell cycle control are other principal areas of current investigation.

1.1.1 Molecular genetic techniques and resources

C. reinhardtii is amenable to a diversity of genetic and molecular manipulations[13] and the toolbox of molecular genetics techniques has been continuously expanded[14-17]. This includes methods for transformation of the nuclear genome by agitation with glass beads[18], electroporation[19] and particle bombardment[20] as well as transformation of chloroplast[21-23] and mitochondrial DNA[24]. Selectable markers that are routinely used for nuclear transformation include the endogenous Chlamydomonas

[i] Chlamydomonas will be used as a proper noun in this work to refer to the common laboratory species, *Chlamydomonas reinhardtii*. Other species will be named specifically.

genes *ARG7*[25, 26] and *NIT1*[27] as well as the bacterial resistance genes such as the *ble* gene[28] coding for zeocin resistance or an engineered version of the *aph7''* conferring hygromycin resistance[29]. A number of reporter constructs to study promoter function have been developed. Reporter genes include arylsulfatase[30], luciferase[31, 32] and a green fluorescent protein[33] adapted to *C. reinhardtii* codon usage. Targeted disruption of nuclear genes in *Chlamydomonas reinhardtii* is not effective due to the rarity of homologous insertion. Post transcriptional gene silencing, or RNAi, is a promising tool for inactivating the expression of specific genes[34].

The Chlamydomonas genome project[35] marks the beginning of the post-genomic era in Chlamydomonas research. Various sequencing efforts have been bundled and the 3rd version of the draft genome sequence, which is subject to a massive manual curation effort, has been released recently[36]. The availability of the genome sequence has enabled the construction of cDNA- and oligonucleotide microarrays for global transcript profiling[13, 37] and has already led to a multitude of gene expression studies on the effects of various environmental stimuli[38], including the response to low or high CO_2 concentrations[39, 40], acclimation to phoshorus[41] and sulfur[42] deprivation, the dissection of cell cycle regulatory genes[43] or flagellar regeneration[44]. The availability of genomic sequences dramatically reduces the knowledge required to identify and study proteins[45] and methodological advances have fueled a number of studies on the Chlamydomonas proteome[46]. Topics studied include specific compartments such as the flagellar proteome[47], specialized protein classes like thylakoid membrane protein complexes[48], protein phosphorylation[49] or the response to highlight stress[50]. With the extensive cDNA and genomic sequence information new data mining techniques are enabled. This is highlighted by the identification of genes implicated in human disease such as the Bardet-Biedl syndrome[51], polycystic kidney disease[52] or primary cilia diskinesis[53]as a result of the application of comparative genomics to the flagellar/ basal body proteome of Chlamydomonas.

This haploid organism grows rapidly in axenic cultures, on both solid and liquid medium, with a sexual cycle that can be precisely controlled. *C. reinhardtii* is heterothallic and isogamous: Sexual reproduction involves fusion of two gametes of different mating types (+ and –) that appear morphologically identical. Differentiation into sexually competent gametes can easily be triggered by growth in nitrogen-limited media. The mitotic cell cycle is characterized by division into two equal daughter cells with two or more mitotic divisions taking place in rapid succession. Daughter cells are retained within a common mother cell wall and released simultaneously on secretion of a vegetative lytic enzyme acting specifically on the sporangial mother cell wall[54]. Cells can be synchronized in their cell cycle progression by maintaining cultures in 12:12, 14:10, or 16:8 light-dark cycles. Vegetative diploids are readily selected through the use of complementing auxotrophic markers and are useful for analyses of deleterious recessive alleles. These genetic features have permitted the generation and characterization of a wealth of mutants with lesions in structural, metabolic and regulatory genes.

1.1.2 Adaptation of *Chlamydomonas reinhardtii* to its nutrient environment

Due to its simplicity and tractability the Chlamydomonas experimental system has been used extensively to characterize mechanisms and regulation of nutrient uptake and response to nutrient stress situations.

Acclimation to nutrient limitation involves responses specific for the limiting nutrient as well as responses that are more general and occur when an organism experiences different stress conditions. Specific responses enable organisms to efficiently scavenge the limiting nutrient and may involve the induction of high-affinity transport systems and the synthesis of hydrolytic enzymes that facilitate the release of the nutrient from extracellular organic molecules or from internal reserves. General responses include changes in cell division rates and global alterations in metabolism to adjust for nutrient availability and growth potential. In photosynthetic organisms, for example, there must be precise regulation of photosynthetic activity since when severe nutrient limitation prevents continued cell growth, excitation of photosynthetic pigments could result in the formation of reactive oxygen species, which can severely damage structural and functional features of the cell.

1.1.2.1 Nitrogen

Wild-type strains of *C. reinhardtii* can assimilate nitrogen as nitrate, nitrite, ammonium, or other small molecules such as urea or acetamide[12]. NO_3 is the major source of inorganic N in the soil and serves as a substrate for N assimilation. Chlamydomonas synthesizes several transport systems that are specifically involved in acquisition of NO_3 and NO_2[55]. The accumulation of transcripts from the components of these systems is repressed by NH_4^+, whereas the transcripts are most abundant when cells are exposed to NO_3. Nitrate uptake is mediated by high- and low-affinity proton symporters. In the cytosol, nitrate is reduced to nitrite by NAD(P)H-dependent nitrate reductase. Further reduction of nitrite to ammonium by nitrite reductase takes place in the plastid. Most of the nitrate assimilatory genes are regulated at the transcriptional level. Ammonium is a key regulator repressing the expression of genes encoding nitrate and nitrite reductase and the nitrate/ nitrite transporters. Ammonium, whether transported directly into the cell or generated by nitrate/ nitrite reduction enters metabolism via the glutamine synthetase (GS)/ glutamine-2-oxoglutarate aminotransferase (GOGAT) system. Chlamydomonas possesses two GS isoforms. GS1 is localized in the cytosol, while GS2 is present in the chloroplast. GOGAT is present in two isoforms as well, differing in the co-factor used for reduction, NADH and ferredoxin, respectively. Both activities are localized in the chloroplast.

Cells no longer grow and divide upon N depletion and concurrent with metabolic adaptations to low nitrogen differentiation into gametes in initiated[56]. It appears that one or more of the changes that facilitate survival during nitrogen starvation has been co-opted as a signal for the programme of gametic differentiation as gametes are metabolically adapted to survive prolonged periods of nitrogen starvation and sexually competent cells of opposite mating type fuse to form zygotes which are

specialized to endure harsh environmental conditions. When conditions become more amenable to growth, the zygotes germinate into haploid vegetative cells.

Mature gametes can return to the vegetative state by addition of nitrogen. Low nitrogen levels trigger the formation of pregametes, cells which are competent to respond to blue light as second independent extrinsic signal for the transition into mature gametes. Competence for the blue light signal is attained only after five hours of continuous N deprivation[57]. Gametogenesis, if cells are exposed to light, usually is completed ten hours after transfer to nitrogen-free medium.

Carbon and nitrogen metabolism are linked because they must share organic carbon and energy supplied directly from photosynthetic electron transport and CO_2 fixation, or from respiration of fixed carbon via glycolysis, the tricarboxylic acid (TCA) cycle and the mitochondrial electron transport chain. The integration of these two important metabolic processes involves extensive regulation between the two pathways[58].

Nitrate reductase (NR) and phosphoenolpyruvate carboxylase (PEPc) have been described as two major metabolic checkpoints for coordination of primary N and C assimilation[8]. NR, controlling flux into N assimilation is regulated by many factors including light, nitrate, Gln, and sugars. PEPc catalyses carboxylation of phosphoenolpyruvate (PEP) to form oxaloacetate (OA) and enables the provision of C-skeletons through the TCA cycle for inorganic N assimilation. Ammonia incorporation requires 2-oxoglutarate (2OG) and amino acid synthesis downstream the GS/GOGAT system relies on appropriate allocation of assimilated carbon.

The initial steps in nitrogen assimilation result in metabolite changes that activate glycolysis at the level of pyruvatekinase (PK) and PEPc. This activation causes metabolite changes that signal the need to direct carbon to respiration from either starch, sucrose, or the reductive pentose phosphate pathway, depending on the tissue. During photosynthesis, the metabolic demands of nitrogen assimilation are transduced to the photosynthetic apparatus to balance ATP and NADPH production with the energy requirements. The extra reductant demanded in assimilating NO_3 changes the initial priority of carbon flow in tissues where photosynthetic energy is inadequate to meet the electron demands. In such cases, the oxidative pentose phosphate pathway (OPPP) is activated to provide reducing power. The nitrogen and carbon metabolic pathways are interconnected through regulatory signals that include allosteric metabolite effectors, phosphorylation, and redox regulations. Carbon and nitrogen metabolism are interdependent processes, so neither can continue to operate to the detriment of the other. Nutrient status, either of carbohydrate levels or nitrogen compounds are important factors in determining the priority of resource use between these two pathways.

1.1.2.2 **Iron**

Chlamydomonas reinhardtii was shown to exhibit a similar response to iron deficiency as strategy I plants, that involves an inducible Fe^{3+}- reductase activity and regulated iron uptake[59-61]. Iron reduction at the cell surface is a key step in mobilizing iron for uptake[62]. Genetic and biochemical evidence suggests that the multi-copper oxidase Fox1 and the putative permease Ftr1 are additional components

in the high-affinity iron uptake system[63]. While there is evidence that copper deficient cells are unable to activate high-affinity iron uptake in response to removal of iron from growth medium[64], copper deficiency does not lead to chlorosis[65], which is typical for the iron deficient phenotype. This implicates the existence of additional iron transport systems in Chlamydomonas, highlighted by the *crd2* mutant that shows conditional high iron requirement in copper-deficient but not copper replete medium[66].

Activation of assimilation pathways is logically a first line of defense in response to iron deprivation. Indeed, *FOX1* and *FTR1* expression is increased substantially when the iron content of the medium is reduced to 1 μM. Iron-deficiency symptoms such as chlorosis and inhibition of cell division become evident only after iron content is reduced to sub-micromolar amounts, at which point iron supply is insufficient for the maintenance of all iron-containing enzymes.

Besides activating iron assimilation pathways, iron-deficient Chlamydomonas cells re-adjust metabolism by reducing light delivery to photosystem I (PSI) to avoid photo-oxidative damage resulting from compromised FeS clusters[67]. In an iron-replete cell, the light harvesting complex I (LHCI) is well "coupled" to PSI so that the energy of the photons absorbed by chlorophyll bound to Lhca subunits migrates effectively to the special pigments in PSI where photochemistry occurs. In the iron-deficient state, the structure of PSI is modified so that part of the LHCI pigments are no longer effectively connected. Under severe iron limitation, Chlamydomonas cells initiate sequential degradation of the LHCI subunits and both photosystems. The signal transduction pathways for these responses are completely unknown, but it has been deduced that they directly sense iron nutrition rather than damaged PSI because transfer to iron deficient conditions can save PSI-defective mutants that are light sensitive in iron replete medium[67].

1.1.2.3 **Phosphorus**

Phosphorus (P) is assimilated and utilized mainly as phosphate ion (P_i). P_i is an important structural component in nucleic acids and phospholipids and has a critical role in energy conversion in the form of high-energy phosphoester bonds. It is an important substrate and regulatory factor in photosynthesis and respiration and protein phosphorylation/ dephosphorylation is one of the central mechanisms of regulation of protein activity. Due to its low solubility and high sorption capacity in soil, P supply is often limiting to plant growth. Chlamydomonas responds to phosphorus limitation with induction of high-affinity phosphate transport and the expression of extracellular phosphatases that can cleave phosphate from organic compounds in the environment[55]. Alkaline phosphatase activity starts to increase rapidly 20 hours after exposure to P-free conditions and reaches a maximum after 48 h with a 300fold increase relative to unstarved cells[68]. *PHOX* encodes a calcium-dependent periplasmic alkaline phosphatase that accounts for more than 80% of alkaline phosphatase activity. *PHOX* mRNA levels increase dramatically during P deprivation[41].

Chlamydomonas cells possess electron dense vacuoles containing large amounts of pyrophosphate (PP_i) and short and long chain polyphosphate alongside with magnesium, calcium and zinc[69]. They

presumably serve as P_i storage and buffer a critical P_i concentration in the cytoplasma, although also P-starved cells contain polyphosphate bodies of the normal size[70] and most of the inorganic phosphate taken up by P_i-starved Chlamydomonas cells is still accumulated as polyphosphate[71]. Therefore, it has been suggested that apart from P_i storage these organelles may serve also as internal calcium stores and may have a role in inositol-1,4,5-trisphosphate/ calcium signaling[70].

The *Chlamydomonas reinhardtii* transcription factor Psr1 is required for the control of activities involved in scavenging phosphate from the environment during periods of phosphorus limitation[72]. *PSR1* appears to exert transcriptional control on the P_i transporters identified in the Chlamydomonas genome as well as on *PHOX*. Psr1 also controls genes encoding proteins that can serve as alternative electron acceptors that help prevent photodamage caused by overexcitation of the photosynthetic electron transport system. For example, transcript levels of the alternative oxidase gene *AOX1* increase in wild-type cells, while the *psr1* mutant shows only a transient increase in *AOX1* levels after 4 h of P deprivation that is not maintained. In accordance with this finding, phosphorus-starved *psr1* mutants die when subjected to elevated light intensities; at these intensities, the wild-type cells still exhibit rapid growth[41].

Acclimation to phosphorus deprivation also involves a reduction in the levels of transcripts encoding proteins involved in photosynthesis and both cytoplasmic and chloroplast translation as well as an increase in the levels of transcripts encoding stress-associated chaperones and proteases[41]. The onset and intensity of these transcriptional changes suggests that *psr1* mutant cells need to activate the general stress response more rapidly than wild-type cells, possibly because of the inactivity to scavenge P from external resources or internal stores. Regulation of photosynthetic electron transport has been characterized as a general response to adjust metabolism and sustain viability when nutrient levels fall[55]. Both P and S limitation, result in a 75% decrease of maximal O_2 evolution that correlates with the reduction of electron flow through photosystem II, although with P-deprivation a longer treatment is needed to observe the effect[73]. Decline in PS II electron flow is, besides loss of reaction center activity, a consequence of the formation of Q_B nonreducing centers to resist photoinhibition and possibly dissipate excess absorbed light energy. P- or S-limited cells also exhibit increased non-photochemical quenching and undergo a transition to state II with regard to localization of chlorophyll antennae.

1.1.2.4 **Sulfur**

Sulfur (S) is an essential element for all organisms and is present in proteins, lipids, carbohydrates, and various metabolites. S is mostly taken up as sulfate anion (SO_4^{2-}). The first step of assimilation into organic compounds is activation of sulfate by the enzyme ATP sulfurylase (ATS). Adenosine phosphosulfate (APS), the activated form of SO_4^{2-}, can serve as a substrate for reduction or can be phosphorylated by APS kinase to yield 3'-phosphoadenosine-phosphosulfate (PAPS). PAPS can be used by sulfotransferases to catalyze the sulfation of choline, glucosides, proteins and other metabolites. In the reductive sulfate assimilation pathway, the S of APS is reduced to sulfite by APS

reductase (APR). Sulfite is further reduced to sulfide and incorporated into the amino acid cysteine, which is the main hub for synthesis of S-containing compounds including methionine, the methyl donor S-adenosylmethionine, and the antioxidant glutathione.

Cysteine is synthesized by condensation of *O*-Acetylserine (OAS) and sulfide. OAS is formed from serine and acetyl-CoA. The sequential reaction is catalyzed by two enzymes, serine acetyltransferase (SAT) and *O*-acetylserine (thiol) lyase (OAS-TL) which are integrated into the hetero-oligomeric cysteine synthase complex (CSC)[74]. The reversible association of the CSC, accompanied by activation of SAT and inactivation of OAS-TL, in response to changes of cellular concentrations of the key effector metabolites sulfide and OAS provides an intricate mechanism for regulation of sulfate uptake and reduction in plants.

C. reinhardtii synthesizes a prominent, extracellular arylsulfatase (ARS) in response to S limitation[75, 76]. The extracellular location of ARS allows it to hydrolyze soluble SO_4^{2-} esters in the medium, releasing free SO_4^{2-} for assimilation by the cells. Both transcripts and activity for enzymes involved in the uptake and assimilation of SO_4^{2-} increase substantially during S deprivation, including ARS, ATS, APR, SAT, and OAS-TL, although mRNA levels for sulfite reductase and APS kinase change very little[42, 77]. S starvation of *C. reinhardtii* causes a 10fold increase in the V_{max} and a 7fold decrease in the K_M for SO_4^{2-} transport[78].

The *sac* mutants of *C. reinhardtii* are deficient in the response to sulfur-limiting conditions[79]. The *sac1* and *sac2* mutants are deficient in inducing arylsulfatase, whereas *sac3* constitutively expresses arylsulfatase in sulfate-replete medium. All three mutants are unable to increase sulfate transport to the same extent as wild-type cells when deprived of sulfate. In addition, *sac1*, but not *sac2* or *sac3*, is unable to down-regulate photosynthesis in response to sulfur starvation[80]. *SAC1* sequence shows characteristics of Na^+/SO_4^{2-} transporters and is an important regulator of many aspects of both the specific and general response to S starvation[81]. Many of the enzymes of the S assimilation pathway, such as ARS, ATS, APR and sulfite reductase are regulated in a *SAC1* dependent manner[42]. Furthermore, the *sac1* mutant exhibits lower sulfate transport activity and dies much more rapidly under conditions of S deprivation than wild-type cells[55].

The Chlamydomonas cell wall consists primarily of hydroxyproline-rich glycoproteins and is known to be extensively sulfated[82]. The accumulation of cell wall polypeptides which have no or very few sulfur-containing amino acids during S deprivation suggests that restructuring of the cell wall upon the imposition of sulfur starvation may be important for the efficient utilization of sulfur-containing amino acids and possibly for reallocation of sulfur present in cell wall components of unstarved cells[83]. Sac1 mutants fail to accumulate transcripts for these specialized cell wall constituents, which highlights the pivotal role of *SAC1* in the response to S starvation.

1.1.3 **Amino acid metabolism: arginine biosynthesis**

Arginine biosynthesis has been one of the first metabolic processes studied in *Chlamydomonas reinhardtii*[12]. The reaction sequence resembles the Arg biosynthesis pathways in

yeast, *Neurospora crassa*[84] and higher plants[85] with synthesis of ornithine from glutamate and synthesis of arginine from the ornithine intermediate (Figure 1). Orn is synthesized from Glu via a series of acetylated intermediates by sequential activity of N-Acetylglutamate synthase (NAGS), N-Acetylglutamate kinase (NAGK), N-Acetylglutamate-5-P reductase (NAGPR) and N^2-Acetylornithine aminotransferase (NAOAT). Acetylation of Glu commits it to Orn biosynthesis. Orn is formed as the acetyl moiety of N^2-acetylornithine (NAO) is transferred to glutamate, regenerating *N*-acetylglutamate (NAG), in a reaction catalyzed by N^2-acetylornithine:*N*-acetylglutamate acetyltransferase (NAOGAcT). This step completes the so-called "cyclic pathway" for Orn synthesis, which conserves the acetyl moiety that is contributed in catalytic amounts to this pathway by NAGS. Synthesis of Arg from Orn proceeds via enzymes of the urea cycle. Ornithine transcarbamoylase (OTC) catalyzes carbamoylation of the δ-amino group of Orn forming citrulline. Argininosuccinate synthase (ASS) and Argininosuccinate lyase (ASL) activities transform the citrulline backbone to Arg.

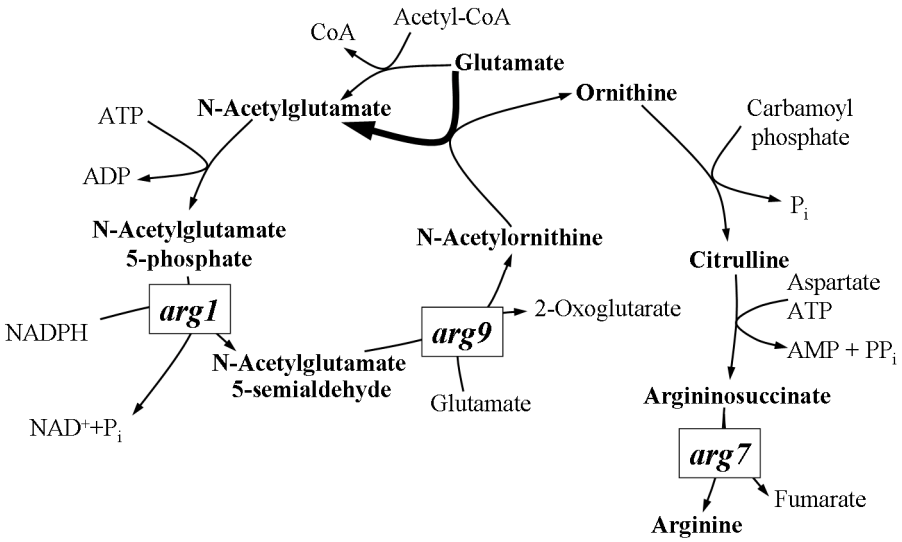

Figure 1:Synthesis of Arg in Chlamydomonas. *N*-Acetylglutamate is synthesized from glutamate mainly by transacetylation from N^2-Acetylornithine (bold arrow). Position of enzymes deficient in the *arg1*, *arg7* and *arg9* mutant strains which have been characterized in this study are indicated.

Feedback inhibition of NAGK by Arg appears to be the major checkpoint for metabolic control of the pathway. Expression of NAGS, NAGK, NAOGAcT appears to be coordinated in response to changes in Arg demand. Allocation of the common carbamoyl-P intermediate coordinates synthesis of Arg with pyrimidine nucleotide synthesis. In *Saccharomyces cerevisiae* NAGS/NAGK are integrated into a functional complex (metabolon) with co-ordinated catalytic activities and feed-back regulation by Arg[86]. An additional layer of control which links sensing of global nitrogen status to Arg synthesis appears to be exerted by modulation of NAGK activity through binding of a PII regulatory protein as has been demonstrated in *Arabidopsis thaliana*[87] and cyanobacteria[88].

In Chlamydomonas, Arg is the only amino acid with a regulated carrier-mediated uptake[89], possibly due to its eligibility as generic N-source. Although substantial evidence in favour of uptake of a

number of amino acids has been presented[12], to date Arg is the only amino acid for which auxotrophic mutants could be isolated. Mutants for six of the individual steps in the biosynthetic pathway for Arg have been described[12]. Among these are mutants affected in the loci for *ARG1* (deficient in NAGPR), *ARG9* (deficient in NAOAT) and *ARG7* (deficient in ASL) (Figure 1). In Chlamydomonas, only ASL has been characterized in detail[26, 90]. The gene is 7.8 kb long and is thought to contain 14 exons. Both the genomic and cDNA have been used to engineer constructs to exploit Arg auxotrophy as selectable marker for transformation and for gene tagging.

1.2 Metabolomic Analysis

Metabolites form an integral part of the molecular interaction network and play diverse roles from structural building blocks to energy sources and signaling molecules. The comprehensive study of the changes of metabolite composition, or metabolomics, in response to environmental, genetic or developmental signals is an important complement of other functional genomic techniques in the effort to develop an understanding of how genes, proteins and metabolites are all integrated into a seamless and dynamic network to sustain cellular functions. The unbiased and complete representation and quantification of the suite of metabolites in a biological sample is an ambitious concept and recent improvements of analytical performance, innovative bioinformatics tools and new data mining strategies are just beginning to extend the relevance of metabolomic data from the observation of global or systemic properties and responses to more refined analyses of metabolic regulation and control.

1.2.1 Scope and objectives

The proximate objective of metabolomic analysis is to obtain measurements that truly reflect the in-vivo amounts of cellular metabolites. Metabolites can be detected directly or as chemical derivates specific for the individual compounds. Several issues regarding this proximate goal are important to consider: The analysis should include as many metabolites as possible, ideally all, and avoid bias towards certain compound classes defined by molecular structure or physicochemical properties such as polarity or volatility. Furthermore, artifact signals, which can be of various origin, should be avoided or must be removed from the set of measurements. Dynamic range presents a further challenge for the correct quantification of metabolites as individual components can vary in concentration seven to nine orders of magnitude within tissue extracts[91]. Depending on the analytical platform, some metabolites may be below their limit of detection, while others may be present in significant amounts and be out of the range of linear detection or even of the detection capacity of the hardware.

Ideally, quantification would allow establishing absolute amounts of the different compounds. Due to largely different analytical sensitivity of individual metabolites which depends on the detection system used, relative quantification can be restricted to comparisons of the amounts of individual metabolites

between differently treated samples, rather than allowing the comparison of the amounts of different metabolites in one or more samples.

A major challenge to the generation of metabolomic data is the diverse chemical nature of small organic compounds which limits the number and type of metabolites that can be extracted, detected and identified with any single method of sample preparation and measurement. Depending on the type of question asked, the scope of metabolite analysis should be adapted to the cause, as the general notion in metabolite analysis is that with currently available technology comprehensiveness and accuracy are partly conflicting objectives. For example, adaptation of the sample preparation protocol and detection method to the physicochemical properties and in-vivo abundance of a certain compound class of special interest will be suitable to determine these compounds with high precision while other compounds may not be adequately extracted or detected. Consequently, metabolite analysis may be restricted to the substrate(s) or product(s) of a particular enzyme or metabolic process (metabolite target analysis), e.g. when hypotheses on specific metabolites are tested, or to a group of metabolites implicated in a metabolic pathway of interest or belonging to certain compound classes defined by molecular structure (metabolite profiling). If compounds are not selected in advance, the resulting data will contain a broad spectrum of metabolites (metabolomics) and will, besides recognized molecules, include a substantial number of analytes without an assigned chemical structure due to current limitations in compound identification (see 1.2.2.2). Metabolomic data which is not or only to a small degree annotated has worthwhile applications, notably for sample classification or the general characterization of metabolite changes in response to environmental or genetic perturbations; such metabolic phenotypes have been shown to very sensitively differentiate biological samples[6] and for a number of purposes sample classification in itself is of great importance. When sample classification is the main focus, identification or even separation of individual analyte signals may not be needed (metabolic fingerprinting). However, depending on the methodology used, classification can identify metabolites accounting for the difference between samples and lead to targeted identification efforts for the most relevant analytes.

The capability of metabolomic approaches to cover potentially important novel or unknown compounds is generally regarded as an advantage and analytes without assigned chemical structure still convey information on global changes of metabolism or highlight the impact of individual unknown compounds. However, to exploit metabolomic data to its fullest, to integrate it with other datasets of genomic scale and with the vast body of experimental evidence from established targeted biochemical analyses, identification is a key step. Identification therefore can be seen as the link between the proximate (metabolite measurement) and the ultimate objective of metabolomic analysis which is to apply metabolite measurements to study regulation and control of metabolism, to identify regulational circuitries and determine how the flux of energy and matter is conducted and coordinated within and between metabolic pathways.

1.2.2 **Methods**

Harvest, extraction and preparation of the extract for metabolite measurement are the first steps of metabolomic analysis and are crucial for the quality of the result. Important parameters during sample preparation are rapid inactivation of metabolism to preserve in-vivo metabolite concentrations (quenching), quantitative and comprehensive extraction of metabolites, prevention of metabolite degradation or modification, complete and reproducible derivatization and comparability between samples. Studies which provide a synthetic view on the many parameters entailed in the sample preparation process for metabolite analysis and compare alternative methods for quenching, extraction, or derivatization have begun to appear only recently, including studies on sample preparation and derivatization of *Arabidopsis thaliana*[92] and microorganisms such as *Saccharomyces cerevisiae*[93] or *Escherichia coli*[94, 95]. A range of analytical techniques such as gas chromatography coupled to mass spectrometry (GC-MS), H-1 NMR spectroscopy, liquid chromatography-mass spectrometry (LC-MS), Fourier Transform mass spectrometry (FT-MS), high performance liquid chromatography (HPLC) and electrochemical array (EC-array) have been applied to maximize the number of metabolites that can be identified in a matrix[96, 97]. GC-MS in particular has been widely used due to unsurpassed sensitivity, chromatographic separation power, high dynamic range and reproducibility and is employed also in this study. The following paragraphs highlight the methodology of metabolomic analysis and in particular methods in GC-MS based approaches.

1.2.2.1 **Sample preparation for metabolite measurement**

Environmental stimuli of any kind are suitable to provoke rapid changes in metabolite concentrations, especially for intermediates which participate in reactions with high turnover rates. To generate an authentic picture of the metabolic composition of a biological system it is therefore crucial to stop biochemical activity instantly as the material is removed from the original growth conditions for harvest. Enzyme inactivation can be reached by protein denaturation or rapid freezing. Denaturation occurs after sudden pH change, e.g. mixing with strong acid (perchloric or trichloroacetic acid) or alkali reagents (NaOH or KOH), or mixing with organic solvents. Treatments with acids or alkali reagents have often been applied to inactivate enzymes and extract metabolites at the same time. Acidic and alkalinic extraction methods have commonly been used for the extraction of acid and alkaline stable compounds, respectively (see below).

Rapid freezing to low temperatures will slow and eventually stop enzymic reactions. Freezing does not eliminate the need for permanent destruction of enzyme activity but enables rapid quenching of metabolism in larger objects such as organs, or objects which have structural barriers (e.g. cell walls) which prevent rapid mixing with acids, alkali, or organic solvents and require homogenization prior to the application of denaturing agents. During homogenization and until application of denaturing agents the material must be kept at low temperatures.

Whereas plant material can be freeze-clamped or flash-frozen in liquid nitrogen directly, the situation is different for analysis of microbial cells from suspension cultures. Although freezing of entire

microbial cultures with subsequent analysis of the metabolite composition have been reported[98], separation of the cells from the medium is highly desirable. The separation is a prerequisite for differentiation of intra- and extracellular metabolites and enables sample concentration in view of the usually small ratio between biomass and culture medium. In addition, it provides the possibility to eliminate large amounts of constituents of the growth medium from the sample, which may not be compatible with the use of highly sensitive separation or detection methods.

A commonly used method for metabolite analysis of yeast cultures that enables separation of cells from the culture medium while stopping cell metabolism is based on rapid sampling into a cold methanol solution as proposed by de Koning and van Dam[99]. Cells can then be collected by centrifugation[100] or filtration[101] requiring sample handling at low temperatures to minimize turnover of metabolites prior to cell extraction.

A critical factor for the use of cold aqueous methanol solution for quenching is the preservation of the integrity of the cells. Yeast cells[93], like bacterial cells[102-104] are sensitive to cold methanol solutions (50% v/v final methanol concentration) in that leakage of certain intracellular metabolites, e.g. significant amounts of glucose-6-phosphate (G6P), ATP and NAD^+, is observed during quenching[100]. Methanol concentrations as low as 25% v/v appear to compromise membrane stability of yeast cells, although it is not known whether this results in significant metabolite leakage[93]. Minimizing exposure time to cold methanol solution reduces the amount of metabolite leakage in yeast[93].

To extract metabolites efficiently from plant tissues, the tissue must be homogenized properly first. Various techniques have been applied for this, e.g., grinding with a mortar and pestle together with liquid nitrogen, homogenization with a ball mill with pre-chilled holders[105], a metal pestle connected to an electric drill[106], and ultra-turrax devices[107]. In Chlamydomonas simple freezing and thawing is sufficient for the release of soluble enzymes[108]. Sonication, the French press, homogenization with glass beads, and grinding of cell pellets with mortar and pestle are used to prepare more particulate homogenates[12]. Mostly, these cell disruption techniques have been applied in Chlamydomonas without special regard or need to preserve metabolite levels during homogenization and have been described for aqueous extraction solutions rather than organic solvent extractants.

The most common way to extract metabolites is to incubate and agitate the homogenized material at low or high temperatures in organic solvents, solvent mixtures[105, 109, 110] or perform sequential extractions with different solvents. For polar metabolites, methanol, ethanol, and water are often used, while for lipophilic compounds chloroform is commonly applied. A number of techniques has been used to increase extraction efficiency including supercritical fluid extraction (SFE)[111] microwave-assisted extraction[112, 113] (MAE), and pressurized liquid extraction (PLE)[114, 115].

De Koning and van Dam[99] adapted a methodology originally designed for extraction of total lipids from animal tissues[116] based on buffered methanol-water mixture and chloroform to extract polar metabolites from a yeast cell suspension. Their method has recently been applied for intracellular metabolite analysis of a variety of microorganisms[94, 101, 102, 117, 118]. The combination of methanol,

water, and chloroform has been shown to yield excellent recoveries of amino acids, organic acids and sugar alcohols, and, in contrast to using pure or diluted methanol, is able to adequately recover phosphorylated compounds[93, 102, 118].

Metabolite extraction at extreme pH is suited for the measurement of acid-stable and alkali-stable compounds, respectively. These methods have been widely used in the extraction of metabolites from animal[119] and plant[120-122] tissues and microorganisms[9, 94, 103, 123]. Acidic extraction is commonly used for the extraction of nucleotides and water-soluble metabolites[9, 124], but for metabolome studies it is evident that not all metabolites are stable at the extreme pH, and destruction of some nucleotides has been reported during acidic extractions[123]. Data acquisition methods should be carefully chosen in order to eliminate the interferences of high salt concentrations that may occur as a result of neutralizing the extraction solution. Compounds such as pyruvate, nucleotides, and phosphorylated sugars are poorly recovered under extreme acidic or alkaline pH [94]. In addition, the neutralization of the extracts may increase the losses of metabolites by absorbing to the $KClO_4$ precipitate. When both acid- and alkali-stable metabolites have to be determined, the extraction has to be carried out on two separate samples, making it difficult to reproduce cell sampling and quenching. Furthermore, there are metabolites which are unstable in both high and low pH extraction solutions[100]. Metabolite extracts are concentrated prior to GC-MS measurement by lyophilization or solvent evaporation[93]. Removal of polar solvents is also usually a prerequisite for chemical derivatization to increase volatility of polar compounds for GC-MS analysis.

Many of the constituents of a crude metabolite extract are nonvolatile and are in their underivatized form not amenable to GC analysis[92]. The most common way to derivatize polar compounds containing acidic protons as in –OH, –SH, or –NH groups, is to introduce a trimethylsilyl (TMS) group, and form TMS ethers, TMS sulfides or TMS amines, respectively[125]. For monosaccharides TMS derivatization usually results in five tautomeric forms (open chain, two pyranose, and two furanose anomers) of the reducing sugars[126, 127]. This causes major problems for the identification and quantification of complex mixtures of carbohydrates due to equilibrium shifts and separation constraints in complex matrices. The number of tautomeric forms can be reduced by conversion of the aldehyde and keto groups into oximes using hydroxyamines or alkoxyamines before forming TMS ethers. This results in the formation of only *syn* and *anti* forms due to the limited rotation along the C=N bond[105]. The choice of reagents for oximation and silylation is guided by setting priorities between maximizing reaction efficiency, to ensure that as few metabolites as possible remain underivatized, and minimizing formation of unexpected side products[128]. Evidence suggests that alkoxyamine and TMS derivatization are more suitable for the identification of compounds by GC/MS compared to hydroxylamine and TMS derivatization[105]. MSTFA (*N*-methyl-*N*-trimethylsilyltrifluoroacetamide) has been widely used for silylation of sugars and plant metabolites in combination with oximation[105, 129, 130]. The silylation donor power of MSTFA is similar to that of BSTFA (*N,O*-bistrimethylsilyltrifluoroacetamide) and BSA (*N,O*-bistrimethylsilylacetamide), but MSTFA is more volatile and thus more suitable for direct

GC analysis of the derivatization reaction[125]. Reagents, such as potassium acetate, pyridine, TMCS, and TMBS, can enhance the silylation power of silylation reagents[125]. The choice of solvent can also affect the silylation efficiency[121, 125].

GC-MS analyses easily yield peak information reaching and exceeding 1000 separate analytical signals. As illustrated with reducing sugars above, original metabolites can produce several derivate peaks due to tautomeric conversions or varying degrees of derivatization. Other chromatographic peaks may be the result of compound degradation or modification during extract preparation due to metabolite instability under extraction conditions, e.g. oxidation[131] or allomerization[132]. Side reactions and residues of the TMS derivatization reaction are detected as numerous signal in GC-MS analyses[128]. A further source of bogus peaks may be contamination of reagents, solvents and reaction vessels used. Rarily, systematic strategies are reported to differentiate and eliminate these artifact signals which is especially important if conclusions are based on the analysis of both known and unknown peaks.

1.2.2.2 Metabolite measurement with GC-MS: detection and identification

GC-MS is a combined system where compounds are first separated by GC and then detected traditionally by electron-impact mass spectrometers. The combination of these analytical techniques provides high chromatographic resolution and high sensitivity. Typically, limits of detection are in the pico- or nanomolar range. A diverse array of small organic compounds is amenable to analysis by GC-MS, but this range is, in general terms, restricted to thermally stable volatile compounds or compounds that can be chemically transformed into stable volatile derivatives. Non-volatile, high-MW compounds or certain polyphosphorylated or activated intermediates may therefore not adequately be covered. Volatile, low-MW metabolites have been sampled and analyzed directly, without further need for derivatization including breath[133] and plant[134, 135] volatiles.

Small aliquots of derivatized samples are analyzed by split and splitless injection setups on GC columns of differing polarity. In metabolomic analyses, the goal is to maximize the number of metabolites analyzed in a single GC-MS run, and therefore extracts usually are not fractionated, in contrast to procedures for analyzing specific metabolites from complex matrices. This results in a complex data output, containing hundreds of analyte peaks. Although extending run times increases GC separation power[136], complete chromatographic resolution is difficult or impossible to achieve under these conditions. Recent studies probe the potential of two-dimensional gas chromatography for a substantial enhancement of chromatographic resolution in metabolomics approaches[137-140].

Several bioinformatics tools have been introduced to process GC-MS raw data[129, 141, 142] in addition to proprietary software offered by suppliers of GC-MS systems, such as ChromaTOF (Leco Inc., St. Joseph, MI, USA). Data transformation algorithms include automated computation of peak apexes and mass spectra, peak deconvolution, which aims at the mass spectral correction for co-eluting analytes, calculation of retention time indices and automated assignment of mass fragments suitable

for selective quantification. Alignment of chromatographic peaks from large sample series is required when metabolite responses are to be compared for a large number of samples or conditions. Tools proposed for the simultaneous processing of large chromatographic data sets include the software packages MSFACTS[129], MetAlign[143] and the curve resolution approaches by Jonsson et al.[130, 144].

However, no generally adopted procedure to transform metabolite raw data has yet been proposed that can be used independently from its technological platform which is due to the dependency of GC-MS data on a significant number of technical parameters and sample-specific requirements. Currently, no automated tool appears to be an adequate substitute for expert input to correct wrong assignments during annotation and identification of peaks.

With appropriate external and internal calibration GC-MS can provide exact absolute quantification of the level of a given metabolite in a concentration range of up to four orders of magnitude[96]. External calibration is labour intensive and not all metabolites are commercially available to enable preparation of standard solutions. General and substance-specific losses can occur during all stages of sample preparation and measurement and are matrix-dependent[92, 93]. Stable isotope labeling with isotopomers for each compound or xenobiotic stereoisomers which can be differentiated by specific mass fragments and different retention behavior, respectively, would be ideally suited for standardization[145, 146].

Currently, the vast majority of analytes in a typical GC-MS analysis remains unidentified. Though there have been advances in de-novo structure elucidation[147, 148], identification usually relies on comparison of both the chromatographic retention times or indices and mass-spectrum of sample peaks with those of authentic standard compounds in mass spectral libraries[149]. These libraries are created in identification efforts in many laboratories and are often adapted to the specific analytical set-ups in use[150-154]. Recent efforts to develop resources that facilitate exchange of metabolomic data and integrate mass spectral collections from different laboratories highlight the importance of mass spectral libraries as a reference for compound identification[5, 155, 156].

1.2.2.3 **Metabolomic data analysis and applications**

To study metabolism, analysis of metabolite concentrations are one approach complementary to the analysis of metabolic fluxes[157, 158] and of enzyme activities[159].

Metabolite levels are regarded as a “downstream” result of gene expression and as more direct indicators for relating genes to functions at a cellular or systems level[160]. Changes in the metabolome are expected to be amplified relative to changes in the transcriptome and the proteome[161]. In addition, both theoretical[162, 163] and empirical[164] evidence indicates that although changes in the quantities of individual enzymes might have little effect on metabolic fluxes, they can have significant effects on the concentrations of individual metabolites.

Metabolomic data is in its nature multivariate and in many investigations the number of variables (metabolites) exceeds the number of observations (samples) by far. A variety of multivariate techniques has been tested to exploit metabolomic data, detect and explain statistically significant

structural dependencies and derive hypotheses on the origin of sample variance. Cluster analysis, e.g. hierarchical cluster analysis (HCA) is widely used for classification of samples[143]. Factor analytic techniques like principal components analysis (PCA) and partial least squares (PLS[165]) or independent components analysis (ICA[166]) can be used to extract common factors which account for orthogonal or independent sources of variance and to reduce the dimensionality of the data. Self-organizing maps (SOM[167, 168]), mutual information[169], and machine learning[170, 171] are additional tools that have been applied to detect dependencies between the variates measured.

Probably due to its firm anchorage in basic statistical theory and well-developed understanding regarding terms of use and significance, the concept of linear correlation is a popular measure of the dependency of pairs of individual metabolites[6, 172-174] though in the context of metabolic control it may be inadequate to detect many types of dependencies occurring in the biochemical network of the cell[175].

To date, metabolomic data is often used for sample classification with or without determination of the most discriminative metabolites and for the characterization of differences of individual metabolites or sets of metabolites between different conditions. Metabolomic data allow the detection of effects of genetic or environmental perturbations on the metabolite level which are not known or presumed a priori. This allows to assess the effectiveness of heterologous expression that aim at the accumulation or depletion of specific compounds and monitor, apart from the desired effect, the formation of side products[176]. Transformation of tomato with a stilbene synthase from grape[177] resulted in the accumulation of trans-resveratrol and its glucopyranoside but also of ascorbate and glutathione. As an extension of this concept, global metabolite data has been interrogated to associate quantitative trait loci with metabolic loci that have potential for crop breeding[173]. The comprehensive analysis of metabolite levels and the comparison of metabolic phenotypes have been suggested as a possible measure for substantial equivalence to assess the degree of similarity/ of difference between transgenic and wild-type plants. In this way, substantial equivalence of genetically modified potatoes which, apart from the targeted changes, had similar total metabolite composition as conventional varieties was established. Apart from applications in bioengineering the broad scope of metabolomic analysis has potential for the analysis of the regulation and control of metabolism on a complex level. The inducible activation of a cytosolic invertase from yeast in growing potato tubers and comparison with the effects of constitutive overexpression of the same gene allowed primary effects of increased sucrose mobilization to be distinguished from pleiotropic secondary effects such as switch from starch synthesis to respiration[178]. The analysis of tissue specific metabolic phenotypes can suggest their possible biochemical roles in whole-organism processes and, vice versa, distinction of cellular areas by metabolite composition can point to different biochemical function[179]. Global metabolite levels are a valuable tool to characterize biochemical effects during developmental or environmental transitions like the adaptation to cold-stress[7] or sulfur starvation which leads to enhanced glucosinolate biosynthesis[180]. The complementary nature of metabolomic analysis in functional genomics

approaches is illustrated by the temporal offset of transcriptional changes and reactions on metabolite level after infestation of tomato plants with *Tetranychus urticae*[181]. Cellular processes are regulated at several layers and the integration of metabolomic data with transcriptomics or proteomics aims to capture the regulational properties of the molecular interaction networks more appropriately[182]. This can aid in determining gene functions[183, 184] or regulatory metabolites and genes[168]. The comprehensive analysis of metabolite levels has supported a paradigm change from pathways to reaction and regulation networks[160] and a major goal of metabolomics is to adequately describe complex traits like optimized carbon partitioning or protein content and develop an understanding of the underlying metabolic network. For example, heterologous, seed-specific expression of a bacterial PEPc in beans lead to a flux shift from sugars and starch to organic acids and free amino acids[185]. Sulfur deficiency in *Arabidopsis thaliana* leads not only to a rebalancing of cellular sulfur, but also of carbon and nitrogen resourses[186].

The network model of cellular metabolism implies that the concept of biochemical engineering may be fundamentally flawed and will work only efficiently when metabolic pathways and their mutual dependencies are fully understood and a dedicated strategy for genetic modification can be designed[187]. Accordingly, reconstruction of the metabolic network, deduction of reaction routes and regulational circuitries from metabolomic data is a major focus. A variety of theoretical approaches have been suggested for how metabolomic data can be employed to develop models of metabolism either based on metabolic fluxes or biochemical stoichiometry[3]. Metabolic control analysis[162] provides a fundament on which current extensions like co-response analysis[188] or elementary flux modes[189, 190] are used to reveal stoichiometric constraints that restrict possible network topologies. Network motifs[191, 192] are arrangements of reactions with recurrent types of regulational control, including feedback and feed-forward loops[193] and are being exploited to unravel possible network topologies too. Algorithms like correlation metric construction have been developed for the reconstruction of metabolic networks from metabolomic data after perturbations[194] or from time series data[195] but are currently restricted to reaction systems which do not reach the complexity level of cellular metabolism.

1.3 **Objectives**

To date, genome-scale analyses in *Chlamydomonas reinhardtii* are centered on transcript profiling and proteomic approaches. This work sets out to extend the scope of available functional genomics techniques for this important model organism and develop and apply a metabolite profiling technique for multiparallel analysis of small organic compounds. Being a well studied model organism, a wealth of physiological and molecular genetic techniques and well characterized mutants with defects in structural, metabolic or regulatory genes are available and allow expanding the characterization of the affected cellular processes by comprehensive analysis of metabolite levels. As a test case for metabolite profiling in Chlamydomonas, the response to macro-nutrient and iron deficiency will be characterized. The adaptation to sulfur deficiency will be analyzed with greater temporal resolution

and responses of wild-type cells will be compared with mutant cells lacking *SAC1*, an important regulator of the sulfur deficiency response. For most of the steps in Arg biosynthesis in Chlamydomonas mutants have been isolated that are deficient in the respective enzyme activities. This presents the unique opportunity to probe the potential of metabolite analysis for elucidating regulation of amino acid biosynthesis in a photosynthetic eukaryote and analyze the response to withdrawal of externally supplied Arg and activation of endogenous Arg biosynthesis by determining the levels of the pathway intermediates.

2 Material and Methods

2.1 Cell Culture

Chlamydomonas reinhardtii strains CC-125 wt mt+ and CC-400 *cw15* mt+ were acquired from the Chlamydomonas Genetics Center (CGC). The arginine-requiring strains CC-48 *arg2* mt+ (deficient in argininosuccinate lyase[196])[i], CC-861 *arg1* mt+ (deficient in *N*-acetylglutamate-5-phosphate reductase[197]) and CC-2958 *arg9-2 shf1-253* mt– (deficient in N^2-acetylornithine-aminotransferase[198]) were also obtained from CGC.

Generally algae were cultured in TRIS-acetate-phosphate (TAP) medium[12] at 25°C under constant illumination with cool white fluorescent bulbs at a fluence rate of 90 $\mu mol \times m^{-2} \times s^{-1}$ and with continuous shaking.

Analysis of macronutrient and iron deficiency

Single colonies were used to inoculate a starter culture which was harvested at late log-phase and used to inoculate a new culture at a starting density of 5×10^5 cells/ml. After 48 h, cells were harvested by centrifugation, washed twice with sterile 20 mM TRIS pH 7.0 supplied with 300 µM $CaCl_2$, 400 µM $MgCl_2$ and 7 mM KCl, and resuspended at a starting density of 1×10^6 cells/ml in TRIS buffered media depleted of nitrogen[199], sulfur[79], phosphorus[68] or iron[64] prepared as described earlier, grown for 24 h and harvested at final densities of $5\text{-}8 \times 10^6$ cells/ml.

Metabolomic analysis of S deprivation

For the detailed analysis of sulfur deficiency a *sac1* mt+ mutant and the parental strain CC-1690 mt+ were used. The mutant *sac1* strain was generated by backcrossing the original *sac1* cells[79, 80] isolated from a mutagenized population of strain CC-425 *cw15 arg7-8* mt+ three times to the wild type strain CC-1690. Both mutant and parental strain were obtained from Jeffrey Moseley (Carnegie Institution, Stanford, CA, USA).

For each strain, single colonies were used to inoculate a TAP starter culture which was harvested at late log-phase and used to inoculate a new culture at a starting density of 5×10^5 cells/ml. Cells were grown for 24 h to late log-phase, harvested and used to inoculate a 1 L culture at the same starting density to yield sufficient cellular material for the experiment. Cells were harvested after 24 h and resuspended twice in ice-cold Tris-buffered medium depleted of sulfur. After each round cells were collected by centrifugation for 5 min at 2000g and 4°C. Cells were then resuspended in ice-cold sulfur-deplete medium at a high concentration and stored on ice. An appropriate amount of cells was used to make a culture stock in sulfur-depleted medium at RT which was then used to inoculate separate 200 ml culture flasks to be harvested after 2, 5, 10 and 24 hours sulfur deprivation. Sulfur replete control samples were generated by resuspending the needed amount of the washed and

[i] The *arg2* allele (=*arg7-8*) is considered to be an allele at the *ARG7* locus, showing intragenic complementation with various *arg7* alleles in diploids.

resuspended cell concentrate into standard TAP medium (200 ml final volume). For each strain, condition and time point the cell concentration to start the culture were adjusted so that each culture was harvested at mid-log phase (OD_{750} between 0.4-0.5). The required starting concentrations for each strain, condition and time point were experimentally determined in advance. Cultures were handled sterile until the individual flasks were harvested. The entire experiment was conducted three times independently. Correlation between turbidity and cell density was verified in advance by hemocytometer cell count with an optical density (λ=750 nm) of one corresponding to 1.5×10^7 cells/ml. Chlorophyll a and b levels were determined spectrophotometrically[12, 200]. Growth of arginine auxotrophic strains was maintained by addition of 50 mg/l L-Arginine to liquid media prior to sterilization. Solid media were supplemented with 4 g yeast extract per liter medium.

2.2 Harvest, Quenching, and Extraction

At the incubation site the cell suspension was injected into a quenching solution (40% methanol in water). The quenching solution was pre-chilled at –32°C and used at a ratio of 7:1 v/v of quenching solution to cell suspension for rapid cooling of cells. During injection, the quenching solution was stirred to facilitate rapid mixing and cooling. Centrifuge tubes were cooled throughout the harvest procedure in an ethanol/ dry ice bath to keep sample temperature below –20°C. Cells were collected by centrifugation at 2500 g for 20 min with centrifuge and rotor pre-cooled at –20°C. Supernatants were decanted and residual liquid carefully removed. Pellets were flash frozen in liquid nitrogen. Cells were resuspended in 125 µl extraction solution (methanol:chloroform:water 10:3:1 v/v/v) per milliliter cell suspension based on unit optical density of the harvested cell culture; extraction volume for more dilute cultures was adjusted accordingly. Five microliter of a 0.2 g/L [U-^{13}C]-sorbitol (Isotec, Miamisburg, OH, USA) in H_2O stock solution were added per milliliter extraction solution prior to its use. Resuspended material was transferred to new tubes containing 1 ml glass beads (0.25-0.3 mm diameter, B.Braun Biotech, Melsungen, Germany), vigorously vortexed and incubated for 30 min at –25°C with occasional vortexing to facilitate extraction. Extracts were transferred to new centrifugation tubes and particulate material was pelleted by centrifugation for 30 min at 50000 g and –20°C and the clear supernatant was used for aliquotation of GC-MS samples. Polar phase separation and derivatization for specialized analysis of hydrophilic compounds only were essentially carried out as described earlier[146]. In brief, extracts were separated into a lipophilic and polar phase by adding 0.4 volume parts water to the clear extract and centrifugation for 15 min at 25000 g and –20°C using a swing-out rotor. Aliquoted samples were dried by vacuum evaporation over night, flushed with argon, tightly capped and stored at –20°C until GC-MS measurement.

For manual derivatization, 10 µl of a freshly prepared solution of 40 mg *O*-Methylhydroxylamine per ml pyridine were added to the dried samples and incubated for 90 min at 30°C with continuous shaking. Silylation reactions were started by adding 90 µl MSTFA and incubation for 30 min at 37°C. MSTFA was spiked with 2 µl retention index marker mix per milliliter prior to use. Retention index marker mix stock solution contained the fatty acid methyl ester amounts specified in Table 1 solved in

25 ml chloroform and stored at 4°C. Prior to aliquotation into autosampler vials derivate solutions were centrifuged for 10 min at 20000 g at RT to sediment any precipitates.

name	sum formula	CAS registry	m [mg]	retention index
Methylcaprylate	$C_9H_{18}O_2$	111-11-5	20	262320
Methylpelargonate	$C_{10}H_{20}O_2$	1731-84-6	20	323120
Methylcaprate	$C_{11}H_{22}O_2$	110-42-9	20	381020
Methyllaurate	$C_{13}H_{26}O_2$	111-82-0	20	487220
Methylmyristate	$C_{15}H_{30}O_2$	124-10-7	20	582620
Methylpalmitate	$C_{17}H_{34}O_2$	112-39-0	20	668720
Methylstearate	$C_{19}H_{38}O_2$	112-61-8	10	747420
Methyleicosanoate	$C_{21}H_{42}O_2$	1120-28-1	10	819620
Methyldocosanoate	$C_{23}H_{46}O_2$	929-77-1	10	886620
Lignoceric Acid Methylester	$C_{25}H_{50}O_2$	2442-49-1	10	948820
Methylhexacosanoate	$C_{27}H_{54}O_2$	5802-82-4	10	1006900
Methyloctacosanoate	$C_{29}H_{58}O_2$	55682-92-3	10	1061700
Triacontanoic Acid Methylester	$C_{31}H_{62}O_2$	211-113-1	10	1113100

Table 1: Composition of retention index marker mix. Retention times were converted to the indices indicated.

2.3 Control of Metabolite Leakage during Quenching

Strains CC-125 and CC-400 had been grown for 22 h from a starting density of 1×10^6 cells/ml in unlabeled TAP medium to a density of 6.8×10^6 cells/ml.

10 µl [U-^{14}C]-acetate (Amersham, 200 µCi×ml^{-1}) were added to 10 ml of the cell suspension which was put back to the same culture conditions. After three hours of incubation cells were harvested by centrifugation for 5 min at 2000 g and 4°C. The culture supernatant was carefully removed and residual medium extracted with a pipette. Cells were gently resuspended in 10 ml ice-cold (unlabeled) TAP medium to wash off all remaining activity from medium residuals and interstitial spaces. Resuspended cells were collected by centrifugation for 5 min at 2000 g and 4°C and the supernatant was carefully removed. The pellet was resuspended in 10 ml of room-temperature (unlabeled) TAP and gently agitated on a shaker for 15 min in the light at room temperature to allow for equilibration of the cells after two rounds of centrifugation.

Aliquots of 170 µl of the cell suspension were subjected to the quenching procedure described above. The quenched samples were prepared in six replicates: Cells from three of the samples were harvested after 3 min by centrifugation, whereas the other three were kept for 30 min at –25°C before pelleting. 625 µl of the supernatant, corresponding to 125 µl cell suspension was used for scintillation. Measurements of the total amount of incorporated radioactivity were made by using 125 µl of the washed and equilibrated cell suspension with an addition of 500 µl quench solution directly for scintillation.

Control samples for leakage inflicted by the centrifugation itself were prepared by harvesting an aliquot of the washed and equilibrated cell suspension at 2500 g for 5 min and 4°C and subjecting the supernatant to quenching in parallel with the cell suspension.

Using 10 ml scintillation cocktail (Ready Safe, Beckman Coulter, Fullerton, CA, USA) per sample, scintillation for ^{14}C was performed on a LS 6500 Scintillation Counter (Beckman Coulter, Fullerton, CA, USA).

2.4 GC-TOF Measurement

Analysis of polar phase extracts was performed on an HP5890 gas chromatograph with splitless injection of 1 µl at 230°C and 15°C/min GC temperature ramping from 85°C (2 min isocratic) to 360°C, using a 30 m MDN35 column (0.32 mm I.D., 0.25 µm film, Supelco), at a constant flow rate of 2 ml/min. The Pegasus II TOF (LECO, St. Joseph, MI, USA) mass spectrometer ion source operated at –70kV filament voltage with ion source and transfer line temperature set at 250°C. Data were acquired at a rate of 20 spectra per second in the mass range of m/z 85 to 500.

Complete extracts were automatically derivatized prior to GC-MS measurement with 10 µl of a 40 mg/ml solution of *O*-methylhydroxylamine in DMF for 180 min at 42°C with continuous shaking. Silylation reactions were started by adding 90 µl MSTFA and incubation for 30 min at 37°C. One microliter retention index marker mix was added to each sample prior to injection. Analysis of complete extracts was performed on an HP5890 gas chromatograph with splitless injection of 1.5 µl into a DTD-injector at 85°C. Injector temperature increased to 290°C with a rate of 4°C/s. GC temperature ramping extended from 85°C (210 s isocratic) to 360°C at a rate of 15°C/min, using the same 30 m MDN35 column (0.32°mm I.D., 0.25 µm film, Supelco) at a constant flow rate of 2 ml/min. Mass spectrometer settings were identical to polar phase extracts analysis.

2.5 Solvents and Chemicals

HPLC grade methanol and chloroform were supplied by Merck (Darmstadt, Germany). MSTFA was supplied by Macherey-Nagel (Düren, Germany). [U-^{13}C] sorbitol was purchased from Isotec (Miamisburg, OH, USA). All other chemicals, in the highest grade available, were supplied by Sigma-Aldrich (Taufkirchen, Germany).

2.6 Data Analysis

2.6.1 ChromaTOF data processing methods

Chromatographic files were processed with the ChromaTOF software (version 1.0, Pegasus driver 1.6). For baseline computation and peak finding the following settings were used: Baseline offset: 1.0; number of data points for smoothing: 10; Peak width continuously broadening from 2.5 (0 s) to 4.0 (1000 s); upper limit for peak finding: 9999. Peaks were reported above a S/N threshold of 20.0. Retention indices were calculated based on the retention indices of the 13 retention index markers (Table 1). Analyte spectra were searched against custom spectrum libraries and identified based on retention index and spectrum similarity match. Best library hits for all analytes were retrieved based on spectrum similarity match by searching the NIST spectrum library EINST_MSRI_136 which encompasses all other special purpose spectra libraries used in this study[149, 155]. Pooled sample

chromatograms were used to generate chromatogram references against which all sample chromatograms of the experiment were compared. Chromatogram references were checked for false positive library hit annotations. In addition, the reference chromatogram was searched manually for metabolites from core biochemical pathways which are represented in custom spectra libraries acquired by the measurement of genuine pure standard substances. Unique masses identified by the peak finding algorithm were generally used for peak area quantification. For all annotated peaks, quantification masses were checked to represent a genuine mass fragment of the analyte spectrum. Sample chromatograms peaks were matched to the reference within a retention index window of ±2000 RI units with a spectral similarity threshold of 700 and a S/N minimum of five. The result of the reference comparison of all sample chromatograms was further analyzed in Microsoft Office Excel 2003 and Matlab (version 6.5, release 13; Mathworks, Natick, USA).

2.6.2 **Preparative data analysis**

Metabolomic Analysis of S deprivation

Peaks of the reference peak list were analyzed with respect to matching consistency. Only analytes that were consistently found in at least one experimental class, i.e. samples corresponding to one combination of strain, experimental condition and time point, were retained in the dataset (only replicates with the largest aliquot volumes are considered). Analyte responses in each sample were normalized to internal standard. Each experimental class of each independent experiment was represented by at least two samples with different aliquot volumes (500 and 250 µl). Corresponding samples were used to calculate peak area aliquot ratios for each analyte (large aliquot divided by small aliquot). The distribution of the median aliquot ratios for each analyte was fitted to a non-parametric normal fit set to auto-bandwidth and positive domain. Only analytes with ten or more calculated aliquot ratio values were considered. The local minimum in the resulting bimodal normal fit was set as minimum threshold of the aliquot ratio mean for analytes to be retained in the dataset.

Analytes were considered true low values below detection limit, if the peak was missing from the class entirely, i.e. was never reported in any of the sample chromatograms derived from independent experiments and different aliquot volumes (type I missing value). For these missing values, zero was imputed. Missing values in sample chromatograms were regarded as missed due to failures of the automatic deconvolution and peak detection (type II missing value) whenever the analyte was reported at least once for the respective class. Missing values of the second type were imputed with the median of the normalized peak response in each class. The imputed data matrix was used for exploratory data analysis with multivariate methods. Visualization of the results was aided by the Mapman[201] Software (Version 1.8.1).

Analysis of macronutrient deficiency and of Arg auxotroph strains

For arginine auxotroph strains metabolite analysis was confined to intermediates of the Arg biosynthetic pathway and the TCA-cycle. Metabolites that were not yet represented as reference

spectra in custom mass spectral libraries were purchased as authentic standards whenever available, and reference mass spectra and retention information were acquired. Peaks of the target metabolites were checked in each sample chromatogram for correct assignment and peak area integration.

2.6.3 **Multivariate statistical analysis**

2.6.4 **Principal Component Analysis**

Principal component analysis was generally performed with standardized variables, i.e. transformation to unit variance and zero mean.

2.6.5 **Hierarchical Cluster Analysis**

Hierarchical cluster analysis was performed with analyte response profiles after averaging response values in each experimental class, normalizing to the mean response of the relevant control samples and $\log_2$-transform the normalized data.

	treatment			
control (+24)	-2 h	-5 h	-10 h	-24 h
1	0	1	1	1
1	1	0	1	1
0	1	0	1	1
1	1	1	0	1
0	1	1	0	1
1	0	0	1	1
1	0	1	0	1
0	0	1	0	1
1	0	1	1	0
1	1	0	0	1
0	1	0	0	1
1	1	0	1	0
0	1	0	1	0
1	0	0	0	1
1	0	0	1	0
1	0	1	0	0

Table 2: Excluded response profile patterns. Zero signifies response below LOD, one signifies a measured response. Times indicate duration of S deprivation.

With respect to zero values of analytes below the limit of detection, the following imputation scheme was used: Response of analytes below LOD in control samples was set to ⅛ of the minimum of all available measurements for this analyte prior to normalization and log-transformation. Any other class due to be normalized by the selected control and exhibiting analyte response below LOD is imputed with the same value. Log-transformation requires analyte responses >0 even if the control sample value exists. In these cases, the overall minimum value of all available log-transformed ratios minus three, equivalent to 2^{-3} with regard to log-transformation, was imputed for the normalized and log-transformed response to establish a uniform response value for analytes below the limit of detection. For the purpose of clustering, profiles of an analyte in individual strains were treated as separate

objects. To further decrease the presence of false negative observations in the data set, profiles which showed erratic behavior with respect to detection of the analyte were removed from the dataset (Table 2). In addition, only profiles which exhibited an absolute value <4 for the $\log_2$-transformed response of the 2h sulfur replete sample were retained in the dataset to focus on effects due to the imposition of sulfur deprivation, rather than effects due to handling of cell cultures. For the purpose of clustering, the correlation metric was used as proximity measure between individual analyte response profiles. To derive a hierarchical cluster structure, the Ward method was used. At each time point, for each analyte, a two-way t-test was conducted to assess the significance of the relative analyte abundance levels. Each t-test considered the unaveraged but normalized data for each analyte. The + and – patterns displayed in Table 7 depict the significance threshold at α=0.05.

methanol % v/v	35	40	45	50	55	60
freezing temperature °C	–28,0	–33,6	–43,0	–51,1	–56,4	–63,4

Table 3: Freezing temperatures of methanol-water solutions. Solutions were continuously stirred while being cooled at a rate of app. 1 K/min. The freezing temperature was determined as the temperature when first ice particle became visible.

methanol %v/v	quenching solution excess	T_{start}	T_{max}
35	4	–25,1	–11,9
	5	–25,0	–13,4
	6,5	–24,8	–15,6
	8	–25,0	–17,8
	10	–25,0	–18,8
40	4	–29,9	–13,7
	5	–31,9	–17,8
	6,5	–31,9	–20,9
	8	–31,8	–22,9
	10	–31,2	–24,2
45	4	–36,1	–17,7
	5	–36,2	–20,8
	6,5	–36,2	–23,3
	8	–36,2	–25,3
	10	–36,2	–27,4
50	4	–40,0	–19,2
	5	–40,1	–23,3
	6,5	–40,8	–26,4
	8	–40,8	–28,6
	10	–40,8	–30,9
55	4	–45,0	–20,0
	5	–45,3	–25,1
	6,5	–46,2	–29,7
	8	–46,6	–33,0
	10	–44,6	–35,8
60	4	–50,0	–24,6
	5	–50,0	–28,1
	6,5	–50,0	–31,6
	8	–50,0	–33,8
	10	–50,0	–36,1

Table 4: Temperature rise after quenching. A quenching solution excess of four signifies four parts quenching solution and one part cell suspension. T_{start} is the temperature in °C before addition of cell suspension, T_{max} is the maximum temperature in °C reached after cell suspension was injected.

3 Results

3.1 A Protocol for Metabolite Analysis in Cell Cultures

3.1.1 Overview

To obtain metabolomic data which correctly measure amount of substance and reflect the levels of intracellular metabolites a multi-step procedure was developed that conceptually can be divided into cell harvest and extraction, sample preparation for the acquisition of GC-TOF data, and processing of the analytical signal obtained.

Harvest and extraction essentially comprise the injection of the cell suspension into a quenching solution to stop enzymic reactions, recovery of the cells by centrifugation, homogenization of the material, and metabolite extraction. Extracts can be processed further by separating the crude extract into a lipophilic and a polar phase, depending on the GC-MS injection type used. Metabolites are concentrated and derivatized to increase compound volatility for separation of the complex mixture by gas chromatography. Once the samples have been measured by GC-TOF the raw data chromatograms are processed to find analyte peaks, compare individual samples and to identify analytes by mass spectral comparison with custom mass spectral libraries of pure standards. The initial peak lists are filtered for false negatives, artifact peaks and contaminants. Normalization to the amount of sample material and internal standards enables comparison and evaluation of the metabolic profiles.

3.1.2 Metabolite analysis in cell cultures needs rapid quenching of metabolism before extraction

Taking up an approach originally suggested for rapid sampling of yeast cultures[99] the cell suspensions are injected into an excess of cold solution of methanol-water prior to collecting the cells to stop metabolic activity. Methanol concentration and ratio of cell suspension to quenching solution were optimized to allow rapid cooling and handling of cells at temperatures below –20°C throughout the procedure. The minimum temperature a methanol-water solution can be cooled to depends on the methanol concentration (Table 3). To measure the actual temperature rise after addition of algal suspension culture, different amounts of cell suspension were added to quenching solutions with various methanol concentrations cooled to just above their freezing temperatures (Table 4). The set objective of keeping temperature below –20°C throughout harvest requires lower initial temperatures of the quenching solution and hence increased methanol concentration for higher proportions of cell suspensions to be quenched (Figure 2). In the effort to minimize the methanol concentration to ensure integrity of the cells after injection while maintaining the capability to harvest even large sample volumes methanol concentration was set to 40% v/v. This quenching solution was pre-chilled to –32°C and used at a ratio of 7:1 (quenching solution to cell suspension) to harvest cells as described in the material and methods.

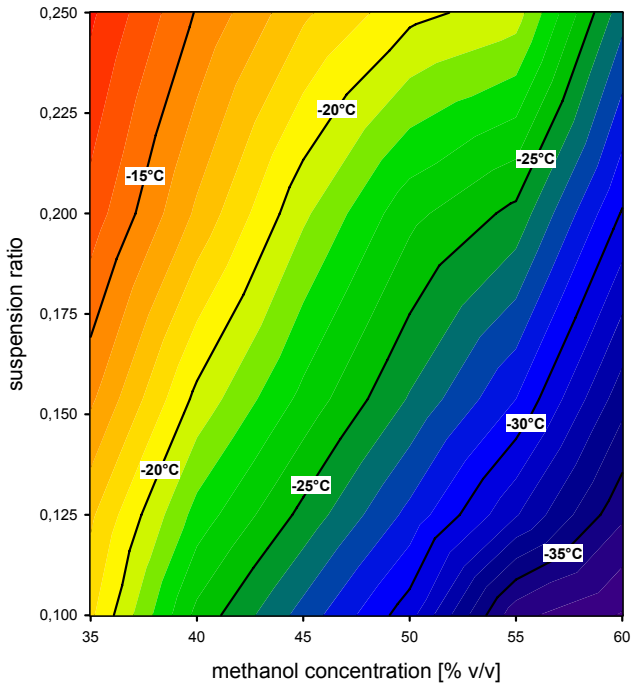

Figure 2: Maximum temperature of quenched cells as a function methanol concentration and ratio of cell suspension volume to quenching solution volume (suspension ratio).

3.1.3 Chlamydomonas cells are resistant to the quenching solvent

To demonstrate that the quenching procedure does not compromise the integrity of the cells to an extent where significant leakage of intracellular matter into the quenching solution occurs, cells of a late log-phase culture were cultivated in TAP-medium in the presence of labeled [U-^{14}C]-acetic acid as reduced carbon source. After three hours of cultivation with the labeled substrate, cells were harvested and the culture medium containing the labeled substrate carefully removed. After equilibration of the cells for 15 min in TAP medium without labeled acetate, cells were subjected to the quenching procedure. To account for leakage due to centrifugation itself, aliquots of the equilibrated cell suspensions were centrifuged and the supernatants treated in parallel with the samples containing whole suspension aliquots. Both the walled wild-type strain CC-125 and the wall-less strain CC-400 were tested in this way (Table 5).

After three hours of growth, 19.5% and 8.7% of the entire amount of radioactivity remains with the cells of strain CC-125 and CC-400 after removal of the growth medium, washing and equilibration in normal TAP medium, respectively.

Of the incorporated radioactivity, 1.9% is found in the supernatant of CC-125 cells after quenching and immediate sedimentation of cells. Incubation of the cells in quenching solution for 30 min at –25°C after prior to centrifugation increases this value to 2.4%. After centrifugation of the cell suspension and addition of the supernatant to the quenching solution, 1.3% of the activity can be found in the quenched sample.

For the wall-less strain CC-400, 4.8% of the incorporated activity are found in the supernatant of the quenched sample. This value increases to 6.2% when the sample is stored for 30 min at

–25°C prior to centrifugation. Addition of the supernatant of the centrifuged cell suspension to quench solution accounts for 2.0% of the activity.

To ensure that the detection limit of ^{14}C-scintillation would allow for spotting metabolite leakage exceeding 1% of the incorporated label, the amount of radioactivity added (20 kBq×ml^{-1} cell suspension) and the actual volume of cell suspension used for scintillation (125 µl) were chosen accordingly.

These results indicate that even after prolonged handling of cells during quenching, leakage of intracellular substances is below an acceptable level. For the walled strain CC-125 this is well below 2%, whereas with the cell wall deficient strain CC-400 leakage appears to be slightly higher. Still, also with CC-400 after 30 min suspension in methanol-water at –25°C less than 5% of the activity taken up by the cells is lost as a result of quenching, if the activity in the supernatant of the quenched sample is corrected by the activity found in the control accounting for leakage due to mechanical stress during harvest.

sample	CC-125 wt mt+		CC-400 cw15 mt+	
	Bq	%	Bq	%
cell suspension after 3h labeling	5051.6 ± 20.8		5558.2 ± 42.5	
cells after resuspension in unlabeled medium	984.1 ± 2.3	100.0	483.6 ± 1.5	100.0
quenched cells centrifugation after 3 min	18.6 ± 0.7	1.9	23.0 ± 1.8	4.8
quenched cells centrifugation after 30 min	24.0 ± 1.4	2.4	30.2 ± 0.8	6.2
controls for leakage due to harvest	12.8 ± 0.1	1.3	9.7 ± 0.2	2.0

Table 5: Resistance of *Chlamydomonas reinhardtii* suspended in quenching solution to leakage. Activities refer to one ml of cell suspension and for the quench samples to the corresponding volume of quench supernatant. The quenching was performed in triplicates. Mean and standard error for the measured activities are indicated, percentage values refer to means.

3.1.4 An extraction solution for Chlamydomonas samples

Cells are collected by centrifugation at –20°C. After careful removal of the supernatant, the cell pellet is flash frozen in liquid nitrogen, rendering it biologically inert. The material is resuspended and homogenized at –20°C in methanol-chloroform-water (MCW) for extraction.

Composition of the extraction mixture was optimized to maximize extraction capacity, measured as the capacity to quantitatively extract chlorophyll, and minimize the volume needed for extraction to concentrate extracted compounds (Figure 3). As a result, the original extraction formulation of 10:4:4 v/v/v MCW, which had been used for extraction of plant material[146], was changed to a composition of 10:3:1 v/v/v MCW. The reduced water content of the new formulation compensates for the interstitial liquid contained in the cell pellet that led to phase separation between a chloroform containing lipophilic phase and polar methanol-water phase already during resuspension of the homogenized material, prior to removal of particulate material from the preparation, when the original formulation was used for algal cells. Moderate reduction of the chloroform content to three volume parts enables

complete extraction of cell chlorophyll with only a quarter of extractant compared to the original extraction mix composition and performs equally well for chlorophyll extraction as the standard protocol using 80% v/v acetone (Figure 3). MCW volumes of 2-fold or more extract app. 2.7 µg chlorophyll per 10^6 cells and produce completely discolored cell pellets. Re-extraction of the pellets with MCW and acetone produced supernatants which contained 0.037 µg and 0.048 µg chlorophyll per 10^6 cells, respectively, indicating that residual chlorophyll content was less than 2% of total chlorophyll for the MCW-extracted samples. Under these conditions extraction of smaller polar compounds is surmised to be quantitative, as relative methanol-water content of the extraction mix is even higher than with the original formulation.

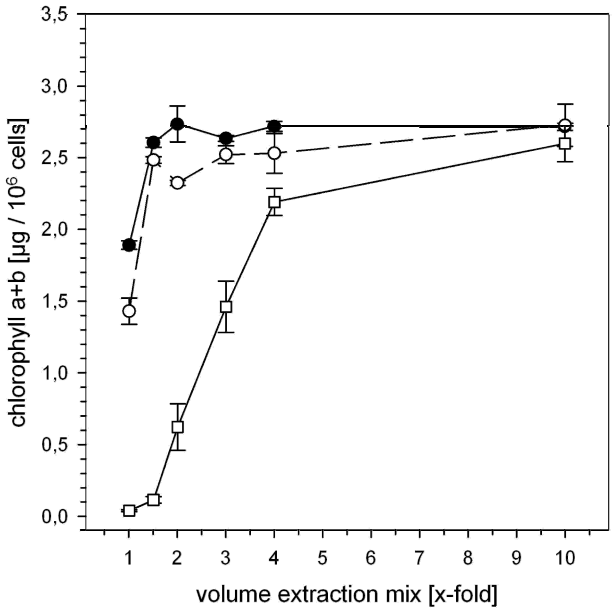

Figure 3: Extraction capacity of methanol-chloroform-water (MCW). Changing the ratio of MCW from 10:4:1 v/v/v (open squares) to a ratio of 10:3:1 (closed circles) increases extraction capacity 4-fold, as assessed by extraction of cell chlorophyll. In direct comparison with standard acetone extraction of chlorophyll (open circles), chlorophyll extraction with MCW 10:3:1 performs equally well. Extraction mix volume relates to the use of 3 ml of extraction mix for 1.2×10^9 cells. Standard errors of triplicate experiments are indicated.

3.2 Metabolite Profiling of *Chlamydomonas reinhardtii* under Nutrient Deprivation

3.2.1 Polar phase extracts contain numerous analytes and a variety of compound classes

Extracts were used to prepare polar phase samples and acquire GC-TOF data as described in material and methods. In chromatograms of *C. reinhardtii* polar phase metabolite extracts, more than 800 analytes were detected routinely (Figure 4). Among the most prominent peaks were found Ala, pyruvate, Glu, glycerolphosphate (GlyP), and AMP. Also, isotopically labeled sorbitol, which was introduced as an internal standard and a number of unidentified analytes produced prominent peaks. Originating from residual culture medium, TRIS (2-amino-2-(hydroxymethyl)-1,3-propanediol) and orthophosphate were observed with very high detector signal intensities. The former regularly

exceeded detector capacity impeding analysis of analytes co-eluting with the TRIS signal. Although reduction of TRIS peak size can be achieved by additional washes of the pelleted cells with quench solution (data not shown), this would require handling of cells for a prolonged period of time before rendering the material inert in liquid nitrogen and still yield chromatograms with a prominent TRIS peak.

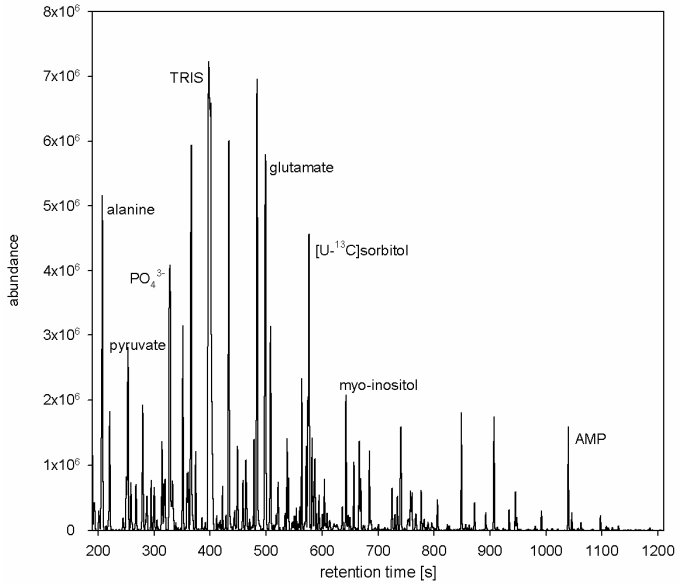

Figure 4: Analytical signal for *C. reinhardtii* polar phase extract after GC-TOF measurement. Total ion chromatogram (TIC) of wild type strain CC-125. In a retention time window from 180 s to 1200 s after sample injection, fragment ion intensities for all m/z in the mass range from 85 to 500 are recorded. The TIC is a composite signal of the sum of all m/z values in each recorded spectrum. Identity of prominent identified peaks is indicated.

GC-TOF chromatograms contain detector signal intensities for each m/z value in the chosen mass range for every spectrum acquired during the run. By mass spectral similarity and retention index comparison with custom libraries of authentic compounds, more than 100 of the detected peaks could be assigned a chemical structure, including amino acids, carbohydrates, phosphorylated intermediates, nucleotides and organic acids. The diverse chemical nature of the compounds identified underlines the usefulness of this technique to detect metabolites in a multi-parallel and unbiased manner.

3.2.2 Macronutrient and iron deficiency produce highly distinct metabolic phenotypes

To demonstrate the relevance of the method, it was analyzed how nutrient availability is reflected in metabolite profiles under conditions of nitrogen, sulfur, phosphorus and iron depletion, respectively. Table 6 shows metabolite peak area normalized to cell number and the internal standard [U-^{13}C] sorbitol for 77 abundant primary metabolites after 24 hours of nutrient starvation and for controls. A large number of metabolites undergo marked changes in at least one of the conditions applied. In iron deficient cells, the levels of succinate (SUC), threonic acid (THRa) and citrate (CIT) all rise more than twofold. While the rise in SUC is specific for Fe-depleted cells, CIT is elevated 4-fold also under P

Table 6: Levels, response ratios and PCA loadings of metabolites in Fe, N, S and P limited and TAP control conditions. Mean and standard error (n=5) of metabolite levels in arbitrary units are shown. Response ratios above 2.5 or below 0.4 are underlined. Loadings for principal components 1 and 2 are given in powers of 10^{-2}, i.e. 1,23 designates 0,0123. LOD indicates response below limit of detection. NA indicates not applicable.

metabolite	TAP	–Fe	–N	–S	–P	–Fe/ TAP	–N/ TAP	–S/ TAP	–P/ TAP	loading PC1	loading PC2
1,3-Dihydroxyaceton	0,48 ± 0,04	0,05 ± 0,003	0,097 ± 0,005	0,062 ± 0,006	0,17 ± 0,01	0,10	0,20	0,13	0,36	-8,93	7,67
2-Aminoadipate	0,026 ± 0,001	0,024 ± 0,002	0,248 ± 0,004	0,202 ± 0,005	0,045 ± 0,003	0,90	9,42	7,66	1,69	9,00	-2,00
2-Ketoglutaric acid	0,49 ± 0,02	1,11 ± 0,05	0,223 ± 0,005	0,136 ± 0,004	1 ± 0,4	2,28	0,46	0,28	2,03	-6,92	-4,71
2-Ketovaline	0,44 ± 0,03	0,65 ± 0,04	0,034 ± 0,006	0,008 ± 0,008	0,042 ± 0,006	1,47	0,08	0,02	0,10	-6,39	9,32
2-Phosphoglycolic acid	0,014 ± 0,002	0,009 ± 0,003	0,011 ± 0,002	0,0111 ± 0,0008	0,016 ± 0,002	0,61	0,79	0,79	1,14	-7,13	-3,18
3-Hydroxybutyric acid	2,72 ± 0,04	1,64 ± 0,04	0,077 ± 0,005	LOD	2,6 ± 0,1	0,60	0,03	NA	0,96	-12,69	-0,70
3-Hydroxypyridine	10,5 ± 0,8	11 ± 1	7,9 ± 0,4	11,9 ± 0,8	10,3 ± 0,9	1,08	0,76	1,14	0,98	-8,05	0,31
3-Isopropylmalic acid	5,3 ± 0,1	2,39 ± 0,04	LOD	LOD	2,53 ± 0,1	0,45	NA	NA	0,47	-11,72	6,74
4-Hydroxybenzoic Acid	0,103 ± 0,01	0,086 ± 0,01	0,053 ± 0,003	0,073 ± 0,008	0,104 ± 0,009	0,84	0,51	0,70	1,01	-11,23	0,30
4-Hydroxyproline	0,24 ± 0,01	0,202 ± 0,007	0,201 ± 0,005	12,6 ± 0,4	0,27 ± 0,03	0,84	0,84	52,27	1,11	9,10	1,79
5-Oxoproline	0,83 ± 0,05	0,64 ± 0,02	0,19 ± 0,03	0,315 ± 0,006	0,71 ± 0,02	0,77	0,23	0,38	0,85	-12,29	1,13
6-Phosphogluconic acid	0,8 ± 0,2	0,4 ± 0,1	0,047 ± 0,007	0,23 ± 0,05	0,15 ± 0,02	0,50	0,06	0,29	0,19	-7,41	11,02
Adenine	4,32 ± 0,07	1,8 ± 0,2	0,39 ± 0,01	0,57 ± 0,04	2,51 ± 0,07	0,43	0,09	0,13	0,58	-11,88	5,22
Alanine	9,9 ± 0,4	2,6 ± 0,09	0,61 ± 0,03	2,57 ± 0,06	6 ± 0,2	0,26	0,06	0,26	0,61	-11,13	4,04
Asparagine	4 ± 0,1	1,29 ± 0,06	0,73 ± 0,03	2,27 ± 0,1	3,1 ± 0,1	0,32	0,18	0,57	0,78	-10,59	2,27
Aspartic Acid	26,9 ± 0,4	11,4 ± 0,2	16,8 ± 0,3	50 ± 2	40 ± 2	0,42	0,63	1,85	1,49	-2,99	-8,65
Benzoic acid	0,99 ± 0,05	0,91 ± 0,03	0,72 ± 0,03	0,53 ± 0,03	1,05 ± 0,06	0,92	0,73	0,54	1,07	-11,12	-2,58
Citramalic acid	1,56 ± 0,05	0,74 ± 0,02	0,115 ± 0,003	0,077 ± 0,003	1,09 ± 0,07	0,47	0,07	0,05	0,70	-12,42	3,29
Citric Acid	21,6 ± 0,6	53 ± 1	12,19 ± 0,07	11,4 ± 0,1	88 ± 2	2,45	0,56	0,53	4,06	-8,10	-12,25
Citrulline	1,4 ± 0,3	1,4 ± 0,3	0,33 ± 0,03	2,4 ± 0,4	1,1 ± 0,2	0,97	0,23	1,74	0,76	-3,47	6,51
Cysteine	0,243 ± 0,006	0,13 ± 0,03	0,33 ± 0,04	0,06 ± 0,01	6,1 ± 0,4	0,54	1,35	0,25	25,13	-5,84	-14,85
Cystine	LOD	LOD	LOD	LOD	43 ± 2	NA	NA	NA	NA	-5,73	-14,96
D-Fructose-1,6-bisphosphate	0,064 ± 0,007	0,08 ± 0,03	0,043 ± 0,003	0,18 ± 0,05	0,23 ± 0,02	1,21	0,67	2,90	3,61	-3,18	-12,61
D-Fructose-6-phosphate	0,86 ± 0,07	0,92 ± 0,04	0,55 ± 0,02	1,2 ± 0,07	0,85 ± 0,05	1,07	0,64	1,40	0,99	-8,13	2,13
D-Glucose-6-phosphate	3,2 ± 0,3	3,9 ± 0,2	2,87 ± 0,03	10,2 ± 0,2	3 ± 0,2	1,21	0,89	3,17	0,95	8,30	3,72
Dihydroxyaceton phosphate	0,22 ± 0,01	0,13 ± 0,006	0,056 ± 0,003	0,13 ± 0,01	0,108 ± 0,003	0,58	0,25	0,59	0,48	-9,71	9,95
D-Ribose-5-phosphate	0,0145 ± 0,001	0,016 ± 0,002	0,014 ± 0,002	0,025 ± 0,003	0,025 ± 0,002	1,13	0,99	1,72	1,70	-4,23	-10,32
Fructose	0,58 ± 0,07	0,13 ± 0,02	LOD	0,15 ± 0,02	0,46 ± 0,09	0,22	NA	0,27	0,79	-10,31	1,16
Fumaric acid	13,2 ± 0,2	6,1 ± 0,1	2,07 ± 0,05	0,58 ± 0,07	7,6 ± 0,2	0,46	0,16	0,04	0,57	-12,11	5,26

metabolite	TAP	–Fe	–N	–S	–P	–Fe/ TAP	–N/ TAP	–S/ TAP	–P/ TAP	loading PC1	loading PC2
Galactinol	0,94 ± 0,05	0,45 ± 0,03	0,87 ± 0,03	2,1 ± 0,2	0,85 ± 0,05	0,47	0,92	2,22	0,90	5,89	0,86
Galactonic acid	0,144 ± 0,006	0,186 ± 0,007	0,0155 ± 0,0008	0,024 ± 0,003	0,165 ± 0,008	1,29	0,11	0,17	1,15	-11,27	-1,01
Glucose-1-phosphate	7,7 ± 0,4	8,3 ± 0,3	4,7 ± 0,2	6,9 ± 0,5	5,8 ± 0,3	1,07	0,61	0,89	0,75	-9,25	7,18
Glutamic acid	10,2 ± 0,2	8,5 ± 0,2	1,8 ± 0,06	3,3 ± 0,1	8,4 ± 0,2	0,83	0,18	0,32	0,83	-12,30	2,05
Glutamine	40 ± 2	28 ± 1	4,1 ± 0,1	21,8 ± 0,9	47 ± 2	0,70	0,10	0,55	1,18	-11,75	-2,61
Glyceraldehyde-3-phosphate	0,101 ± 0,002	0,123 ± 0,004	0,1 ± 0,01	0,05 ± 0,003	0,21 ± 0,01	1,22	0,98	0,50	2,05	-8,29	-11,32
Glycerate-3-Phosphate	2,07 ± 0,09	5,7 ± 0,3	3,3 ± 0,1	7,7 ± 0,2	4,8 ± 0,1	2,73	1,61	3,74	2,31	3,58	-9,31
Glyceric acid	1,51 ± 0,03	0,84 ± 0,03	0,88 ± 0,04	2,27 ± 0,06	6,4 ± 0,2	0,55	0,58	1,51	4,24	-6,02	-14,02
Glycerol	26 ± 3	20 ± 2	20 ± 2	160 ± 30	18 ± 2	0,78	0,77	6,23	0,70	8,09	3,13
Glycine	5,1 ± 0,3	2,33 ± 0,1	1,79 ± 0,08	2,97 ± 0,1	4,28 ± 0,08	0,46	0,35	0,58	0,84	-11,42	1,04
Glycolic acid	0,9 ± 0,03	0,64 ± 0,01	0,4 ± 0,02	0,83 ± 0,06	1,3 ± 0,08	0,71	0,44	0,92	1,44	-10,08	-8,37
Histidine	8 ± 1	1,7 ± 0,6	4 ± 1	1,4 ± 0,5	3,2 ± 0,5	0,21	0,55	0,17	0,40	-5,46	5,29
Hydroxylamine	8 ± 2	8,9 ± 0,9	10,4 ± 0,7	10 ± 1	8,2 ± 0,7	1,18	1,39	1,31	1,10	-0,35	-1,61
Iminodiacetic acid	0,6 ± 0,01	0,168 ± 0,007	0,329 ± 0,005	0,427 ± 0,008	1,71 ± 0,09	0,28	0,55	0,71	2,86	-7,27	-12,56
Inositol-beta-galactoside	24,1 ± 0,8	8,6 ± 0,1	2,44 ± 0,06	3,62 ± 0,08	8,8 ± 0,4	0,36	0,10	0,15	0,37	-10,47	9,23
Isoleucine	19,1 ± 0,4	9,7 ± 0,2	48 ± 2	82 ± 3	17,1 ± 0,8	0,51	2,50	4,28	0,90	10,83	0,25
Leucine	1,53 ± 0,02	0,54 ± 0,01	0,91 ± 0,03	1,65 ± 0,06	0,63 ± 0,02	0,35	0,59	1,08	0,41	-1,57	12,20
Lysine	10,6 ± 0,2	8,8 ± 0,2	4,45 ± 0,08	5,4 ± 0,1	10,7 ± 0,6	0,83	0,42	0,51	1,00	-12,69	-1,48
Malic Acid	8,32 ± 0,09	8,9 ± 0,1	2,14 ± 0,05	0,62 ± 0,02	8,9 ± 0,2	1,07	0,26	0,07	1,07	-12,05	-1,58
Maltose	0,51 ± 0,05	0,26 ± 0,02	0,32 ± 0,03	0,37 ± 0,01	1,4 ± 0,08	0,51	0,62	0,72	2,73	-7,53	-12,49
Methionine	0,67 ± 0,02	0,61 ± 0,06	0,123 ± 0,007	LOD	1,4 ± 0,2	0,91	0,18	NA	2,09	-10,17	-8,73
myo-Inositol	19,6 ± 0,6	6,2 ± 0,2	2,49 ± 0,06	2,53 ± 0,04	23,4 ± 0,4	0,32	0,13	0,13	1,19	-11,59	-3,99
Myristic acid	0,47 ± 0,08	0,51 ± 0,06	0,39 ± 0,03	0,55 ± 0,05	0,5 ± 0,05	1,10	0,84	1,18	1,07	-7,31	1,31
N-acetyl-galactosamine	0,041 ± 0,003	0,035 ± 0,003	0,024 ± 0,002	0,024 ± 0,004	0,077 ± 0,006	0,86	0,59	0,60	1,89	-9,42	-10,81
N-acetyl-L-Glutamic Acid	3,4 ± 0,2	1,4 ± 0,2	0,34 ± 0,01	0,4 ± 0,1	0,6 ± 0,05	0,40	0,10	0,13	0,18	-8,88	11,41
N-acetyl-Ornithine	0,48 ± 0,05	0,43 ± 0,03	LOD	0,24 ± 0,02	0,125 ± 0,009	0,90	NA	0,50	0,26	-7,82	11,62
Nicotinamide	5,1 ± 0,3	2,4 ± 0,4	0,85 ± 0,08	1 ± 0,2	2,3 ± 0,3	0,48	0,17	0,20	0,46	-10,65	7,29
Ornithine	11,5 ± 0,5	10,2 ± 0,2	0,7 ± 0,1	1,8 ± 0,1	9 ± 0,5	0,88	0,06	0,15	0,78	-12,03	2,51
Oxalic acid	6,1 ± 0,6	5,9 ± 0,7	5,7 ± 0,3	7,4 ± 1	6,7 ± 0,5	0,97	0,94	1,21	1,09	-5,43	-4,60
Phenylalanine	13,4 ± 0,2	5 ± 0,1	5,9 ± 0,1	20,1 ± 0,7	5,2 ± 0,2	0,37	0,44	1,50	0,39	0,77	12,09
Phosphoenolpyruvic Acid	1,48 ± 0,04	0,95 ± 0,05	0,279 ± 0,005	0,42 ± 0,01	0,39 ± 0,02	0,65	0,19	0,29	0,26	-9,11	12,17
Prephenic Acid	0,034 ± 0,003	0,078 ± 0,002	0,032 ± 0,001	LOD	0,04 ± 0,01	2,27	0,94	NA	1,16	-6,16	-0,56
Proline	86 ± 4	61 ± 4	29,5 ± 0,6	180 ± 10	35 ± 3	0,71	0,34	2,06	0,41	3,37	10,29

metabolite	TAP	–Fe	–N	–S	–P	–Fe/ TAP	–N/ TAP	–S/ TAP	–P/ TAP	loading PC1	loading PC2
Putrescine	18,7 ± 0,5	13,2 ± 0,4	1,78 ± 0,05	0,129 ± 0,008	5,5 ± 0,3	0,71	0,09	0,01	0,29	-10,27	9,86
Pyruvic Acid	4,1 ± 0,3	2,9 ± 0,3	1,05 ± 0,06	0,53 ± 0,02	1,28 ± 0,08	0,70	0,25	0,13	0,31	-9,49	10,47
Ribose	0,46 ± 0,03	0,32 ± 0,03	1,1 ± 0,1	1,8 ± 0,09	2,2 ± 0,2	0,68	2,36	3,89	4,85	-0,43	-15,10
Sedoheptulose 1,7-bisphosphate	LOD	LOD	LOD	0,033 ± 0,006	0,015 ± 0,003	NA	NA	NA	NA	3,82	-8,53
Serine	2 ± 0,03	0,71 ± 0,02	0,277 ± 0,007	3,28 ± 0,07	1,71 ± 0,06	0,35	0,14	1,64	0,85	-3,44	1,82
Shikimic acid	94,9 ± 1	37,9 ± 0,6	LOD	LOD	LOD	0,40	NA	NA	NA	-8,29	13,35
sn-Glycerol 3-phosphate	2,2 ± 0,2	0,8 ± 0,1	0,79 ± 0,07	7 ± 0,5	1,1 ± 0,2	0,37	0,36	3,25	0,49	5,88	5,48
Succinic Acid	2,97 ± 0,09	7,4 ± 0,1	2,41 ± 0,06	2,72 ± 0,06	2,84 ± 0,05	2,48	0,81	0,92	0,96	-4,26	2,44
Threonic acid	1,42 ± 0,04	3,5 ± 0,1	0,56 ± 0,01	3,3 ± 0,1	12,8 ± 0,5	2,47	0,39	2,33	9,04	-6,10	-14,52
Threonine	7,3 ± 0,3	5,5 ± 0,3	17,9 ± 0,7	21,7 ± 0,5	11,5 ± 0,9	0,75	2,46	2,99	1,58	7,80	-6,09
Trehalose	0,15 ± 0,01	0,093 ± 0,003	0,036 ± 0,002	0,051 ± 0,003	0,043 ± 0,003	0,63	0,24	0,35	0,29	-8,83	12,32
Tryptophane	0,6 ± 0,1	0,33 ± 0,07	2,9 ± 0,7	1,2 ± 0,3	0,43 ± 0,07	0,55	4,95	2,11	0,73	5,62	-1,10
Tyrosine	8,1 ± 0,2	4,16 ± 0,05	9 ± 0,1	36,5 ± 0,5	5,8 ± 0,2	0,51	1,11	4,51	0,71	9,78	3,18
Uracil	6,86 ± 0,09	1,3 ± 0,1	0,68 ± 0,07	1,4 ± 0,4	1,44 ± 0,06	0,19	0,10	0,20	0,21	-8,56	11,09
Valine	9,3 ± 0,1	3,9 ± 0,1	3,1 ± 0,1	11,6 ± 0,4	4,6 ± 0,3	0,42	0,33	1,25	0,50	-3,54	10,73

deprivation and THRa levels increase 2-fold and 9-fold in S- and P-deprived cells, respectively. THRa, but not CIT, is significantly decreased in N-deprived cultures. Fe deficiency leads to an almost 3-fold rise in 3-phosphoglycerate (3PGA). 3PGA levels are elevated also in the other nutrient stress conditions although less pronounced in N-stressed cells. Prephenate, which is an intermediate in the biosynthetic pathway for Phe and Tyr is increased more than 2-fold under Fe deficiency, appears unchanged in N and P deprived cells and could not be detected under S deficiency. Interestingly, shikimate, which is an important intermediate for the synthesis of both Trp and the other two aromatic amino acids Phe and Tyr, is reduced under Fe deficiency and could not be detected at all in the other stress conditions. Levels of these three aromatic amino acids dropped to half or less of the control level. A number of other compounds is reduced too, among them the amino acids Ala, Asn, His, Leu and Ser. Other noteworthy reductions include fructose, myo-inositol (MI) and inositol-β-galactoside (IbGAL). Fructose levels are below LOD in N-deprived cultures and are similarly reduced under S-deficiency. MI is markedly reduced as well in N- and S-deficient conditions, while IbGAL is always significantly reduced in comparison to control. On the contrary, sedoheptulose 1,7-bisphosphate (S17P) could be detected only in S- and P-deficient samples. The pattern of the response of the amino acids after nutrient deprivation appears to be highly characteristic for each nutrient limitation. Phe is reduced under Fe-, N-, and P-deficiency but slightly elevated in S-deficient conditions. Tyr is slightly decreased also in P-deficiency, at control level in N-deficiency and markedly increased in S-deficiency. Trp, however, is markedly increased in N-deficient cells, slightly increased in S-deficiency and slightly reduced in –P-cells. Specific patterns are observed also for many other amino acids, including the uniform rise in Thr except in Fe-deficient conditions, and the marked increase of Ile in N- and S-deficiency. Ala and Lys exhibit strong reductions in N- and S-deficient conditions but only slight reductions in P-deficient cells. Interestingly, 2-aminoadipate, which is implicated in lysine biosynthesis and catabolism, is, on the contrary, strongly accumulated under N- and S-deficiency, with only a slight increase in P-deficient cells. A number of metabolites implicated in nitrogen assimilation and downstream pathways like arginine biosynthesis exhibit marked decreases in N-deficient cells, such as Glu, Gln, Asn, *N*-Acetylglutamate (NAG), N^2-Acetylornithine (NAO), citrulline and ornithine (Orn). While a strong decrease of Gln and Asn is observed specifically in N-deprived cells, others exhibit marked reductions also in other stress conditions: Glu in S-deficiency, NAG in both S- and P-deficiency, NAO in P-deficiency and Orn in S-deficiency. Sulfur depleted cells exhibited the largest increase of any single compound: Here, 4-hydroxyproline (Hyp) accumulated more than 50-fold compared to control conditions while undergoing only slight changes with the other treatments. Sulfur-containing amino acids exhibited lower levels: Cys pools were lowered to 25% while Met decreased below the limit of detection in S-depleted cells. Met levels were reduced also in N-deplete conditions. Under P-deficiency, however, accumulation of Met (2-fold) and Cys (25-fold) is observed. In addition, cystine could be detected only in P-deficient cells. A number of phosphorylated intermediates such as 3PGA, GlyP, G6P and fructose-1,6-bisphosphate (FBP) increased more than

threefold under sulfur-depleted conditions. Decreases for a number of organic acids like malic, citramalic, 3-isopropylmalic, 3-hydroxybutyric, galactonic and fumaric acid occurred similarly in N- and S-deplete conditions. A number of important primary metabolites appeared to be similarly affected by N- P- and S- deficiency. This includes marked reductions in 2OG, 6-phosphogluconate (6PG), PEP and pyruvate. Similarly, adenine and uracil exhibited reductions in all nutrient stress situations, suggesting depletion of intermediates also in nucleotide metabolism. Taken together, many important primary metabolic modules are affected in each of the macronutrient stress condition, but for sulfur stress, specifically carbohydrate metabolism seemed to be more dramatically affected, providing evidence for the hypothesis that a plethora of metabolic responses would result from nutrient depletion. While the response of N- and S-depleted cells share a certain extent of similarity regarding the decrease or increase of individual metabolites, the overall pattern of the metabolite changes appear to be highly specific in response to diminishing supply of each nutrient.

A data matrix of 170 metabolites including both known compounds and unidentified analyte peaks was manually inspected for false negatives and subsequently used for PCA. Projection of the resulting sample scores for the first and second principal component which together account for 54% of the total sample variance clearly separated the five experimental groups (Figure 5), indicating a high suitability of metabolic readouts to study environmental effects in Chlamydomonas.

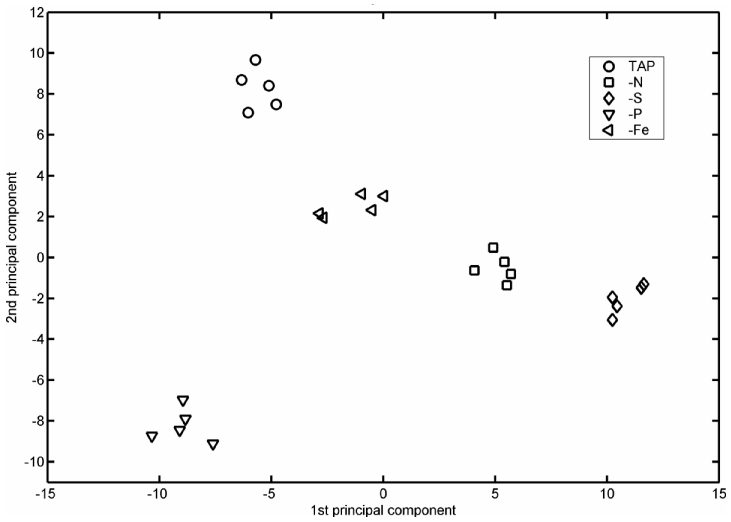

Figure 5: Sample scores for the first and second principal component extracted from the normalized peak response data of the five experimental groups. Each group is represented by five samples. The first and second principal component account for 35.2% and 19.1% of the total sample variance, respectively.

It was apparent that the replicate analysis of samples of each individual treatment gave very similar profiles, which validates high reproducibility of the experimental procedure from cell harvest to data analysis. Distances between the groups of samples give a measure of the overall difference between the metabolite profiles of different treatments. The contribution of individual metabolites to the differences observed is quantified via the loading of the metabolite for the respective principal component. Among the group of metabolites with high absolute loading values for the first principal

component are G6P, Tyr, Trp (high positive loadings), glyceraldehyde-3-phosphate (GAP) and Lys (small negative loadings). A high positive loading value usually indicates abundance of these metabolites in samples with high score value for the corresponding principal component, whereas for small negative loadings metabolite levels and score value are inversely correlated. This is confirmed for Tyr (PC1 loading = 0.098) with pool ratios increasing from 0.51 (–Fe) to 1.11 (–N) and 4.51 (–S) and GAP (PC1 loading = –0.0829) with pool ratios decreasing from 1.22 (–Fe) to 0.98 (–N) and 0.50 (–S). TAP cultured cells and –P cells, which are not very well discriminated by the first PC, nevertheless can be clearly separated using the linear combination of metabolite responses that constitutes the second principal component. Here, PEP and shikimate have among the highest positive loadings, whereas NAO and maltotriose have very small negative loadings. Interestingly, score values for the first and second principal components for the –Fe, –N and –S samples correlate. This suggests that the first two principal components, rather than explaining specific effects of adaptation to Fe, N or S deprivation, measure parameters of the general response to nutrient deficiency with common effects in all three treatments with the most severe impact observed under sulfur depleted conditions. P deprivation, however, is transduced mainly as difference in score value for principal component two, suggesting that adjustment to P deficiency may share the general response developing in the other nutrient stress situations during 24 h treatment only to a limited extent. This notion is supported by the varying growth rates (controls: 1.6 doublings per day, –Fe: 1.6, –N: 0.7, –S: 0.7 and –P: 1.3) during the 24 h period of treatment.

3.3 Metabolomic Analysis of Adaptation to Sulfur Deficiency

To gain insight into the adaptation of *Chlamydomonas reinhardtii* during sulfur deprivation both the *sac1* mutant and its parental wild-type strain CC-1690 were analyzed. Cells were harvested, extracted and the extracts measured as described under material and methods. Metabolites were extracted from sulfur deprived cells harvested at four different times (2, 5, 10 and 24 h). Cells were grown in standard TAP cultures and harvested after two and 24 hours served as controls.

3.3.1 One in ten analyte peaks can be positively identified

As a result of the chromatogram reference processing, library hit annotation and further manual search for spectra of 214 metabolites from core biochemical pathways 90 of the 839 analytes in the reference peak list could be established as derivates of known chemical compounds and hence classified as “Knowns”. A total of 108 chromatograms were analyzed and compared to the chromatogram reference. Of the 839 analytes in the reference peak list 305 were found to have missing values in each class. These inconsistently found analytes were removed from the dataset. The remaining 534 analytes, including 83 of the 90 Knowns, were subject of a detailed data analysis.

3.3.2 Aliquot ratio analysis systematically reduces the number of artifactual peaks

In GC-TOF analysis numerous artifact peaks are observed which do not relate to compounds extracted from the biological matrix. For metabolites genuinely extracted from a biological matrix, the necessary condition can be set that their response must be directly proportional to the amount of substance, provided that the response is measured in the analyte's linear range of detection. In order to eliminate undesired peaks the concept of aliquot ratios is introduced here and used to systematically remove peaks from the dataset for which peak area response is not proportional to the amount of biological material extracted. Aliquot ratios are computed as ratio of the normalized analyte response (normalized to response of internal standard) in replicates of the same extract with different aliquot volumes. As a consequence of the sample preparation protocol, the amount of internal standard is directly proportional to volume of extract which in turn is directly proportional to the number of cells harvested. Thus, extracted metabolites detected within their linear range of detection should have an aliquot ratio of one. Deviations of the aliquot ratio from one point to violations of the condition pointed out above. For compounds unrelated to the biological matrix, the aliquot ratio is expected to equal the inverse of the aliquot volume ratio. The sulfur deficiency experiments used aliquot volumes of 500µl and 250µl, respectively. Indeed are the expected aliquot ratios (one and ½) observed as maxima of the distribution of the aliquot ratios of all analytes (Figure 6).

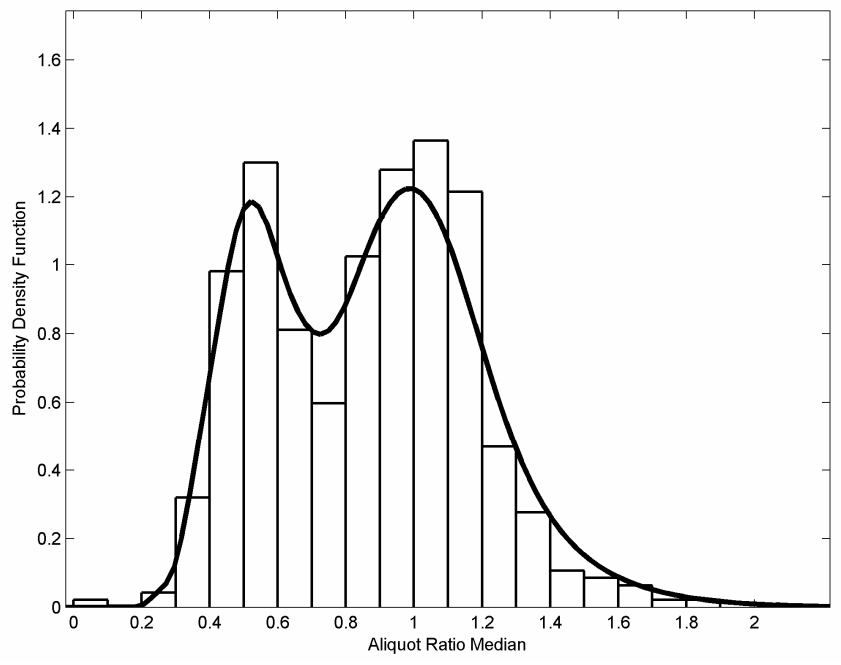

Figure 6: Distribution of aliquot ratio median values. Only analytes with at least ten aliquot ratio values were considered.

The normalized peak areas were subjected to an aliquot ratio analysis. The distribution of the medians of the aliquot ratios of each analyte identified a local minimum in the bimodal non-parametric fit at 0.725 (Figure 6). Accordingly, only analytes were retained which had an aliquot ratio median larger

Table 7: Response of identified metabolites represented in the final dataset during sulfur deprivation[a]

Metabolite[a]	Profile dissimilarity[b]	Response profile assignment[c]		Direction of change in analyte level[d]		Analyte level[e] (log2 ratio) for									
						CC-1690					*sac1*				
		CC-1690	*sac1*	CC-1690	*sac1*	+2h	-2h	-5h	-10h	-24 h	+2h	-2h	-5h	-10h	-24 h
2-Isopropylmalic acid	6,82	A2	A4	– – – – –	– – – – –	-0,90	-3,13	LOD	LOD	LOD	-0,70	-2,66	-3,94	LOD	LOD
2-Ketoglutaric acid	3,47	D12	00	. – – – +	– + – + –	-0,06	-0,43	-0,67	-2,43	0,55	-4,63	0,67	-0,09	1,05	-0,54
4-Hydroxyproline	1,76	C20	C10	– + . . .	+ + + . –	-0,37	1,49	1,07	0,44	0,43	0,42	1,08	0,34	0,13	-1,33
Adenine	1,60	A3	A1	. . . . –	– – – – –	-0,45	-0,55	-0,47	-0,55	-1,52	-0,04	-1,37	-2,07	-1,90	-2,77
Alanine	1,92	A1	A3	– – – – –	– – – – –	-0,35	-3,74	-3,61	-4,11	-5,22	-0,27	-2,34	-3,53	-2,20	-6,80
Aspartic acid	0,52	B11	B13	– – – – –	+ – – – –	-0,36	-1,70	-1,62	-1,44	-0,68	0,26	-2,12	-1,79	-0,92	-0,82
Citric Acid	2,49	A2	C17	. . – – –	. . . . .	0,08	-1,04	-2,05	-1,86	-1,65	0,44	0,14	0,42	0,63	-0,04
Cysteine	1,37	A1	A3	. . – – –	. – – – –	-0,48	-0,49	-0,87	-0,97	-1,42	-0,13	-1,33	-1,06	-1,22	-2,79
D-Fructose-6-phosphate	0,98	E18	A1	–	– . . . –	-1,34	0,12	-0,11	-0,87	-0,03	-0,70	-0,65	-0,56	-0,73	-1,01
D-Gluconic acid	9,47	00	00	. – + – –	– . – – –	0,08	-0,82	0,64	LOD	-2,22	-4,63	0,11	-1,71	-1,29	-1,60
D-Glucose	2,33	E18	E15	– . + – .	+	-0,41	-0,31	2,38	-0,80	0,26	0,10	-0,17	0,05	0,26	-0,57
D-Glucose-1-phosphate	0,63	A2	A3	. . – – –	– . – . –	-0,14	-0,07	-0,54	-0,61	-0,29	-0,14	-0,16	-0,49	-0,42	-0,91
D-Glucose-6-phosphate	1,49	D7	A2	. + . + +	–	0,03	0,58	0,19	0,24	1,25	-0,13	-0,26	-0,30	-0,46	-0,24
D-Phosphoglyceric acid	4,49	B5	C17	. . – – .	– . . + .	1,23	0,55	-1,29	-0,67	1,40	-0,24	1,41	3,19	2,46	-1,00
Fumaric acid	0,71	A2	A2	– – – – –	. . . . .	-0,33	-0,97	-1,56	-1,62	-1,61	0,12	-0,27	-1,25	-0,94	-0,94
Galactonic acid γ-lactone	9,67	A3	C10	+ – + . –	. + . + –	0,33	-0,41	0,35	0,13	LOD	0,79	0,58	0,21	0,48	-1,10
Glutamic acid	1,75	A2	E15	– – – – –	– – – . –	-0,34	-1,63	-2,41	-2,42	-2,08	-0,11	-0,98	-1,43	-0,67	-1,99
Glutamine	0,84	A1	A3	. – – – –	– – – – –	-0,23	-2,16	-2,99	-3,42	-3,79	-0,07	-2,05	-2,22	-2,58	-4,60
Glycerol	0,85	B11	A6	– – . . .	– – – . .	-0,74	-0,55	-0,19	-0,38	-0,11	-0,24	-1,04	-0,98	-0,37	-0,96
Glycerolphosphate	1,47	A2	A1	. . – – .	– – – – –	-0,17	-0,24	-0,40	-0,55	-0,29	-0,56	-0,66	-1,37	-0,98	-1,76
Glycerolphosphate	0,99	A3	A1	. . – – –	– – – – –	0,19	0,01	-0,48	-0,55	-1,08	-0,47	-0,48	-1,23	-1,13	-2,08
Heptadecanoic acid	1,24	B5	E18	. . . . .	. . . – .	-0,32	-0,50	-0,78	-0,50	0,51	0,95	0,74	0,19	-1,12	0,22
Hydroxybutanoic acid	1,93	A3	A3	– – – – –	– . – – –	-0,56	-0,69	-2,39	-3,86	LOD	-0,76	0,32	-1,23	-1,92	LOD
Inositol-1-phosphate	1,50	C8	A1	. . . . .	– . – – –	0,05	0,40	-0,54	0,01	-0,45	-0,48	-0,48	-1,49	-0,93	-1,95
Inositol-β-galactoside	4,60	D9	A3	+ + + + +	. . . . .	1,94	2,29	2,37	1,69	1,48	0,91	-0,13	0,22	-0,39	-3,11
Isoleucine	0,92	B5	B16	– – – – +	– – – . +	-0,47	-1,08	-1,38	-0,97	0,64	-0,35	-0,94	-1,06	-0,05	0,52
Leucine	0,83	D7	C19	. + . + +	– . . + +	0,09	0,40	0,38	0,56	1,61	-0,20	0,20	0,23	1,39	0,78
Lysine	9,03	A3	A3	– . . . –	+ – . . –	-0,87	-0,05	0,03	0,41	-1,73	0,09	-0,95	-0,34	-0,13	LOD

Metabolite[a]	Profile dissimilarity[b]	Response profile assignment[c]		Direction of change in analyte level[d]		Analyte level[e] (log2 ratio) for									
						CC-1690					*sac1*				
		CC-1690	*sac1*	CC-1690	*sac1*	+2h	-2h	-5h	-10h	-24 h	+2h	-2h	-5h	-10h	-24 h
Malic Acid	1,15	A4	A1	. – – – –	+ . – – –	-0,01	-0,93	-1,85	-2,42	-2,21	0,04	-0,51	-1,17	-1,27	-1,68
Maltose	1,45	D7	A6	– . . . +	– – – . –	-0,68	-0,22	0,14	0,09	0,46	-0,57	-0,93	-0,81	-0,40	-0,99
Mannose	2,83	E18	C17	. . + – .	. . . + .	0,28	0,17	0,97	-0,94	0,49	0,75	0,88	0,72	1,89	0,56
myo-Inositol	1,19	B11	A2	– – – – .	– – – – –	-0,23	-0,58	-0,41	-0,59	0,03	-0,16	-0,60	-1,16	-0,77	-1,17
Myristic Acid	1,79	D12	A4	. . . . .	+ . . – .	0,80	0,07	-0,11	-0,33	1,04	0,34	0,64	-0,29	-0,91	-0,75
Nicotinamide	0,78	A2	00	. – – – –	– – – – –	-0,11	-0,88	-1,74	-1,76	-1,67	-4,63	-0,38	-1,16	-1,41	-2,45
Oxoproline	0,59	A2	A1	– – – – –	– – – – –	-0,41	-0,96	-1,38	-1,41	-1,19	-0,09	-0,97	-1,33	-0,81	-1,64
Palmitic acid	1,45	D12	A2	. . . . .	– – – – –	-0,01	-0,11	-0,26	-0,14	0,41	-0,32	-0,62	-1,16	-1,15	-1,03
Palmitoleic acid	1,85	B5	A1	. . . . .	– – – – –	-0,03	-0,29	-0,40	-0,22	0,14	-0,25	-1,21	-1,31	-1,41	-1,71
Phenylalanine	0,80	B5	B5	– – – – .	– – – – –	-0,60	-1,68	-1,84	-1,38	-0,05	-0,60	-1,83	-2,26	-1,24	-0,85
Phosphate	0,91	A4	A3	+ . – – –	– . . . –	0,38	0,08	-0,41	-0,47	-0,61	-0,26	-0,10	-0,85	-0,64	-1,52
Proline	2,32	C20	C10	– + + – –	– + + + –	-0,63	2,14	1,17	-0,50	-0,96	-0,76	2,86	2,60	1,82	-1,97
Putrescine	3,31	A4	E14	. . – – –	. . . . –	-0,88	0,10	-1,61	-2,46	-4,21	0,40	-3,20	-2,04	-2,39	-4,75
Pyruvic Acid	8,64	00	A4	. – – – .	– + . – –	-0,49	-2,27	-1,25	LOD	-0,61	-1,06	0,60	-0,22	-2,12	-1,15
Serine	1,03	C8	C10	– . – – –	– + . . –	-0,23	0,33	-0,71	-0,80	-1,00	-0,26	1,34	-0,11	0,14	-2,03
Serine	1,84	A3	C8	. . . – –	– . – – –	0,61	0,04	0,40	-0,75	-1,20	-0,77	1,00	-1,44	-0,68	-2,21
Shikimic Acid	3,00	A2	A6	– – – – –	– – – – –	-1,38	-7,76	LOD	LOD	LOD	-0,87	LOD	LOD	LOD	LOD
Threonic acid	1,25	A2	A2	. . – – .	– . – – –	-0,09	-0,66	-0,94	-1,18	-0,67	-0,86	-0,67	-1,86	-1,92	-1,92
Threonine	0,94	B5	B13	– – – – +	– – – – –	-0,66	-1,21	-1,43	-1,11	0,21	-0,23	-1,01	-1,44	-0,43	-0,73
Thymine	1,46	A2	A2	– – – – –	– . – . –	-0,76	-1,23	-1,70	-2,02	-1,76	-0,17	-0,63	-1,26	-0,56	-1,03
trans-Squalene	1,26	B5	A2	– – – – –	– – – – –	-1,34	-1,56	-2,90	-2,84	-0,72	-0,08	-0,31	-3,22	-3,20	-1,56
Tyrosine	0,91	B5	B5	. – – – .	– – – – –	-0,09	-1,22	-1,62	-1,42	0,27	-0,43	-1,45	-1,78	-1,16	-0,63
Valine	1,36	B11	B13	– – – – –	– – – – –	-0,75	-1,45	-1,79	-1,60	-0,56	-0,29	-1,05	-1,03	-0,23	-0,70

[a] Metabolite represented by the respective analyte derivate.
[b] The dissimilarity between the analyte profile recorded for the mutant and the parental strain measured by the Chebychev metric, i.e. the maximum absolute difference at any time point.
[c] Indicates the assignment of the individual profiles to the pattern groups and clusters. 00 indicates that the profile was not used for HCA.
[d] Difference in analyte abundance (+ or –; a dot indicates no statistically significant change) relative to controls (24 h sulfur replete conditions). The five symbols represent 2h (sulfur replete conditions), 2, 5, 10, 24 h (sulfur deplete conditions).
[e] LOD indicates analyte levels below the limit of detection. This corresponds to the value –10.76 in cluster analysis plots.

than 0.725. Of the 346 analytes selected in this way, 52 are Knowns, including the internal standard (Table 7). This final set of analytes contains metabolites which can be reliably quantified in the available dynamic range and which likely originate from the cellular material, while for the excluded analytes aliquot ratio analysis casts doubt on either their reliable quantification or biological origin.
The resulting data matrix contained 4.9% missing values of type I (true low values below detection limit) and 23.5% missing values of type II (false negatives) which were filled-in according to imputation strategy detailed in material and methods.

3.3.3 Numerous metabolites undergo marked changes during S deprivation

There were 51 metabolites for CC-1690 and 86 for the *sac1* mutant for which relative levels exhibited a ≥4-fold alteration for at least one time point during S starvation (see Table 7 and Table A1 in appendix). Thirty-five of these metabolites were selected for both strains. For 30 out of 35 metabolites regulation exhibited the same direction. In four instances metabolites that increased in CC-1690 decreased in *sac1*, and in one instance the metabolite decreased in the parental strain while it increased in the mutant. Thus, of the metabolites represented in the dataset used for HCA 18% for the wild-type and 31% for *sac1* mutant exhibited marked changes (4-fold or more). If changes exceeding 2-fold accumulation or depletion are considered, these proportions increase to 43% for CC-1690 and 85% for *sac1*. The extremely high value in the mutant strain is due to 221 out of 280 metabolites exhibiting ratios ≤0.5 for at least one time point.
Both shikimic and 2-isopropylmalic acid exhibit marked decreases after 2 h S deprivation and are below the limit of detection after 5 h in the wild-type strain. They are depleted to levels below the LOD also in the mutant, although the timing here is different: shikimate could not be detected already after 2 h, while 2-isopropylmalate decreased below LOD only after 10 h. Galactonic acid γ-lactone was among the ten metabolites decreasing below LOD in CC-1690 after 24 h S deprivation, but was only moderately decreased in the mutant. Ala, Glu, Gln and putrescine are greatly reduced in both strains during prolonged S deprivation. The same behavior is observed for levels of malate and citrate, which are reduced more than 4-fold after 10 and 5 h S deprivation, respectively, in CC-1690. While malate is regulated quite similarly in *sac1*, citrate levels are maintained in the mutant, rather than depleted. The terpenoid trans-squalene is also greatly reduced upon imposition of S deprivation, but increases after 24 h almost to control levels in CC-1690 and, to a lesser extent, in *sac1*. 2OG in CC-1690 decreases more than 4-fold after 10 h S deprivation, but increases to control levels in the 24 h S deplete samples. Modulation of glucose levels in CC-1690 is characterized by slight decreases below control levels at 2 and 10 h S deprivation and a marked ≥4-fold increase at 5 h S deprivation. Glucose levels in *sac1* exhibit only slight deviations from control levels. Proline exhibits transient ≥4-fold increases in both strains, although the increase is more pronounced with respect to magnitude and duration in the *sac1* mutant. After 24 h Pro levels are markedly decreased relative to control levels in both strains.

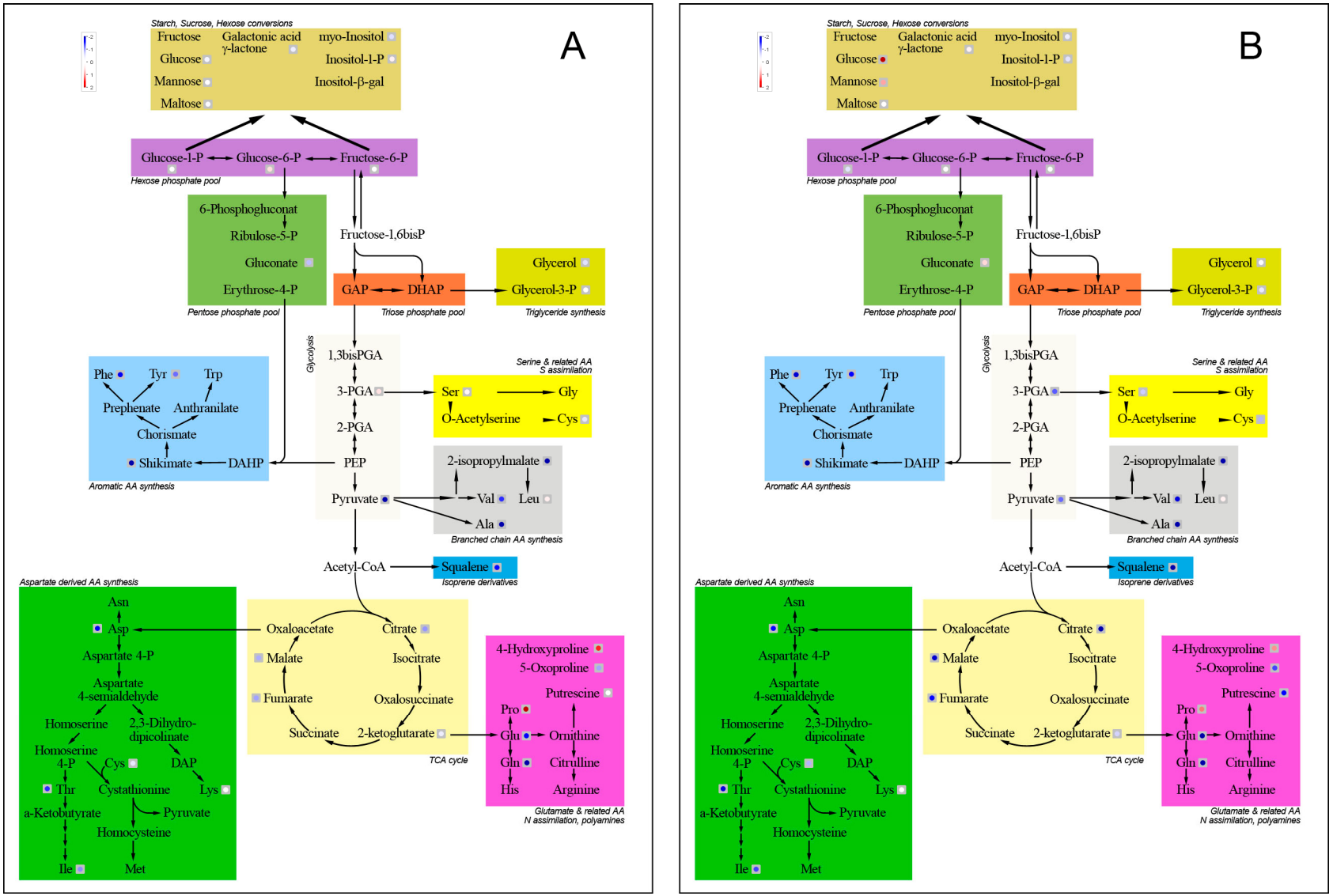

Figure 7: Metabolic changes in CC-1690 during S deprivation. Red indicates accumulation relative to controls, blue indicates depletion. (A) 2 h S deprivation (B) 5 h S deprivation.

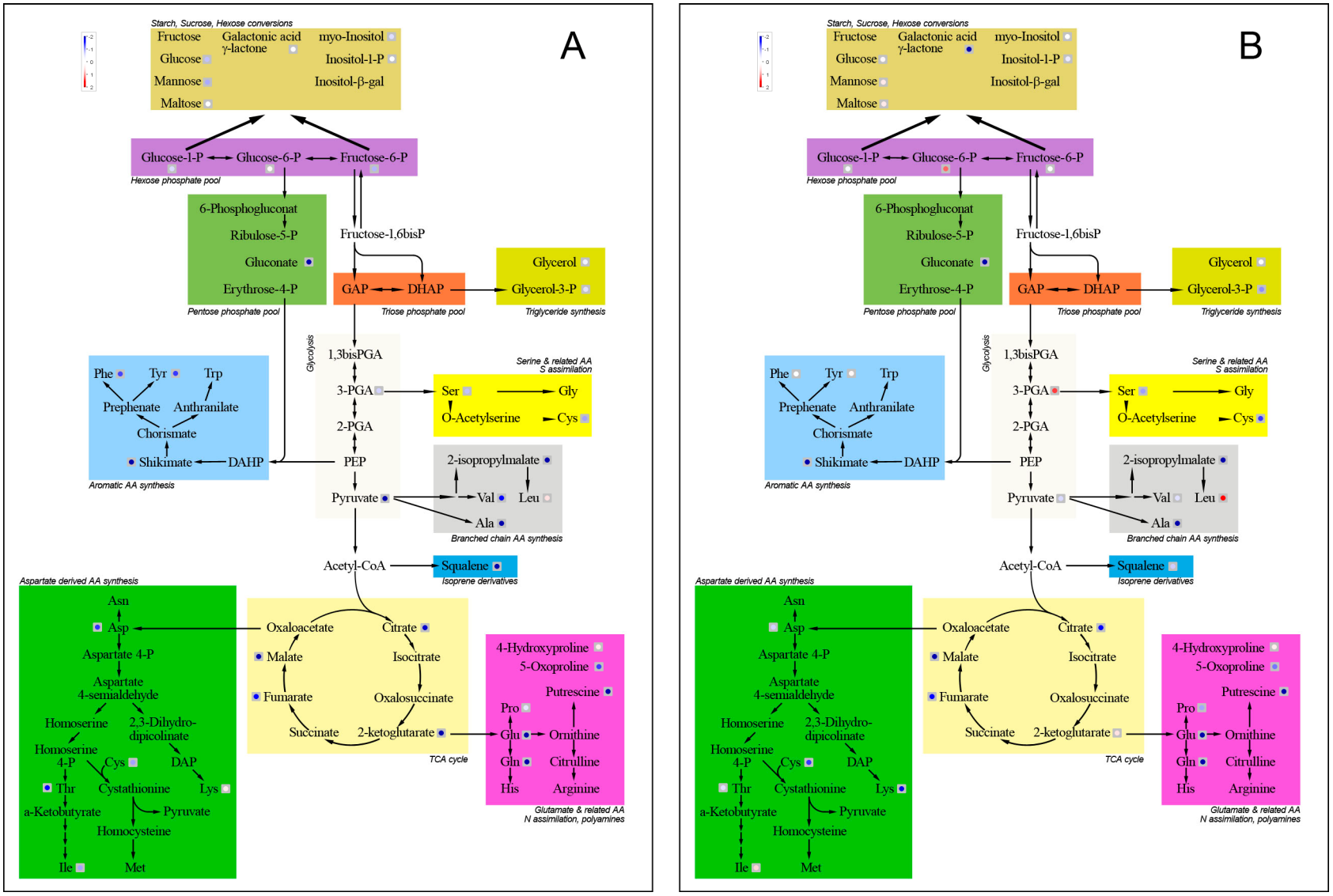

Figure 8: Metabolic changes in CC-1690 during S deprivation. Red indicates accumulation relative to controls, blue indicates depletion. (A) 10 h S deprivation (B) 24 h S deprivation.

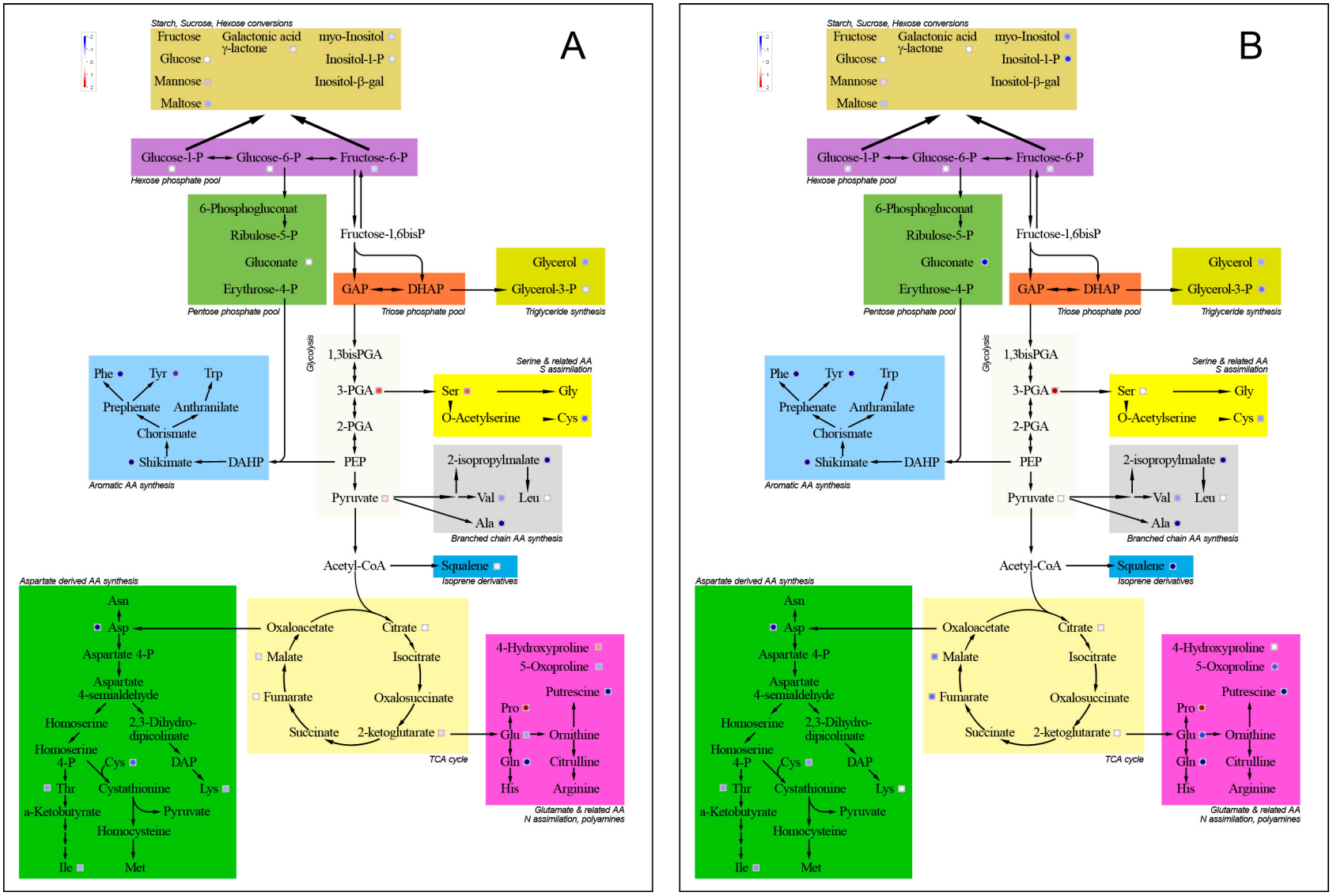

Figure 9: Metabolic changes in *sac1* during S deprivation. Red indicates accumulation relative to controls, blue indicates depletion. (A) 2 h S deprivation (B) 5 h S deprivation.

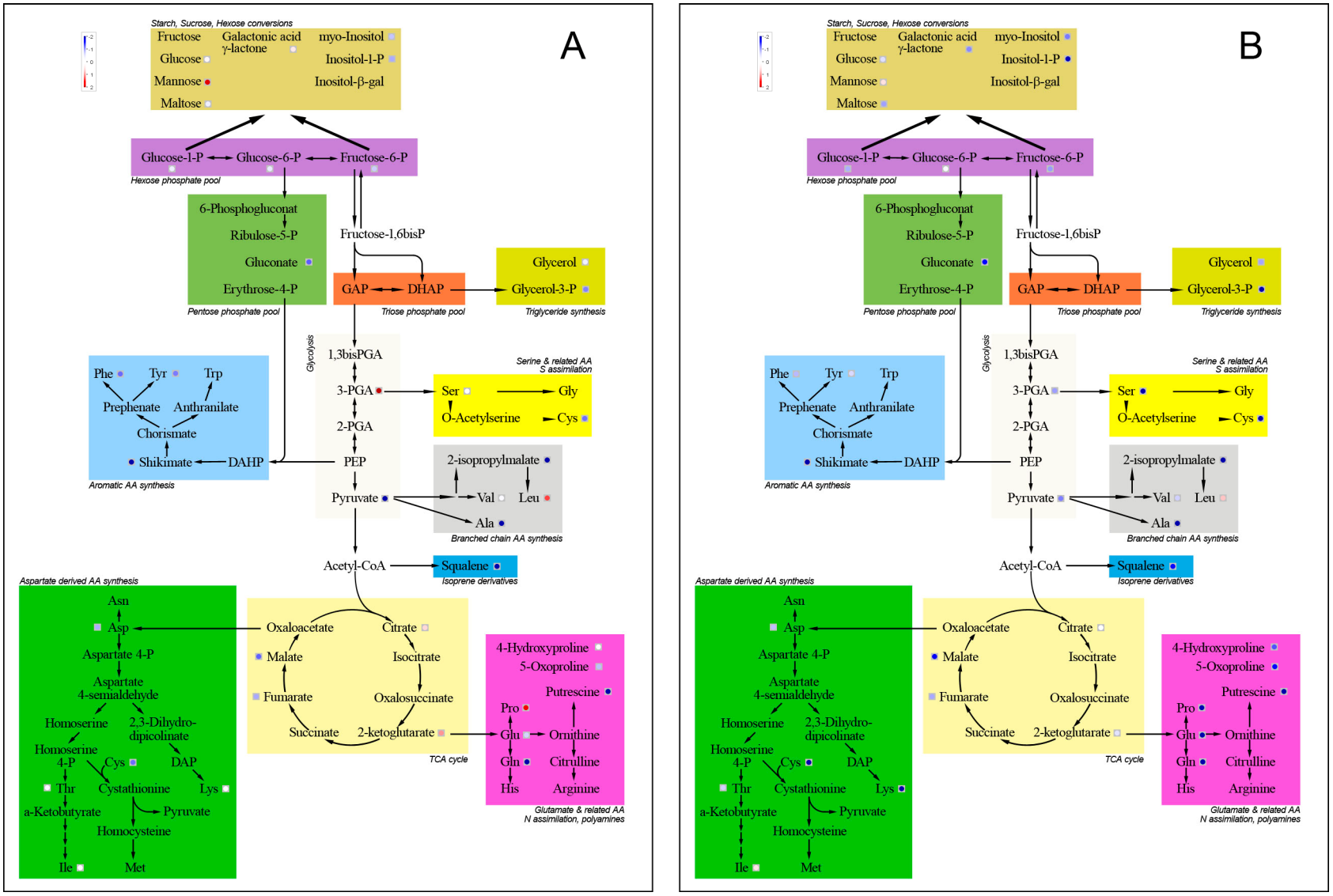

Figure 10: Metabolic changes in *sac1* during S deprivation. Red indicates accumulation relative to controls, blue indicates depletion. (A) 10 h S deprivation (B) 24 h S deprivation.

3.3.4 A number of metabolites are differentially regulated in the *sac1* mutant

Some of the metabolites exhibiting marked changes in the wild-type background showed deviating regulation in *sac1*. Among these are shikimic, 2-isopropylmalic and citric acid and galactonic acid γ-lactone, which are described also with respect to regulation in *sac1* in the preceding paragraph. Apart from these metabolites, there are others that show more intense changes in the mutant strain. This is the case, for example, for Lys, which is reduced app. 3-fold in CC-1690 and is below LOD in *sac1* after 24 h S deprivation. While 3PGA exhibits slight decreases in CC-1690 after 5 and 10 h S starvation, it accumulates more than 8- and 4-fold, respectively, at these time points in *sac1*. In addition, the data contains a considerable number of metabolites which show qualitative and quantitative differences between the two strains in response to S deprivation but could not be positively identified (see Table A1 in appendix). This includes yCR5253fa36#63 which accumulates only at 2 h after the onset of S deprivation in the *sac1* strain or yCR5253fa36#296 which increases markedly during 2, 5, and 10 h in *sac1* but shows only modest increases in the wild-type strain. Analyte yCR5253fa36#473 sets an example for early transient accumulation in the wild-type strain (cluster 10) while this analyte is immediately depleted in the mutant (cluster 3). yCR5253fa36#299 shows permanently increased levels in the wild-type while on the contrary being significantly reduced in the mutant.

3.3.5 S deprivation affects metabolite pools in many primary metabolic pathways

Figures 7-10 illustrate the changes of a number of compounds represented in the dataset in the context of important metabolic pathways of primary plant metabolism during 24 h of S starvation.

Regarding the hexose phosphate pools in CC-1690, after 2 h S deprivation G1P and F6P maintain their control level, while the level of G6P is slightly up-regulated, as are the levels of 3PGA and its downstream product, serine (Figure 7). Pyruvate, which is a downstream product in glycolysis, however, is markedly decreased, as are intermediates of the TCA cycle. Also most amino acids, that are synthesized from either pyruvate or carbon backbones of the TCA cycle show reduced levels with the exception of Lys, which is maintained at control level, and Leu (slight increase) and Pro (marked increase). This pattern of amino acid pool changes is generally maintained also after 5 h S starvation. By this time, however, distinct decreases also of 3PGA and serine below control level are observed. Glucose, mannose, and the pools of gluconate and galactonate γ-lactone, in contrast, are markedly increased after 5 h S deprivation (Figure 7). This is reversed after 10 h S deprivation (Figure 8), where glucose, mannose and gluconic acid have reduced levels. Hexose phosphate pools, in particular G1P and F6P are also markedly reduced. The pattern of amino acid pools is maintained also after 10 h. The initial marked increase in proline levels, however, is not maintained after 10 h and proline levels decrease further after 24 h S starvation. At the final time point of the experiment, the pattern of amino acid pools is slightly different: aromatic amino acids Phe and Tyr have returned app. to control levels

and Lys level now is clearly reduced. While citrate, malate and fumarate exhibit distinctly reduced levels also after 24 h S deprivation, 2-ketoglutarate appears to be increased now, as are other intermediates such as 3PGA and G6P. Slight increases above control level are also observed for glucose, mannose and maltose.

In the *sac1* mutant strain no increase of hexose phosphate pools could be observed, rather, a slight decrease of F6P could be observed after 2 h (Figure 9). 3PGA and serine, however, are strongly increased and, in contrast to the wild-type strain, pyruvate appears to be slightly increased too. Though the measured intermediates of the TCA cycle are decreased, the down-regulation is not as marked as in the wild-type. The pattern of amino acid pools generally resembles that of the wild-type, though Lys is clearly decreased in the mutant. Notably, putrescine levels are markedly decreased in the mutant but not in the wild-type after 2 h S deprivation. After 5 h, in contrast to the wild-type situation, the strong increase of 3PGA continues and both serine and pyruvate levels are not decreased in the mutant. Apart from slightly elevated mannose levels, no increase in hexose backbones could be observed in the mutant after 5 h, rather, levels of gluconic acid are distinctly reduced. Another contrasting feature is the maintenance of high levels of citrate and 2OG in the mutant, which is even more pronounced after 10 h S deprivation (Figure 10). A distinct increase of mannose is observed after 10 h S starvation and 3PGA levels are kept high, whereas pyruvate levels decrease below control levels. Proline levels are increased in the mutant also after 10 h, but are markedly decreased below control level after 24 h S starvation. Neither the G6P nor the 3PGA increase after 24 h in the wild-type are observed in the mutant.

Cysteine levels are declining in both the wild-type strain and the mutant during S deprivation. During the first 10 hours of S deprivation the decrease is moderate in CC-1690, after 24 h there is a marked decrease in Cys levels. In the *sac1* strain, Cys levels appear to be depleted more rapidly than in the wild-type. While OAS, which is a key regulatory element in the sulfur assimilation pathway, can be readily measured with GC-MS, it coelutes with the TRIS buffer component in GC-TOF chromatograms of *Chlamydomonas reinhardtii* samples and could therefore not be evaluated. OAS is synthesized from Ser, which is represented in the data by two analytes, which differ in their derivatization. For both analytes the general regulation pattern described above is similar which demonstrates their equivalence for measuring serine and confirms the steps undertaken in data acquisition and analysis.

3.3.6 Principal component analysis resolves time- and strain-specific metabolic phenotypes

Prior to the application of factor analytic techniques, the remaining set of 345 analytes, excluding the internal standard, was evaluated with regard to the distribution of the response for each analyte (Figure 11). The differences in variance between individual analytes are substantial. Not only does the variance among the variables differ greatly, analytes are also measured on individual scales, as their analytical sensitivity can vary greatly depending on ionization efficiency and detector response in the

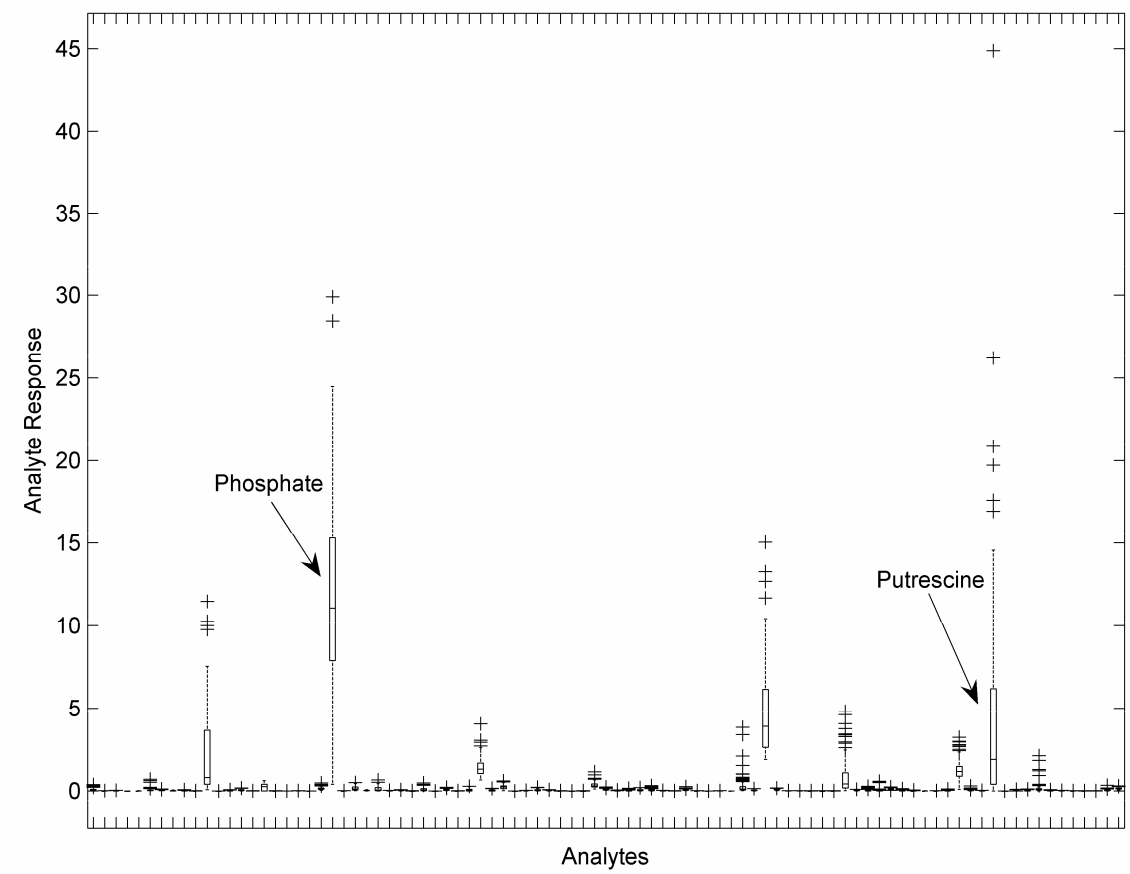

Figure 11: Distribution of analyte response values for 90 out of 345 analytes over all samples. Boxes extend from lower to upper quartile values. The median is indicated. Dashed lines indicate the dispersion of the rest of the values with the exception of data points more than 1.5 times the interquartile range away from the top or bottom of the box.

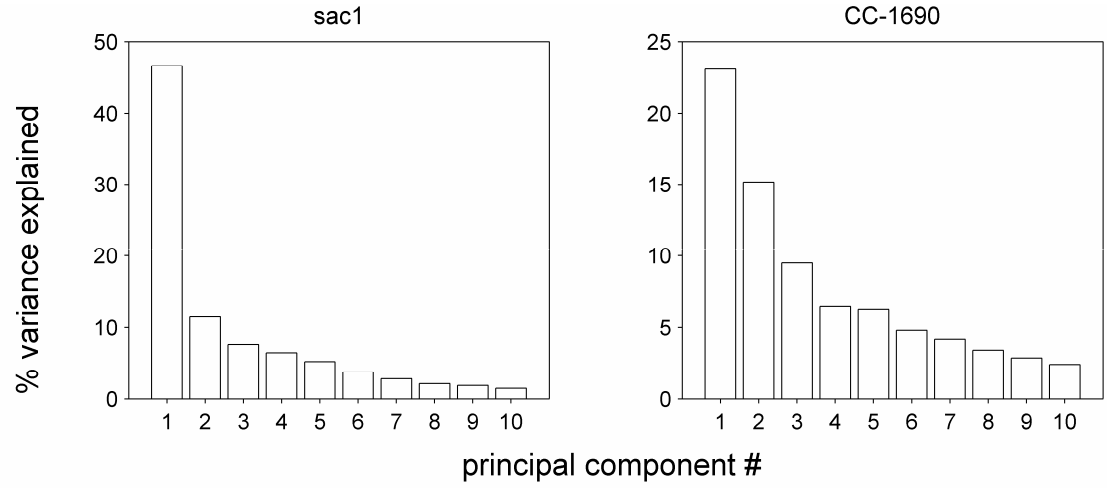

Figure 12: Variance explained by the first ten principal components of each analysis.

mass spectrometer for each compound. To ensure that each variable is given the same weight it is therefore highly appropriate to standardize the response for each analyte to unit variance prior to the application of variance-optimizing techniques such as principal component analysis. Standardization appears as prerequisite to detect variations of analyte response excited by biochemical regulation rather than separating samples by analytes which show large variance merely due to scaling effects.
Accordingly, all data was standardized to unit variance prior to performing PCA. Principal components were extracted for both the mutant strain *sac1* and the parental wild-type strain CC-1690. Eigenvalues of the principal components were normalized to the sum of all eigenvalues in each PCA and multiplied by 100 to retrieve the percentage of variance explained by each component (Figure 12). Projection of the score values of the individual samples for different pairs of principal components successfully separates the different biological groups (Figure 13, Figure 14). While no single principal component separates all groups, each of the selected components separates one or more classes with respect to duration of sulfur deficiency, strain or sulfur replete/ deplete conditions. This underlines the relevance of the factors extracted by principal components for the distinction of the metabolic phenotypes of the different groups. Prior to interpretation of the individual factors, analysis of the eigenvalues and of the distribution of the individual observations for each factor were conducted to retain only factors which account for (i) a substantial percentage of total variance and (ii) describe a biological, rather then technical cause.

	sac1	CC-1690
Kaiser criterion	22	31
Difference criterion	9	10
Scree test	2	2

Table 8: Number of principal components to retain

3.3.6.1 The difference criterion is a generalization of the Scree test and is useful for metabolomic data matrices to determine the number of factors to retain

To estimate the number of components that actually measure sources of variance attributable to common factors rather than sample to sample variation, three different criteria were used (Table 8). The Kaiser-criterion[202] retains all components with eigenvalues greater than one which essentially stipulates that a factor explains at least as much variation as the equivalent of one original variable. The scree test, as a graphical method[203], determines where the decrease of eigenvalues or explained variance levels off with increasing index of the factors. In applying this method to Figure 12, two factors in each PCA are retained. While both of these criteria appear to be very useful under circumstances where the number of samples is large and the number of variables is small, in data sets from metabolic profiling experiments the number of variables exceeds the number of samples considerably. Under these circumstances, the Kaiser criterion appears to select far more principal components than appear meaningful, while the scree-test retains inappropriately few components. Therefore, in addition to the Kaiser-criterion and the scree test, the following difference criterion is

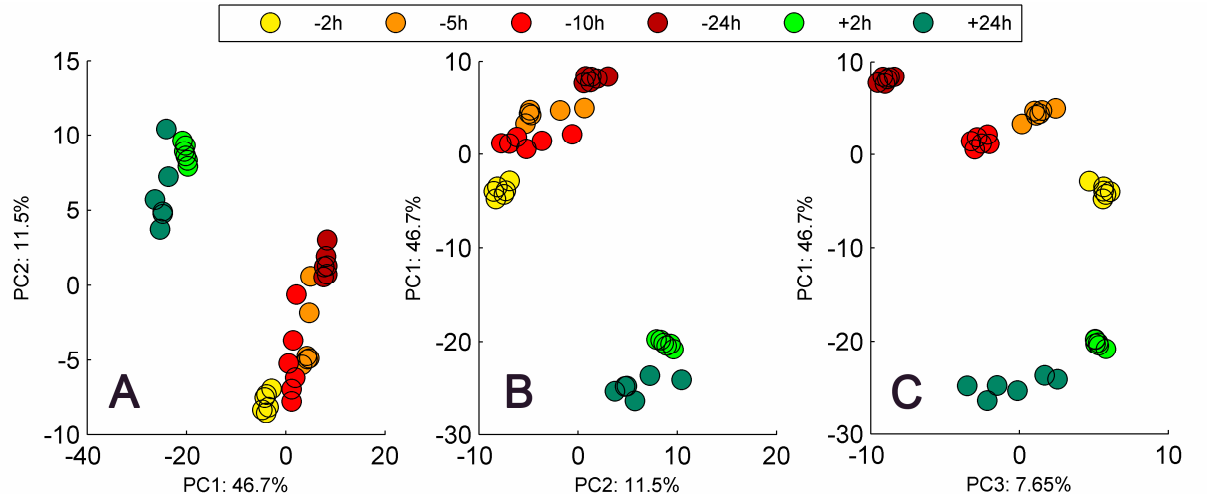

Figure 13: Projections of sample scores of components for strain *sac1* with range coefficients < 0.5. PC 1 is plotted against PC 2 (A), all other components are plotted against PC 1 (B and C). Component index and variance explained by each component are indicated in the axes labels.

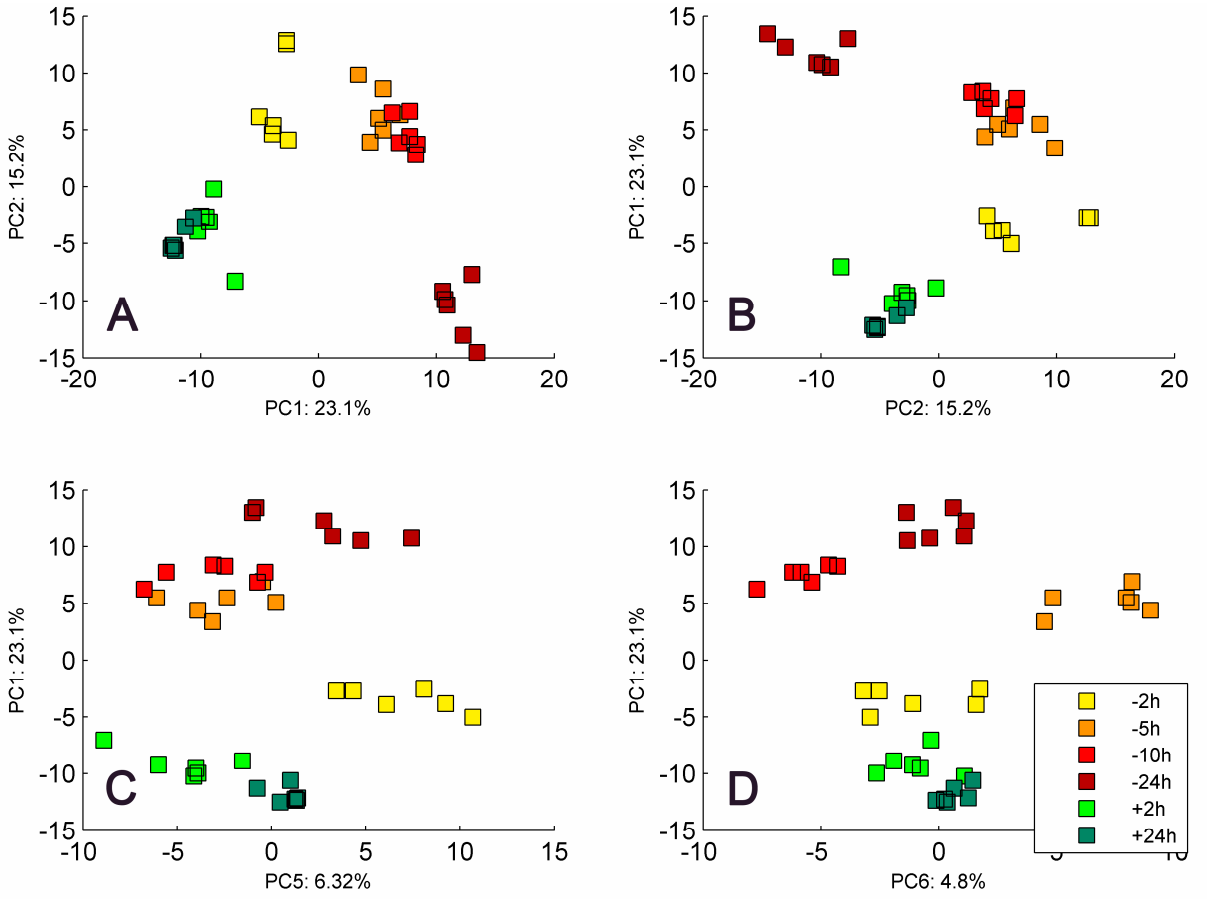

Figure 14: Projections of sample scores of components for strain CC-1690 with range coefficients < 0.5. PC 1 is plotted against PC 2 (A), all other components are plotted against PC 1 (B-D). Component index and variance explained by each component are indicated in the axes labels.

proposed: After computing the difference of the eigenvalues from one component to the next, the last component which exhibits a difference >1 is determined. All preceding components and the last one are selected. This criterion is proposed as a generalization of the scree-test in that all components where the decrease of eigenvalues levels off with differences ≤1 are not retained. Application of the difference criterion retains 30-50% of the components selected by the Kaiser criterion and thus preserves the most distinct factors while principal components with low absolute eigenvalues and low differences in eigenvalues are sorted out (Table 9).

PC index	*sac1*	CC-1690
1	**160,982**	**79,683**
2	**39,716**	**52,338**
3	**26,392**	**32,754**
4	**22,375**	**22,496**
5	**18,043**	**21,816**
6	**13,041**	**16,546**
7	**9,732**	**14,442**
8	**7,422**	**11,784**
9	**6,438**	**9,925**
10	5,134	**8,347**
11	4,907	6,921
12	4,262	6,457
13	3,348	5,681
14	2,733	5,446
15	2,304	5,192
16	2,190	5,035
17	1,971	4,163
18	1,732	3,940
19	1,660	3,346
20	1,475	3,151
21	1,207	2,940
22	1,076	2,628
23		2,554
24		2,382
25		2,186
26		2,045
27		1,835
28		1,629
29		1,412
30		1,375
31		1,235

Table 9: Eigenvalues of the factors extracted by PCA. The table comprises all factors with eigenvalues greater than 1 (Kaiser criterion). Factors in bold satisfy the difference criterion.

All further steps of the analysis were restricted to the first 10 components of each PCA, 10 being the maximum number of components selected by the difference criterion for any one of the two analyses.

3.3.6.2 Range coefficients can be used to distinguish technical and biological sources of variance

In order to distinguish between factors which exhibit large within-group variation compared to variation between groups, range coefficients for each component were calculated as the maximum of all group ranges of scores for that component divided by the overall range of scores for the same

component (Table 10). By definition, range coefficient values are in the interval [0,1]. The maximum value of 1 is reached if and only if the minimum and maximum score values are from samples belonging to the same group of biological replicates. The hereby defined range coefficients are proposed to distinguish between factors which describe technical (large values) and biological (small values) sources of sample variation. Large range coefficients indicate a substantial variation of score values within at least one biological group of replicates which points to a technical rather than biological source for the variation explained by this factor. Vice versa, the smaller the range coefficient, the smaller is the within-group variation in any one biological group and the more clearly the separation between groups which indicates a biological source of the variation explained by this factor.

PC index	*sac1*	CC-1690
1	**0,065**	**0,136**
2	**0,377**	**0,320**
3	**0,388**	1,000
4	1,000	0,624
5	0,991	**0,431**
6	0,901	**0,296**
7	0,543	0,970
8	1,000	1,000
9	1,000	1,000
10	0,946	0,892

Table 10: Range Coefficients of principal components. Range coefficients smaller than 0.5 are printed in bold.

To distinguish between factors that are likely to describe merely technical parameters of the experiment, a cut-off value of 0.5 for the range coefficient was used. Only components with a range coefficient smaller 0.5 were investigated further. The set of principal components obtained by the chosen cut-off value was remarkably consistent with manual inspection of score plots of the principal components and estimation of acceptable within-group variation in the plot (Figure 15). As a result, factors 1, 2, 3 from PCA with *sac1* and factors 1, 2, 5, 6 from PCA with CC-1690 were selected (Table 10). The small within-group variation of the different treatment groups associated with these principal components allows for the substitution of individual score values by the mean score value for each group (Figure 16). This representation shows how the intensity of the complex biological factor defined by each principal component develops as cells continue to grow under sulfur deplete conditions. These factors, which appear to describe biological variation related to the development of and adaptation to sulfur starvation, were investigated in detail.

3.3.6.3 PCA reveals concurrent metabolite accumulation and depletion as sources of sample variance

Differences in the metabolic composition correspond to differences in the score values of samples for the individual principal components. Individual metabolites can have either a positive or negative loading for any one principle component and hence are either positively or negatively correlated with

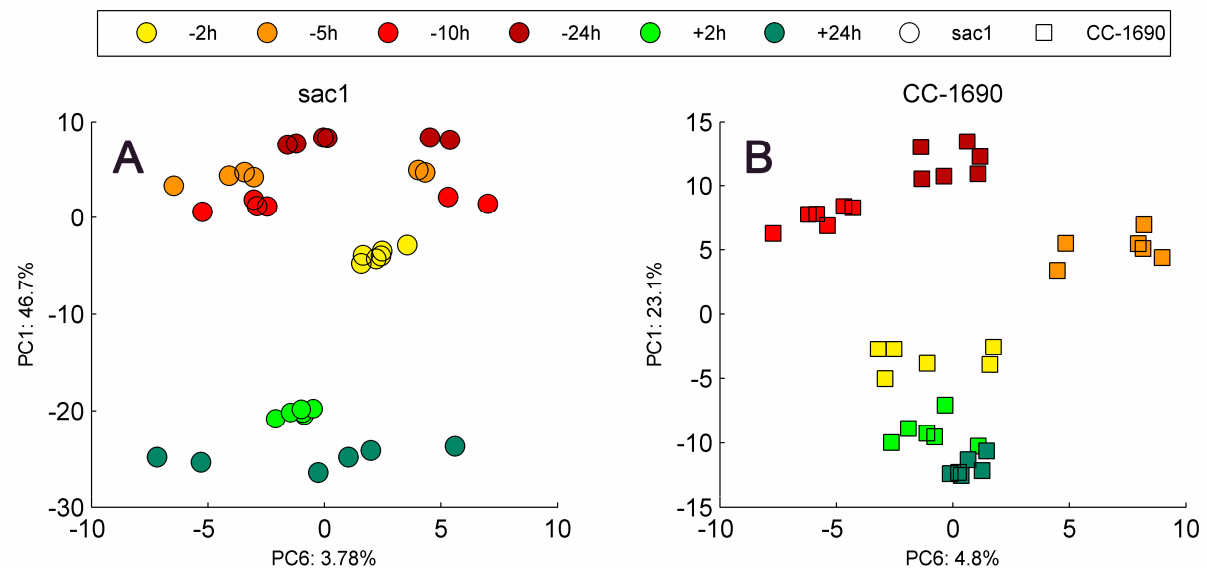

Figure 15: Sample scores of PC 6 vs. PC 1. (A) The substantial within-group variation of the scores in the +24 h group of biological replicates effects a range coefficient of 0.901. (B) For CC-1690 the within-group variation is moderate in all groups. This is reflected in a small range coefficient of 0.296. Axes labels indicate the percentage of variance explained for the respective PC.

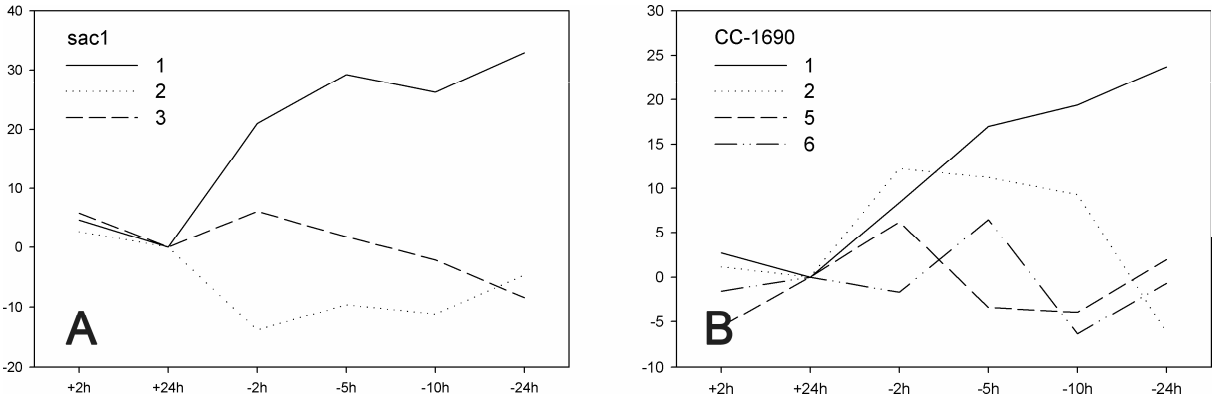

Figure 16: Centroid score values for components with range coefficients < 0.5 for individual strains. (A) *sac1*, (B) CC-1690. Component index in each panel is indicated in the panel's legend. In each panel values are normalized to the score value of the 24 h sulfur replete control.

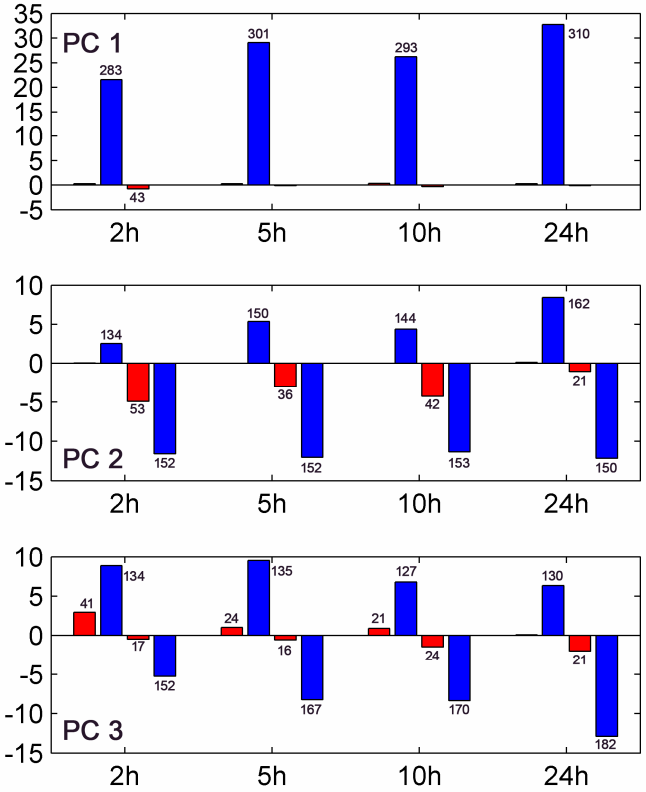

Figure 17: Contributions to score value differences in *sac1*. Red color indicates metabolite accumulation, blue color indicates metabolite depletion. For each time-point the contribution of 4 types of metabolites is indicated in the following sequence: accumulation, positive correlation (red upward), depletion and negative correlation (blue, upward), accumulation and negative correlation (red, downward), depletion and positive correlation (blue, downward). Numbers above/ below the bars indicate the number of metabolites falling in the respective category; they are omitted if the contribution is insignificantly small. Times refer to the duration of S depletion.

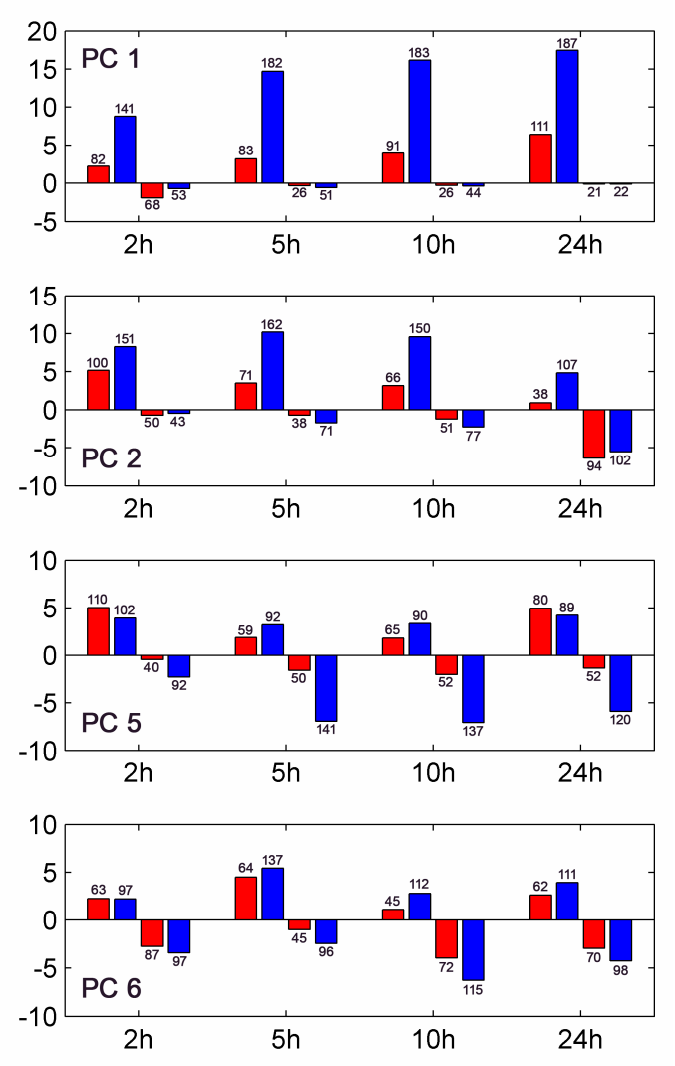

Figure 18: Contributions to score value differences in CC-1690. Color scheme and display order as in Figure 17.

the factor. When comparing score value differences between time points, a positive contribution to the total score value difference is effected by both increasing levels of positively correlated analytes and decreasing levels of negatively correlated analytes. Negative contributions occur whenever analyte level difference and loading have different signs. Sign of the loading and direction of change of the analyte therefore define four different groups of analytes which contribute differently to the magnitude of the principal components extracted: accumulating analytes with positive loadings (PP-Type), depleted analytes with negative loadings (MM-Type), accumulating analytes with negative loadings (PM-Type) and depleted analytes with positive loadings (MP-Type). The contributions of each of these four types to the difference in mean score value between the control samples and every S starvation sample for each principal component are shown in Figure 17 (*sac1*) and Figure 18 (CC-1690).

For the *sac1* mutant the first three principal components appear to describe biological features of the adaptation to S deficiency. The first PC, which explains almost 50% of the metabolic variation in the *sac1* samples, is characterized by a steep increase in score value upon imposition of S deprivation with score values reaching a plateau after 5 hours (Figure 16). Accordingly, S-deprived samples are very well separated from control samples and a slight separation is achieved also between the different time points of S starvation with maximum score values reached after 24 h of S starvation (Figure 13). Metabolites with the ten highest and lowest loadings remain unknown apart from GlyP (–0.077). The score value increase is almost exclusively accounted for by decreasing values of negatively correlated metabolites, like GlyP (Figure 17). Accordingly, principal component 1 in *sac1* reflects the immediate massive decrease in the levels of many metabolites with levels decreasing further as S deprivation continues.

The second PC has a minimum value at 2 h into S deprivation and gradually increases almost to control level after 24 hours (Figure 16) and especially differentiates –2 h samples apart from controls (Figure 13). Three main features contribute to the score value decrease (Figure 17): (i) a constant contribution by decreases of positively correlated metabolites, (ii) a decreasing contribution of accumulating and negatively correlated analytes and (iii) an increasing contribution of negatively correlated analytes that are decreasing in their levels. The gradual increase of the factor therefore reflects the gradual decreases of metabolites which at first accumulate after the onset of S deprivation, while the general offset with regard to control samples is effected by a substantial decrease of metabolites during all S starvation time points.

PC 3 attains similar values in both the S deplete and replete samples harvested after 2 h. Possibly this factor describes changes that occur due to the recent handling of cell cultures, which are unrelated to the imposition of sulfur deficiency.

In the parental strain wild-type strain CC-1690 the principal components 1, 2, 5 and 6 were selected for detailed analysis. The first principal component explains 23.1% of the variance and exhibits increasing values for the progression of S deprivation and separates the samples of the corresponding

four time points from each other (Figure 16, Figure 14). Organic acids like fumarate and malate have among the smallest negative loadings for this component and also isopropylmalic, shikimic and glutamic acids have negative loadings and are significant MM-type contributors. The score value increase can be attributed mainly to the steadily increasing contribution of MM-type analytes and, to a lesser extent, to the increasing contribution of PP-type analytes (Figure 18). Thus, this factor reflects both steadily decreasing values for about 180 metabolites and the concurrent increase of others during the entire course of S deprivation.

The second PC still accounts for 15.2% of the variance and separates the 2, 5, and 10 h S deprivation samples from the controls as well as from the 24 h S deprivation samples. In comparison to the +24 h control sample, changes in the metabolite composition of the 2, 5, and 10 h samples are characterized by significant contributions of both PP- and MM-type with the aforementioned amino acids in the latter group (Figure 18). After 24 h, the situation is reversed: almost 2/3 of the positively correlated metabolites that were increased before, are now lower than in controls and app. 1/3 of the negatively correlated metabolites that were decreased before, are after 24 h higher than in control values. Thus, this factor sets apart processes that occur during the ten first hours of adaptation to S deficiency which are characterized by concurrent metabolite accumulation and, more so, depletion. Low negative loadings indicate that depletion of the pools of the aromatic amino acids Phe and Tyr as well as of Val, Thr and the downstream product Ile may be indicative of this process.

Principal component 5 slightly sets apart the 2 h S deprivation samples (Figure 14) due to transient increases in the levels of at least 51 of the positively correlated metabolites, proline being an example. These PP-type contributions are high also in the 24 h S deprivation sample but are counterbalanced there by strong decreases of the rest of the positively correlated analytes (Figure 18).

Principal component 6 differentiates both the 5 h S deprivation samples (higher score value) and the 10 h S deprivation samples (lower score values) (Figure 14). The 5 h sample is characterized by transient increases of positively correlated analytes, which are more pronounced than in the other S deprivation samples and similarly, transient decreases of a number of negatively correlated analytes. In the 10 h sample, these processes are exactly reversed, i.e. positively correlated metabolites which increase or decrease only moderately, are decreased here more strongly and negatively correlated metabolites accumulate at 10 h whereas they might be decreasing during other time points. In summary, this factor describes processes that are observed during 5 h into S starvation and is reversed during 10 h. Glucose, gluconic acid and mannose have high positive loadings for this factor, indicating that carbohydrate metabolism may play a role here.

3.3.6.4 **Conclusions from PCA analysis**

In summary, principal component analysis is able to separate the different biological groups by their metabolic composition. For the mutant strain *sac1*, three orthogonal factors reflecting biological sources of variance could be extracted which together account for more than 65% of the sample variance. While the third of these factors may mirror short term changes in the algal cultures not

related to S deprivation, the first two factors appear to illustrate the major quantitative changes in terms of overall variance covered in the *sac1* strain. Imposition of S deficiency results in quick decreases for a large number of metabolites, and the overall depletion of metabolite pools is enhanced as S deprivation continues. The second largest independent source of variance reflects another process which can be described as diminishing levels of accumulation or even depletion of certain metabolites as S deprivation continues. Continuing depletion of metabolite pools also in the parental wild-type strain accounts for much of the variance. However, in contrast to the mutant strain this is accompanied by concurrent and continued accumulation of certain compounds. Principal component 2 shows characteristics of adaptational processes that are active during the first 10 h of S starvation but are not sustained after 24 h. Factors 5 and 6 can tentatively be identified as adaptational processes being most distinct after 2 and 5 hours S starvation. Metabolite loadings for the individual components rarily exceed absolute values of 0.2 which does not permit to pinpoint the biological processes reflected in the principal components to individual metabolites. However, the multiple occurrences of amino acids among metabolites with low negative loadings for factor 2 for CC-1690 data may indicate a role for amino acid biosynthesis in the adaptation to S deficiency, where especially pools of aromatic and branched chain amino acids are depleted.

criterion	*sac1*	CC-1690
(1) erratic course of detection	13	22
(2) abs(+2h)>4	41	14
(1) or (2)	48	30

Table 11: Number of analyte response profiles excluded from the dataset prior to HCA.

3.3.7 Hierarchical cluster analysis reveals five main patterns of metabolic response to S deprivation and incapability of the *sac1* mutant to sustain certain adaptational responses

Hierarchical cluster analysis (HCA) was performed using $\log_2$ values of the averaged analyte response data normalized to the control response (24 h sulfur replete conditions). Object proximities were based on the correlation distance metric and object hierarchy was computed using the Ward method. A small number of profiles which exhibited extreme changes between the 2 h and 24 h S replete samples or exhibited an erratic course of detection was removed from the dataset (Table 11). The resulting partition of the dataset of 612 individual profiles into 22 clusters is shown in Figure 19. Application of other linkage methods such as centroid, average or complete linkage identified essentially the same cluster structures (data not shown). Application of the Ward method was advantageous in that it successfully separated profiles which were below LOD after 2, 5, 10 and 24 h of detection into different clusters. LOD instances are indicated by the uniformly assigned value –10.76[i]. HCA revealed

[i] As detailed in materials and methods, this corresponds to a value three $\log_2$ units below the total minimum of all data points after normalization and log-transformation.

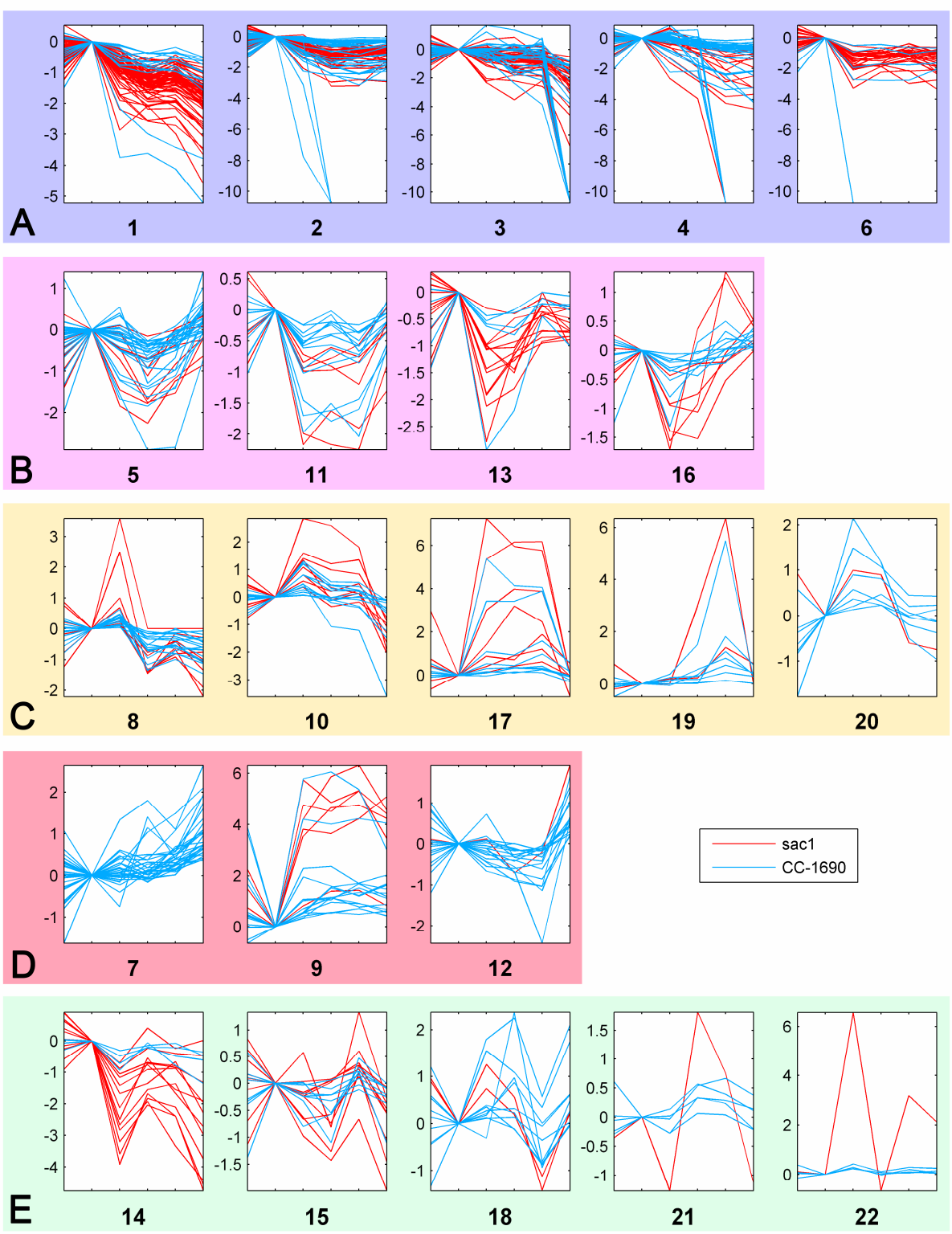

Figure 19: HCA of analyte response profiles Clusters are indexed by descending size (number of profiles assigned) and arranged in five main pattern groups A-E (see text). Data are shown along the x-axis in the following sequence: +2h, +24h, –2h, –5h, –10h, –24h. Displayed are the $\log_2$ values of the analyte response normalized to the control (24h sulfur replete conditions).

cluster index	number of profiles			pattern group	General profile characteristics
	total	*sac1*	CC-1690		
1	88	74	14	A	Steady decline
2	77	43	34	A	moderate to pronounced decline during first 05h, then level including below LOD after 5h
3	71	45	26	A	Level to moderate steady decline, further decline after 10h including below LOD after 24 h
4	47	14	33	A	moderate to pronounced decline during first 10h, then level including below LOD after 10h
5	35	8	27	B	moderate to pronounced decline during first 05h, then rise to control level after 24 h
6	34	29	5	A	moderate to pronounced decline during first 02h, then level including one profile LOD after 2h
7	31	0	31	D	steady increase (only small changes)
8	25	8	17	C	elevated after 2h then dropping to control level or moderate decline
9	21	6	15	D	elevated after 2h, staying on that level or moderate decrease above control level after 24 h
10	20	8	12	C	elevated after 2h, then continuously decreasing to or below control level after 24 h
11	20	6	14	B	moderate to pronounced decline after 2h, keeping the low level and recovery after 24 h
12	19	1	18	D	level, moderate increase after 24 h
13	18	13	5	B	decrease during first 2h, then increase to control level after 5-10h
14	17	13	4	E	decreased after 2h, recovery after 5h, then moderate to pronounced decrease
15	17	9	8	E	decrease during first 5h, increase after 10h, decrease after 24 h
16	16	6	10	B	decrease during first 2h, then steady increase to control level
17	16	7	9	C	elevated after 2h, keeping the elevated level to 10h, then decrease to control level after 24 h
18	12	2	10	E	increase during first 2-5h, decrease to or below control level at 10h, increase at 24 h
19	9	2	7	C	Rising to a maximum at 10h, returning to control levels after 24 h
20	8	1	7	C	Rising to a maximum at 2h, return to control level after 10h
21	6	1	5	E	minimum at 2h, maximum at 5-10h, returning to or below control levels after 24 h
22	5	1	4	E	maximum at 2h, return to control level at 5h, elevated level after 10-24 h

Table 12: Size and characteristics of the 22-cluster-HCA solution for strains *sac1* and CC-1690.

five main pattern groups of metabolites responses over the entire course of experimental observation: depletion (A), depletion and recovery (B), transient accumulation or peaking (C), accumulation (D) and oscillation (E). Clusters could be grouped into five different pattern groups A-E according to the general type of regulation shown by the elements of each cluster for which a descriptive summary is given in Table 12. Group A, with the largest number of profiles, contains analytes for which the hallmark is gradual depletion through the course of 24 h sulfur deprivation. Due to the chosen correlation distance metric group A also comprises metabolites which show no statistically significant response to S deprivation and retain their control levels or even exhibit slight transient increases. The extent of the actual decrease of individual metabolites ranges from modest to below the limit of detection. Decline below limit of detection is observed especially after 10 and 24 h S deprivation (clusters 4 and 3, respectively) but for a small number of metabolites also after 2 (cluster 6, one instance for each strain) and 5 h (cluster 2, 3 instances in CC-1690) S starvation. Group B combines analytes which show moderate to marked depletion too, but for which the levels recover or even reach the control level after 24 h sulfur deprivation. Analytes which show a distinct peak in response to sulfur deprivation are merged into group C. The timing and duration of the transient accumulation vary. For example, while cluster 8 contains analytes which show a sharp maximum two hours after the imposition of sulfur deficiency, the elements in cluster 19 show a late maximum after ten hours sulfur deprivation and cluster 17 contains elements which exhibit a broad temporal window of accumulation ranging from 2 to 10 hours after imposition of sulfur deficiency. Group D is characterized by accumulating substances, i.e. analyte levels after 24 h sulfur deprivation are higher than in the control. As in group A, the values do not necessarily increase monotonically over the course of the experiment. Group E comprises profiles which can be described as oscillating, as the relative changes are recorded in both plus and minus directions during the time course. For some metabolite profiles assigned to this pattern group, the amplitude of these changes is, however, relatively small and differences are only partly statistically significant (see Table 7 and Table A1).

In the wild-type strain CC-1690, 36% of the metabolites are assigned to one of the clusters in pattern group A (Figure 20), making modest to marked gradual depletion of metabolite pools the most prominent feature of the adaptation to S starvation. The second largest number of metabolites (20%), however, is assigned to pattern group D, which shows that adaptation to S starvation is a regulated process that leads to accumulation of certain substances in varying degrees. In contrast, in the mutant strain *sac1* almost 70% of all metabolites are assigned to pattern group A, while the number of elements in groups B-D is significantly reduced, with only 2% of the metabolites being assigned to pattern group C. The reduced share of metabolites in groups B-D is almost exclusively due to the fact that metabolites which belong to groups B-D in the wild-type are assigned to group A in the mutant strain (Table 13). For example, of the 52 metabolites showing transient accumulation of some sort (group C) in the wild-type strain, 31 are assigned to group A in the mutant strain. This reflects the massive incapability of the *sac1* mutant to sustain processes that normally lead to transient or

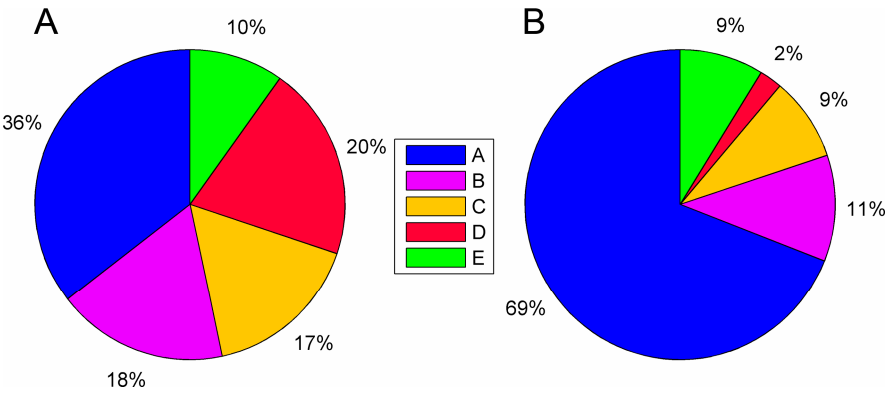

Figure 20: Relative contributions of response pattern groups in the metabolite response. (A) Wild-type strain CC-1690, (B) mutant strain *sac1*. Pattern groups are indicated in the legend.

strain		CC-1690						
	pattern group	0	A	B	C	D	E	row sum
sac1	0	13	13	9	5	5	3	48
	A	10	80	35	31	32	17	205
	B	2	3	10	2	13	3	33
	C	4	7	1	7	4	3	26
	D	1	2	0	1	1	2	7
	E	0	7	1	6	9	3	26
	column sum	30	112	56	52	64	31	345

Table 13: Distribution of metabolite response profiles among pattern groups. Individual cells indicate the number of metabolites found in the corresponding pattern groups for *sac1* (in rows) and CC-1690 (in columns), respectively. Pattern group zero indicates metabolite profiles that were excluded from the dataset prior to HCA for either strain.

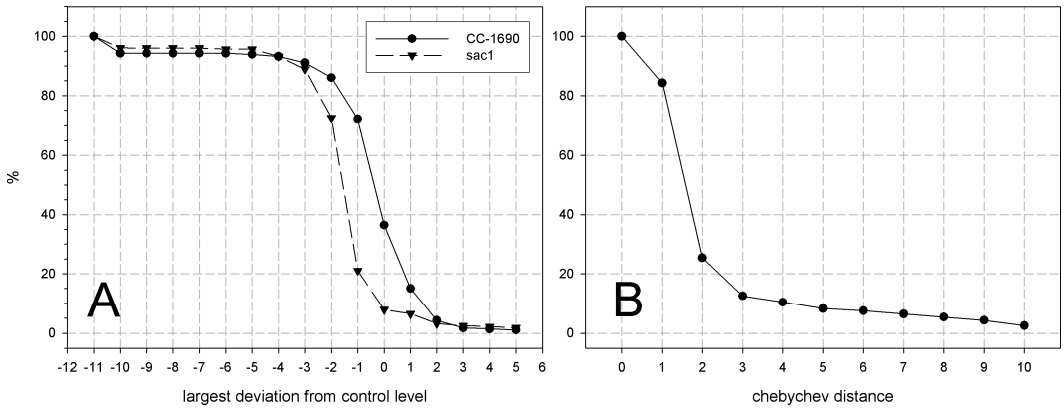

Figure 21: Comparative metabolomic analysis. (A) Cumulative density of changes in metabolite levels induced by S starvation. For each strain, the plot shows the percentage of metabolites exhibiting a maximum deviation from control levels larger than the indicated $\log_2$ values for at least one time point. (B) Cumulative density of dissimilarity between metabolite profiles in *sac1* and the parental strain CC-1690. The plot shows the percentage of metabolites exhibiting a maximum absolute difference in $\log_2$ values (Chebychev distance) larger than the indicated values.

permanent accumulation of the levels of certain metabolites. The inability to maintain or elevate levels of certain metabolites is further illustrated in Figure 21. The fraction of metabolites for which control levels are maintained for at least one time point during S deprivation is reduced to less than 10% in the mutant whereas this is true for almost 40% of the metabolites in the wild-type strain.

The dissimilarity of metabolite profiles of the same metabolite in the mutant and parental wild-type strain can serve as indication of differential regulation and control by *SAC1*. The maximum difference of the log-transformed relative metabolite levels at any time point was used to quantitate profile dissimilarity (Chebychev distance). While the median of the Chebychev distance relating to the entire set of metabolites is about 1.5, more than 10% of all metabolites exhibit differences greater than 4 (Figure 21) which indicates a prominent role for *SAC1* in the regulation of certain metabolite levels during acclimation to S deficiency.

In summary, these results demonstrate how metabolite levels react in a time dependent manner and in different general regulation types to the imposition of sulfur deficiency. Based on cluster sizes and feature group assignments, most analytes decrease in their levels as sulfur deprivation continues. The response in *sac1* cells is characterized by the inability to sustain processes which lead to transient or permanent up-regulation of metabolite levels as part of the S deprivation response which leads to an even higher proportion of metabolites that decline in their levels.

3.4 Different Enzymatic Blocks of Arg Biosynthesis are Reflected in the Pool Sizes of its Intermediates

A total of eight different strains carrying lesions in different steps of Arg biosynthesis were obtained from CGC. Only for five of them a clear Arg requirement for growth could be established (Figure 22 and Table 14). For strains CC-48 (*arg2*), CC-861 (*arg1*), CC-2000 (*arg8*), CC-2001 (*arg9*), and CC-2958 (*arg9*) the Arg auxotrophic phenotype could be reproduced. CC-48, CC-2000, and CC-2958 had a strict requirement for externally supplied Arg, while strains CC-861 and CC-2001 showed residual growth. Both strains exhibited severely reduced growth rates without external Arg supply in liquid cultures (Table 14). On solid media, CC-2001 did not grow while CC-861 exhibited marginal growth (Figure 22).

In contrast, strains CC-1997 *arg4* mt+, CC-2002 *arg10* mt+, CC-2391 *arg9-2* mt+ grew equally well without addition of Arg, raising the possibility that the original mutations in these strains are suppressed or reverted. From the two strains representing the *arg9* mutation, CC-2958 was chosen for further analysis as it exhibited a clear Arg requirement in both liquid and solid culture. Strain CC-2000, in contrast to all other strains, turned out to be incompatible with the chosen quenching and harvest procedure as cells adhered tightly to the inner wall of the centrifugation containers after quenching and could not be collected by centrifugation (data not shown).

For the three remaining Arg auxotrophic strains that had been characterized previously as lacking *N*-Acetylglutamate-5-P reductase (CC-861 *arg1*), N^2-Acetylornithine aminotransferase (CC-2958 *arg9*) and Argininosuccinate lyase (CC-48 *arg2*) pools of intermediates of the arginine biosynthetic pathway

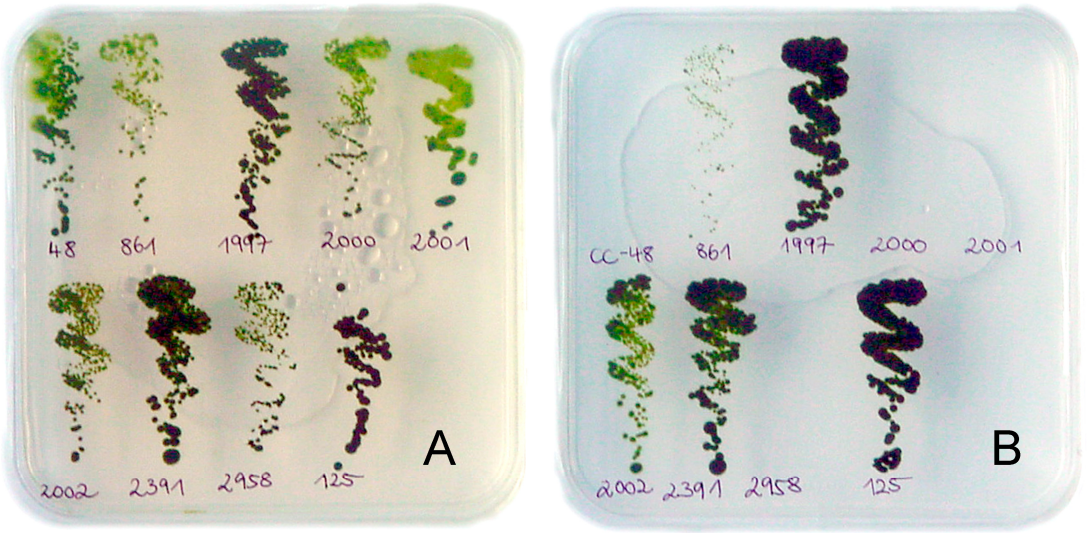

Figure 22: Growth of Arg⁻ strains on solid media. (A) TAP-Agar supplemented with yeast extract as Arg source, (B) TAP-Agar without yeast extract. Numbers indicate CGC strain index. Wild-type strain CC-125 is used as positive growth control.

strain	growth rate [h^{-1}]		growth rate ratio
	+Arg	-Arg	
CC-125 wt mt+	0,083	0,087	1,045
CC-48 *arg2* mt+	0,080	0,008	0,095
CC-861 *arg1* mt+	0,049	0,030	0,612
CC-1997 *arg4* mt+	0,063	0,042	0,658
CC-2000 *arg8-1* mt+	0,074	0,001	0,017
CC-2001 *arg9-1* mt+	0,081	0,033	0,403
CC-2002 *arg10* mt+	0,080	0,077	0,965
CC-2391 *arg9-2* mt+	0,079	0,084	1,057
CC-2958 *arg9-2 shf1-253* mt–	0,053	0,004	0,072

Table 14: Growth rates of *arg*⁻ strains in TAP medium. Growth was monitored over 48 h in liquid cultures with (+Arg) and without (–Arg) supplementation of 50 mg/l L-Arginine. Growth rate ratio (–Arg/+Arg) is indicated.

and of the TCA-cycle were determined 24 h after withdrawal of external Arg supply. Metabolite pools in CC-125 were determined as wild-type reference[i]. Due to the unavailability of authentic standards (*N*-Acetylglutamate-5-P (NAG5P), *N*-Acetylglutamate-5-semialdehyde (NAGSA)) or insufficient compound stability during sample preparation and derivatization, some compounds could not be measured. Notably, internal Arg levels could not be measured reliably due to fragmentation of the molecule.

Each enzymatic block resulted in a highly specific modulation of the pools of the intermediates of the Arg biosynthetic pathway. Compared to the wild-type reference, the changes encompass five orders of

[i] All Arg auxotrophic strain mentioned in the text were originally generated in the CC-125 background (Elizabeth Harris, CGC, personal communication).

magnitude ranging from a reduction of 2OG to less than 4% to a nearly 500-fold accumulation of argininosuccinate (Table 15).

metabolite	levels				ratio		
	CC-125 wt	CC-48 *arg2*	CC-861 *arg1*	CC-2958 *arg9*	*arg2*/wt	*arg1*/wt	*arg9*/wt
2-Oxoglutarate	0,079 ± 0,002	0,0029 ± 0,0002	0,0291 ± 0,0008	0,0288 ± 0,0004	0,037	0,368	0,364
Argininosuccinate	0,0021 ± 0,0004	1,023 ± 0,005	0,0015 ± 0,0001	0,00068 ± 0,00007	495,244	0,742	0,330
Aspartate	0,039 ± 0,001	0,119 ± 0,002	0,79 ± 0,02	0,579 ± 0,009	3,047	20,321	14,828
cis-Aconitate	0,0103 ± 0,0005	0,0045 ± 0,0002	0,0187 ± 0,0003	0,0073 ± 0,0003	0,432	1,805	0,708
Citrate	1,55 ± 0,01	0,242 ± 0,003	1,02 ± 0,01	0,984 ± 0,005	0,157	0,660	0,635
Citrulline	0,025 ± 0,001	0,07 ± 0,004	0,039 ± 0,001	0,0099 ± 0,0004	2,752	1,542	0,389
Fumarate	0,318 ± 0,004	0,038 ± 0,002	0,494 ± 0,006	0,149 ± 0,001	0,119	1,555	0,468
Glutamate	0,0124 ± 0,0002	0,0072 ± 0,0003	0,0508 ± 0,0007	0,0326 ± 0,0005	0,575	4,084	2,623
Malate	1,56 ± 0,04	0,081 ± 0,001	1 ± 0,03	0,98 ± 0,02	0,052	0,639	0,628
N-Acetylglutamate	0,0188 ± 0,0005	0,074 ± 0,002	0,652 ± 0,008	0,0502 ± 0,0005	3,955	34,708	2,672
N^2-Acetylornithine	0,0108 ± 0,0005	0,0067 ± 0,0001	0,0394 ± 0,0007	0,0012 ± 0,0002	0,620	3,645	0,114
Ornithine	0,629 ± 0,005	0,165 ± 0,003	0,521 ± 0,005	0,032 ± 0,001	0,263	0,829	0,050
Succinate	0,32 ± 0,003	0,0164 ± 0,0005	0,192 ± 0,002	0,0773 ± 0,0009	0,051	0,600	0,241

Table 15: Response of intermediates of Arg biosynthesis and TCA cycle to withdrawal of externally supplied Arg. Metabolite levels are shown in arbitrary units relating to peak area integration. Standard errors are indicated (n=5, except for CC-48 n=4).

In the context of the biochemical pathway for Arg synthesis it is evident that a block in ASL (*arg2*, *arg7*) results in massive accumulation of the substrate for this reaction, argininosuccinate (Figure 23). Interestingly, while citrulline (last but one enzymatic conversion) exhibits a comparably slight increase, Orn and NAO levels are decreased. NAG levels however, increase 4-fold. These results indicate that, except for the disabled last step, the Arg biosynthesis pathway is highly active upon withdrawal of external arginine supply in the *arg7* mutant. Pathway flux is presumably high, with elevated levels of the product of the first commited step, NAG, and accumulation of the last two intermediates of the pathway, citrulline and especially ArgSuc. In addition, levels of all measured TCA-cycle intermediates are greatly decreased, indicating reduced carbon channeling and respiration which is consistent with the rapid cessation of growth in CC-48 *arg2*.

Precursor accumulation is observed also in the CC-861 *arg1*. The direct precursor and product of the NAGPR reaction, N-Acetylglutamate-5-phosphate and N-Acetylglutamate-5-semialdehyde, respectively, could not be evaluated due to the unavailability of standards for these substances. NAG, which commits the Glu backbone to Orn synthesis, however, increased more than 30-fold. Interestingly, also NAO, which is considered a downstream product of the NAGPR reaction, accumulates more than 3-fold. Not only can all other downstream intermediates of the pathway – Orn, citrulline, and ArgSuc - clearly be detected in *arg1* cells; their levels even appear only slightly

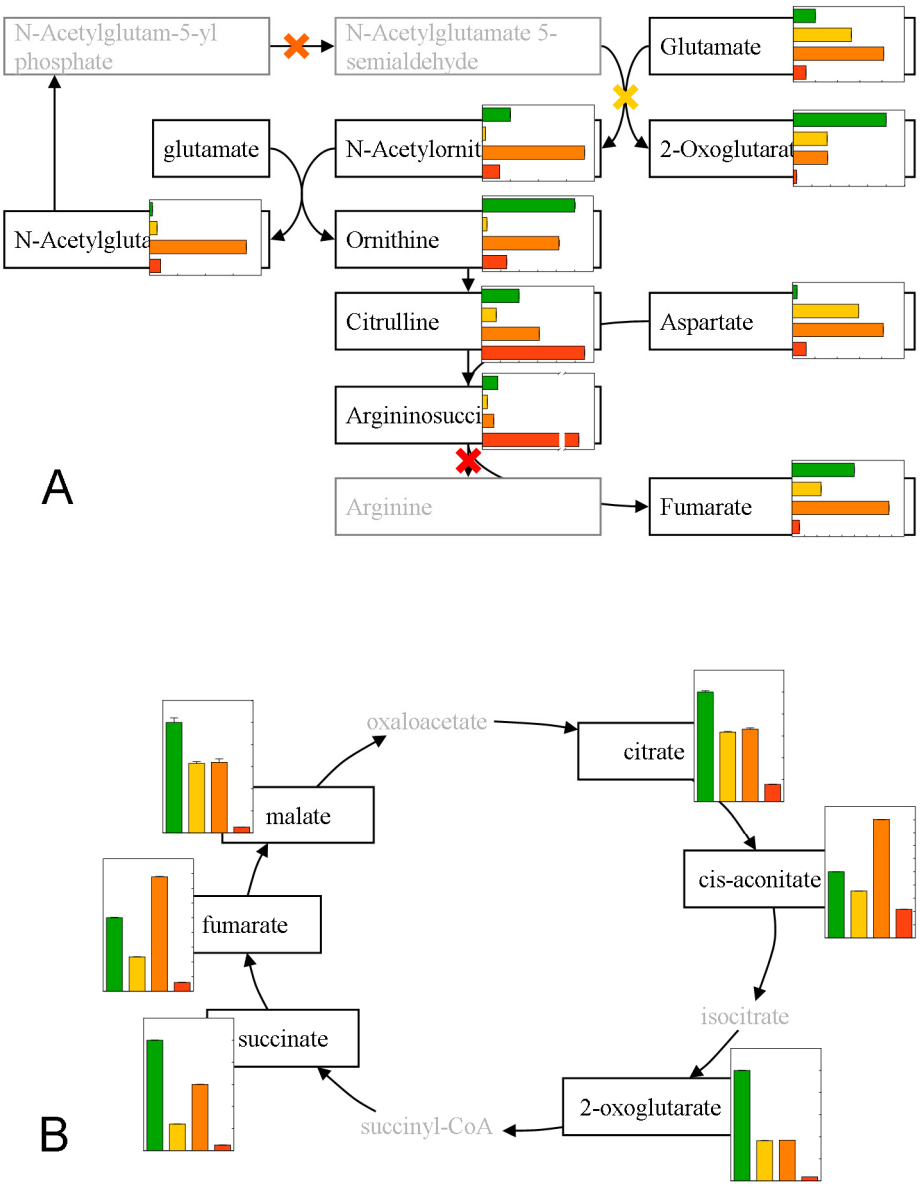

Figure 23: Response of *arg*⁻ strains to withdrawal of externally supplied Arg. (A) intermediates of Arg biosynthesis, (B) intermediates of TCA cycle. Green bars indicate level in wild-type (Arg prototroph).Yellow bars: *arg9*, deficient in N^2-Acetylornithine-aminotransferase, Orange bars: *arg1*, deficient in *N*-Acetylglutamate-5-P reductase, Red bars: *arg7*, deficient in argininosuccinate lyase. Note that a broken bar is used to indicate extremely high levels of argininosuccinate in *arg7*. Crosses indicate actual enzymatic block for each mutant strain. Bar heights correspond to relative quantitation of GC-MS signals and allow comparison of metabolite levels among different strains for the same compound, but not among compounds. Compounds that could not be measured by GC-MS are shaded in grey. Standard errors are indicated (n=5, except for CC-48 n=4).

depleted (Orn, ArgSuc) or exhibit slight accumulation (citrulline). The existence of significant amounts of these intermediates may explain the capacity for residual growth observed with strain CC-861 *arg1*, harboring the corresponding mutation. Glu and Asp accumulate app. 4- and 20-fold, respectively, which may indicate alternative channeling of nitrogen into N-storage amino acids. In contrast to *arg2* and *arg9* cells, intermediates of the TCA-cycle are not uniformly reduced in the *arg1* cells, as fumarate and aconitate accumulate 1.5- and 1.8-fold, respectively.

Cells deficient in NAOAT (CC-2958 *arg9*), show a dramatic reduction of NAO, one of the products of the reaction. As in *arg1* cells, Glu, which is also the donor of the amino-group in the impaired reaction, and Asp are markedly increased, more than 2- and 14-fold, respectively. The direct precursor of the NAO, NAGSA, could not be evaluated as no standard could be made available. Pools of all three downstream intermediates Orn, citrulline and ArgSuc were detected, albeit at reduced levels. Apparently, these decreased levels are insufficient to provide the Arg supply needed to sustain cellular growth in this mutant. TCA-cycle intermediates were all reduced compared to wild-type, though the decrease was less dramatic as in the *arg2* strain.

4 Discussion

4.1 Overview

This study introduces a method for comprehensive analysis of metabolite levels in *Chlamydomonas reinhardtii*. Drawing on protocols for metabolite analysis in yeast and vascular plants the method was adapted for Chlamydomonas and validated especially with respect to harvest, quenching and quantitative extraction, which, due to the diversity of cell structures even within the eukaryote kingdom, cannot simply be adopted from procedures that were designed for a specific group of organisms. Metabolite profiling of Chlamydomonas cells under macronutrient and iron deficiency was used as a test case for the relevance of metabolomic approaches for the characterization of different physiological states in Chlamydomonas.

The comprehensive study of metabolite levels was used to help elucidate the effects of S starvation in *C. reinhardtii*. A metabolomic analysis was used to identify patterns of how metabolite levels are either positively or negatively regulated as cells become starved for S and to define those metabolites that appear to be involved in processes controlled by the transcription factor Sac1. As part of the metabolomic analysis, peak area aliquot ratios are proposed as a tool for systematic reduction of artifact peaks. Multivariate techniques like PCA and HCA are used to characterize the metabolite response to sulfur starvation. A difference criterion and the concept of range coefficients are proposed in order to decide which principal components to retain to characterize relevant biological sources of variance.

Enzyme activities are key factors determining the dynamic and structural properties the metabolic network of the cell. To determine the effects of the loss of specific enzyme activites on the performance of the affected biochemical pathway mutants deficient in enzyme activities in the Arg biosynthetic pathway were examined.

4.2 Methodical Aspects of Metabolite Analysis

Due to its tractability under laboratory conditions Chlamydomonas allows for sampling of large amounts of homogeneous cellular material with growth conditions that can be precisely controlled. Therefore, among photosynthetic eukaryote models, the Chlamydomonas system presents unique opportunities for the generation of high-quality metabolomic data which offers the possibility to address issues such as reproducibility, artifact recognition or applicability of multivariate techniques.

4.2.1 Sample preparation

Sample preparation protocols for metabolite analysis in microbial cultures have been reported for both prokaryotic and eukaryotic systems. The budding yeast *Saccharomyces cerevisiae* generally appears to be a suitable reference point to adapt existing protocols for metabolite extraction for *Chlamydomonas reinhardtii*. For yeast, sampling into a cold methanol solution is a widely applied method that enables separation of cells from the culture medium while stopping cell metabolism.

Critical parameters during the quenching process are the maximum temperature of the biomass and the resistance of the cells to the organic solvent solution used for cooling the material. The Chlamydomonas protocol adopts the widely used rationale to cool and handle cells below –20°C to stop enzymic conversions and preserve metabolite concentrations. The parameters of the quenching step were measured in detail and allow for easy adaptation of the quenching procedure to sample cells at even lower temperatures. However, this would require either increasing the ratio between quenching solution and cell suspension or increasing methanol concentration. Increasing the proportion of quenching solution will reduce yield while increasing methanol concentration may lead to considerable metabolite leakage. Leakage of significant amounts of certain intracellular metabolites has been reported for both yeast and bacteria during exposure in cold methanol solutions containing 50% v/v methanol. Minimizing methanol concentration while maintaining the capability to process large sample volumes up to 100 ml cell suspension has therefore been the aim to settle on the optimal combination of methanol content and mixing ratio. Chlamydomonas cells are quenched in 40% v/v methanol and the results of the isotope-labeling experiments indicate that metabolite leakage is within acceptable limits and is lower than 5% even with cell-wall deficient strains after prolonged exposure to the quenching solution. This indicates that the protocol could be applied to a wide range of Chlamydomonas wild-type and mutant strains and also may be an alternative for published quenching procedures for other microorganisms. However, even though the amount of labeled compounds leaking into the quenching solution was low, the contributing molecular species were not determined. It cannot be ruled out that integrity of Chlamydomonas cells is compromised in a specific way that causes certain low abundant compound classes preferentially to leak from the cells in significant amounts.

For metabolomic approaches, extraction of intracellular metabolites must be both quantitative and comprehensive. The first requirement was measured as the possibility to completely extract cellular chlorophyll from Chlamydomonas cells. Extraction of chlorophyll indicates extensive damage of membranes and other cellular structures and the extraction of low-molecular weight compounds is surmised to be quantitative under these conditions. The combination of chloroform, methanol and water has been routinely used for comprehensive metabolite extraction in higher photosynthetic eukaryotes[7, 146] as well as in other microorganisms[94, 102, 118] and was characterized as an extraction method with high recovery rates for compounds from many different compound classes including phosphorylated compounds[93]. Indeed, compounds from a variety of compound classes, including phosphorylated intermediates, can be found in metabolite profiles from Chlamydomonas in both polar phase extracts and unfractionated extracts. While this indicates that the methanol-chloroform-water mix is generally suitable for broadly unbiased extraction of metabolites from Chlamydomonas, proportions of the three constituents were adapted to account for the elevated water content of cell culture samples and achieve maximum concentration of the extract. In summary, the method presented here is suited for the comprehensive analysis of intracellular metabolites from *Chlamydomonas reinhardtii* and the protocol

has been optimized to ensure rapid inactivation of metabolite conversion, quantitative and unbiased metabolite extraction and maximum extract concentration.

4.2.2 **Artifact recognition and removal**

Besides derivatives of genuine intracellular metabolites, GC-MS chromatograms contain artifact peaks due to compound degradation or modification, side reactions and residues of the derivatization reaction, contamination of reagents, solvents or reaction vessels. While some artifact signals like residues of the stationary phase of the GC capillary column can be recognized by their mass spectrum, artifact peaks of the abovementioned origins in general do not have a universal signature that would allow their distinction by mass spectral features or retention behavior. Artifact signal recognition and removal is therefore difficult to generalize and automate and is usually performed by manual evaluation. Attention must be paid to the artifact issue especially in metabolomics approaches of the actual sense, i.e. where unknown peaks are generally included to study systemic properties of the metabolite complement or search for potentially important novel compounds. Artifact recognition is less an issue in targeted approaches or metabolite profiling where the scope of the analysis is often constrained to a list of peaks which are unambiguously annotated as derivates of established metabolites.

A powerful approach not only for artifact recognition but also, and even more important, for reliable quantification and standardization is in vivo labeling with stable isotopes[204, 205] but requires elaborate strategies for data analysis and comparison of labeled and unlabeled extracts for the purpose of artifact recognition.

Aliquot ratios as introduced in this study provide a straightforward means to recognize and reduce the number of artifacts in a metabolomics dataset and retain only analytes that exhibit proportionality between amount of substance (peak area/ peak height, whichever is used for quantification) and the extracted biomass. The condition is satisfied if and only if the corresponding aliquot ratio reaches the value one. Accumulating analytical errors can lead to deviation from this theoretical value. Thus aliquot ratios set a criterion not only for the recognition of genuine metabolites but also for reliable quantification: Detection of intracellular metabolites which are present in amounts exceeding their linear range of detection will also result in lowered aliquot ratio values and hence be removed from the dataset. In the experiment involving strains CC-1690 and *sac1*, each sample was measured in two different aliquot volumes to provide for a broad base for calculation of aliquot ratios. Generally, a smaller number of ratio values per analyte will be sufficient to obtain a reliable aliquot ratio value so that only a small number of samples needs to be measured in more than one aliquot volume. As sample pairs that are used to calculate the ratio values are derived from the same extract, aliquot ratios are independent of the experimental conditions and thus could be used for artifact recognition across experiments provided that the analyte is detected within linear range. Aliquot ratios appear to be suitable especially for recognition of artifacts that are formed not stoichiometrically in relation to intracellular metabolites. Hence, preferentially artifacts formed during derivatization as side products and residues or contaminations of the reagents and artifacts

originating from contaminations of the reaction vessels or other sources, e.g. injector or solid phase of the capillary column will be exposed by aliquot ratio analysis. Artifacts originating from degradation or modification of the extracted metabolites can be identified if they are formed not stoichiometrically with regard to the original metabolites. Contaminations of the extraction solution will generally not be recognized by an aliquot ratio analysis. Aliquot ratio values for the same analyte calculated from different pairs of samples differ to a certain extent which makes the median value of all calculated aliquot ratios a more robust estimate for the aliquot ratio value of an analyte. Differences of the individual aliquot ratios may be caused by current limitations of automatic peak annotation and quantification (see below). Currently available algorithms may not accurately determine peak areas especially in complex samples, which causes aliquot ratios to vary. Some metabolites may reach intensities out of their range of linear detection under certain experimental conditions and thus produce aliquot ratios that differ significantly. Generally, the precision of aliquot ratios is limited by the repeatability that can be achieved on the analytical platform used for measurement.

As a result of the aliquot ratio analysis for analytes measured in the metabolomic analysis of sulfur starvation, 64.8% of the analytes in the dataset were retained. Among the removed analytes are all added retention index markers and a large number of peaks known to originate from residues of the stationary phase of the capillary column ("column bleeding"), which underlines the usefulness of the approach. The substantial number of peaks removed after aliquot ratio analysis indicates that metabolomic datasets can contain a significant proportion of peaks which are not suitable for further analysis either because automatic quantification is inadequate or they originate from sources other than the extracted biomass.

4.2.3 Peak annotation and identification as major bottlenecks in metabolomic approaches

This study used both metabolite profiling and metabolomics in the actual sense to characterize effects of environmental factors on the metabolite complement in *Chlamydomonas reinhardtii*. The results clearly illustrate the advantages and limitations of either approach in metabolite analysis. Metabolite profiling of Chlamydomonas under deprivation of nitrogen, phosphorus, sulfur and iron focused on analytes which could actually be identified by mass spectral comparison with custom standard libraries. The current limitations of automatic deconvolution and peak annotation become evident especially in such complex mixtures where chromatographic separation does not suffice to resolve all analytes. The deconvolution algorithm compares retention profiles and position of local maxima of fragment ion intensities to resolve overlapping peaks and computationally derive true mass spectra by identification of unique ions for each analyte peak. Identification of corresponding peaks from individual samples involves automatic peak finding and comparison against a chromatogram reference derived from a pooled extract containing equal amounts of extract from all experimental classes involved. Peaks from individual chromatograms are assigned to the reference analytes by virtue of their mass spectral similarity and retention index match. Due to the complexity of the chromatograms, for most analytes mass spectra derived by automatic

deconvolution differ from one chromatogram to the next to a certain extent. This is especially true when comparing different experimental groups that exhibit large differences in total metabolite composition. When setting rigid thresholds for mass spectrometric similarities and retention index match for peak assignment, this procedure may result in a large number of analytes not being reported from individual samples. To exclude such false negatives and ensure that missing values indeed are the consequence of the absence of any detectable analytical signal, all chromatograms were corrected manually for the occurrence of false negative analytes and errors in peak area integration. The restricted scope of the analysis made manual curation of the result of the automatic deconvolution and annotation algorithms feasible. Thus, a complete set of measurements for more than 70 primary metabolites could be obtained. The changes detected within this group are, however, not necessarily the most important changes, as the majority of analytes which lacked identification, were not considered for further analysis or manual curation.

Manual curation of a metabolomics dataset is not feasible if generally all peaks, whether identified or not, are included in the analysis. Accordingly, data analysis has been described as the bottleneck of metabolomic analysis[96] and strategies need to be devised for artifact removal, treatment of missing values and robust estimates of quantification errors. In this study, aliquot ratio analysis is proposed for artifact evaluation (see above). Missing values, which are either due to failures of the automatic deconvolution and peak detection (type II) or true low values below detection limit (type I) are dealt with in several ways. First, this study adopted the strategy that an analyte must be found automatically in all independent samples of at least one experimental class. Metabolites may be abundant only under certain experimental conditions or within a restricted time window. Its signal could therefore be missing or low abundant and therefore inconsistently found in certain classes. Indeed, metabolites whose accumulation is distinctly modulated are of special interest and may be relevant for signaling or metabolic control. Reproducible automatic detection in all samples of at least one class on the other hand indicates general suitability of the analytical method for detection of the analyte which entails adequate sensitivity and restricted impact of matrix effects which could render detection inconsistent. Imputation of missing values consists a second level of missing values treatment in classes where analytes are reported at least once. Successful peak annotation in one instance usually points to type II missing values for samples of the same class, where the peak is not reported. Imputation of the latter with the median of all available measurements from the same class provides a robust estimate for the class-specific abundance of the analyte, although generally this will cause class-specific variance to decrease and may lead to overestimation of the precision of the measurement. A third test comes from the conservative evaluation of response profile patterns. Although it appears generally possible that metabolites fall below the limit of detection and are detected again at the next time point, such discontinuous response profiles were excluded from the analyses. This affected only a small number of analytes with each analyzed strain. As a result of the data pre-processing, 345 analytes (41.1% of the initial reference peak list) containing 51 identified analytes (14.7%) were retained for explorative data analysis. This data matrix contained 23.5% type II missing

values. These numbers illustrate that a well-defined strategy for processing of raw data is essential to produce a dataset that can be used to discern biological causes of metabolite variation. Initial, automatically processed chromatographic data may contain a large number of inconsistently found or quantified peaks and the use of these data without further processing for metabolite analysis is questionable. In both experimental setups the proportion of identified analytes contained in the pre-processed data-sets is low, although libraries of pure standards of primary metabolites were reverse-searched in the chromatogram references. Individual metabolites may be missed due to matrix effects, low concentration in the biological sample, insufficient recovery during sample preparation or a general incapability to be analyzed by GC-MS. However, peak identification is restricted mainly because there is no efficient means for reconstruction of the chemical structures from EI-generated mass spectra. Identification usually relies on comparison with pure standards measured under the same conditions, but such standards are not available for all metabolites implicated in cellular metabolism.

In conclusion, metabolite profiling is advantageous for a restricted set of analytes to be determined and analyzed in greater detail and with higher precision as it allows for manual curation of the computationally derived quantitative data and to maximize the number of identified analytes. Such an analysis may be especially useful for the analysis of specific metabolic pathways or to test a priori hypotheses. Inclusion of a maximal number of variables allows coverage of the main sources of variance in the dataset which is advantageous for establishing general patterns of metabolite response. Large numbers of variables, however necessitate the use of automated procedures for data analysis and have to take into account a certain amount of detection and quantification errors which have to be accounted for by robust strategies for data evaluation.

4.3 GC-MS based metabolite profiling is well suited to analyze metabolites in Chlamydomonas and reveals a variety of metabolic responses during acclimation to nutrient stress

Metabolite analysis of cells deprived of the macronutrients nitrogen, sulfur and phosphorus and the essential trace element iron was used as a test case for a metabolomics approach in *Chlamydomonas reinhardtii*. The GC-MS data obtained contains a wealth of analytical signals and more than 70 metabolites from various compound classes could be positively identified. Detailed investigation of the metabolite response revealed that most of the metabolites under investigation are differentially regulated in response each nutrient limitation. However, some metabolites show qualitatively or even quantitatively concordant changes in two or more of the stress situations. This involves metabolites like pyruvate, PEP or 3PGA which participate in reactions connecting energy metabolism and provisional routes of carbon building blocks for downstream biosynthesis. This corroborates the view that the response to nutrient limitation comprises both specific and general metabolic adaptations. The data also supports the notion that metabolic responses occur as results of the regulation of reaction networks which may exhibit dynamic connectivity in terms of reaction rates and regulational dependencies, rather than as

the result of the uniform activation or repression of entire pathways. This is illustrated by the modulation of the response of metabolites implicated in the biosynthesis of aromatic amino acids: Shikimate, which is a common precursor for tryptophane, tyrosine and phenylalanine, is severely reduced in Fe-deficient cells and reduced to levels below the detection limit in the three other conditions. Chorismate mutase (CM) is considered the committing enzyme in phenylalanine and tyrosine synthesis. Prephenate, which is the product of the reaction catalyzed by CM accumulates under Fe-deficiency, only slightly deviates from control levels in N- and P-deficiency and cannot be detected under S-deficiency. The amino acids themselves also show distinct responses: Iron deprivation leads to levels of 40-50% of the control for all three aromatic amino acids. In N-deprived cells phenylalanine is similarly reduced while tyrosine retains the control level and tryptophane increases 5 fold. S-limitation leads to a slight increase in phenylalanine, a 2 fold increase in tryptophane and a 4.5 fold increase in tyrosine. P deprivation results in decreases of phenylalanine to 40% and slight decreases of tyrosine and tryptophane to about 70%. Thus, metabolite profiling can help to characterize the metabolic response at a more complex level, although the description remains fragmented as the intermediates of established reaction sequences are not covered completely.

Chlamydomonas responds to N deprivation with metabolic adaptations which include up-regulation of N-scavenging uptake systems and active turnover of proteins and nucleic acids to reallocate internal N resources. A second response is the initiation of a developmental programme that results in the formation of sexually competent gametes. Gametogenesis can be seen as one aspect of the cells response to N deprivation as gametes and in particular zygotes appear to be adapted to survive periods of adverse environmental conditions[206]. Both processes appear to share components of the same regulatory gene network[207] and evidence suggests that ammonium may be directly involved in sensing critical internal levels of nitrogen and initiation of the metabolic and developmental response[206]. In this study, cells were assayed after 24 h N deprivation, suggesting that they were fully differentiated gametes, although this was not tested. Using standard TAP-medium, nitrogen is supplied to the cells as ammonium and is assimilated via the GS/GOGAT cycle. Important intermediates of this reaction cycle such as Glu, Gln, and 2OG are severely reduced after 24 h N-starvation which may be a symptom of the general depletion of upstream precursors of N assimilation or reflect generally reduced metabolic acitivity of the gametic state in which the cells essentially stop growing[56, 206]. Chemostat experiments with autotrophically grown and N-limited *Chlamydomonas reinhardtii* and the related Chlorophyceae *Selenastrum minutum* have investigated the integration of carbon and nitrogen metabolism upon resupply of a nitrogen source. Resupply of nitrate, but not ammonium to illuminated cells stimulates carbon respiration and the supply of reductant for nitrate reduction via the oxidative pentose phosphate pathway (OPPP)[208]. Pathway flux is activated by redox regulation of glucose 6-phosphate dehydrogenase (G6PDH), the key regulatory enzyme of the OPPP[209, 210]. Metabolic changes which accompany resupply of nitrate include the immediate and rapid decrease in G6P and increase of 6PG at the onset of nitrate assimilation[208]. Upon NH_4^+ supply, a transient rise in G6P levels is observed too, but 6PG changes only slightly, which is consistent with induction of

starch breakdown as is the increase in G1P[211]. NH_4^+ assimilation leads to a rapid decrease and new lower quasiequilibrium levels for 2OG and Glu and a steady increase in Gln due to provision of 2OG for NH_4^+ assimilation via GS/GOGAT. Immediate decrease of PYR and increase in PEP is consistent with activation of pyruvatkinase (PK) and increased carbon flow via PK through the TCA cycle for de novo production of 2OG as is the decline in malate and the increase in citrate. Furthermore, a rise in FBP, 3PGA and triosephosphate and constant levels of F6P, G6P and isocitrate are observed upon NH_4^+supply to N-limited *Selenastrum minutum*[211]. The different experimental setup does not allow to relate these observations directly to the results obtained with N-starved cells in this study; however, it is noteworthy that the 6PG pool in N-starved cells is extremely reduced (<10%) in comparison with N-replete conditions, while the G6P levels change only slightly (89%). Similarly, Gln and Glu are severly reduced (<20%) while the 2OG level remains relatively high (46%). These data do not allow to reconstruct the dynamic behavior of metabolite levels or their ratios as cells switch between N-sufficient and deficient conditions, but the fact that precursors of the reactions that meet the demands for carbon backbones (GS/GOGAT: 2OG) and electron donors for N assimilation (G6PDH: G6P) are retained at a relatively high level in contrast to the downstream products (6PG, Gln, Glu) and other intermediates (PYR, PEP, DAHP) may indicate a priority for maintaining the capability for immediate N assimilation as N sources become available even under conditions of decreased metabolic activity and arrested growth.

The increase of organic acids in roots, leaves and xylem is a well documented response to Fe-deficiency among higher plants. Specifically the accumulation of citrate is implicated in mechanisms for Fe acquisition, formation of stable water-soluble complexes, cation/ anion homeostasis or supply of reducing power for ferric chelate reduction[212]. *Chlamydomonas reinhardtii* was shown to exhibit a similar response to iron deficiency as in strategy I plants, that involves an inducible Fe^{3+}- reductase activity and regulated iron uptake[59-61]. The finding of elevated levels of organic acids is consistent with these earlier observations. Given the variety of habitats of *C. reinhardtii* and the restricted bioavailability of iron in both terrestrial and aquatic environments[213, 214], the Fe-starvation induced increase in succinate and citrate could well be related to their iron-chelating properties. Hydroxyproline is believed to be formed only in proteins and is a prominent constituent in the Hyp-rich glycoprotein framework forming the Chlamydomonas cell wall[215-217]. In addition, cell wall proteins are known to be extensively sulfated and to be rearranged during S-starvation[82, 83] while several prolyl 4-hydroxylases are down-regulated[42]. Thus the rise in 4-hydroxyproline could be the result of enhanced degradation of cell-wall proteins. An albeit much more modest increase in Hyp has also been observed with Arabidopsis under S-deprivation[186]. Depletion of internal S-levels is reflected in marked decreases in the S-containing amino acids Cys and Met. OAS, which is the direct precursor in Cys biosynthesis could not be measured as it is coeluting with TRIS, which is used as buffering compound in the TAP culture medium. TRIS produces detector signals of very high intensity and prevents detection of any coeluting compounds. Ser levels, in contrast to the other nutrient stress situations, was found to be slightly increased. The pattern of accumulation and depletion for most of the amino acids is consistent with that in *Arabidopsis thaliana* seedlings under S

deprivation[186] with the exceptions of N-containing Asn and Gln, which are reduced in Chlamydomonas but accumulate in S-starved Arabidopsis. Some degree of cross regulation of P- and S-response pathways[81] in Chlamydomonas has been suggested. The accumulation of S-containing amino acids Met and especially Cys in P- but not S-deprived Chlamydomonas cells may indicate an enhanced capacity for S-assimilation also under P-starvation. A number of metabolites is similarly affected by N-, P-, and S-starvation. These changes, rather than pointing to specific responses, may indicate general metabolic responses in unfavourable growth conditions. This notion is supported by the fact that a number of metabolites linking important circuits of primary metabolism (e.g. PYR, 2OG) are affected in this way. Besides cessation of growth, the regulation of photosynthetic electron transport has been characterized as a general response to adjust metabolism and sustain viability when nutrient levels fall[55]. While the decline of photosynthetic electron transport in N-deprived Chlamydomonas cells is due to the loss of the cytochrome b_6f complex[218] during P and S limitation cells undergo a transition of the photosynthetic apparatus to state 2 which allows them to redistribute absorbed excitation energy. Both conditions result in a 75% decrease of maximal O_2 evolution that correlates with the reduction of electron flow through photosystem II, although with P-deprivation a longer treatment is needed to observe the effect[73].

The delayed response of P-deprived cells may be due to the mobilization of internal phosphate reserves. Chlamydomonas cells possess electron dense vacuoles containing large amounts of PP_i and short and long chain polyphosphate alongside with magnesium, calcium and zinc [69]. They presumably serve as P_i storage and buffer a critical P_i concentration in the cytoplasma, although also P-starved cells contain polyphosphate bodies of the normal size[70] and most of the inorganic phosphate taken up by P_i-starved Chlamydomonas cells is still accumulated as polyphosphate[71]. Therefore, it has been suggested that apart from P_i storage these organelles may serve also as internal Calcium stores and may have a role in inositol-1,4,5-trisphosphate/calcium signaling[70].

Apart from investigating differences in the levels of individual metabolites, factor analytic techniques can be used to quantitatively examine the sources of variation between different experimental conditions. Principal component analysis serves to obtain a multivariate measure of the variability of the metabolite profiles between different treatments and the relative homogeneity among replicate samples of each group. It was successfully applied to separate Chlamydomonas samples from different nutrient stress treatments with the biological variance between the groups being distinctly larger than the analytical variance within each group. This indicates that the metabolic readouts are indeed useful to differentiate different physiological conditions in Chlamydomonas. The positional shift of the metabolite profiles for P-deprived cells after projection onto the PC1-PC2 plane as compared to the other treatments may reflect the divergent alteration of metabolism due to the mobilization of internal P_i reserves and alleviation of external phosphate deficiency during the first 24 h of treatment.

4.4 Metabolomic analysis allows to characterize both general and specific aspects of the metabolic response to S deprivation

Metabolomic analysis conceptually differs from metabolic profiling in that it aims at the comprehensive analysis of metabolite signals using essentially all available metabolite data. Apart from the analysis of compounds that can be identified and mapped to specific reactions and metabolic pathways, metabolomic approaches provide the distinctive opportunity to employ measurements of both identified and unidentified analytes to address general, metabolome-wide features of the metabolic response for the biological process under consideration.

The non-linear fashion in which the levels of many metabolites implicated in core metabolic pathways were affected during the 24 h period of sulfur starvation reflects the convoluted nature of plant metabolism and possibly changing phases of the stress response related to the duration of nutrient deprivation and the corresponding impact on the potential to grow and divide. While early responses could be primarily aimed at the activation of mechanisms to make the supply of sulfur more effective, extended periods of nutrient starvation might cause a more general adjustment of metabolic activity to ensure survival of the cell which under severe nutrient limitation may eventually lead to responses that reflect the exhaustion of the capacity for metabolic regulation, rather than maintenance of homeostasis.

As was expected under S-limiting conditions, Cys, into which sulfur from external sources is primarily assimilated after initial reduction, decreased in both the wild-type and the *sac1* mutant strain, although Cys levels appeared to be depleted quicker in the mutant. The *sac1* mutant has been characterized as being deficient of virtually all the specific responses to S deprivation in Chlamydomonas, including mechanisms to upregulate elements for scavenging sulfur from extracellular sources. The marked decrease of cysteine and the strong increase of 3PGA and serine which are both along the biosynthetic pathway of cysteine 2 h after imposition of S deprivation may be indicative of an unabated cysteine consumption and demand in the *sac1* mutant due to the inability to adjust cellular metabolism to the diminished S supply. Consistent with this conjecture, the only slight increases of 3PGA and serine, and the more moderate decrease in cysteine in the wild-type strain are consistent with the adjustment of cellular metabolism for less cysteine consumption as well as increased capacity to scavenge and assimilate residual S through enhanced capacity for uptake and reduction and precursor accumulation. Interestingly, wild-type cells show lowered levels of pyruvate and TCA cycle intermediates already 2 h after imposition of S deprivation, which could indicate an quick decrease of respiratory carbon flow. Generally, mitochondrial activity is believed to continue in the light[219] to provide cells with ATP, NADH, and TCA cycle carbon skeletons for biosynthetic activity[220-223]. Regarding the production of carbon intermediates for biosynthesis, citrate is believed to be the primary carbon skeleton exported[224] and converted in the cytosol to 2OG[219, 225]. In contrast to the reaction in wild-type cells, citrate and 2OG pools are not depleted in the mutant, which may indicate failure to adjust the rate of supply of carbon skeletons for biosynthesis to the nutrient limiting conditions. Possibly, regulational cues that link supply of carbon

skeletons to the rate of consumption of 2OG by ammonia assimilation into glutamate and glutamine, which exhibit rapid decreases in both mutant and parental strains, are compromised in the *sac1* mutant.

Down-regulation of photosynthetic electron transport has been shown to be a critical component of the acclimation of *C. reinhardtii* to S limiting conditions[42, 80] and to be regulated by *SAC1*[73]. In contrast to wild-type cells, 3PGA levels are increased in the mutant during the first 10 h of S deprivation. Being the primary net product of the Calvin cycle, this may be another indicator for the inability of the *sac1* cells to tailor its metabolic machinery to the diminished nutrient supply by failing to adjust rates of photosynthetic carbon fixation.

CC-1690 and the *sac1* mutant display different patterns of accumulation or depletion of hexose pools in response to S deprivation. Specifically, mutant cells fail to accumulate glucose after 5 h while they show elevated levels of mannose especially after 10 h. The *SAC1* gene product bears similarity to anion transporters[226] and the deduced Sac1 polypeptide sequence and phenotype of the *sac1* mutant have some similarities with the Snf3p polypeptide of yeast and the phenotype of the *snf3* mutant, respectively[42]. Snf3p is a yeast plasma-membrane localized glucose-sensing protein at the top of a signal transduction pathway that governs expression of genes involved in hexose transport and utilization[227]. These findings and the observed differences in the modulation of hexose pools raise the possibility that Sac1 has a regulatory role also in hexose utilization as part of the sulfur stress response.

For most amino acids the pattern of pool modulation is similar in both the mutant and wild-type strains, which indicates that certain adaptational responses occur despite loss of function of *SAC1*. Whereas most amino acids show diminishing pools, proline exhibits transient increases in both strains with *sac1* cells showing a longer and higher accumulation. Accumulation of proline in plants under stress conditions has been associated with reduced damage to membranes and proteins[228], regulation of redox state[229], osmoprotection[230], heavy metal detoxification[231] and response to oxidative stress[232]. Increased free Pro levels were shown to provide enhanced tolerance to Cd stress in *C. reinhardtii* by reducing Cd-induced free radical damage and by maintaining higher GSH levels, which facilitates Cd sequestration and detoxification[231]. Several transcripts involved in limiting oxidative stress were found to increase in both wild-type and *sac1* cells following exposure to S deprivation[42] including glutathione peroxidase (GPX1) and chloroplast localized iron superoxide dismutase (FSD1), the latter catalyzing dismutation of superoxides which can form when excess excitation energy is absorbed by the photosynthetic apparatus. Possibly, Pro accumulation under S deficiency reflects an element of the response to encounter oxidative stress experienced by nutrient limited cells and the even higher levels of Pro in the *sac1* mutant reflect more intense oxidative stress in the mutant strain due to the failure to adjust photosynthetic and respiratory electron transport which may provoke formation of higher levels of reactive oxygen species.

After 24 h S starvation wild-type cells exhibit increased levels of G6P, 3PGA and 2OG and levels of Phe, Tyr, Thr and Ile recover to control values and also in the mutant strain these amino acids are distinctly higher than in the 2, 5, and 10 h time points, although they do not reach control levels. Death of *sac1* cells during S deprivation is observed after 24 to 48 h, whereas wild-type cells survive under these conditions

for prolonged periods of time[80]. Possibly, the 10 h to 24 h interval marks transition into a phase in the S starvation response that could involve enhanced protein degradation leading to accumulation of amino acids or direction of carbon flow into starch reserves (rise in G6P in wild-type cells). Transcripts of genes implicated in starch synthesis accumulate under S deprivation and this response was suggested to contribute to control redox poising in the thylakoid membrane[42]. While the physiological implications of the replenishment of these compounds are uncertain, this pattern appears to be a wide-spread phenomenon, as depletion and recovery after 24 h S deprivation is the common pattern for compounds assigned to pattern group B in cluster analysis.

Hierarchical cluster analysis has revealed five main patterns of metabolite regulation in response to sulfur deprivation in *C. reinhardtii* and the prevalence of each regulational type could be quantitated in terms of elements per pattern group and cluster, respectively. Recovery following depletion at one or more time points, as exemplified by the amino acids Phe, Tyr, Thr and Ile, is a common pattern found for 18% and 11% of the metabolites in the wild-type and in the mutant strain, respectively. The most prominent feature is characterized by moderate to marked gradual decrease of metabolite levels of compounds assigned to pattern group A comprising 36% and 69% of metabolites in the wild-type and the mutant strain, respectively. This striking difference is accounted for by the reassignment of a large number of metabolites assigned to one of the pattern groups B-D in CC-1690 to pattern group A in the mutant strain. The chosen metabolomic approach therefore allows to characterize the effect of the *sac1* mutation in a semi-quantitative manner on the whole metabolic network: Inactivation of *SAC1* results in a massive incapability to sustain processes that normally lead to transient or permanent accumulation of the levels of certain metabolites or recovery of metabolite levels after initial down-regulation. This is especially true for metabolites for which accumulation above control level after 24 h S deprivation is observed (pattern group D, 20% in CC-1690, 2% in *sac1*).

Sulfur deprivation leads to widespread changes in metabolite composition in wild-type cells. While both positive and negative regulation of metabolite levels can contribute to adjustment of metabolism to limiting sulfur, transient or permanent accumulation, due to the cost of biosynthesis, intuitively appears to be a feature more likely observed with metabolites that exert an active role in re-shaping the metabolic network. The HCA results allow for a quantitative estimate of the proportion of such metabolites: 17% of the compounds analyzed are found in clusters whose elements transiently increase and 20% of the compounds are found to increase permanently, i.e. for one or more time points towards the end of the experiment. Reduction of these groups of metabolites to 9% and 2%, respectively in the *sac1* strain is consistent with the loss of function phenotype of *sac1* cells and the available evidence that suggests that *SAC1* plays a central role in activating metabolic and physiological S deprivation responses.

When considering possible roles of metabolites in signaling or regulation of flux in metabolic pathways, it must be kept in mind, however, that the dataset used for multivariate analysis contains only a fraction of the suite of metabolites present in Chlamydomonas cells due to the limitations of the sample preparation (see 1.2.2.1) and measurement by GC-MS (see 1.2.2.2) and thus, important elements of the metabolic

reaction network, either known or unknown, may not be represented. Also, to infer causal relationships in terms of exertion of metabolic control, patterns based on correlation of the levels of individual metabolites need to be combined with complementary evidence from the analysis of fluxes or enzyme activities, isotope labeling or effect of compound analogs.

Principal components analysis is frequently used as a tool for classification of samples in metabolomic experiments. In this work, data analysis by PCA was used to actually characterize the driving principles of adaptation to S deficiency which account for the largest source of variance in the metabolic composition of the individual samples. Due to the high dimensionality and comparably small sample size of metabolomic datasets, individual metabolites rarely exhibit high correlation or anti-correlation (high and low loadings, respectively). It is therefore often not possible to single out individual metabolites to interpret principal components. Rather, they usually reflect the correlated changes of many metabolites. In addition to the separation of strain- and time-specific metabolic phenotypes PCA has revealed continuous gradual depletion and transient accumulation of metabolites as the two largest sources of variance between samples. It has also shown that the wild-type response to S deprivation is characterized by concurrent accumulation of certain compounds and that this source of variance is virtually absent in the *sac1* mutant. PCA and HCA therefore provide consistent and complementary descriptions of the global scheme of acclimation to S deficiency by showing that the exposed response patterns are relevant both in terms of numbers of metabolites showing the corresponding behavior and distinguishing different metabolic phenotypes (fraction of total variance explained).

Zhang et al. conducted gene expression analysis of *sac1* and a parental wild-type strain[42]. They observed changes in transcript abundance ≥ 2-fold during 24 h S deprivation for 16.7% and 11.5% of the genes in the wild-type and the mutant strain, respectively. In contrast, this study has established changes ≥2-fold for 43% and 83% of all represented metabolites in wild-type and mutant cells, respectively. If only changes ≥4-fold are considered, still 31% of the metabolites are selected in the mutant and 18% in the wild-type. Due to a number of factors such as the use of different wild-type background strains, different time course of analysis and incomplete representation of both genes and metabolites in either dataset, full integration of the data from both studies appears to be difficult. Nonetheless, the proportion of genes exhibiting altered transcript abundance following S deprivation appears to be higher in the wild-type, whereas the proportion of metabolites exhibiting marked changes is higher in the *sac1* mutant. This observation may reflect the extensive genetic regulation being exerted in a wild-type genetic background to encounter the nutrient stress situation and preserve metabolic homeostasis, whereas malfunction of *SAC1* leads to an impaired transcriptional response with less genes involved that eventually results in widespread metabolic changes and extreme stress.

A number of metabolites have been measured under conditions of S limitation in both the metabolic profiling experiment using strain CC-125 and in the time-resolved metabolomic approach using the mutant strain *sac1* and its parental wild-type strain CC-1690. For a number of metabolites the observed changes exhibit consistency even in terms of quantitative changes and for most metabolites measured in

both experiments the direction of change agrees. For some metabolites, however, direction and magnitude of change after 24 h S deprivation differs in both experiments. This includes levels of MI, IbGAL and 2OG (increased in CC-1690, depleted in CC-125) and Pro, Ser, and Asp levels (depleted in CC-1690, increased in CC-125). However, Pro and Ser exhibit transient increases during S deprivation in CC-1690 as well. When comparing the results of both experiments, the different experimental setup and possible differences between both strains have to be taken into account. For metabolic profiling of Chlamydomonas under N, P, Fe and S deprivation crude extracts were separated into a polar and non-polar phase and only the polar phase analyzed. In contrast, the DTD-technology enabled analysis of complete extracts of CC-1690 and *sac1*. This may affect recovery and derivatization of individual compounds in the mixture. While both CC-1690 and CC-125 are widely used as wild-type references and have served as parental backgrounds for the isolation of numerous mutations in Chlamydomonas research, both strains exhibit important differences, most notably, CC-125 lacks nitrate reductase activity[14]. Taken together, the results of both experiments impart a consistent view on the adaptation of Chlamydomonas to S deprivation. At the same time, this highlights the need for strict standardization[156] of large scale metabolite analysis with respect to the biological system studied, experimental conditions and methods used for sample preparation and measurement.

4.5 Metabolite analysis of Arg auxotrophy provides insight into the regulation of Arg biosynthesis

The arginine biosynthesis pathway presents the opportunity to apply GC-MS based metabolite analysis in Chlamydomonas to a well-defined biochemical module that can be perturbed by setting selective breakpoints through the specific loss of enzymatic activity. The appeal of this system in Chlamydomonas comes from the fact, that for most enzymes implicated in the pathway, mutants have been described. For five of the arginine-requiring strains available from culture collections the arginine-auxotroph phenotype could be confirmed. Three strains representing three different genetic loci were amenable to the sample preparation protocol developed for Chlamydomonas in this study. Metabolite pools in each strain appear to be regulated quite differently after withdrawal of Arg from the growth medium. Presumably, the removal of external Arg triggers endogenous Arg biosynthesis in all the strains, as intracellular Arg levels are depleted by incorporation into protein and other biosynthetic activity. This allows the analysis of the regulation of the Arg biosynthetic pathway by analyzing shifts in the concentrations of the Arg biosynthesis intermediates in comparison to the wild-type situation when individual steps in the reaction sequence are disabled and to characterize how the effects of the genetic perturbation propagate in the biochemical network. At the same time the methodology of metabolic profiling allows to monitor system-wide changes and relate them to the actual biochemical block.

The enormous accumulation of argininosuccinate (500-fold) in the *arg2* strain lacking ASL activity suggests that cells channel considerable resources into Arg biosynthesis in the attempt to compensate for externally supplied Arg. The amassment of ArgSuc suggests that synthesis of this intermediate likely is a

metabolic cul-de-sac in the *arg2* strain, as no other reactions appear to consume ArgSuc. This may indicate that also under wild-type conditions ArgSuc is consumed only by the ASL reaction and entirely committed to Arg biosynthesis. Also, ArgSuc appears not to have any relevance for allosteric regulation or feedback inhibition of the Arg biosynthetic pathway, which would probably prevent accumulation of large amounts of ArgSuc. While also citrulline accumulates in the *arg2* strain, the ASS reaction appears to sustain an equilibrium that allows for massive accumulation of ArgSuc. Levels of the intermediates of the TCA-cycle are severely reduced in the *arg2* strain which links impaired ASL-activity to the main processes of primary metabolism. The severe pool reduction may indicate a greatly reduced overall metabolic activity consistent with quick cessation of growth in the *arg2* mutant.

Surprisingly, levels of the intermediates downstream of the block of the NAGPR catalyzed formation of NAGSA in the CC-861 *arg1* strain are only slightly reduced or, as is the case with NAO and citrulline, exceed wild-type levels. The strain exhibits a residual capacity for growth without externally supplied Arg which is consistent with existence of Arg precursor pools and hence synthesis of a certain amount of endogenous Arg. The dramatic increase of NAG, the entry point for Orn biosynthesis, specifically seen in *arg1* cells supports the idea that the pathway is blocked also in this strain and intermediates start to accumulate upstream of the blockage as NAG or, although this could not be evaluated, as NAG5P. Which biochemical activities could lead to a more than 3-fold increase of NAO, if the default reaction sequence via NAGPR is blocked? Pro and Arg biosynthesis are linked by the activity of ornithine aminotransferase (OAT) which catalyzes the interconversion of glutamate-5-semialdehyde (GSA) and Orn and raises the possibility of an alternate pathway from Glu to Orn without acetylation[85] (Figure 24). Accumulation of NAG could favor consumption of Glu by Δ^1-pyrroline-5-carboxylate synthetase and formation of GSA which is then metabolized to Orn. Orn could then be used as substrate for citrulline synthesis and the ensuing steps of Arg biosynthesis. The unusual amassment of NAG could, however, at the same time shift the equilibrium for the NAOGAcT-reaction in the reverse direction so that the acetyl-group is transferred from NAG to Orn, leading to accumulation of NAO.

As the phenotype of strain CC-861 *arg1* was tested on the level of Arg auxotrophy, rather than enzyme activity, it can, however, not be ruled out, that the cells possess residual NAGPR activity which could account for the formation of NAO and the metabolite levels observed.

OAT activity could account for the residual levels of Orn also in the CC-2958 *arg9* mutant strain lacking NAOAT activity. In contrast to CC-861 *arg1* this strain does not show any residual growth without external Arg supply which suggests that the low endogenous levels of Orn, citrulline, and ArgSuc detected do not suffice to sustain prototrophic growth. Incidently, NAG accumulation is much smaller in this strain than in *arg1* cells, which could indicate that NAGSA is diverted to other biosynthetic activities or exerts feedback control on the activity of the first steps of Orn synthesis.

Strain CC-2958 harbors besides the *arg9* mutation the *shf1-253* mutant allele which leads to impaired flagellar assembly (short flagella) at RT and stop of flagellar assembly at 34°C. Cells with this mutation

have normal ultrastructure and motility at 25°C, so that no interference with the original *arg9* mutant phenotype is assumed.

Both *arg1* and *arg9* cells exhibit markedly increased levels of Glu and especially Asp. Generally, this may reflect reallocation of N to these amino acids when flux into the N-containing intermediates of the Arg-biosynthetic pathway is inhibited. Increase of Asp in *arg7* is much lower than in the other two strains which may be the result of Asp consumption by synthesis and accumulation of ArgSuc in *arg7* cells as major sink for the Asp backbone.

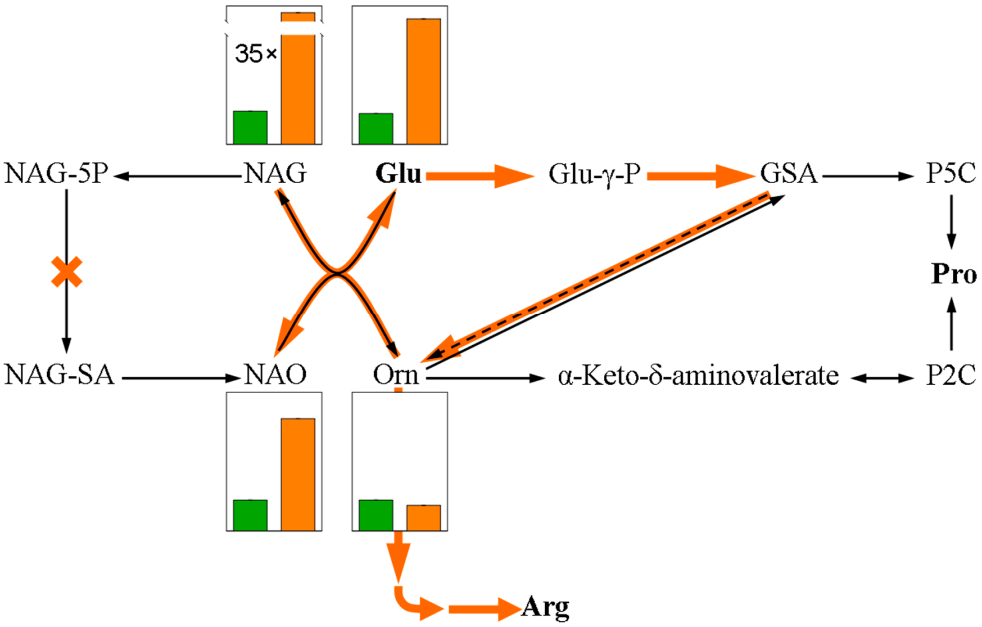

Figure 24: Hypothetical model for synthesis of ornithine in *arg1* cells. Black arrows designate standard reaction routes in arginine and proline synthesis. Orange arrows designate reactions occurring when NAGPR activity (orange cross) is disabled. Orange bars indicate metabolite levels in *arg1* cells relative to the wild-type level (green bars).

5 Conclusions

Metabolomic analysis is a well suited method to detect numerous changes of metabolite levels in response to environmental and genetic perturbations in Chlamydomonas and to complement other functional genomics techniques in Chlamydomonas research. The method introduced here was optimized with regard to several critical aspects of sample preparation, metabolite measurement and data analysis to ensure that the analytical signals represent in-vivo amounts of intracellular metabolites. The sample preparation protocol tailored to the analysis of cells of suspension cultures is amenable to a wide range of Chlamydomonas strains and could generally also applied to suspension cultures of other organisms. The implementation of aliquot ratio analysis for the systematic recognition of GC-MS artifacts, range coefficients for distinction of technical and biological sources of variance and a difference criterion for determination of the numbers of factors to retain when metabolomic data matrices are explored by PCA may be beneficial for the analysis of metabolite data from other biological sources as well. The level of accuracy observed in this study suggests that Chlamydomonas may be highly suitable as a model for metabolomic research, especially in the context of photosynthetic processes. The possibility to control growth conditions precisely and to obtain large amounts of homogeneous sample material is a clear advantage in the attempt to study complex metabolic changes in fine-scaled gradients of conditions or with high temporal resolution.

Metabolite profiling is suitable for the distinction of different metabolic phenotypes. Metabolites implicated in many different processes are affected in their concentration during adaptation to nutrient deprivation corroborating the view that nutrient limitation leads to a system-wide rearrangement of metabolic activity to adjust acquisition and consumption of the limiting nutrient and match its availability with the potential to grow and divide.

Metabolomic analysis has revealed both specific and general characteristics of the response of wild-type cells and *sac1* mutants to S deprivation. Specific aspects of the metabolite response could be related to other findings, e.g. the increase of proline to oxidative stress. Five main types of response patterns of metabolite pools are observed under sulfur deprivation, of which the most prominent is the gradual decline of metabolite pools as S depletion continues. The metabolite response of the *sac1* mutant strain is characterized by a massive incapability to sustain processes that normally lead to transient or permanent accumulation of the levels of certain metabolites or recovery of metabolite levels after initial down-regulation.

Arginine auxotroph mutants were used to probe the potential of metabolite analysis for investigation of how genetic perturbations propagate in the biochemical network. Enzymatic blocks in the Arg biosynthetic pathway could be characterized by precursor accumulation, like the amassment of argininosuccinate in *arg2* cells, and depletion of downstream intermediates, e.g. NAO, Orn, and ArgSuc depletion in *arg9* cells. The parallel examination of a number of pathway intermediates facilitated the generation of hypotheses about alternative pathways to account for residual growth of *arg1* cells lacking *N*-Acetylglutamate reductase.

6 References

1. Kitano, H. Systems biology: A brief overview. Science 295, 1662-1664 (2002).

2. Stelling, J., Sauer, U., Szallasi, Z., Doyle, F. J., 3rd & Doyle, J. Robustness of cellular functions. Cell 118, 675-85 (2004).

3. Fiehn, O. Metabolomics - the link between genotypes and phenotypes. Plant Molecular Biology 48, 155-171 (2002).

4. Kromer, J. O., Sorgenfrei, O., Klopprogge, K., Heinzle, E. & Wittmann, C. In-depth profiling of lysine-producing Corynebacterium glutamicum by combined analysis of the transcriptome, metabolome, and fluxome. J Bacteriol 186, 1769-84 (2004).

5. Bino, R. J. et al. Potential of metabolomics as a functional genomics tool. Trends Plant Sci 9, 418-25 (2004).

6. Weckwerth, W., Loureiro, M. E., Wenzel, K. & Fiehn, O. Differential metabolic networks unravel the effects of silent plant phenotypes. Proc Natl Acad Sci U S A 101, 7809-14 (2004).

7. Cook, D., Fowler, S., Fiehn, O. & Thomashow, M. F. A prominent role for the CBF cold response pathway in configuring the low-temperature metabolome of Arabidopsis. Proc Natl Acad Sci U S A 101, 15243-8 (2004).

8. Foyer, C. H., Parry, M. & Noctor, G. Markers and signals associated with nitrogen assimilation in higher plants. J Exp Bot 54, 585-93 (2003).

9. Buchholz, A., Hurlebaus, J., Wandrey, C. & Takors, R. Metabolomics: quantification of intracellular metabolite dynamics. Biomol Eng 19, 5-15 (2002).

10. Sauer, U. & Schlattner, U. Inverse metabolic engineering with phosphagen kinase systems improves the cellular energy state. Metab Eng 6, 220-8 (2004).

11. Shi, Y., Evans, J. E. & Rock, K. L. Molecular identification of a danger signal that alerts the immune system to dying cells. Nature 425, 516-21 (2003).

12. Harris, E. H. The Chlamydomonas sourcebook : a comprehensive guide to biology and laboratory use (Academic Press, San Diego, 1989).

13. Grossman, A. R. et al. Chlamydomonas reinhardtii at the crossroads of genomics. Eukaryot Cell 2, 1137-50 (2003).

14. Harris, E. H. Chlamydomonas as a model organism. Annual Review of Plant Physiology and Plant Molecular Biology 52, 363-406 (2001).

15. Lefebvre, P. A. & Silflow, C. D. Chlamydomonas: the cell and its genomes. Genetics 151, 9-14 (1999).

16. Rochaix, J. D. Post-transcriptional regulation of chloroplast gene expression in Chlamydomonas reinhardtii. Plant Mol Biol 32, 327-41 (1996).

17. Rochaix, J. D. Chlamydomonas reinhardtii as the photosynthetic yeast. Annu Rev Genet 29, 209-30 (1995).

18. Kindle, K. L. High-frequency nuclear transformation of Chlamydomonas reinhardtii. Methods Enzymol. 297, 27-38 (1998).

19. Shimogawara, K., Fujiwara, S., Grossman, A. & Usuda, H. High-efficiency transformation of Chlamydomonas reinhardtii by electroporation. Genetics 148, 1821-8 (1998).

20. Mayfield, S. P. & Kindle, K. L. Stable nuclear transformation of Chlamydomonas reinhardtii by using a C. reinhardtii gene as the selectable marker. Proc Natl Acad Sci U S A 87, 2087-91 (1990).

21. Rochaix, J., Fischer, N. & Hippler, M. Chloroplast site-directed mutagenesis of photosystem I in Chlamydomonas: electron transfer reactions and light sensitivity. Biochimie 82, 635-45 (2000).

22. Bateman, J. M. & Purton, S. Tools for chloroplast transformation in Chlamydomonas: expression vectors and a new dominant selectable marker. Mol Gen Genet 263, 404-10 (2000).

23. Ramesh, V. M., Bingham, S. E. & Webber, A. N. A simple method for chloroplast transformation in Chlamydomonas reinhardtii. Methods Mol Biol 274, 301-7 (2004).

24. Remacle, C., Cardol, P., Coosemans, N., Gaisne, M. & Bonnefoy, N. High-efficiency biolistic transformation of Chlamydomonas mitochondria can be used to insert mutations in complex I genes. Proc Natl Acad Sci U S A 103, 4771-6 (2006).

25. Debuchy, R., Purton, S. & Rochaix, J. D. The argininosuccinate lyase gene of Chlamydomonas reinhardtii: an important tool for nuclear transformation and for correlating the genetic and molecular maps of the ARG7 locus. Embo J 8, 2803-9 (1989).

26. Auchincloss, A. H., Loroch, A. I. & Rochaix, J. D. The argininosuccinate lyase gene of Chlamydomonas reinhardtii: cloning of the cDNA and its characterization as a selectable shuttle marker. Mol Gen Genet 261, 21-30 (1999).

27. Fernandez, E. et al. Isolation and characterization of the nitrate reductase structural gene of Chlamydomonas reinhardtii. Proc Natl Acad Sci U S A 86, 6449-53 (1989).

28. Stevens, D. R., Rochaix, J. D. & Purton, S. The bacterial phleomycin resistance gene ble as a dominant selectable marker in Chlamydomonas. Mol Gen Genet 251, 23-30 (1996).

29. Berthold, P., Schmitt, R. & Mages, W. An engineered Streptomyces hygroscopicus aph 7" gene mediates dominant resistance against hygromycin B in Chlamydomonas reinhardtii. Protist 153, 401-12 (2002).

30. Ohresser, M., Matagne, R. F. & Loppes, R. Expression of the arylsulphatase reporter gene under the control of the nit1 promoter in Chlamydomonas reinhardtii. Curr Genet 31, 264-71 (1997).

31. Fuhrmann, M. et al. Monitoring dynamic expression of nuclear genes in Chlamydomonas reinhardtii by using a synthetic luciferase reporter gene. Plant Mol Biol 55, 869-81 (2004).

32. Matsuo, T., Onai, K., Okamoto, K., Minagawa, J. & Ishiura, M. Real-time monitoring of chloroplast gene expression by a luciferase reporter: evidence for nuclear regulation of chloroplast circadian period. Mol Cell Biol 26, 863-70 (2006).

33. Fuhrmann, M., Oertel, W. & Hegemann, P. A synthetic gene coding for the green fluorescent protein (GFP) is a versatile reporter in Chlamydomonas reinhardtii. Plant J 19, 353-61 (1999).

34. Schroda, M. RNA silencing in Chlamydomonas: mechanisms and tools. Curr Genet 49, 69-84 (2006).

35. Shrager, J. et al. Chlamydomonas reinhardtii genome project. A guide to the generation and use of the cDNA information. Plant Physiol 131, 401-8 (2003).

36. http://genome.jgi-psf.org/Chlre3/Chlre3.home.html

37. Eberhard, S. et al. Generation of an oligonucleotide array for analysis of gene expression in Chlamydomonas reinhardtii. Curr Genet 49, 106-24 (2006).

38. Lilly, J. W., Maul, J. E. & Stern, D. B. The Chlamydomonas reinhardtii organellar genomes respond transcriptionally and post-transcriptionally to abiotic stimuli. Plant Cell 14, 2681-706 (2002).

39. Miura, K. et al. Expression profiling-based identification of CO2-responsive genes regulated by CCM1 controlling a carbon-concentrating mechanism in Chlamydomonas reinhardtii. Plant Physiol 135, 1595-607 (2004).

40. Im, C. S., Zhang, Z. D., Shrager, J., Chang, C. W. & Grossman, A. R. Analysis of light and CO2 regulation in Chlamydomonas reinhardtii using genome-wide approaches. Photosynthesis Research 75, 111-125 (2003).

41. Moseley, J. L. et al. Genome-based approaches to understanding phosphorus deprivation responses and PSR1 control in Chlamydomonas reinhardtii. Eukaryot Cell 5, 26-44 (2006).

42. Zhang, Z. et al. Insights into the survival of Chlamydomonas reinhardtii during sulfur starvation based on microarray analysis of gene expression. Eukaryot Cell 3, 1331-48 (2004).

43. Bisova, K., Krylov, D. M. & Umen, J. G. Genome-wide annotation and expression profiling of cell cycle regulatory genes in Chlamydomonas reinhardtii. Plant Physiol 137, 475-91 (2005).

44. Stolc, V., Samanta, M. P., Tongprasit, W. & Marshall, W. F. Genome-wide transcriptional analysis of flagellar regeneration in Chlamydomonas reinhardtii identifies orthologs of ciliary disease genes. Proc Natl Acad Sci U S A 102, 3703-7 (2005).

45. Cardol, P. et al. The mitochondrial oxidative phosphorylation proteome of Chlamydomonas reinhardtii deduced from the Genome Sequencing Project. Plant Physiol 137, 447-59 (2005).

46. Stauber, E. J. & Hippler, M. Chlamydomonas reinhardtii proteomics. Plant Physiol Biochem 42, 989-1001 (2004).

47. Pazour, G. J., Agrin, N., Leszyk, J. & Witman, G. B. Proteomic analysis of a eukaryotic cilium. J Cell Biol 170, 103-13 (2005).

48. Hippler, M., Klein, J., Fink, A., Allinger, T. & Hoerth, P. Towards functional proteomics of membrane protein complexes: analysis of thylakoid membranes from Chlamydomonas reinhardtii. Plant Journal 28, 595-606 (2001).

49. Wagner, V. et al. Analysis of the phosphoproteome of Chlamydomonas reinhardtii provides new insights into various cellular pathways. Eukaryot Cell 5, 457-68 (2006).

50. Forster, B., Mathesius, U. & Pogson, B. J. Comparative proteomics of high light stress in the model alga Chlamydomonas reinhardtii. Proteomics (2006).

51. Li, J. B. et al. Comparative genomics identifies a flagellar and basal body proteome that includes the BBS5 human disease gene. Cell 117, 541-52 (2004).

52. Pazour, G. J. Intraflagellar transport and cilia-dependent renal disease: the ciliary hypothesis of polycystic kidney disease. J Am Soc Nephrol 15, 2528-36 (2004).

53. Omran, H. et al. Homozygosity mapping of a gene locus for primary ciliary dyskinesia on chromosome 5p and identification of the heavy dynein chain DNAH5 as a candidate gene. Am J Respir Cell Mol Biol 23, 696-702 (2000).

54. Matsuda, Y., Koseki, M., Shimada, T. & Saito, T. Purification and characterization of a vegetative lytic enzyme responsible for liberation of daughter cells during the proliferation of Chlamydomonas reinhardtii. Plant Cell Physiol 36, 681-9 (1995).

55. Grossman, A. & Takahashi, H. Macronutrient utilization by photosynthetic eukaryotes and the fabric of interactions. Annual Review of Plant Physiology and Plant Molecular Biology 52, 163-210 (2001).

56. Quarmby, L. M. Signal transduction in the sexual life of Chlamydomonas. Plant Mol Biol 26, 1271-87 (1994).

57. Treier, U., Fuchs, S., Weber, M., Wakarchuk, W. W. & Beck, C. F. Gametic Differentiation in Chlamydomonas-Reinhardtii - Light Dependence and Gene-Expression Patterns. Archives of Microbiology 152, 572-577 (1989).

58. Huppe, H. C. & Turpin, D. H. Integration of Carbon and Nitrogen-Metabolism in Plant and Algal Cells. Annual Review of Plant Physiology and Plant Molecular Biology 45, 577-607 (1994).

59. Eckhardt, U. & Buckhout, T. J. Iron assimilation in Chlamydomonas reinhardtii involves ferric reduction and is similar to Strategy I higher plants. Journal of Experimental Botany 49, 1219-1226 (1998).

60. Lynnes, J. A., Derzaph, T. L. M. & Weger, H. G. Iron limitation results in induction of ferricyanide reductase and ferric chelate reductase activities in Chlamydomonas reinhardtii. Planta 204, 360-365 (1998).

61. Weger, H. G. Ferric and cupric reductase activities in the green alga Chlamydomonas reinhardtii: experiments using iron-limited chemostats. Planta 207, 377-384 (1999).

62. Pierre, J. L., Fontecave, M. & Crichton, R. R. Chemistry for an essential biological process: the reduction of ferric iron. Biometals 15, 341-346 (2002).

63. Merchant, S. S. et al. Between a rock and a hard place: Trace element nutrition in Chlamydomonas. Biochim Biophys Acta (2006).

64. Herbik, A., Bölling, C. & Buckhout, T. J. The Involvement of a Multicopper Oxidase in Iron Uptake by the Green Algae Chlamydomonas reinhardtii. Plant Physiol 130, 2039-48 (2002).

65. La Fontaine, S. et al. Copper-dependent iron assimilation pathway in the model photosynthetic eukaryote Chlamydomonas reinhardtii. Eukaryotic Cell 1, 736-757 (2002).

66. Eriksson, M. et al. Genetic dissection of nutritional copper signaling in chlamydomonas distinguishes regulatory and target genes. Genetics 168, 795-807 (2004).

67. Moseley, J. L. et al. Adaptation to Fe-deficiency requires remodeling of the photosynthetic apparatus. Embo J 21, 6709-20 (2002).

68. Quisel, J. D., Wykoff, D. D. & Grossman, A. R. Biochemical characterization of the extracellular phosphatases produced by phosphorus-deprived Chlamydomonas reinhardtii. Plant Physiol 111, 839-48 (1996).

69. Ruiz, F. A., Marchesini, N., Seufferheld, M., Govindjee & Docampo, R. The polyphosphate bodies of Chlamydomonas reinhardtii possess a proton-pumping pyrophosphatase and axe similar to acidocalcisomes. Journal of Biological Chemistry 276, 46196-46203 (2001).

70. Siderius, M. et al. Chlamydomonas eugametos (chlorophyta) stores phosphate in polyphosphate bodies together with calcium. Journal of Phycology 32, 402-409 (1996).

71. Hebeler, M., Hentrich, S., Mayer, A., Leibfritz, D. & Grimme, L. H. Phosphate Regulation and Compartmentation in Chlamydomonas-Reinhardtii Studied by Invivo P-31-Nmr. Photosynthesis Research 34, 199-199 (1992).

72. Wykoff, D. D., Grossman, A. R., Weeks, D. P., Usuda, H. & Shimogawara, K. Psr1, a nuclear localized protein that regulates phosphorus metabolism in Chlamydomonas. Proc Natl Acad Sci U S A 96, 15336-41 (1999).

73. Wykoff, D. D., Davies, J. P., Melis, A. & Grossman, A. R. The regulation of photosynthetic electron transport during nutrient deprivation in Chlamydomonas reinhardtii. Plant Physiol 117, 129-39 (1998).

74. Wirtz, M. & Hell, R. Functional analysis of the cysteine synthase protein complex from plants: structural, biochemical and regulatory properties. J Plant Physiol 163, 273-86 (2006).

75. Lien, T. & Schreiner, O. Purification of a Derepressible Arylsulfatase from Chlamydomonas-Reinhardti - Properties of Enzyme in Intact-Cells and in Purified State. Biochimica Et Biophysica Acta 384, 168-179 (1975).

76. de Hostos, E. L., Schilling, J. & Grossman, A. R. Structure and expression of the gene encoding the periplasmic arylsulfatase of Chlamydomonas reinhardtii. Mol Gen Genet 218, 229-39 (1989).

77. Ravina, C. G. et al. The sac mutants of Chlamydomonas reinhardtii reveal transcriptional and posttranscriptional control of cysteine biosynthesis. Plant Physiol 130, 2076-84 (2002).

78. Yildiz, F. H., Davies, J. P. & Grossman, A. R. Characterization of Sulfate Transport in Chlamydomonas reinhardtii during Sulfur-Limited and Sulfur-Sufficient Growth. Plant Physiol 104, 981-987 (1994).

79. Davies, J. P., Yildiz, F. & Grossman, A. R. Mutants of Chlamydomonas with Aberrant Responses to Sulfur Deprivation. Plant Cell 6, 53-63 (1994).

80. Davies, J. P., Yildiz, F. H. & Grossman, A. Sac1, a putative regulator that is critical for survival of Chlamydomonas reinhardtii during sulfur deprivation. Embo J 15, 2150-9 (1996).

81. Pollock, S. V., Pootakham, W., Shibagaki, N., Moseley, J. L. & Grossman, A. R. Insights into the acclimation of Chlamydomonas reinhardtii to sulfur deprivation. Photosynth Res 86, 475-89 (2005).

82. Hallmann, A. Extracellular matrix and sex-inducing pheromone in Volvox. Int Rev Cytol 227, 131-82 (2003).

83. Takahashi, H., Braby, C. E. & Grossman, A. R. Sulfur economy and cell wall biosynthesis during sulfur limitation of Chlamydomonas reinhardtii. Plant Physiol 127, 665-73 (2001).

84. Davis, R. H. Compartmental and regulatory mechanisms in the arginine pathways of Neurospora crassa and Saccharomyces cerevisiae. Microbiol Rev 50, 280-313 (1986).

85. Slocum, R. D. Genes, enzymes and regulation of arginine biosynthesis in plants. Plant Physiol Biochem 43, 729-45 (2005).

86. Pauwels, K., Abadjieva, A., Hilven, P., Stankiewicz, A. & Crabeel, M. The N-acetylglutamate synthase/N-acetylglutamate kinase metabolon of Saccharomyces cerevisiae allows co-ordinated feedback regulation of the first two steps in arginine biosynthesis. Eur J Biochem 270, 1014-24 (2003).

87. Ferrario-Mery, S., Besin, E., Pichon, O., Meyer, C. & Hodges, M. The regulatory PII protein controls arginine biosynthesis in Arabidopsis. FEBS Lett 580, 2015-20 (2006).

88. Maheswaran, M., Urbanke, C. & Forchhammer, K. Complex formation and catalytic activation by the PII signaling protein of N-acetyl-L-glutamate kinase from Synechococcus elongatus strain PCC 7942. J Biol Chem 279, 55202-10 (2004).

89. Kirk, D. L. & Kirk, M. M. Carrier-mediated Uptake of Arginine and Urea by Chlamydomonas reinhardtii. Plant Physiol 61, 556-560 (1978).

90. Purton, S. & Rochaix, J. D. Characterization of the Arg7 Gene of Chlamydomonas-Reinhardtii and Its Application to Nuclear Transformation. European Journal of Phycology 30, 141-148 (1995).

91. Dunn, W. B. & Ellis, D. I. Metabolomics: Current analytical platforms and methodologies. Trac-Trends in Analytical Chemistry 24, 285-294 (2005).

92. Gullberg, J., Jonsson, P., Nordstrom, A., Sjostrom, M. & Moritz, T. Design of experiments: an efficient strategy to identify factors influencing extraction and derivatization of Arabidopsis thaliana samples in metabolomic studies with gas chromatography/mass spectrometry. Anal Biochem 331, 283-95 (2004).

93. Villas-Boas, S. G., Hojer-Pedersen, J., Akesson, M., Smedsgaard, J. & Nielsen, J. Global metabolite analysis of yeast: evaluation of sample preparation methods. Yeast 22, 1155-1169 (2005).

94. Maharjan, R. P. & Ferenci, T. Global metabolite analysis: the influence of extraction methodology on metabolome profiles of Escherichia coli. Analytical Biochemistry 313, 145-154 (2003).

95. Koek, M. M., Muilwijk, B., van der Werf, M. J. & Hankemeier, T. Microbial metabolomics with gas chromatography/mass spectrometry. Analytical Chemistry 78, 1272-1281 (2006).

96. Kopka, J., Fernie, A., Weckwerth, W., Gibon, Y. & Stitt, M. Metabolite profiling in plant biology: platforms and destinations. Genome Biol 5, 109 (2004).

97. Griffin, J. L. The Cinderella story of metabolic profiling: does metabolomics get to go to the functional genomics ball? Philosophical Transactions of the Royal Society B-Biological Sciences 361, 147-161 (2006).

98. Barsch, A., Patschkowski, T. & Niehaus, K. Comprehensive metabolite profiling of Sinorhizobium meliloti using gas chromatography-mass spectrometry. Funct Integr Genomics 4, 219-30 (2004).

99. de Koning, W. & van Dam, K. A method for the determination of changes of glycolytic metabolites in yeast on a subsecond time scale using extraction at neutral pH. Anal Biochem 204, 118-23 (1992).

100. Gonzalez, B., Francois, J. & Renaud, M. A rapid and reliable method for metabolite extraction in yeast using boiling buffered ethanol. Yeast 13, 1347-55 (1997).

101. Ruijter, G. J. G. & Visser, J. Determination of intermediary metabolites in Aspergillus niger. Journal of Microbiological Methods 25, 295-302 (1996).

102. Jensen, N. B. S., Jokumsen, K. V. & Villadsen, J. Determination of the phosphorylated sugars of the Embden-Meyerhoff-Parnas pathway in Lactococcus lactis using a fast sampling technique and solid phase extraction. Biotechnology and Bioengineering 63, 356-362 (1999).

103. Letisse, F. & Lindley, N. D. An intracellular metabolite quantification technique applicable to polysaccharide-producing bacteria. Biotechnology Letters 22, 1673-1677 (2000).

104. Wittmann, C., Kromer, J. O., Kiefer, P., Binz, T. & Heinzle, E. Impact of the cold shock phenomenon on quantification of intracellular metabolites in bacteria. Anal Biochem 327, 135-9 (2004).

105. Fiehn, O., Kopka, J., Trethewey, R. N. & Willmitzer, L. Identification of uncommon plant metabolites based on calculation of elemental compositions using gas chromatography and quadrupole mass spectrometry. Analytical Chemistry 72, 3573-3580 (2000).

106. Edlund, A., Eklof, S., Sundberg, B., Moritz, T. & Sandberg, G. A Microscale Technique for Gas Chromatography-Mass Spectrometry Measurements of Picogram Amounts of Indole-3-Acetic Acid in Plant Tissues. Plant Physiol 108, 1043-1047 (1995).

107. Orth, H. C., Rentel, C. & Schmidt, P. C. Isolation, purity analysis and stability of hyperforin as a standard material from Hypericum perforatum L. J Pharm Pharmacol 51, 193-200 (1999).

108. Fernandez, E. & Cardenas, J. Regulation of the nitrate-reducing system enzymes in wild-type and mutant strains of Chlamydomonas reinhardii. Mol Gen Genet 186, 164-9 (1982).

109. Johansen, H. N., Glitso, V. & Knudsen, K. E. B. Influence of extraction solvent and temperature on the quantitative determination of oligosaccharides from plant materials by high-performance liquid chromatography. Journal of Agricultural and Food Chemistry 44, 1470-1474 (1996).

110. Streeter, J. G. & Strimbu, C. E. Simultaneous extraction and derivatization of carbohydrates from green plant tissues for analysis by gas-liquid chromatography. Analytical Biochemistry 259, 253-257 (1998).

111. Huie, C. W. A review of modern sample-preparation techniques for the extraction and analysis of medicinal plants. Analytical and Bioanalytical Chemistry 373, 23-30 (2002).

112. Brachet, A., Christen, P. & Veuthey, J. L. Focused microwave-assisted extraction of cocaine and benzoylecgonine from coca leaves. Phytochemical Analysis 13, 162-169 (2002).

113. Kaufmann, B. & Christen, P. Recent extraction techniques for natural products: Microwave-assisted extraction and pressurised solvent extraction. Phytochemical Analysis 13, 105-113 (2002).

114. Benthin, B., Danz, H. & Hamburger, M. Pressurized liquid extraction of medicinal plants. Journal of Chromatography A 837, 211-219 (1999).

115. Ong, E. S. Chemical assay of glycyrrhizin in medicinal plants by pressurized liquid extraction (PLE) with capillary zone electrophoresis (CZE). Journal of Separation Science 25, 825-831 (2002).

116. Folch, J., Lees, M. & Stanley, G. H. S. A Simple Method for the Isolation and Purification of Total Lipides from Animal Tissues. Journal of Biological Chemistry 226, 497-509 (1957).

117. Cremin, P., Donnelly, D. M. X., Wolfender, J. L. & Hostettmann, K. Liquid Chromatographic-Thermospray Mass-Spectrometric Analysis of Sesquiterpenes of Armillaria (Eumycota, Basidiomycotina) Species. Journal of Chromatography A 710, 273-285 (1995).

118. Smits, H. P., Cohen, A., Buttler, T., Nielsen, J. & Olsson, L. Cleanup and analysis of sugar phosphates in biological extracts by using solid-phase extraction and anion-exchange chromatography with pulsed amperometric detection. Analytical Biochemistry 261, 36-42 (1998).

119. Conneely, A. et al. Isolation of bound residues of nitrofuran drugs from tissue by solid-phase extraction with determination by liquid chromatography with UV and tandem mass spectrometric detection. Analytica Chimica Acta 483, 91-98 (2003).

120. Chen, Z. L., Landman, P., Colmer, T. D. & Adams, M. A. Simultaneous analysis of amino and organic acids in extracts of plant leaves as tert-butyldimethylsilyl derivatives by capillary gas chromatography. Analytical Biochemistry 259, 203-211 (1998).

121. Adams, M. A., Chen, Z. L., Landman, P. & Colmer, T. D. Simultaneous determination by capillary gas chromatography of organic acids, sugars, and sugar alcohols in plant tissue extracts as their trimethylsilyl derivatives. Analytical Biochemistry 266, 77-84 (1999).

122. Bouchereau, A., Guenot, P. & Lather, F. Analysis of amines in plant materials. Journal of Chromatography B-Analytical Technologies in the Biomedical and Life Sciences 747, 49-67 (2000).

123. Hajjaj, H., Blanc, P. J., Goma, G. & Francois, J. Sampling techniques and comparative extraction procedures for quantitative determination of intra- and extracellular metabolites in filamentous fungi. Fems Microbiology Letters 164, 195-200 (1998).

124. Martins, A. M. T. B. S., Cordeiro, C. A. A. & Freire, A. M. J. P. In situ analysis of methylglyoxal metabolism in Saccharomyces cerevisiae. Febs Letters 499, 41-44 (2001).

125. Blau, K. & Halket, J. M. Handbook of derivatives for chromatography (Wiley, Chichester ; New York, 1993).

126. Curtius, H. C., Muller, M. & Vollmin, J. A. Studies on Ring Structures of Ketoses by Means of Gas Chromatography and Mass Spectroscopy. Journal of Chromatography 37, 216-& (1968).

127. Asres, D. D. & Perreault, H. Monosaccharide permethylation products for gas chromatography mass spectrometry: how reaction conditions can influence isomeric ratios. Canadian Journal of Chemistry-Revue Canadienne De Chimie 75, 1385-1392 (1997).

128. Little, J. L. Artifacts in trimethylsilyl derivatization reactions and ways to avoid them. J Chromatogr A 844, 1-22 (1999).

129. Duran, A. L., Yang, J., Wang, L. J. & Sumner, L. W. Metabolomics spectral formatting, alignment and conversion tools (MSFACTs). Bioinformatics 19, 2283-2293 (2003).

130. Jonsson, P. et al. A strategy for identifying differences in large series of metabolomic samples analyzed by GC/MS. Anal Chem 76, 1738-45 (2004).

131. Peng, S. & Jayallemand, C. Use of Antioxidants in Extraction of Tannins from Walnut Plants. Journal of Chemical Ecology 17, 887-896 (1991).

132. Brereton, R. G., Rahmani, A., Liang, Y. Z. & Kvalheim, O. M. Investigation of the Allomerization Reaction of Chlorophyll-Alpha - Use of Diode-Array Hplc, Mass-Spectrometry and Chemometric Factor-Analysis for the Detection of Early Products. Photochemistry and Photobiology 59, 99-110 (1994).

133. Deng, C. H., Zhang, X. M. & Li, N. Investigation of volatile biomarkers in lung cancer blood using solid-phase microextraction and capillary gas chromatography-mass spectrometry. Journal of Chromatography B-Analytical Technologies in the Biomedical and Life Sciences 808, 269-277 (2004).

134. Perera, R. M. M., Marriott, P. J. & Galbally, I. E. Headspace solid-phase microextraction - comprehensive two-dimensional gas chromatography of wound induced plant volatile organic compound emissions. Analyst 127, 1601-1607 (2002).

135. Verdonk, J. C. et al. Regulation of floral scent production in petunia revealed by targeted metabolomics. Phytochemistry 62, 997-1008 (2003).

136. Roessner, U., Wagner, C., Kopka, J., Trethewey, R. N. & Willmitzer, L. Simultaneous analysis of metabolites in potato tuber by gas chromatography-mass spectrometry. Plant Journal 23, 131-142 (2000).

137. Shellie, R. A. Comprehensive two-dimensional gas chromatography-mass spectrometry and its use in high-resolution metabolomics. Australian Journal of Chemistry 58, 619-619 (2005).

138. Mohler, R. E., Dombek, K. M., Hoggard, J. C., Young, E. T. & Synovec, R. E. Comprehensive two-dimensional gas chromatography time-of-flight mass spectrometry analysis of metabolites in fermenting and respiring yeast cells. Analytical Chemistry 78, 2700-2709 (2006).

139. Adahchour, M., Beens, J., Vreuls, R. J. J. & Brinkman, U. A. T. Recent developments in comprehensive two-dimensional gas chromatography (GC x GC) II. Modulation and detection. Trac-Trends in Analytical Chemistry 25, 540-553 (2006).

140. Adahchour, M., Beens, J., Vreuls, R. J. J. & Brinkman, U. A. T. Recent developments in comprehensive two-dimensional gas chromatography (GC X GC) I. Introduction and instrumental set-up. Trac-Trends in Analytical Chemistry 25, 438-454 (2006).

141. Stein, S. E. An integrated method for spectrum extraction and compound identification from gas chromatography/mass spectrometry data. Journal of the American Society for Mass Spectrometry 10, 770-781 (1999).

142. Krupcik, J., Mydlova, J., Spanik, I., Tienpont, B. & Sandra, P. Computerized separation of chromatographically unresolved peaks. Journal of Chromatography A 1084, 80-89 (2005).

143. Tikunov, Y. et al. A novel approach for nontargeted data analysis for metabolomics. Large-scale profiling of tomato fruit volatiles. Plant Physiol 139, 1125-37 (2005).

144. Jonsson, P. et al. High-throughput data analysis for detecting and identifying differences between samples in GC/MS-based metabolomic analyses. Anal Chem 77, 5635-42 (2005).

145. Fiehn, O. et al. Metabolite profiling for plant functional genomics. Nature Biotechnology 18, 1157-1161 (2000).

146. Roessner, U. et al. Metabolic profiling allows comprehensive phenotyping of genetically or environmentally modified plant systems. Plant Cell 13, 11-29 (2001).

147. Steinbeck, C. The automation of natural product structure elucidation. Curr Opin Drug Discov Devel 4, 338-42 (2001).

148. Wolfender, J. L., Ndjoko, K. & Hostettmann, K. Liquid chromatography with ultraviolet absorbance-mass spectrometric detection and with nuclear magnetic resonance spectroscopy: a powerful combination for the on-line structural investigation of plant metabolites. J Chromatogr A 1000, 437-55 (2003).

149. Schauer, N. et al. GC-MS libraries for the rapid identification of metabolites in complex biological samples. FEBS Lett 579, 1332-7 (2005).

150. Veriotti, T. & Sacks, R. High-speed characterization and analysis of orange oils with tandem-column stop-flow GC and time-of-flight MS. Anal Chem 74, 5635-40 (2002).

151. Kienhuis, P. G. & Geerdink, R. B. A mass spectral library based on chemical ionization and collision-induced dissociation. J Chromatogr A 974, 161-8 (2002).

152. Herzler, M., Herre, S. & Pragst, F. Selectivity of substance identification by HPLC-DAD in toxicological analysis using a UV spectra library of 2682 compounds. J Anal Toxicol 27, 233-42 (2003).

153. Saint-Marcoux, F., Lachatre, G. & Marquet, P. Evaluation of an improved general unknown screening procedure using liquid chromatography-electrospray-mass spectrometry by comparison with gas chromatography and high-performance liquid-chromatography--diode array detection. J Am Soc Mass Spectrom 14, 14-22 (2003).

154. Wagner, C., Sefkow, M. & Kopka, J. Construction and application of a mass spectral and retention time index database generated from plant GC/EI-TOF-MS metabolite profiles. Phytochemistry 62, 887-900 (2003).

155. Kopka, J. et al. GMD@CSB.DB: the Golm Metabolome Database. Bioinformatics 21, 1635-8 (2005).

156. Jenkins, H. et al. A proposed framework for the description of plant metabolomics experiments and their results. Nat Biotechnol 22, 1601-6 (2004).

157. Fernie, A. R., Geigenberger, P. & Stitt, M. Flux an important, but neglected, component of functional genomics. Curr Opin Plant Biol 8, 174-82 (2005).

158. Ratcliffe, R. G. & Shachar-Hill, Y. Measuring multiple fluxes through plant metabolic networks. Plant J 45, 490-511 (2006).

159. Gibon, Y. et al. A Robot-based platform to measure multiple enzyme activities in Arabidopsis using a set of cycling assays: comparison of changes of enzyme activities and transcript levels during diurnal cycles and in prolonged darkness. Plant Cell 16, 3304-25 (2004).

160. Goodacre, R., Vaidyanathan, S., Dunn, W. B., Harrigan, G. G. & Kell, D. B. Metabolomics by numbers: acquiring and understanding global metabolite data. Trends Biotechnol 22, 245-52 (2004).

161. Urbanczyk-Wochniak, E. et al. Parallel analysis of transcript and metabolic profiles: a new approach in systems biology. Embo Reports 4, 989-993 (2003).

162. Fell, D. Understanding the control of metabolism. Portland Press ; London ; Miami, 1997.

163. Kell, D. B. & Mendes, P. in Technological and Medical Implications of Metabolic Control Analysis (eds. Cornish-Bowden, A. J. & Cárdenas, M. L.) 3-25 (Kluwer Academic Publishers, 2000).

164. Raamsdonk, L. M. et al. A functional genomics strategy that uses metabolome data to reveal the phenotype of silent mutations. Nat Biotechnol 19, 45-50 (2001).

165. Kemsley, E. K. Discriminant analysis of high-dimensional data: A comparison of principal components analysis and partial least squares data reduction methods. Chemometrics and Intelligent Laboratory Systems 33, 47-61 (1996).

166. Scholz, M., Gatzek, S., Sterling, A., Fiehn, O. & Selbig, J. Metabolite fingerprinting: detecting biological features by independent component analysis. Bioinformatics 20, 2447-2454 (2004).

167. Toronen, P., Kolehmainen, M., Wong, C. & Castren, E. Analysis of gene expression data using self-organizing maps. Febs Letters 451, 142-146 (1999).

168. Hirai, M. Y. et al. Elucidation of gene-to-gene and metabolite-to-gene networks in arabidopsis by integration of metabolomics and transcriptomics. J Biol Chem 280, 25590-5 (2005).

169. Ricard, J. Reduction, integration and emergence in biochemical networks. Biol Cell 96, 719-25 (2004).

170. Konig, R. et al. Discovering functional gene expression patterns in the metabolic network of Escherichia coli with wavelets transforms. BMC Bioinformatics 7, 119 (2006).

171. Baumgartner, C. & Baumgartner, D. Biomarker discovery, disease classification, and similarity query processing on high-throughput MS/MS data of inborn errors of metabolism. J Biomol Screen 11, 90-9 (2006).

172. Morgenthal, K., Weckwerth, W. & Steuer, R. Metabolomic networks in plants: Transitions from pattern recognition to biological interpretation. Biosystems 83, 108-117 (2006).

173. Schauer, N. et al. Comprehensive metabolic profiling and phenotyping of interspecific introgression lines for tomato improvement. Nat Biotechnol 24, 447-54 (2006).

174. Schuster, S., Klamt, S., Weckwerth, W., Moldenhauer, F. & Pfeiffer, T. Use of network analysis of metabolic systems in bioengineering. Bioprocess and Biosystems Engineering 24, 363-372 (2002).

175. Steuer, R. Review: On the analysis and interpretation of correlations in metabolomic data. Brief Bioinform 7, 151-158 (2006).

176. Ralley, L. et al. Metabolic engineering of ketocarotenoid formation in higher plants. Plant J 39, 477-86 (2004).

177. Giovinazzo, G. et al. Antioxidant metabolite profiles in tomato fruit constitutively expressing the grapevine stilbene synthase gene. Plant Biotechnology Journal 3, 57-69 (2005).

178. Junker, B. H. et al. Temporally regulated expression of a yeast invertase in potato tubers allows dissection of the complex metabolic phenotype obtained following its constitutive expression. Plant Mol Biol 56, 91-110 (2004).

179. Desbrosses, G. G., Kopka, J. & Udvardi, M. K. Lotus japonicus metabolic profiling. Development of gas chromatography-mass spectrometry resources for the study of plant-microbe interactions. Plant Physiol 137, 1302-18 (2005).

180. Hirai, M. Y. et al. Global expression profiling of sulfur-starved Arabidopsis by DNA macroarray reveals the role of O-acetyl-L-serine as a general regulator of gene expression in response to sulfur nutrition. Plant Journal 33, 651-663 (2003).

181. Kant, M. R., Ament, K., Sabelis, M. W., Haring, M. A. & Schuurink, R. C. Differential timing of spider mite-induced direct and indirect defenses in tomato plants. Plant Physiol 135, 483-95 (2004).

182. Hirai, M. Y. et al. Integration of transcriptomics and metabolomics for understanding of global responses to nutritional stresses in Arabidopsis thaliana. Proc Natl Acad Sci U S A 101, 10205-10 (2004).

183. Mercke, P. et al. Combined transcript and metabolite analysis reveals genes involved in spider mite induced volatile formation in cucumber plants. Plant Physiology 135, 2012-2024 (2004).

184. Tohge, T. et al. Functional genomics by integrated analysis of metabolome and transcriptome of Arabidopsis plants over-expressing an MYB transcription factor. Plant J 42, 218-35 (2005).

185. Rolletschek, H. et al. Seed-specific expression of a bacterial phosphoenolpyruvate carboxylase in Vicia narbonensis increases protein content and improves carbon economy. Plant Biotechnology Journal 2, 211-219 (2004).

186. Nikiforova, V. J. et al. Systems rebalancing of metabolism in response to sulfur deprivation, as revealed by metabolome analysis of Arabidopsis plants. Plant Physiol 138, 304-18 (2005).

187. Trethewey, R. N. Metabolite profiling as an aid to metabolic engineering in plants. Curr Opin Plant Biol 7, 196-201 (2004).

188. Hofmeyr, J. H. & Cornish-Bowden, A. Co-response analysis: a new experimental strategy for metabolic control analysis. J Theor Biol 182, 371-80 (1996).

189. Stelling, J., Klamt, S., Bettenbrock, K., Schuster, S. & Gilles, E. D. Metabolic network structure determines key aspects of functionality and regulation. Nature 420, 190-193 (2002).

190. Schuster, S., Dandekar, T. & Fell, D. A. Detection of elementary flux modes in biochemical networks: a promising tool for pathway analysis and metabolic engineering. Trends in Biotechnology 17, 53-60 (1999).

191. Yeger-Lotem, E. et al. Network motifs in integrated cellular networks of transcription-regulation and protein-protein interaction. Proc Natl Acad Sci U S A 101, 5934-9 (2004).

192. Milo, R. et al. Network motifs: simple building blocks of complex networks. Science 298, 824-7 (2002).

193. Mangan, S. & Alon, U. Structure and function of the feed-forward loop network motif. Proc Natl Acad Sci U S A 100, 11980-5 (2003).

194. Vance, W., Arkin, A. & Ross, J. Determination of causal connectivities of species in reaction networks. Proceedings of the National Academy of Sciences of the United States of America 99, 5816-5821 (2002).

195. Ross, J. New approaches to the deduction of complex reaction mechanisms. Acc Chem Res 36, 839-47 (2003).

196. Strijkert, P. J., Loppes, R. & J.S., S. Actual Biochemical Block in Arg-2 Mutant of Chlamydomonas-Reinhardi. Biochemical Genetics 8, 239-248 (1973).

197. Ebersold, W. T. Crossing over in Chlamydomonas-Reinhardi. American Journal of Botany 43, 408-410 (1956).

198. Loppes, R. & Heindricks, R. New Arginine-Requiring Mutants in Chlamydomonas-Reinhardtii. Archives of Microbiology 143, 348-352 (1986).

199. Farr, T. J., Huppe, H. C. & Turpin, D. H. Coordination of Chloroplastic Metabolism in N-Limited Chlamydomonas-Reinhardtii by Redox Modulation .1. The Activation of Phosphoribulosekinase and Glucose-6-Phosphate- Dehydrogenase Is Relative to the Photosynthetic Supply of Electrons. Plant Physiology 105, 1037-1042 (1994).

200. Wintermans, J. & Demots, A. Spectrophotometric Characteristics of Chlorophylls a and B and Their Pheophytins in Ethanol. Biochimica Et Biophysica Acta 109, 448-& (1965).

201. Usadel, B. et al. Extension of the visualization tool MapMan to allow statistical analysis of arrays, display of corresponding genes, and comparison with known responses. Plant Physiol 138, 1195-204 (2005).

202. Kaiser, H. F. The Application of Electronic-Computers to Factor-Analysis. Educational and Psychological Measurement 20, 141-151 (1960).

203. Cattell, R. B. Scree Test for Number of Factors. Multivariate Behavioral Research 1, 245-276 (1966).

204. Birkemeyer, C., Luedemann, A., Wagner, C., Erban, A. & Kopka, J. Metabolome analysis: the potential of in vivo labeling with stable isotopes for metabolite profiling. Trends in Biotechnology 23, 28-33 (2005).

205. Patzelt, H., Kessler, B., Oschkinat, H. & Oesterhelt, D. The entire metabolite spectrum of the green alga Scenedesmus obliquus in isotope-labelled form. Phytochemistry 50, 215-217 (1999).

206. Beck, C. F. & Haring, M. A. Gametic differentiation of Chlamydomonas. International Review of Cytology - a Survey of Cell Biology, Vol 168 168, 259-302 (1996).

207. Abe, J., Kubo, T., Saito, T. & Matsuda, Y. The regulatory networks of gene expression during the sexual differentiation of Chlamydomonas reinhardtii, as analyzed by mutants for gametogenesis. Plant and Cell Physiology 46, 312-316 (2005).

208. Huppe, H. C., Vanlerberghe, G. C. & Turpin, D. H. Evidence for Activation of the Oxidative Pentose-Phosphate Pathway During Photosynthetic Assimilation of No3- but Not Nh4+ by a Green-Alga. Plant Physiology 100, 2096-2099 (1992).

209. Huppe, H. C. & Turpin, D. H. A role for glucose-6-phosphate dehydrogenase in short- and long-term regulation of photosynthetic and respiratory carbon and nitrogen metabolism in nitrogen-limited Chlamydomonas reinhardtii. Biochem Soc Trans 24, 767-70 (1996).

210. Huppe, H. C., Farr, T. J. & Turpin, D. H. Coordination of Chloroplastic Metabolism in N-Limited Chlamydomonas-Reinhardtii by Redox Modulation .2. Redox Modulation Activates the Oxidative Pentose-Phosphate Pathway During Photosynthetic Nitrate Assimilation. Plant Physiology 105, 1043-1048 (1994).

211. Smith, R. G., Vanlerberghe, G. C., Stitt, M. & Turpin, D. H. Short-Term Metabolite Changes During Transient Ammonium Assimilation by the N-Limited Green-Alga Selenastrum-Minutum. Plant Physiology 91, 749-755 (1989).

212. Abadia, J., Lopez-Millan, A. F., Rombola, A. & Abadia, A. Organic acids and Fe deficiency: a review. Plant and Soil 241, 75-86 (2002).

213. Guerinot, M. L. & Yi, Y. Iron: Nutritious, Noxious, and Not Readily Available. Plant Physiol 104, 815-820 (1994).

214. Behrenfeld, M. J. & Kolber, Z. S. Widespread iron limitation of phytoplankton in the south pacific ocean. Science 283, 840-3 (1999).

215. Imam, S. H., Buchanan, M. J., Shin, H. C. & Snell, W. J. The Chlamydomonas Cell-Wall - Characterization of the Wall Framework. Journal of Cell Biology 101, 1599-1607 (1985).

216. Voigt, J., Munzner, P. & Vogeler, H. P. The Cell-Wall Glycoproteins of Chlamydomonas-Reinhardtii - Analysis of the Invitro Translation Products. Plant Science 75, 129-142 (1991).

217. Voigt, J. & Frank, R. 14-3-3 proteins are constituents of the insoluble glycoprotein framework of the Chlamydomonas cell wall. Plant Cell 15, 1399-1413 (2003).

218. Peltier, G. & Schmidt, G. W. Chlororespiration - an Adaptation to Nitrogen Deficiency in Chlamydomonas-Reinhardtii. Proceedings of the National Academy of Sciences of the United States of America 88, 4791-4795 (1991).

219. Kromer, S. Respiration During Photosynthesis. Annual Review of Plant Physiology and Plant Molecular Biology 46, 45-70 (1995).

220. Hoefnagel, M. H. N., Atkin, O. K. & Wiskich, J. T. Interdependence between chloroplasts and mitochondria in the light and the dark. Biochimica Et Biophysica Acta-Bioenergetics 1366, 235-255 (1998).

221. Peltier, G. & Thibault, P. O(2) Uptake in the Light in Chlamydomonas: Evidence for Persistent Mitochondrial Respiration. Plant Physiol 79, 225-230 (1985).

222. Xue, X., Gauthier, D. A., Turpin, D. H. & Weger, H. G. Interactions between Photosynthesis and Respiration in the Green Alga Chlamydomonas reinhardtii (Characterization of Light-Enhanced Dark Respiration). Plant Physiol 112, 1005-1014 (1996).

223. Husic, D. W. & Tolbert, N. E. Inhibition of glycolate and D-lactate metabolism in a Chlamydomonas reinhardtii mutant deficient in mitochondrial respiration. Proc Natl Acad Sci U S A 84, 1555-1559 (1987).

224. Hanning, I. & Heldt, H. W. On the Function of Mitochondrial Metabolism during Photosynthesis in Spinach (Spinacia oleracea L.) Leaves (Partitioning between Respiration and Export of Redox Equivalents and Precursors for Nitrate Assimilation Products). Plant Physiol 103, 1147-1154 (1993).

225. Hanning, I. I., Baumgarten, K., Schott, K. & Heldt, H. W. Oxaloacetate transport into plant mitochondria. Plant Physiol 119, 1025-32 (1999).

226. Davies, J. D. & Grossman, A. R. in The molecular biology of chloroplasts and mitochondria in Chlamydomonas (eds. Rochaix, J., Goldschmidt-Clermont, M. & Merchant, S.) 613-635 (Kluwer Academic Publishers, Dordrecht, Boston, 1998).

227. Johnston, M. & Kim, J. H. Glucose as a hormone: receptor-mediated glucose sensing in the yeast Saccharomyces cerevisiae. Biochem Soc Trans 33, 247-52 (2005).

228. Alia, Saradhi, P. P. & Mohanty, P. Involvement of proline in protecting thylakoid membranes against free radical-induced photodamage. Journal of Photochemistry and Photobiology B-Biology 38, 253-257 (1997).

229. Hare, P. D. & Cress, W. A. Metabolic implications of stress-induced proline accumulation in plants. Plant Growth Regulation 21, 79-102 (1997).

230. Taylor, C. B. Proline and water deficit: Ups, downs, ins, and outs. Plant Cell 8, 1221-1224 (1996).

231. Siripornadulsil, S., Traina, S., Verma, D. P. & Sayre, R. T. Molecular mechanisms of proline-mediated tolerance to toxic heavy metals in transgenic microalgae. Plant Cell 14, 2837-47 (2002).

232. Matysik, J., Alia, Bhalu, B. & Mohanty, P. Molecular mechanisms of quenching of reactive oxygen species by proline under stress in plants. Current Science 82, 525-532 (2002).

7 Acknowledgments

I am grateful to **Prof. Lothar Willmitzer** for his supervision, continuous support, inspiration and incentive. I have benefited a lot from his expert knowledge and experience.

I would like to acknowledge the support of **Prof. Oliver Fiehn**, who gave me the opportunity to join this project and the scope for development of own ideas.

I very much would like to thank **Dr. Wolfram Weckwerth** for providing me with laboratory space and the entire **Integrative Proteomics and Metabolomics Research Group** for their good spirits and work atmosphere.

I specially would like to thank **Dr. Jeffrey Moseley** for backcrossing and providing the *sac1* mutant strain.

I very much would like to thank **Änne Eckardt** for her excellent and priceless support in GC-MS measurements.

I would like to thank the undergraduate students who at different times have greatly supported and advanced these studies with their work and commitment: **Anja Kunert**, **Dennis Dauscher**, **Janine Turner**, **Jenny Wrede** and **Matthias Pietzke**.

I would like to thank **Dr. Joachim Kopka** for sharing GC-MS library resources and for many helpful discussions.

I am obliged to **Dr. Wolfgang Lein** and **Dr. Oliver Bläsing** for the liberal use of laboratory equipment and storage space.

I'd like to thank **Dr. Oliver Lerch** for his practical introduction to the DTD-technology.

I am indebted to the members of the Infrastructure Support Groups for their invaluable help in having made and kept things going: **Technical Support Group**, **Laboratory Preparation Service**, **IT Service**, **Campus Store**, and **Rita Quade**, our librarian.

I am thankful to the members of the **Metabolomic Analysis Research Group** for various helpful inputs and support.

A warm thank you goes out to **my family** and all **friends** who took interest and have supported me during these studies.

8 Appendices

Table A1: Metabolite Response during sulfur deprivation.

Analyte ID[a]	Hit ID[b]	Metabolite/ Best Library Hit[c]	Profile dissimilarity[d]	Response profile assignment[e]		Direction of change in analyte level[g]		Analyte level[h] (log2 ratio) for									
								CC-1690					sac1				
				CC-1690	*sac1*	CC-1690	*sac1*	+2h	-2h	-5h	-10h	-24 h	+2h	-2h	-5h	-10h	-24 h
5253fa36_3	1653	M000100_A105001-101_CONT-METB_190250_EINS_Lactic acid, DL- (2TMS)	0,81	E14	A6	. . . . –	– – . – –	-0,29	-0,94	-0,06	-0,78	-1,36	-0,04	-1,75	-0,82	-1,41	-1,20
5253fa36_9	2296	M000443_A116002-101_METB_230340_EIFIEHN_Butyric acid, 2-oxo- (1MEOX) (1TMS)	1,35	C8	A1	. . – – –	– . – – –	0,32	0,09	-1,16	-0,80	-1,12	-0,23	-0,26	-1,65	-1,56	-2,47
5253fa36_12		Alanine	1,92	A1	A3	– – – – –	– – – – –	-0,35	-3,74	-3,61	-4,11	-5,22	-0,27	-2,34	-3,53	-2,20	-6,80
5253fa36_15	2657	M000517_A106002-101_CONT-MST_206867_EINS_Glycolic acid (2TMS)	0,88	B16	B5	. – . . .	+ . – . .	-0,27	-1,31	0,13	0,50	0,09	0,37	-0,46	-0,70	-0,38	-0,24
5253fa36_24		Pyruvic Acid	8,64	00	A4	. – – – .	– + . – –	-0,49	-2,27	-1,25	LOD	-0,61	-1,06	0,60	-0,22	-2,12	-1,15
5253fa36_38	198	M000000_AE050823-101_MST_440820_EICAT_y-158	1,80	C19	A1	+ . + + +	+ – – – –	0,24	0,09	0,56	0,99	0,40	0,19	-1,04	-1,19	-0,73	-1,40
5253fa36_40	252	M000000_AE050823-101_MST_246430_EICAT_y-acid-34	1,62	C17	B13	. . . . .	– – – . –	0,11	0,17	0,12	0,27	-0,08	0,00	-0,98	-1,50	0,00	-1,02
5253fa36_41		Hydroxybutanoic acid	1,93	A3	A3	– – – – –	– . – – –	-0,56	-0,69	-2,39	-3,86	LOD	-0,76	0,32	-1,23	-1,92	LOD
5253fa36_53		Valine	1,36	B11	B13	– – – – –	– – – – –	-0,75	-1,45	-1,79	-1,60	-0,56	-0,29	-1,05	-1,03	-0,23	-0,70
5253fa36_62	336	M000000_AE041126-101_METB_684710_EIFIEHN_Octane, 1,8-diamino-	12,68	A4	D12	– – – – –	+ . – . +	-2,01	-2,24	-2,16	LOD	LOD	0,11	0,12	-0,71	-0,20	1,92
5253fa36_63	2977	M000606_A188004-101_METB_582135_EINS_Fructose, D- (1MEOX) (5TMS)	14,35	00	C8	– – – – –	. + . . .	LOD	LOD	LOD	LOD	LOD	*0,75*	*3,59*	*0,00*	*0,00*	*0,00*
5253fa36_65	196	M000000_AE050823-101_MST_448180_EICAT_hydroxyproline-163	1,40	A2	A3	– – – – –	– – – – –	-0,47	-1,44	-1,90	-2,41	-1,82	-0,24	-0,77	-0,82	-1,01	-1,99
5253fa36_67	2296	M000443_A116002-101_METB_230340_EIFIEHN_Butyric acid, 2-oxo- (1MEOX) (1TMS)	1,67	C17	E14	. . . . .	– – – – –	0,20	-0,03	0,16	0,12	-0,31	-0,26	-1,17	-0,77	-1,56	-1,91
5253fa36_70		Glycerol	0,85	B11	A6	– – . . .	– – – . .	-0,74	-0,55	-0,19	-0,38	-0,11	-0,24	-1,04	-0,98	-0,37	-0,96
5253fa36_74	2335	M000456_A136001-101_METB_392490_EINIST_Uracil (2TMS)	0,41	A2	A2	. . – – .	– – – – –	-0,09	-0,33	-0,67	-0,57	-0,29	-0,36	-0,40	-1,08	-0,77	-0,63
5253fa36_78	2977	M000606_A188004-101_METB_582135_EINS_Fructose, D- (1MEOX) (5TMS)	10,31	00	A2	– + + – +	+ – – – –	LOD	0,89	0,36	LOD	0,67	0,74	-0,30	-1,25	-0,45	-0,77
5253fa36_79		Leucine	0,83	D7	C19	. + . + +	– . . + +	0,09	0,40	0,38	0,56	1,61	-0,20	0,20	0,23	1,39	0,78
5253fa36_85	2232	M000427_A122003-101_MST_300730_EIMOR_Malonic acid (2TMS)	1,58	E14	A1	. – . – –	+ – – – –	0,04	-0,48	-0,22	-0,49	-0,61	0,17	-1,50	-1,67	-1,59	-2,19
5253fa36_92		Isoleucine	0,92	B5	B16	– – – – +	– – – . +	-0,47	-1,08	-1,38	-0,97	0,64	-0,35	-0,94	-1,06	-0,05	0,52
5253fa36_93	2198	M000421_A114006-101_METB_235710_EIFIEHN_Maleimide, N-ethyl-	2,55	C8	C10	. . – . .	. + . . –	-0,07	0,63	-1,35	-0,70	-0,59	0,47	1,60	1,21	1,35	-0,89
5253fa36_96	850	M000028_A182002-101_METB-METB_570427_EINS_Ornithine, DL- (4TMS)	1,74	E21	B5	. . . . .	– . – – .	-0,29	-0,27	0,07	0,04	-0,21	-0,95	-0,45	-1,68	-0,83	-0,18
5253fa36_98		Serine	1,84	A3	C8	. . . – –	– . – – –	0,61	0,04	0,40	-0,75	-1,20	-0,77	1,00	-1,44	-0,68	-2,21
5253fa36_99	875	M000028_A162001-101_METB-METB_490485_EITTMS_Ornithine, L- (3TMS)	7,42	A3	A6	. . – – –	+ – – – –	-0,92	-0,42	-1,51	-1,46	LOD	0,02	-3,29	-2,26	-2,16	-3,35
5253fa36_101	1530	M000075_A129001-101_METB_333520_EIQTMS_Phosphoric acid (3TMS)	0,90	A4	A1	+ . – – –	– . . – –	0,30	-0,04	-0,49	-0,58	-0,75	-0,34	-0,94	-0,84	-1,14	-1,61
5253fa36_102		Phosphate	0,91	A4	A3	+ . – – –	– . . . –	0,38	0,08	-0,41	-0,47	-0,61	-0,26	-0,10	-0,85	-0,64	-1,52
5253fa36_103	229	M000000_AE050823-101_MST_333620_EICAT_phosphoric acid-88	0,88	C8	A1	. + – – –	– . . – –	0,04	0,26	-0,51	-0,63	-0,69	-0,27	-0,54	-0,80	-1,11	-1,57
5253fa36_104	1528	M000075_A129001-101_METB_333520_EIFIEHN_Phosphoric acid (3TMS)	2,25	D9	B13	+ + + + +	+	1,67	1,95	1,59	1,20	1,64	0,13	-0,30	-0,40	-0,11	-0,27
5253fa36_105	2593	M000510_A232002-101_METB_767060_EINS_Fructose-6-phosphate (1MEOX) (6TMS)	0,69	C8	A3	. + – . –	–	-0,11	0,37	-0,71	-0,57	-0,68	-0,84	0,03	-0,02	-0,20	-0,52
5253fa36_106		Proline	2,32	C20	C10	– + + – –	– + + + –	-0,63	2,14	1,17	-0,50	-0,96	-0,76	2,86	2,60	1,82	-1,97
5253fa36_109	1539	M000075_A129001-101_METB_333520_EITTMS_Phosphoric acid (3TMS)	7,82	A3	A3	. – – – –	– – – – –	-0,02	-0,39	-1,11	-1,19	-2,94	-0,44	-0,43	-1,59	-0,94	LOD
5253fa36_115	430	M000000_AE041126-101_METB_348370_EIFIEHN_Oxamic acid	1,20	E21	C8	. . . . .	. . . . .	-0,24	-0,28	0,34	0,24	-0,21	0,21	0,14	-0,87	-0,37	-1,00
5253fa36_117	2723	M000563_A280001-101_IS (RI05)_943980_EIFIEHN_Octacosane, n-	1,37	D7	B11	. . . . +	– – – – .	-0,01	-0,01	0,11	0,46	1,03	-0,37	-0,85	-0,61	-0,76	-0,35
5253fa36_119	2157	M000364_A127002-101_METB_340357_EIROE_Urea (2TMS)	10,73	C20	00	– + . – –	+ . – – –	-0,84	0,14	0,23	-0,03	-0,14	0,54	-0,08	-0,38	LOD	-0,35
5253fa36_120	608	M000015_A138001-101_METB_357523_EINS_Serine, DL- (3TMS)	1,77	C8	E15	– . – . –	+ + – + .	-0,78	0,45	-0,95	-0,43	-0,89	0,43	0,58	-0,81	1,34	-0,30
5253fa36_122	607	M000015_A138001-101_METB_357523_EINS_Serine, DL- (3TMS)	0,77	C8	C10	– + – – –	– . . . –	-0,22	0,48	-0,68	-0,54	-1,04	-0,37	0,80	-0,04	0,24	-1,65
5253fa36_124		Serine	1,03	C8	C10	– . – – –	– + . . –	-0,23	0,33	-0,71	-0,80	-1,00	-0,26	1,34	-0,11	0,14	-2,03
5253fa36_126	223	M000000_AE050823-101_MST_358060_EICAT_serine-103	10,02	00	A3	. . – + –	+ – – – –	-0,10	-0,10	LOD	0,54	LOD	0,46	-0,45	-0,74	-0,65	-1,34
5253fa36_131	221	M000000_AE050823-101_MST_365240_EICAT_threonine-109	1,14	A4	A3	– – . – –	+ . . . –	-0,33	-0,30	-0,08	-0,68	-0,61	0,15	-0,31	-0,86	-0,92	-1,75
5253fa36_133	1494	M000074_A134001-101_METB_365427_EINS_Succinic acid (2TMS)	8,68	00	A2	– + – . –	+ – – – –	LOD	0,58	-0,21	0,01	LOD	0,17	-1,37	-2,10	-2,09	-2,08
5253fa36_135	1494	M000074_A134001-101_METB_365427_EINS_Succinic acid (2TMS)	1,13	A4	A1	. . . – –	+ – – – –	0,20	-0,11	0,09	-0,86	-0,39	0,13	-0,85	-1,04	-0,66	-1,26
5253fa36_140		Threonine	0,94	B5	B13	– – – – +	– – – – –	-0,66	-1,21	-1,43	-1,11	0,21	-0,23	-1,01	-1,44	-0,43	-0,73
5253fa36_141		Thymine	1,46	A2	A2	– – – – –	– . – . –	-0,76	-1,23	-1,70	-2,02	-1,76	-0,17	-0,63	-1,26	-0,56	-1,03
5253fa36_142	2335	M000456_A136001-101_METB_392490_EINIST_Uracil (2TMS)	2,26	A2	A3	– – – – –	– . . . –	-0,56	-1,47	-1,91	-2,43	-2,27	0,00	-0,15	-0,34	-0,17	-1,71

Analyte ID[a]	Hit ID[b]	Metabolite/ Best Library Hit[c]	Profile dissimilarity[d]	Response profile assignment[e]		Direction of change in analyte level[g]		Analyte level[h] (log2 ratio) for									
								CC-1690					sac1				
				CC-1690	*sac1*	CC-1690	*sac1*	+2h	-2h	-5h	-10h	-24 h	+2h	-2h	-5h	-10h	-24 h
5253fa36_144		Fumaric acid	0,71	A2	A2	– – – – –	. . . . .	-0,33	-0,97	-1,56	-1,62	-1,61	0,12	-0,27	-1,25	-0,94	-0,94
5253fa36_145	3141	M000638_A189008-101_METB_625030_EIGTMS_Gluconic acid-1,5-lactone, D- (4TMS)	10,85	A3	B5	. – – – –	–	-0,19	-0,89	-0,63	-0,47	LOD	-0,63	0,10	-0,16	-0,01	0,08
5253fa36_152	1678	M000102_A143001-101_METB_415730_EITTMS_Glutaric acid (2TMS)	3,16	D9	E21	. . + + +	– – . + –	0,35	0,57	1,55	1,71	2,02	-0,36	-1,26	1,81	0,75	-1,14
5253fa36_154	215	M000000_AE050823-101_MST_378400_EICAT_glycerol2(put.)-121	1,40	C19	A6	. . . + .	+ – – – –	0,10	0,25	0,29	0,71	0,44	0,62	-1,02	-1,05	-0,65	-0,96
5253fa36_161	1420	M000067_A137001-101_METB_371255_EITTMS_Fumaric acid (2TMS)	1,50	C17	A6	. . . . .	+ – – – –	-0,09	0,11	0,33	0,42	-0,22	0,49	-1,19	-1,17	-0,89	-1,29
5253fa36_170	169	M000000_AE050823-101_MST_507120_EICAT_glutamic acid-208	0,72	E15	B5	. . . . .	– . – . .	-0,39	-0,24	-0,21	0,09	-0,21	-0,13	-0,06	-0,93	0,03	0,32
5253fa36_179	207	M000000_AE050823-101_MST_404410_EICAT_y-139	15,05	00	00	+ + . + +	+ – – – +	*4,20*	*4,29*	*0,00*	*3,62*	*4,44*	0,08	LOD	-0,98	-0,50	0,29
5253fa36_193	1953	M000186_A151005-101_METB-METB_466925_EINS_Putrescine (3TMS)	3,76	A4	E14	. . . – –	. – . . –	-1,13	-0,16	-1,09	-3,02	-4,09	0,30	-3,92	-1,68	-2,40	-4,58
5253fa36_199	413	M000000_AE041126-101_METB_425580_EIFIEHN_Naphthalene, 1,2,3,4-tetrahydro-1,1,6-trimethyl-	2,02	A3	00	+ + + + –	– – + – –	0,18	1,72	1,38	0,66	LOD	-4,63	-0,30	0,24	-0,66	LOD
5253fa36_207	1728	M000106_A220002-101_METB_728760_EINS_Spermidine (4TMS)	2,59	A3	A1	. . – – –	– – – – –	-0,33	-0,29	-1,63	-2,17	-3,81	-0,32	-2,87	-2,08	-2,98	-4,59
5253fa36_209	2465	M000477_A176004-101_MST_558110_EIFIEHN_Glucosone, 3-deoxy- (2MEOX) (3TMS)	1,49	C19	A6	. . . + .	+ – – – –	-0,13	0,16	0,17	0,44	0,29	0,36	-1,14	-1,27	-1,05	-1,11
5253fa36_211	56	M000000_AE050823-101_MST_756640_EICAT_y-390	1,30	D7	B5	. . . . .	–	-0,60	0,07	0,18	0,64	1,05	-1,40	-0,09	-1,12	-0,10	0,35
5253fa36_213		Malic Acid	1,15	A4	A1	. – – – –	+ . – – –	-0,01	-0,93	-1,85	-2,42	-2,21	0,04	-0,51	-1,17	-1,27	-1,68
5253fa36_215	1573	M000078_A156001-101_METB_458330_EINS_Threonic acid (4TMS)	1,50	B5	A2	. . . . .	– . – . .	-0,24	-0,42	-0,62	-0,19	0,64	-1,41	-0,89	-1,52	-0,84	-0,86
5253fa36_221		4-Hydroxyproline	1,76	C20	C10	– + . . .	+ + + . –	-0,37	1,49	1,07	0,44	0,43	0,42	1,08	0,34	0,13	-1,33
5253fa36_222	3153	M000639_A189003-101_METB_618870_EIFIEHN_Galactonic acid-1,4-lactone, DL- (4TMS)	1,66	D7	A2	. . . . .	–	0,41	0,30	-0,07	0,39	0,50	-1,15	-0,74	-1,34	-1,27	-0,75
5253fa36_227	2929	M000592_A172006-101_METB_553540_EITTMS_Adipic acid, 2-amino-, DL- (3TMS)	8,59	00	B11	. – + + +	– – – – –	0,06	LOD	0,73	1,12	1,71	-0,40	-2,17	-1,63	-1,91	-1,30
5253fa36_230		Aspartic acid	0,52	B11	B13	– – – – –	+ – – – –	-0,36	-1,70	-1,62	-1,44	-0,68	0,26	-2,12	-1,79	-0,92	-0,82
5253fa36_231		Threonic acid	1,25	A2	A2	. . – – .	– . – – –	-0,09	-0,66	-0,94	-1,18	-0,67	-0,86	-0,67	-1,86	-1,92	-1,92
5253fa36_233	1427	M000069_A182004-101_METB-METB_592883_EINS_Citric acid (4TMS)	1,34	A2	B13	– . – – .	+ – – – –	-0,58	-0,16	-0,61	-0,60	-0,35	0,14	-1,50	-1,28	-0,73	-0,73
5253fa36_236	2839	M000582_A168002-101_METB_500740_EITRAPTMS_Ribose, D- (1MEOX) (4TMS)	9,92	A3	A2	. . . . –	+ – – – –	-0,09	0,03	0,02	0,02	LOD	0,06	-0,73	-1,41	-0,92	-0,84
5253fa36_238	1414	M000067_A137001-101_METB_371255_EIBOEL_Fumaric acid (2TMS)	4,55	C17	D9	. + . + .	. + + + +	*0,00*	*5,38*	*4,14*	*4,05*	*0,00*	*0,75*	*4,20*	*5,86*	*6,31*	*4,55*
5253fa36_240	3149	M000639_A189003-101_METB_618870_EIGTMS_Galactonic acid-1,4-lactone, D(-)- (4TMS)	2,95	B5	00	. . . . .	– – . . –	0,04	0,40	-0,69	-0,24	1,04	-4,63	-1,55	-0,43	-0,80	-1,91
5253fa36_242	2261	M000432_A116005-101_MST_253950_EINIST_Hexanoic acid, 2-ethyl- (1TMS)	0,79	A2	A1	. – – – –	– – – – –	-0,02	-2,26	-2,53	-2,77	-2,88	-0,13	-2,20	-2,57	-2,42	-3,66
5253fa36_246	864	M000028_A162001-101_METB-METB_490485_EIGTMS_Ornithine, DL- (3TMS)	1,96	D7	B16	. . . . .	. . . . .	-1,63	0,25	1,03	1,49	2,10	0,26	-1,71	0,37	1,24	0,41
5253fa36_247		2-Isopropylmalic acid	6,82	A2	A4	– – – – –	– – – – –	-0,90	-3,13	LOD	LOD	LOD	-0,70	-2,66	-3,94	LOD	LOD
5253fa36_249	426	M000000_AE041126-101_METB_379620_EIFIEHN_Geraniol	9,17	A1	A3	– – – – –	– – – – –	-0,60	-0,83	-1,02	-0,87	-1,59	-0,59	-2,24	-1,83	-1,19	LOD
5253fa36_250	276	M000000_AE041126-101_METB_1052100_EIFIEHN_Vitamin D3	1,10	A2	C8	. . . . .	. . – . –	0,11	-0,17	-0,39	-0,18	-0,24	0,87	0,39	-0,77	-0,41	-1,33
5253fa36_251		Cysteine	1,37	A1	A3	. . – – –	. – – – –	-0,48	-0,49	-0,87	-0,97	-1,42	-0,13	-1,33	-1,06	-1,22	-2,79
5253fa36_253	581	M000014_A192003-101_METB_615467_EINS_Lysine (4TMS)	8,04	A3	E14	. . . – –	– – . – –	-0,15	-0,52	-1,45	-1,82	LOD	-0,07	-2,50	-0,55	-1,67	-2,73
5253fa36_257	68	M000000_AE050823-101_MST_731340_EICAT_y-369	10,25	C10	A3	+ + + + –	– . – – –	0,10	0,79	0,42	0,26	-0,52	-0,49	-0,77	-1,37	-1,29	LOD
5253fa36_260	1168	M000043_A191002-101_METB-METB_587270_EINS_Galactose, D- (1MEOX) (5TMS)	1,32	C20	00	+ + + . .	– + . + –	0,57	0,90	0,81	0,20	0,23	-4,63	0,39	0,23	0,63	-1,10
5253fa36_262	6	M000000_AE050823-101_MST_1077300_EICAT_cholesterol-D(RI marker)-505	1,10	C8	A3	– + – – –	– – – – –	-0,56	0,32	-1,32	-0,99	-1,46	-0,34	-0,58	-0,86	-1,09	-2,56
5253fa36_263	152	M000000_AE050823-101_MST_539340_EICAT_yfatty acid-234	1,03	D12	A2	– . – – .	– . – . .	-1,20	-0,22	-0,55	-1,14	0,66	-0,03	-0,21	-0,75	-0,18	-0,36
5253fa36_267	1620	M000085_A185013-101_METB_606980_EIFIEHN_Gulonic acid, 2-oxo-, DL- (1MEOX) (5TMS)	2,43	D7	E15	. . . . +	– . . . –	-0,15	-0,40	0,09	0,65	1,37	-1,13	-0,66	-0,57	0,12	-1,07
5253fa36_268	373	M000000_AE041126-101_METB_541310_EIFIEHN_Galactose, 3,6-anhydro-	0,62	A6	00	– – – – –	– – – – –	-0,98	-1,97	-1,73	-1,80	-1,67	-4,63	-1,51	-1,77	-1,26	-2,29
5253fa36_269	319	M000000_AE041126-101_METB_814940_EIFIEHN_Bis-trispropane	1,28	D7	00	. . . + +	– – – – –	-0,30	0,20	-0,16	0,29	0,66	-4,63	-0,92	-0,84	-0,79	-0,61
5253fa36_273	3210	M000663_A283001-101_METB_979380_EIFIEHN_Squalene, all-trans-	1,07	A4	A1	. . – – –	– . – – –	0,05	-0,20	-0,31	-0,40	-0,50	-0,43	-0,40	-0,92	-0,88	-1,57
5253fa36_281	2229	M000427_A122003-101_MST_300730_EINIST_Malonic acid (2TMS)	0,53	E14	A3	. – . . .	– . . . –	0,03	-0,72	-0,20	-0,21	-0,36	-0,04	-0,19	-0,44	-0,03	-0,86
5253fa36_283		Oxoproline	0,59	A2	A1	– – – – –	– – – – –	-0,41	-0,96	-1,38	-1,41	-1,19	-0,09	-0,97	-1,33	-0,81	-1,64
5253fa36_284		Glutamic acid	1,75	A2	E15	– – – – –	– – – . –	-0,34	-1,63	-2,41	-2,42	-2,08	-0,11	-0,98	-1,43	-0,67	-1,99
5253fa36_285	169	M000000_AE050823-101_MST_507120_EICAT_glutamic acid-208	1,17	A4	A4	+ + – – –	+ . – – –	0,35	0,86	-0,67	-1,53	-2,45	0,12	-0,01	-0,99	-2,70	-3,24
5253fa36_286	2071	M000296_A283011-101_METB_926665_EINS_Gentiobiose (1MEOX) (8TMS)	0,70	A4	A4	– . . – –	+ . . – –	-0,61	0,32	-0,18	-0,69	-0,59	0,23	-0,38	-0,69	-1,23	-1,02
5253fa36_287	2727	M000563_A280001-101_IS (RI05)_943980_EITTMS_Octacosane, n-	1,21	D7	E15	. . . . .	+	0,02	-0,10	-0,09	0,02	0,73	0,06	-0,23	-0,74	0,33	-0,48
5253fa36_288	1086	M000037_A153002-101_METB-METB_506483_EINS_Pyroglutamic acid, DL- (2TMS)	12,00	C19	00	. . . + +	+ – – – –	-0,11	-0,06	0,36	1,24	0,35	0,78	-0,66	-0,95	LOD	-0,67
5253fa36_291	6	M000000_AE050823-101_MST_1077300_EICAT_cholesterol-D(RI marker)-505	1,13	D9	E15	. + + + +	. . . . –	0,47	0,71	1,13	0,92	0,57	0,83	-0,20	0,07	0,38	-0,56
5253fa36_292		Nicotinamide	0,78	A2	00	. – – – –	– – – – –	-0,11	-0,88	-1,74	-1,76	-1,67	-4,63	-0,38	-1,16	-1,41	-2,45
5253fa36_293		Putrescine	3,31	A4	E14	. . – – –	. . . . –	-0,88	0,10	-1,61	-2,46	-4,21	0,40	-3,20	-2,04	-2,39	-4,75
5253fa36_294	205	M000000_AE050823-101_MST_408950_EICAT_erythritol-141	4,56	D7	D9	. – + . +	. + + + +	-0,04	-0,75	1,40	0,39	1,75	*0,75*	*3,82*	*3,64*	*4,23*	*5,09*

Analyte ID[a]	Hit ID[b]	Metabolite/ Best Library Hit[c]	Profile dissimilarity[d]	Response profile assignment[e]		Direction of change in analyte level[g]		Analyte level[h] (log2 ratio) for									
								CC-1690					sac1				
				CC-1690	*sac1*	CC-1690	*sac1*	+2h	-2h	-5h	-10h	-24 h	+2h	-2h	-5h	-10h	-24 h
5253fa36_296	165	M000000_AE050823-101_MST_518850_EICAT_y-216	10,76	00	C17	– + + + –	. + + + .	LOD	1,46	0,66	0,60	LOD	*0,75*	*7,25*	*5,95*	*5,76*	*0,00*
5253fa36_299	6	M000000_AE050823-101_MST_1077300_EICAT_cholesterol-D(RI marker)-505	7,23	D9	A6	+ . + . +	– – – – –	*3,88*	*4,21*	*4,01*	*4,23*	*4,06*	-0,40	-2,77	-1,90	-3,00	-2,77
5253fa36_300		2-Ketoglutaric acid	3,47	D12	00	. – – – +	– + – + –	-0,06	-0,43	-0,67	-2,43	0,55	-4,63	0,67	-0,09	1,05	-0,54
5253fa36_304	24	M000000_AE050823-101_MST_906020_EICAT_fatty acid-455	2,10	D9	B13	. + + + +	+ – – – –	0,49	1,02	1,15	1,35	1,32	0,34	-1,08	-0,93	-0,72	-0,75
5253fa36_305	6	M000000_AE050823-101_MST_1077300_EICAT_cholesterol-D(RI marker)-505	1,56	A4	A3	. . – – –	– . – – –	-0,20	-0,09	-0,31	-0,49	-0,65	-0,61	-0,61	-1,41	-1,08	-2,21
5253fa36_306	1367	M000060_A209002-101_METB_653910_EITTMS_Inositol, myo- (6TMS)	9,82	00	A3	. – – – –	– – – – –	-0,37	-1,08	-2,84	LOD	-1,40	0,00	-0,81	-0,61	-0,94	-1,78
5253fa36_308		Phenylalanine	0,80	B5	B5	– – – – .	– – – – –	-0,60	-1,68	-1,84	-1,38	-0,05	-0,60	-1,83	-2,26	-1,24	-0,85
5253fa36_310	49	M000000_AE050823-101_MST_772990_EICAT_y-400	1,98	D12	00	. – – – .	– + . + .	-0,46	-0,45	-0,91	-1,04	0,22	-4,63	1,12	0,74	0,95	0,57
5253fa36_317	1086	M000037_A153002-101_METB-METB_506483_EINS_Pyroglutamic acid, DL- (2TMS)	2,32	B11	00	– – – – –	– – – – –	-1,03	-1,97	-1,50	-2,04	-0,63	-4,63	-0,87	-1,40	-0,99	-2,95
5253fa36_318	372	M000000_AE041126-101_METB_543600_EIFIEHN_Bis-acrylamide	0,86	A6	A2	– – – – –	– – – – –	-1,59	-2,72	-2,80	-2,78	-2,07	-0,23	-2,09	-2,96	-2,81	-2,93
5253fa36_320	1950	M000186_A151005-101_METB-METB_466925_EIGTMS_Putrescine (3TMS)	4,06	C10	E14	. . . – –	. . . . .	-0,67	0,47	-1,07	-1,21	-3,63	0,64	-3,59	-1,83	-2,11	-3,75
5253fa36_322	331	M000000_AE041126-101_METB_700690_EIFIEHN_Glucosamine, N-acetyl-	2,15	D9	00	. . + . +	– – – – –	0,34	0,56	0,96	0,91	0,68	-4,63	-1,19	-0,88	-1,23	-0,41
5253fa36_324	1110	M000038_A183001-101_METB-METB_605940_EIFIEHN_Citrulline, DL-, -H2O (3TMS)	1,06	B5	A2	. . – – .	– – – – –	-0,11	-0,28	-0,55	-0,43	0,23	-0,74	-0,67	-1,35	-0,86	-0,83
5253fa36_334	569	M000013_A168001-101_METB_550100_EITTMS_Asparagine, DL- (3TMS)	9,53	00	A6	. – – – –	– – – – –	-0,34	-1,04	-1,54	LOD	-1,24	-0,07	-1,53	-1,31	-1,23	-1,84
5253fa36_335	476	M000007_A185001-101_METB_577930_EIMOR_Quinic acid, D(-)- (5TMS)	10,62	00	00	. – – – –	– – – – –	-0,18	-0,54	LOD	LOD	-0,15	-0,23	LOD	-1,87	-1,24	LOD
5253fa36_338		Glycerolphosphate	1,47	A2	A1	. . – – .	– – – – –	-0,17	-0,24	-0,40	-0,55	-0,29	-0,56	-0,66	-1,37	-0,98	-1,76
5253fa36_346		D-Glucose-1-phosphate	0,63	A2	A3	. . – – –	– . – . –	-0,14	-0,07	-0,54	-0,61	-0,29	-0,14	-0,16	-0,49	-0,42	-0,91
5253fa36_351	2484	M000479_A166003-101_CONT-METB_527860_EITTMS_Dodecanoic acid, n- (1TMS)	11,09	A3	00	+ + + – –	– – – . –	0,31	0,34	0,33	-0,29	LOD	-0,58	-0,86	LOD	-0,03	-1,67
5253fa36_357	2484	M000479_A166003-101_CONT-METB_527860_EITTMS_Dodecanoic acid, n- (1TMS)	1,54	00	00	– – + + –	– – – – –	LOD	LOD	0,21	0,55	-1,48	-0,77	LOD	-1,34	-0,42	-1,77
5253fa36_361	2096	M000328_A177002-101_METB_574230_EIGTMS_Glycerol-3-phosphate, DL- (4TMS)	9,52	A3	A2	+ + . . –	– – – – –	0,30	1,23	0,07	-0,16	LOD	-0,38	-0,67	-1,08	-1,74	-1,25
5253fa36_364		Glycerolphosphate	0,99	A3	A1	. . – – –	– – – – –	0,19	0,01	-0,48	-0,55	-1,08	-0,47	-0,48	-1,23	-1,13	-2,08
5253fa36_365	2100	M000328_A177002-101_METB_574230_EIFIEHN_Glycerol-3-phosphate, DL- (4TMS)	8,38	A3	A6	. – – + –	. – – – –	-0,01	-0,23	-0,85	0,83	LOD	0,58	-1,95	-1,71	-1,21	-2,38
5253fa36_366	2029	M000248_A172001-101_METB_557320_EIFIEHN_Glucose, 1,6-anhydro, beta-D- (3TMS)	1,41	C10	A1	. . . . .	+ – – – –	-0,05	0,09	-0,12	0,03	-0,21	0,05	-1,06	-1,05	-1,15	-1,61
5253fa36_367	2087	M000328_A177002-101_METB_574230_EINS_Glycerol-3-phosphate, DL- (4TMS)	1,58	A4	C10	. . . – .	+ + + + –	0,05	0,17	-0,36	-0,74	-0,54	0,35	1,40	0,99	0,84	-0,77
5253fa36_369	138	M000000_AE050823-101_MST_573260_EICAT_glycerolphosphate alpha-260	11,62	A2	A3	+ . – – –	+ + + – –	0,07	-0,35	LOD	LOD	LOD	0,40	0,69	0,86	-0,58	LOD
5253fa36_372	229	M000000_AE050823-101_MST_333620_EICAT_phosphoric acid-88	0,86	A4	A1	. . . – .	–	-0,06	0,35	-0,12	-0,43	-0,25	-0,33	-0,42	-0,98	-0,44	-1,06
5253fa36_374		Mannose	2,83	E18	C17	. . + – .	. . . + .	0,28	0,17	0,97	-0,94	0,49	0,75	0,88	0,72	1,89	0,56
5253fa36_376	2259	M000431_A164005-101_MST_500320_EIFIEHN_Valeric acid, 5-amino- (3TMS)	2,71	A3	E14	. . – – –	+ – – – –	-0,27	0,04	-1,45	-1,04	-3,52	0,89	-2,67	-1,55	-1,37	-2,97
5253fa36_378		Shikimic Acid	3,00	A2	A6	– – – – –	– – – – –	-1,38	-7,76	LOD	LOD	LOD	-0,87	LOD	LOD	LOD	LOD
5253fa36_380	2318	M000454_A154001-101_MST_442640_EINS_Erythronic acid (4TMS)	0,82	C8	A4	. . – – –	– – – – –	-0,10	0,39	-0,62	-0,53	-1,10	-0,23	-0,35	-0,72	-1,24	-1,92
5253fa36_383		D-Glucose	2,33	E18	E15	– . + – .	+	-0,41	-0,31	2,38	-0,80	0,26	0,10	-0,17	0,05	0,26	-0,57
5253fa36_384		Citric Acid	2,49	A2	C17	. . – – –	. . . . .	0,08	-1,04	-2,05	-1,86	-1,65	0,44	0,14	0,42	0,63	-0,04
5253fa36_387	2222	M000426_A340005-101_IS (RI05)_1107200_EIFIEHN_Tetratriacontane, n-	1,40	C10	A1	. . . . –	– – – – –	0,05	0,18	-0,01	-0,10	-0,38	-0,37	-0,86	-1,26	-1,00	-1,78
5253fa36_388	1351	M000060_A209002-101_METB_653910_EINS_Inositol, myo- (6TMS)	10,76	00	00	+	– – – – –	*4,12*	*0,00*	*0,00*	*0,00*	*0,00*	-4,63	-0,22	-0,79	-0,92	LOD
5253fa36_389		Inositol-β-galactoside	4,60	D9	A3	+ + + + +	. . . . .	1,94	2,29	2,37	1,69	1,48	0,91	-0,13	0,22	-0,39	-3,11
5253fa36_390	264	M000000_AE041126-101_METB_1107900_EIFIEHN_Corticosterone, 11-deoxy-	1,73	D9	A2	. + + + +	. – – – –	0,09	0,55	0,54	0,72	0,43	0,69	-0,87	-0,99	-1,01	-1,02
5253fa36_391		Glutamine	0,84	A1	A3	. – – – –	– – – – –	-0,23	-2,16	-2,99	-3,42	-3,79	-0,07	-2,05	-2,22	-2,58	-4,60
5253fa36_393	2555	M000493_A238008-101_MST_835420_EIFIEHN_Eicosatetraenoic acid, 5,8,11,14-(Z,Z,Z,Z)-, n- (1TMS)	1,00	B11	A2	. – . . .	– – – – –	0,00	-0,50	-0,39	-0,35	-0,05	-0,04	-0,51	-1,09	-1,21	-1,06
5253fa36_395	276	M000000_AE041126-101_METB_1052100_EIFIEHN_Vitamin D3	1,26	A2	A1	+ . – – .	– . – – –	0,42	-0,10	-0,33	-0,45	-0,22	-0,46	-0,22	-1,10	-0,93	-1,48
5253fa36_396	2222	M000426_A340005-101_IS (RI05)_1107200_EIFIEHN_Tetratriacontane, n-	1,40	C8	A1	. . . . –	– – – – –	0,01	0,22	-0,10	-0,18	-0,41	-0,49	-0,85	-1,21	-1,00	-1,81
5253fa36_399		D-Phosphoglyceric acid	4,49	B5	C17	. . – – .	– . . + .	1,23	0,55	-1,29	-0,67	1,40	-0,24	1,41	3,19	2,46	-1,00
5253fa36_401	358	M000000_AE041126-101_METB_575930_EIFIEHN_Benzofuranone, 2(4H)- 5,6,7,7a-tetrahydro-4,4,7a-trimethyl-	1,54	C8	A1	+ . – . –	– – – – –	0,24	0,11	-0,16	-0,17	-0,38	-0,26	-0,64	-1,28	-1,26	-1,92
5253fa36_402	3210	M000663_A283001-101_METB_979380_EIFIEHN_Squalene, all-trans-	1,45	D9	A2	. + + + +	. . . . .	-0,01	0,43	0,57	0,49	0,63	0,56	-0,62	-0,88	-0,84	-0,55
5253fa36_403	554	M000013_A168001-101_METB_550100_EINS_Asparagine, DL- (3TMS)	9,47	00	00	– – + – –	– – – – –	-0,42	LOD	0,80	LOD	-0,10	-4,63	-1,29	-1,71	-1,94	-0,85
5253fa36_405	358	M000000_AE041126-101_METB_575930_EIFIEHN_Benzofuranone, 2(4H)- 5,6,7,7a-tetrahydro-4,4,7a-trimethyl-	12,87	E18	A3	. + + . +	. . . –	0,54	1,79	2,25	0,56	2,11	0,61	-0,11	-0,08	0,35	LOD
5253fa36_410	68	M000000_AE050823-101_MST_731340_EICAT_y-369	1,25	E22	A6	. + . . .	+ – – – –	0,08	0,23	0,07	0,06	0,14	0,36	-0,88	-0,96	-0,78	-1,11
5253fa36_413	115	M000000_AE050823-101_MST_615400_EICAT_myristic acid-296	16,50	00	D9	+ – – – –	. + + + +	0,31	LOD	-0,77	-0,40	-0,34	*0,75*	*5,73*	*4,86*	*5,32*	*4,41*
5253fa36_414	342	M000000_AE041126-101_METB_665030_EIFIEHN_Hydantoin, 5-epsilon-hydroxybutyl-	10,11	00	A3	– – – – –	+ . – . –	-0,64	-1,14	LOD	-2,49	-2,00	0,08	-0,06	-0,66	-0,27	-2,24

Analyte ID[a]	Hit ID[b]	Metabolite/ Best Library Hit[c]	Profile dissimilarity[d]	Response profile assignment[e]		Direction of change in analyte level[g]		Analyte level[h] (log2 ratio) for									
								CC-1690					sac1				
				CC-1690	*sac1*	CC-1690	*sac1*	+2h	-2h	-5h	-10h	-24 h	+2h	-2h	-5h	-10h	-24 h
5253fa36_415		Lysine	9,03	A3	A3	– . . . –	+ – . . –	-0,87	-0,05	0,03	0,41	-1,73	0,09	-0,95	-0,34	-0,13	LOD
5253fa36_416		Myristic Acid	1,79	D12	A4	. . . . .	+ . . – .	0,80	0,07	-0,11	-0,33	1,04	0,34	0,64	-0,29	-0,91	-0,75
5253fa36_418	1883	M000158_A332001-101_METB_1114100_EITTBS_Stigmasterol (1TMS)	1,21	B5	A6	– + – – +	+ – – – –	-0,18	0,12	-0,29	-0,15	0,41	0,59	-1,09	-1,31	-1,13	-0,77
5253fa36_419		Galactonic acid γ-lactone	9,67	A3	C10	+ – + . –	. + . + –	0,33	-0,41	0,35	0,13	LOD	0,79	0,58	0,21	0,48	-1,10
5253fa36_420	152	M000000_AE050823-101_MST_539340_EICAT_γfatty acid-234	6,33	A3	E14	– . – – –	– – – – –	-0,30	0,01	-1,84	-1,38	LOD	-0,15	-2,83	-1,93	-3,34	-4,44
5253fa36_421	3210	M000663_A283001-101_METB_979380_EIFIEHN_Squalene, all-trans-	1,63	A2	A1	. . – – .	– – – – –	0,37	-0,23	-0,40	-0,43	-0,31	-0,44	-0,42	-1,10	-1,15	-1,94
5253fa36_426	2197	M000420_A114005-101_METB_235660_EIFIEHN_Valeric acid, 3-hydroxy-3-methyl- (1TMS)	0,93	A4	00	. . – – –	– – – – –	-0,05	-0,19	-0,42	-0,76	-0,74	-4,63	-0,44	-1,30	-0,98	-1,67
5253fa36_428	358	M000000_AE041126-101_METB_575930_EIFIEHN_Benzofuranone, 2(4H)- 5,6,7,7a-tetrahydro-4,4,7a-trimethyl-	0,73	A3	A3	. + . + –	+ . – . –	-0,10	0,35	-0,09	0,53	LOD	1,00	0,01	-0,82	-0,07	LOD
5253fa36_430		D-Gluconic acid	9,47	00	00	. – + – –	– . – – –	0,08	-0,82	0,64	LOD	-2,22	-4,63	0,11	-1,71	-1,29	-1,60
5253fa36_431	358	M000000_AE041126-101_METB_575930_EIFIEHN_Benzofuranone, 2(4H)- 5,6,7,7a-tetrahydro-4,4,7a-trimethyl-	0,96	A2	A6	– – – – –	– – – – –	-0,75	-1,17	-1,69	-1,38	-1,15	-0,11	-2,05	-1,77	-2,20	-2,11
5253fa36_432	358	M000000_AE041126-101_METB_575930_EIFIEHN_Benzofuranone, 2(4H)- 5,6,7,7a-tetrahydro-4,4,7a-trimethyl-	1,57	A1	A1	+ . – – –	– – – – –	0,28	-0,14	-0,38	-0,36	-0,55	-0,54	-0,59	-1,40	-1,34	-2,11
5253fa36_433	3210	M000663_A283001-101_METB_979380_EIFIEHN_Squalene, all-trans-	1,57	A2	A1	. . – – –	– – – – –	0,22	-0,28	-0,51	-0,77	-0,47	-0,51	-0,77	-1,42	-1,63	-2,04
5253fa36_434	1883	M000158_A332001-101_METB_1114100_EITTBS_Stigmasterol (1TMS)	1,40	D7	A1	+ . . . +	– – – – –	0,41	-0,14	0,27	0,24	0,66	-0,08	-0,23	-0,64	-0,59	-0,74
5253fa36_436	264	M000000_AE041126-101_METB_1107900_EIFIEHN_Corticosterone, 11-deoxy-	1,03	C17	A1	. . . . .	+ . . . –	0,12	0,31	0,36	0,32	-0,02	0,09	-0,33	-0,57	-0,67	-1,05
5253fa36_437	3210	M000663_A283001-101_METB_979380_EIFIEHN_Squalene, all-trans-	1,30	A3	A3	. – – – –	– – – – –	0,13	-0,65	-0,58	-0,78	-1,53	-0,21	-1,18	-1,67	-1,41	-2,83
5253fa36_438	2222	M000426_A340005-101_IS (RI05)_1107200_EIFIEHN_Tetratriacontane, n-	1,00	E18	E15	. . + . .	. . . . .	-0,10	0,21	0,87	0,01	0,62	0,63	-0,24	0,02	0,61	-0,38
5253fa36_439	49	M000000_AE050823-101_MST_772990_EICAT_γ-400	2,54	C17	A6	. + + + .	. . . . .	0,37	0,53	0,44	0,99	0,17	-0,01	-2,00	-1,80	-1,55	-1,88
5253fa36_441	6	M000000_AE050823-101_MST_1077300_EICAT_cholesterol-D(RI marker)-505	10,45	A4	00	. – – – –	– . – – –	-0,34	-0,82	-1,39	LOD	LOD	-4,63	0,12	-1,25	-0,32	-1,65
5253fa36_442	269	M000000_AE041126-101_METB_1091500_EIFIEHN_Progesterone	0,96	C17	A1	. . . . .	+ . . . –	0,00	0,31	0,34	0,29	-0,03	0,03	-0,26	-0,62	-0,60	-0,97
5253fa36_455	2528	M000484_A214005-101_METB_734910_EIGTMS_Heptadecanoic acid, n- (1TMS)	0,67	C20	C20	. . . . .	. . + – –	-1,79	0,36	0,23	-0,21	-0,38	0,92	1,00	0,90	-0,60	-0,75
5253fa36_459	84	M000000_AE050823-101_MST_684070_EICAT_γ-340	1,45	A4	C8	. – – – –	– . – . –	-0,02	-0,78	-1,78	-2,36	-2,14	-1,23	0,25	-1,31	-0,91	-1,91
5253fa36_463	24	M000000_AE050823-101_MST_906020_EICAT_fatty acid-455	1,05	E22	A1	. + . . .	. . – – –	-0,15	0,28	-0,02	0,20	0,06	0,53	-0,40	-0,86	-0,66	-0,99
5253fa36_464	6	M000000_AE050823-101_MST_1077300_EICAT_cholesterol-D(RI marker)-505	0,90	A1	A1	– . – – –	– – – – –	-0,42	-0,59	-0,67	-0,64	-0,98	-0,46	-1,21	-1,56	-1,30	-1,85
5253fa36_465	3143	M000638_A189008-101_METB_625030_EIMOR_Gluconic acid-1,5-lactone, D- (4TMS)	1,43	A1	A1	. . . . –	– – – – –	0,15	-0,12	-0,39	-0,38	-0,61	-0,01	-0,71	-1,37	-1,40	-2,04
5253fa36_467	1352	M000060_A209002-101_METB_653910_EINS_Inositol, myo- (6TMS)	4,81	B13	00	. – – . .	– + + + –	0,05	-2,93	-2,20	-0,45	-1,00	-4,63	1,70	2,62	2,29	-1,08
5253fa36_468		myo-Inositol	1,19	B11	A2	– – – – .	– – – – –	-0,23	-0,58	-0,41	-0,59	0,03	-0,16	-0,60	-1,16	-0,77	-1,17
5253fa36_469	50	M000000_AE050823-101_MST_771080_EICAT_γ-399	2,26	D9	A6	. . . . .	. . . . .	-0,64	0,33	0,56	0,71	0,44	0,83	-1,92	-1,16	-1,20	-1,66
5253fa36_470	51	M000000_AE050823-101_MST_770270_EICAT_stearic acid-398	1,80	D12	E18	. . . . .	. . . – .	0,64	-0,55	-0,59	-0,47	1,06	0,89	1,25	0,56	-1,42	0,28
5253fa36_472		Tyrosine	0,91	B5	B5	. – – – .	– – – – –	-0,09	-1,22	-1,62	-1,42	0,27	-0,43	-1,45	-1,78	-1,16	-0,63
5253fa36_473	358	M000000_AE041126-101_METB_575930_EIFIEHN_Benzofuranone, 2(4H)- 5,6,7,7a-tetrahydro-4,4,7a-trimethyl-	2,15	C10	A3	. . . . –	. – – – –	0,09	1,24	0,31	0,21	-0,59	0,50	-0,91	-1,19	-1,10	-2,15
5253fa36_481	88	M000000_AE050823-101_MST_668330_EICAT_γ-330	2,46	D12	A6	. . . – .	– – . – –	1,01	-0,66	-0,87	-1,03	1,65	-0,56	-1,07	-1,15	-1,15	-0,81
5253fa36_482	2478	M000479_A166003-101_CONT-METB_527860_EIMOR_Dodecanoic acid, n- (1TMS)	2,24	D9	B11	+ + + + +	. – – – .	0,42	1,08	1,06	1,68	1,20	0,61	-0,94	-0,78	-0,56	0,04
5253fa36_483	3335	M000706_A274007-101_METB_947757_EINS_Tetracosanoic acid methyl ester, n-	1,04	E21	D9	. . . . .	+ + + + +	-0,05	0,14	0,57	0,39	0,11	1,48	0,82	1,40	1,43	0,83
5253fa36_484	14	M000000_AE050823-101_MST_966040_EICAT_γ-474	1,17	A4	A3	. . – – –	– – – – –	0,07	0,02	-0,58	-0,84	-1,15	-1,12	-0,40	-1,30	-0,85	-2,32
5253fa36_485	432	M000000_A238008-101_MST_835210_EICAT_Eicosatetraenoic acid, 5,8,11,14-(Z,Z,Z,Z)-, n- (1TMS)	1,33	C8	A1	. + – – –	– – – – –	0,02	0,33	-0,33	-0,38	-0,29	-0,78	-0,67	-1,25	-0,83	-1,62
5253fa36_486	2190	M000417_A111001-101_METB_196800_EIFIEHN_Limonene, (+/-)-	1,64	A4	A1	. . . – –	– – – – –	-0,04	0,10	-0,22	-0,52	-0,52	-0,12	-0,81	-1,45	-1,04	-2,17
5253fa36_487	1220	M000048_A277002-101_METB_887905_EINS_Maltose, D- (1MEOX) (8TMS)	10,53	B13	A3	. – – . .	+ – – – –	-0,18	-0,59	-0,66	-0,22	-0,23	0,07	-0,40	-0,19	-0,42	LOD
5253fa36_488	608	M000015_A138001-101_METB_357523_EINS_Serine, DL- (3TMS)	1,14	A4	A3	. . . – –	+ . . . –	-0,11	-0,13	-0,63	-1,30	-1,36	0,07	-0,06	-0,38	-0,44	-2,49
5253fa36_490		Adenine	1,60	A3	A1	. . . . –	– – – – –	-0,45	-0,55	-0,47	-0,55	-1,52	-0,04	-1,37	-2,07	-1,90	-2,77
5253fa36_491	41	M000000_AE050823-101_MST_814750_EICAT_γ-415	1,35	C8	A1	– . . . –	+ – – – –	-0,40	0,04	-0,33	-0,30	-0,61	0,09	-1,13	-1,48	-1,50	-1,96
5253fa36_492	608	M000015_A138001-101_METB_357523_EINS_Serine, DL- (3TMS)	0,62	A3	A3	. . . . –	– . – . –	-0,34	-0,10	-0,56	-0,61	-1,16	-0,08	-0,43	-0,63	-0,26	-1,79
5253fa36_494	2478	M000479_A166003-101_CONT-METB_527860_EIMOR_Dodecanoic acid, n- (1TMS)	2,07	C17	B13	+ + + + +	+ – – – .	0,54	1,09	0,94	1,59	0,58	0,38	-0,98	-0,72	-0,43	-0,30
5253fa36_495	86	M000000_AE050823-101_MST_678620_EICAT_fatty acid-336	0,75	A6	A3	. – . – –	– . . . –	-0,06	-0,93	-0,66	-1,08	-0,84	-0,26	-0,23	-0,96	-0,82	-1,59
5253fa36_496	739	M000019_A146001-101_METB_404940_EITTMS_Homoserine, DL- (3TMS)	10,69	00	A3	– – – – –	+ + – – –	LOD	-0,36	LOD	LOD	-0,37	0,11	0,17	-0,08	-0,31	LOD
5253fa36_499	2977	M000606_A188004-101_METB_582135_EINS_Fructose, D- (1MEOX) (5TMS)	3,00	D9	C17	+ + + + +	+ + + + .	*3,69*	*5,78*	*6,05*	*5,37*	*3,00*	*2,98*	*5,35*	*6,15*	*6,17*	*0,00*
5253fa36_502	2499	M000482_A203002-101_MST_696130_EIFIEHN_Hexadecenoic acid, 9-(Z)-, n- (1TMS)	1,63	D12	A1	. . . . .	– – – – –	0,40	0,09	0,00	-0,17	0,24	-0,16	-0,46	-1,12	-1,12	-1,39

Analyte ID[a]	Hit ID[b]	Metabolite/ Best Library Hit[c]	Profile dissimilarity[d]	Response profile assignment[e]		Direction of change in analyte level[g]		Analyte level[h] (log2 ratio) for									
								CC-1690					sac1				
				CC-1690	*sac1*	CC-1690	*sac1*	+2h	-2h	-5h	-10h	-24 h	+2h	-2h	-5h	-10h	-24 h
5253fa36_503	2553	M000493_A238008-101_MST_835420_EINIST_Eicosatetraenoic acid, 5,8,11,14-(Z,Z,Z,Z)-, n-(1TMS)	1,79	C8	A1	+	– – – – –	0,26	0,21	-0,15	-0,14	-0,07	-0,39	-0,77	-1,51	-1,31	-1,87
5253fa36_504	2504	M000483_A205001-101_METB_487695_EINS_Hexadecanoic acid, n- (1TMS)	14,63	00	C17	. – + – +	. + + + .	-0,01	LOD	0,60	LOD	1,14	*0,75*	*3,00*	*3,97*	*3,86*	*0,00*
5253fa36_506	2503	M000483_A205001-101_METB_487695_EINS_Hexadecanoic acid, n- (1TMS)	1,55	B16	A2	. – – + .	– – – – –	-0,22	-0,52	-0,30	0,32	0,03	-0,44	-0,90	-1,76	-0,94	-1,52
5253fa36_507		Palmitic acid	1,45	D12	A2	. . . . .	– – – – –	-0,01	-0,11	-0,26	-0,14	0,41	-0,32	-0,62	-1,16	-1,15	-1,03
5253fa36_510	80	M000000_AE050823-101_MST_694760_EICAT_palmitoleic acid-349	1,58	B11	A3	. – . – .	– . . – –	0,00	-0,53	-0,21	-0,50	0,11	-0,06	-0,21	-0,68	-0,83	-1,47
5253fa36_511	24	M000000_AE050823-101_MST_906020_EICAT_fatty acid-455	2,74	E18	A1	+	– . – – –	0,59	0,35	-0,12	-0,84	-0,01	-0,89	-0,70	-1,65	-2,12	-2,75
5253fa36_512	1883	M000158_A332001-101_METB_1114100_EITTBS_Stigmasterol (1TMS)	2,03	B5	A2	. – – – .	– – – – –	-0,21	-0,48	-0,73	-0,51	-0,11	-0,50	-1,07	-1,97	-1,86	-2,14
5253fa36_514	2977	M000606_A188004-101_METB_582135_EINS_Fructose, D- (1MEOX) (5TMS)	0,93	A1	00	. – . – –	– – – – –	-0,29	-0,66	-0,64	-0,82	-1,24	-4,63	-0,52	-1,56	-1,72	-1,64
5253fa36_515	2484	M000479_A166003-101_CONT-METB_527860_EITTMS_Dodecanoic acid, n- (1TMS)	9,15	00	00	. – – – –	– . . – –	0,51	LOD	LOD	LOD	-1,08	-0,66	-1,62	-1,81	LOD	-2,83
5253fa36_519	1655	M000100_A105001-101_CONT-METB_190250_EINIST_Lactic acid, DL- (2TMS)	5,09	C17	E14	. + + + .	– – – – –	*0,00*	*3,42*	*3,41*	*3,89*	*0,00*	-0,28	-1,68	-1,36	-0,67	-2,29
5253fa36_520	12	M000000_AE050823-101_MST_987080_EICAT_y-479	1,79	B5	00	. – – . +	– – – – –	0,18	-0,06	-0,51	-0,02	0,16	-4,63	-0,66	-1,15	-1,81	-1,60
5253fa36_521	24	M000000_AE050823-101_MST_906020_EICAT_fatty acid-455	0,76	B11	00	. – – – .	– . . . –	-0,06	-0,61	-0,56	-0,72	-0,21	-4,63	-0,15	-0,45	-0,07	-0,97
5253fa36_523	1387	M000065_A149001-101_METB_440995_EITTMS_Malic acid, DL- (3TMS)	2,00	A3	00	. + + + –	– – – – –	-0,02	0,42	0,26	0,33	LOD	-4,63	-1,25	-1,75	-1,53	LOD
5253fa36_524	2309	M000451_A117005-101_METB_300550_EIFIEHN_Menthol, L-(-)- (1TMS)	1,57	A1	A1	. . . . –	. . . . –	-0,36	-0,78	-0,78	-0,98	-1,26	-0,44	-1,30	-1,94	-1,96	-2,83
5253fa36_527	3141	M000638_A189008-101_METB_625030_EIGTMS_Gluconic acid-1,5-lactone, D- (4TMS)	0,99	A1	A1	– . – – –	– . – – –	-1,50	-0,19	-0,86	-0,63	-1,02	-0,20	-0,90	-1,84	-1,38	-1,98
5253fa36_529	138	M000000_AE050823-101_MST_573260_EICAT_glycerolphosphate alpha-260	1,64	D12	E14	–	+ – – – –	-0,55	-0,11	0,01	-0,17	0,30	0,06	-1,06	-0,69	-0,80	-1,35
5253fa36_532	2501	M000482_A203002-101_MST_696130_EITTMS_	1,25	A2	A3	. . . . .	+ . – – –	0,11	-0,01	-0,29	-0,36	-0,28	0,07	-0,24	-0,91	-0,76	-1,53
5253fa36_534	426	M000000_AE041126-101_METB_379620_EIFIEHN_Geraniol	1,97	A4	A1	. . . . –	– . . . –	-0,71	-0,20	-0,23	-0,54	-0,88	-0,46	-1,74	-2,10	-1,89	-2,85
5253fa36_535	609	M000015_A138001-101_METB_357523_EINS_Serine, DL- (3TMS)	1,65	A2	A1	. . – – .	– . – – –	0,04	-0,03	-0,42	-0,44	-0,30	-0,48	-0,98	-1,51	-1,43	-1,95
5253fa36_537	2309	M000451_A117005-101_METB_300550_EIFIEHN_Menthol, L-(-)- (1TMS)	1,13	A4	A1	. . – – –	– – – – –	0,03	0,01	-0,32	-0,41	-0,52	-0,18	-0,71	-1,09	-1,02	-1,65
5253fa36_538	2309	M000451_A117005-101_METB_300550_EIFIEHN_Menthol, L-(-)- (1TMS)	2,82	D9	A2	. + + + +	. . – . –	0,41	1,08	1,12	1,53	1,12	0,54	-0,98	-1,70	-0,64	-1,02
5253fa36_539		Heptadecanoic acid	1,24	B5	E18	. . . . .	. . . – .	-0,32	-0,50	-0,78	-0,50	0,51	0,95	0,74	0,19	-1,12	0,22
5253fa36_541	426	M000000_AE041126-101_METB_379620_EIFIEHN_Geraniol	1,75	A4	A1	– . . – –	– . – – –	-0,78	-0,30	-0,51	-0,84	-0,94	-0,34	-1,90	-2,06	-1,96	-2,69
5253fa36_543	2096	M000328_A177002-101_METB_574230_EIGTMS_Glycerol-3-phosphate, DL- (4TMS)	1,72	D9	C17	– . + + +	– + + + .	-0,51	0,53	1,52	1,23	1,68	-0,64	0,41	0,90	1,21	-0,03
5253fa36_546	2071	M000296_A283011-101_METB_926665_EINS_Gentiobiose (1MEOX) (8TMS)	7,45	A6	00	– – – – –	– – – – –	-2,26	LOD	LOD	LOD	LOD	-4,63	-3,32	LOD	LOD	LOD
5253fa36_550	3212	M000663_A283001-101_METB_979380_EIMOR_Squalene, all-trans-	0,68	B11	A3	. – . – .	– . . . –	-0,05	-0,44	-0,24	-0,57	-0,19	-0,14	-0,38	-0,48	-0,44	-0,88
5253fa36_551	2707	M000549_A213005-101_METB_873090_EISTR_Octadecanoic acid methyl ester, n-	0,97	A3	A3	– . . . –	+ – – – –	-0,62	-0,07	0,01	-0,33	-0,82	0,04	-0,71	-0,97	-0,59	-1,69
5253fa36_553	291	M000000_AE041126-101_METB_933070_EIFIEHN_	1,98	E18	B16	. + + . .	– – . . .	0,13	1,55	1,09	0,34	1,75	-0,56	-0,44	-0,23	-0,20	0,12
5253fa36_554	50	M000000_AE050823-101_MST_771080_EICAT_y-399	1,31	A2	A3	. . . . .	– . . – –	0,01	-0,11	-0,52	-0,55	-0,34	-0,79	-0,17	-0,58	-0,73	-1,65
5253fa36_555	2556	M000496_A342003-101_MST_1121400_EIFIEHN_Triacontanoic acid, n- (1TMS)	9,79	A4	00	. . – – –	– – – – –	0,02	0,01	-0,52	-0,67	-0,97	-4,63	-0,63	-0,68	-0,65	LOD
5253fa36_556	2036	M000249_A290012-101_METB_959360_EIFIEHN_	0,48	D7	00	– + . + +	– . – . +	-0,67	0,18	0,01	0,46	1,10	-4,63	-0,06	-0,47	0,09	1,08
5253fa36_557	291	M000000_AE041126-101_METB_933070_EIFIEHN_	1,43	B5	A2	. . . . .	– . – – –	-0,41	0,33	-0,35	-0,10	0,37	-0,25	-0,92	-1,64	-1,30	-1,06
5253fa36_558	57	M000000_AE050823-101_MST_752260_EICAT_y-cho-P (put.)-388	1,39	B5	A3	. . . . .	– . – . –	0,01	-0,26	-0,53	-0,17	0,14	-0,99	-0,02	-0,63	-0,28	-1,25
5253fa36_559	57	M000000_AE050823-101_MST_752260_EICAT_y-cho-P (put.)-388	0,92	E18	C10	. . . – .	–	-0,10	0,38	0,23	-0,85	-0,04	-0,28	0,35	-0,34	-0,18	-0,96
5253fa36_561	3210	M000663_A283001-101_METB_979380_EIFIEHN_Squalene, all-trans-	1,16	B5	A2	– . – . .	– – – – –	-0,33	0,02	-0,38	-0,33	0,07	-0,15	-0,78	-1,28	-0,88	-1,09
5253fa36_562	6	M000000_AE050823-101_MST_1077300_EICAT_cholesterol-D(RI marker)-505	10,76	00	00	. – – – –	. + . . +	0,20	-0,42	-1,89	LOD	-2,73	*0,75*	*5,73*	*0,00*	*0,00*	*4,03*
5253fa36_564	50	M000000_AE050823-101_MST_771080_EICAT_y-399	1,13	B11	A3	. – . – .	– . . . –	0,23	-0,95	-0,64	-0,86	-0,36	-0,26	-0,14	-0,65	-0,72	-1,49
5253fa36_565	2597	M000510_A232002-101_METB_767060_EIBOEL_Fructose-6-phosphate (1MEOX) (6TMS)	9,51	00	00	– – – – –	– – – – –	LOD	-0,09	LOD	LOD	LOD	-4,63	-0,75	-2,66	-1,26	LOD
5253fa36_568		D-Fructose-6-phosphate	0,98	E18	A1	–	– . . . –	-1,34	0,12	-0,11	-0,87	-0,03	-0,70	-0,65	-0,56	-0,73	-1,01
5253fa36_569	52	M000000_AE050823-101_MST_767400_EICAT_octadecanoic acid 3xTMS (put.)-396	1,62	B5	A1	. . – . .	– . – – –	0,19	-0,05	-0,35	-0,32	-0,06	-0,34	-0,39	-1,30	-1,26	-1,69
5253fa36_570	2554	M000493_A238008-101_MST_835420_EIMOR_Eicosatetraenoic acid, 5,8,11,14-(Z,Z,Z,Z)-, n-(1TMS)	1,57	D12	A6	. . . . .	– – – – –	0,07	0,09	-0,12	-0,32	0,62	-0,32	-0,92	-1,16	-0,96	-0,95
5253fa36_571	52	M000000_AE050823-101_MST_767400_EICAT_octadecanoic acid 3xTMS (put.)-396	1,50	B5	A1	. . – – .	– – – – –	-0,02	-0,17	-0,36	-0,26	-0,05	-0,41	-0,80	-1,44	-1,18	-1,55
5253fa36_572	51	M000000_AE050823-101_MST_770270_EICAT_stearic acid-398	1,02	D12	A2	. . . . .	+ – – – –	-0,28	-0,05	-0,17	-0,11	0,45	0,06	-0,54	-0,82	-0,81	-0,57
5253fa36_573	50	M000000_AE050823-101_MST_771080_EICAT_y-399	1,55	B16	A2	. – – . +	– – – – –	-0,08	-0,34	-0,44	0,02	0,27	-0,53	-0,89	-1,45	-0,90	-1,28
5253fa36_574		D-Glucose-6-phosphate	1,49	D7	A2	. + . + +	–	0,03	0,58	0,19	0,24	1,25	-0,13	-0,26	-0,30	-0,46	-0,24
5253fa36_575	319	M000000_AE041126-101_METB_814940_EIFIEHN_Bis-trispropane	1,37	E15	00	. – – . .	– – – – .	-0,33	-0,33	-1,10	0,47	-0,01	-4,63	-0,80	-1,39	-0,90	-0,32
5253fa36_579	2554	M000493_A238008-101_MST_835420_EIMOR_Eicosatetraenoic acid, 5,8,11,14-(Z,Z,Z,Z)-, n-(1TMS)	0,69	E15	E15	. . . . .	+ – – . –	-1,38	-0,80	-0,57	0,21	-1,11	0,17	-0,63	-1,26	0,20	-1,47
5253fa36_580	2555	M000493_A238008-101_MST_835420_EIFIEHN_Eicosatetraenoic acid, 5,8,11,14-(Z,Z,Z,Z)-, n-	1,20	D12	A6	. . . . +	– – – – –	-0,22	0,03	-0,15	-0,17	0,57	-0,28	-0,53	-0,69	-0,59	-0,62

Analyte ID[a]	Hit ID[b]	Metabolite/ Best Library Hit[c]	Profile dissimilarity[d]	Response profile assignment[e]		Direction of change in analyte level[g]		Analyte level[h] (log2 ratio) for									
								CC-1690					sac1				
				CC-1690	*sac1*	CC-1690	*sac1*	+2h	-2h	-5h	-10h	-24 h	+2h	-2h	-5h	-10h	-24 h
		(1TMS)															
5253fa36_581	50	M000000_AE050823-101_MST_771080_EICAT_y-399	1,74	A2	A1	+ . – – –	– – – – –	0,26	-0,03	-0,34	-0,30	-0,34	-0,66	-0,77	-1,68	-1,52	-2,08
5253fa36_582	2555	M000493_A238008-101_MST_835420_EIFIEHN_Eicosatetraenoic acid, 5,8,11,14-(Z,Z,Z,Z)-, n-(1TMS)	1,52	A2	A1	. . . . .	– – – – –	-0,11	-0,10	-0,20	-0,06	-0,10	-0,42	-1,00	-1,34	-1,34	-1,62
5253fa36_588	2190	M000417_A111001-101_METB_196800_EIFIEHN_Limonene, (+/-)-	1,53	B11	A6	– – – – .	– – – – –	-0,36	-1,02	-0,86	-0,74	0,13	-0,25	-1,19	-0,98	-1,38	-1,40
5253fa36_589	52	M000000_AE050823-101_MST_767400_EICAT_octadecanoic acid 3xTMS (put.)-396	1,21	A1	E14	– . – . –	– – . . –	-0,81	-0,28	-0,58	-0,31	-0,77	-0,91	-1,43	-0,92	-0,88	-1,97
5253fa36_590	1883	M000158_A332001-101_METB_1114100_EITTBS_Stigmasterol (1TMS)	1,64	C10	A4	. + . . .	+ . . – –	-0,46	1,19	0,43	0,39	-0,45	0,17	-0,45	-0,09	-1,11	-0,75
5253fa36_591	815	M000026_A110001-101_METB_208565_EINS_Alanine (2TMS)	1,81	A3	A1	– . . . –	. . . . –	-0,48	0,09	-0,10	-0,40	-2,19	0,19	-1,72	-1,56	-1,64	-2,03
5253fa36_592		Inositol-1-phosphate	1,50	C8	A1	. . . . .	– . – – –	0,05	0,40	-0,54	0,01	-0,45	-0,48	-0,48	-1,49	-0,93	-1,95
5253fa36_594	49	M000000_AE050823-101_MST_772990_EICAT_y-400	2,41	C10	A6	. . . . .	. – . . –	-0,11	0,80	0,22	0,24	-0,14	0,55	-1,61	-0,94	-1,12	-1,37
5253fa36_598	14	M000000_AE050823-101_MST_966040_EICAT_y-474	1,79	D12	A2	. . – – .	– – – – –	-0,16	-0,11	-0,68	-0,86	0,18	-0,33	-0,93	-1,65	-1,10	-1,61
5253fa36_602	1728	M000106_A220002-101_METB_728760_EINS_Spermidine (4TMS)	10,33	B13	00	– – . . .	– – . – –	-0,67	-0,44	-0,38	-0,21	-0,26	-0,60	LOD	-0,38	-0,81	-1,16
5253fa36_606	2136	M000347_A128003-101_CONT-METB_348220_EITTMS_Benzoic acid (1TMS)	2,52	B5	00	. . – – .	– – – – –	-0,40	-0,08	-0,91	-0,98	-0,20	-4,63	-1,91	-2,18	-1,26	-2,72
5253fa36_611	3210	M000663_A283001-101_METB_979380_EIFIEHN_Squalene, all-trans-	1,61	A1	A1	. . – – –	– . . . –	0,10	-0,28	-0,78	-0,52	-1,02	-0,56	-1,13	-1,88	-1,93	-2,63
5253fa36_612	2624	M000513_A235002-101_METB-METB_781350_EIBOEL_Glucose-6-phosphate (1MEOX) (6TMS)	5,83	00	00	+ + + + +	+ + . . +	*4,68*	*5,61*	*5,83*	*4,73*	*3,45*	*2,66*	*3,50*	*0,00*	*0,00*	*4,79*
5253fa36_613	2675	M000522_A136003-101_MST_430640_EITTMS_	1,98	B16	B13	. . . . .	– – . . .	-1,25	-0,80	-0,27	-0,22	0,38	-0,42	-2,79	-1,09	-0,25	-0,32
5253fa36_616	57	M000000_AE050823-101_MST_752260_EICAT_y-cho-P (put.)-388	4,42	D12	A3	. . . . +	– . . . –	0,85	0,73	-0,33	-0,42	1,29	-1,49	-0,38	0,04	-0,40	-3,13
5253fa36_617	86	M000000_AE050823-101_MST_678620_EICAT_fatty acid-336	1,44	B11	A1	. . . . .	– . – – –	0,14	-0,25	-0,20	-0,24	-0,05	-0,26	-0,29	-1,01	-0,66	-1,49
5253fa36_618	3381	M000724_A243001-101_METB_789700_EITTMS_Inositol-1-phosphate, myo- (7TMS)	1,84	B5	A1	. . – . .	– – – – –	0,00	-0,12	-0,42	-0,05	0,29	-0,66	-0,68	-1,16	-1,08	-1,55
5253fa36_619	2179	M000415_A141002-101_CONT-METB_404860_EIMOR_Lactic acid dimer, DL- (2TMS)	5,06	E15	D9	+ . – + .	+ + + + +	0,58	0,02	-0,55	0,29	-0,10	*2,25*	*4,76*	*4,51*	*5,31*	*3,44*
5253fa36_620	339	M000000_AE041126-101_METB_676200_EIFIEHN_Myristic acid, 3-hydroxy-, DL-	1,56	D7	A1	. . . . .	– – – – –	0,22	0,16	0,03	0,14	0,38	-0,23	-0,72	-1,08	-0,76	-1,18
5253fa36_622	2036	M000249_A290012-101_METB_959360_EIFIEHN_	1,42	C8	00	. . – . .	– – – – –	0,14	0,14	-0,25	-0,04	-0,19	-4,63	-0,80	-1,25	-0,89	-1,61
5253fa36_623	3254	M000673_A299002-101_METB_940280_EIQTMS_Galactinol (9TMS)	2,85	B5	A6	– . – . .	– – – . –	-0,99	-0,49	-0,72	-0,41	0,56	-0,69	-2,13	-1,72	-0,54	-2,30
5253fa36_626	2071	M000296_A283011-101_METB_926665_EINS_Gentiobiose (1MEOX) (8TMS)	2,41	B5	A2	– + – . +	– – – – –	-1,98	0,34	-0,27	0,08	0,69	-0,72	-0,62	-1,87	-1,41	-1,72
5253fa36_631		Palmitoleic acid	1,85	B5	A1	. . . . .	– – – – –	-0,03	-0,29	-0,40	-0,22	0,14	-0,25	-1,21	-1,31	-1,41	-1,71
5253fa36_637	2624	M000513_A235002-101_METB-METB_781350_EIBOEL_Glucose-6-phosphate (1MEOX) (6TMS)	2,71	D7	E15	+ + + + +	–	0,51	1,33	1,80	1,11	2,64	-0,70	0,03	0,08	0,34	-0,08
5253fa36_640	24	M000000_AE050823-101_MST_906020_EICAT_fatty acid-455	1,62	A2	A1	. . – – –	– . – – –	0,15	-0,13	-0,61	-0,32	-0,39	-0,53	-0,84	-1,62	-1,24	-2,01
5253fa36_644	2287	M000440_A189017-101_MST_645560_EIFIEHN_Pyridoxine (3TMS)	15,53	A4	D9	. + . – –	. + + + +	-0,22	0,39	0,05	LOD	LOD	*0,75*	*3,54*	*4,66*	*4,76*	*4,24*
5253fa36_645	34	M000000_AE050823-101_MST_853860_EICAT_y-433	1,13	C20	A3	– . + . .	– . . . –	-0,78	0,20	0,47	0,06	-0,13	-0,40	-0,01	0,10	0,23	-1,26
5253fa36_646	33	M000000_AE050823-101_MST_855370_EICAT_fatty acid-434	3,42	C10	E14	. . . . .	. – . . .	-0,58	1,29	0,55	0,53	-0,13	0,69	-2,13	-0,72	-0,85	-1,33
5253fa36_650	185	M000000_AE050823-101_MST_470240_EICAT_adipic acid-181	2,17	D7	A2	. . . + +	– – – – –	0,32	0,08	0,47	0,59	1,01	-0,81	-1,17	-1,49	-0,91	-1,16
5253fa36_651	2071	M000296_A283011-101_METB_926665_EINS_Gentiobiose (1MEOX) (8TMS)	11,32	A4	00	– + + – –	+ – – – –	-0,08	0,48	0,56	LOD	LOD	0,49	-0,88	LOD	-2,23	LOD
5253fa36_655		Maltose	1,45	D7	A6	– . . . +	– – – . –	-0,68	-0,22	0,14	0,09	0,46	-0,57	-0,93	-0,81	-0,40	-0,99
5253fa36_656	21	M000000_AE050823-101_MST_928380_EICAT_y-460	1,32	D7	C8	– . . . +	– + – – –	-0,64	0,07	-0,13	0,15	0,56	-0,08	0,16	-1,32	-0,81	-0,76
5253fa36_658	6	M000000_AE050823-101_MST_1077300_EICAT_cholesterol-D(RI marker)-505	1,17	A4	00	. . – – –	– – – – –	-0,08	0,06	-0,29	-0,52	-0,80	-4,63	-0,53	-1,32	-1,10	-1,97
5253fa36_659	30	M000000_AE050823-101_MST_877600_EICAT_y-441	1,06	A2	A1	. . – – –	– . – – –	0,10	-0,23	-1,01	-0,80	-0,62	-0,18	-0,26	-1,47	-1,21	-1,68
5253fa36_661	30	M000000_AE050823-101_MST_877600_EICAT_y-441	3,37	E15	A1	. . . . .	. . . . .	0,06	-0,01	-0,10	0,15	-0,08	-1,05	-1,76	-2,59	-2,72	-3,45
5253fa36_662	1228	M000048_A277002-101_METB_887905_EIQTMS_Maltose, D- (1MEOX) (8TMS)	1,51	A2	B13	–	– – . . .	-1,11	-0,37	-0,57	-0,27	-0,41	-1,25	-1,89	-1,17	-0,38	-0,57
5253fa36_664	29	M000000_AE050823-101_MST_880080_EICAT_fatty acid-442	2,49	C19	C8	– . . . +	– + – . .	-0,50	0,01	0,01	1,82	0,73	-0,11	2,50	-1,45	-0,15	-0,29
5253fa36_665	6	M000000_AE050823-101_MST_1077300_EICAT_cholesterol-D(RI marker)-505	9,68	00	A2	+ + – – +	– – – – –	0,11	0,32	LOD	-0,27	0,46	-0,60	-0,21	-1,09	-0,78	-0,80
5253fa36_668	2036	M000249_A290012-101_METB_959360_EIFIEHN_	10,25	A4	00	. . . – –	– – – – –	-0,01	0,28	-0,20	-0,50	-0,51	-4,63	-0,43	-1,39	-0,97	LOD
5253fa36_669	2084	M000323_A178012-101_METB_558940_EIFIEHN_Mannopyranoside, 1-O-methyl-, alpha-D-(4TMS)	2,33	A3	A1	. . – . –	– . – – –	0,06	-0,15	-0,46	-0,25	-1,18	-0,85	-1,70	-2,55	-2,42	-3,52
5253fa36_671	271	M000000_AE041126-101_METB_1082400_EIFIEHN_Cholecalciferol	1,07	C10	A2	. . . . .	– – – – –	0,07	0,06	-0,02	-0,01	-0,11	-0,67	-0,75	-1,10	-1,04	-1,12
5253fa36_675	56	M000000_AE050823-101_MST_756640_EICAT_y-390	1,79	B13	A2	– – – . .	. – – – –	-1,42	-0,53	-0,33	0,00	-0,07	0,49	-0,95	-2,12	-1,16	-1,56
5253fa36_678	12	M000000_AE050823-101_MST_987080_EICAT_y-479	1,14	A4	A1	. . . . –	– – – – –	0,07	0,00	-0,22	-0,27	-0,40	-0,84	-0,81	-1,15	-0,92	-1,53
5253fa36_681	2202	M000423_A115004-101_METB_244690_EIFIEHN_Propan-1,3-diol, 2-methyl-2-amino- (2TMS)	17,11	00	C19	– – + – –	. . + + .	LOD	LOD	4,65	LOD	LOD	*0,75*	*0,00*	*3,00*	*6,34*	*0,00*
5253fa36_682	96	M000000_AE050823-101_MST_654560_EICAT_y-cho-alc-321	2,44	D9	A3	+ . + + .	. – . – –	0,57	0,35	1,15	0,78	0,88	0,63	-0,53	-0,28	-0,66	-1,56
5253fa36_683	2478	M000479_A166003-101_CONT-METB_527860_EIMOR_Dodecanoic acid, n- (1TMS)	0,99	E22	A4	+	– – – – –	0,39	0,24	0,00	0,10	0,05	-0,53	-0,28	-0,59	-0,89	-0,77
5253fa36_684	30	M000000_AE050823-101_MST_877600_EICAT_y-441	1,54	C10	A1	. . . . –	– – – – –	-0,10	0,37	-0,08	-0,34	-1,50	-0,13	-1,07	-1,63	-1,85	-2,86

Analyte ID[a]	Hit ID[b]	Metabolite/ Best Library Hit[c]	Profile dissimilarity[d]	Response profile assignment[e]		Direction of change in analyte level[g]		Analyte level[h] (log2 ratio) for									
								CC-1690					sac1				
				CC-1690	*sac1*	CC-1690	*sac1*	+2h	-2h	-5h	-10h	-24 h	+2h	-2h	-5h	-10h	-24 h
5253fa36_685	135	M000000_AE050823-101_MST_577470_EICAT_y-cho-264	10,90	E18	00	. . . . .	– . – – –	-0,44	0,11	0,13	-0,36	0,03	-4,63	-0,08	LOD	LOD	-1,00
5253fa36_686	2066	M000284_A307003-101_METB_1054900_EIFIEHN_Adenosine-5-monophosphate (5TMS)	1,09	B11	A1	. . . – .	– – – – –	-0,05	-0,38	-0,08	-0,67	-0,28	-0,22	-0,72	-0,96	-1,06	-1,37
5253fa36_688	2071	M000296_A283011-101_METB_926665_EINS_Gentiobiose (1MEOX) (8TMS)	6,52	00	B16	– – – – –	+ – – + .	-5,07	-4,71	-2,37	-5,17	-3,72	0,03	-1,56	-0,92	1,35	0,51
5253fa36_696	20	M000000_AE050823-101_MST_930590_EICAT_y-461	1,19	A6	C8	– . – – –	– + – . –	-0,80	-0,50	-0,44	-0,64	-0,68	-0,17	0,69	-1,38	-0,61	-1,06
5253fa36_697	2484	M000479_A166003-101_CONT-METB_527860_EITTMS_Dodecanoic acid, n- (1TMS)	2,85	C10	A3	. . . – –	– . – – –	0,25	0,47	-0,20	-0,38	-1,24	-0,23	-1,09	-1,80	-1,89	-4,09
5253fa36_700	3258	M000673_A299002-101_METB_940280_EIQTMS_Galactinol (9TMS)	1,64	B16	A2	. . . . .	– – – – –	0,09	-0,21	-0,17	0,01	0,07	-0,08	-1,16	-1,49	-1,43	-1,58
5253fa36_704	19	M000000_AE050823-101_MST_937290_EICAT_y-465	1,33	B11	A4	. . . . .	– – – – –	-0,45	-0,24	-0,02	-0,37	-0,05	-0,35	-0,63	-1,01	-1,64	-1,38
5253fa36_705	18	M000000_AE050823-101_MST_938800_EICAT_y-466	6,20	C19	E22	. . + . .	+ + – . .	-0,05	0,37	1,51	5,49	0,22	0,11	6,57	-0,65	3,18	2,11
5253fa36_707	17	M000000_AE050823-101_MST_941220_EICAT_y-468	0,84	B13	A2	– – – . –	– – – – –	-0,97	-0,64	-0,80	-0,11	-0,34	-0,39	-0,66	-1,36	-0,81	-1,18
5253fa36_708	2071	M000296_A283011-101_METB_926665_EINS_Gentiobiose (1MEOX) (8TMS)	3,14	B5	A3	. – – . .	– . – –	-0,41	-0,50	-0,94	-0,28	0,54	-0,25	0,18	0,00	-0,59	-2,59
5253fa36_711	17	M000000_AE050823-101_MST_941220_EICAT_y-468	0,81	A1	A1	– – – – –	– – – – –	-0,77	-0,45	-0,36	-0,51	-0,65	-0,38	-0,75	-1,15	-1,23	-1,46
5253fa36_712	2967	M000599_A173009-101_METB_487133_EISTR_Tetradecanoic acid methyl ester, n-	1,59	B5	00	. . – – +	– – – – –	-0,13	0,05	-0,36	-0,11	0,26	-4,63	-0,89	-1,35	-1,03	-1,33
5253fa36_713	21	M000000_AE050823-101_MST_928380_EICAT_y-460	1,47	E15	A6	–	– – – – –	-0,30	-0,04	0,06	0,22	-0,10	-0,52	-1,38	-1,41	-1,02	-1,55
5253fa36_714	17	M000000_AE050823-101_MST_941220_EICAT_y-468	1,49	C19	A3	. . . . .	– – – . –	0,01	0,01	0,03	0,13	0,02	-1,00	-0,33	-0,74	-0,14	-1,47
5253fa36_715	3413	M000779_A266004-101_METB_930670_EIFIEHN_Xanthosine (5TMS)	3,44	00	00	– + + + +	– . + + +	LOD	2,49	2,94	3,82	4,34	-4,63	1,75	2,55	3,41	0,90
5253fa36_717	2484	M000479_A166003-101_CONT-METB_527860_EITTMS_Dodecanoic acid, n- (1TMS)	1,71	D7	B11	. . . . .	. . – – .	-0,79	0,30	0,03	0,51	0,72	0,50	-0,72	-0,91	-1,20	-0,21
5253fa36_718	3258	M000673_A299002-101_METB_940280_EIQTMS_Galactinol (9TMS)	1,93	D7	E14	+ . . . +	. – . . .	1,07	-0,16	1,15	0,57	1,94	0,92	-0,70	0,41	-0,25	0,01
5253fa36_719	1427	M000069_A182004-101_METB-METB_592883_EINS_Citric acid (4TMS)	1,90	E22	A6	. . . . +	– – – – –	0,04	0,43	0,11	0,29	0,25	-0,45	-1,47	-1,54	-1,12	-1,65
5253fa36_721	2977	M000606_A188004-101_METB_582135_EINS_Fructose, D- (1MEOX) (5TMS)	1,19	A4	A1	– – – – –	– – – – –	-0,67	-0,33	-0,39	-0,61	-0,68	-0,64	-0,88	-1,17	-1,21	-1,86
5253fa36_722	64	M000000_AE050823-101_MST_738300_EICAT_y-375	10,55	B16	00	. – . . .	+ – – – –	-0,06	-0,30	-0,22	-0,09	0,25	0,15	-0,88	LOD	-0,46	-0,66
5253fa36_723		trans-Squalene	1,26	B5	A2	– – – – –	– – – – –	-1,34	-1,56	-2,90	-2,84	-0,72	-0,08	-0,31	-3,22	-3,20	-1,56
5253fa36_724	291	M000000_AE041126-101_METB_933070_EIFIEHN_	2,02	D7	B16	. . . . +	– – – . .	-0,33	0,44	0,50	0,51	1,09	-0,40	-1,39	-1,52	-0,52	-0,01
5253fa36_725	31	M000000_AE050823-101_MST_872060_EICAT_y-fatty acid-440	2,60	E21	A6	. . + + +	– – – – –	0,02	-0,03	0,54	0,66	0,37	-0,82	-1,86	-1,77	-1,42	-2,23
5253fa36_727	49	M000000_AE050823-101_MST_772990_EICAT_y-400	3,75	C20	00	. . . . .	– – – – –	-0,28	0,57	0,31	-0,01	0,13	-4,63	-1,38	-3,44	-3,07	-0,85
5253fa36_729	30	M000000_AE050823-101_MST_877600_EICAT_y-441	2,95	D7	B11	. . . + +	– – – – –	-0,16	0,06	-0,04	0,70	0,79	-0,87	-1,99	-2,17	-2,25	-0,91
5253fa36_738	1889	M000158_A332001-101_METB_1114100_EIFIEHN_Stigmasterol (1TMS)	1,98	A1	A1	. . . . .	–	0,09	-0,10	-0,38	-0,19	-0,52	-1,25	-0,82	-1,86	-1,72	-2,50
5253fa36_742	24	M000000_AE050823-101_MST_906020_EICAT_fatty acid-455	1,24	B16	B13	. – . . .	– – – – –	0,14	-0,18	-0,02	0,02	0,10	-0,35	-1,43	-1,12	-0,84	-0,82
5253fa36_743	24	M000000_AE050823-101_MST_906020_EICAT_fatty acid-455	1,85	B16	B13	. . . . .	– – – – –	0,19	-0,06	-0,06	0,20	0,15	-1,39	-1,92	-1,22	-0,95	-0,88
5253fa36_744	413	M000000_AE041126-101_METB_425580_EIFIEHN_Naphthalene, 1,2,3,4-tetrahydro-1,1,6-trimethyl-	2,45	D12	A6	. . . . .	–	-0,70	-0,27	-0,31	-0,25	0,53	-0,96	-1,74	-1,90	-1,44	-1,92
5253fa36_750	2036	M000249_A290012-101_METB_959360_EIFIEHN_	1,77	D7	A2	. . . + +	– – – – –	0,24	-0,04	0,10	0,27	0,55	-0,41	-0,70	-1,67	-1,13	-0,91
5253fa36_751	3076	M000626_A316001-101_METB_1070600_EIGTMS_Tocopherol, alpha- (1TMS)	1,06	B5	A1	. . – – .	– – – – –	0,06	-0,22	-0,46	-0,36	0,20	-0,71	-0,45	-0,83	-0,64	-0,85
5253fa36_752	3447	M000799_A327001-101_METB_1051900_EITTMS_Ergosterol (1TMS)	1,28	B5	A1	. . – . .	– – – – –	-0,06	-0,15	-0,27	-0,16	-0,03	-0,62	-0,69	-1,20	-1,04	-1,30
5253fa36_757	1728	M000106_A220002-101_METB_728760_EINS_Spermidine (4TMS)	2,20	A3	A1	. . . . .	. . . . .	0,15	-0,13	-0,51	0,03	-0,88	-1,23	-1,08	-2,19	-2,17	-3,07
5253fa36_761	50	M000000_AE050823-101_MST_771080_EICAT_y-399	4,38	00	00	+ + . + .	–	*3,86*	*3,82*	*0,00*	*3,20*	*0,00*	-4,63	-0,56	-1,17	-1,16	-2,50
5253fa36_763	2036	M000249_A290012-101_METB_959360_EIFIEHN_	1,22	B16	A2	. . . . .	– – – – –	0,10	-0,15	-0,20	0,12	0,33	-0,20	-0,53	-1,41	-0,86	-0,84
5253fa36_764	3073	M000626_A316001-101_METB_1070600_EIFIEHN_Tocopherol, alpha- (1TMS)	9,85	00	A2	. . – – +	– – – – –	0,15	-0,02	-0,24	LOD	0,28	-0,44	-0,66	-1,22	-0,92	-0,92
5253fa36_766	2478	M000479_A166003-101_CONT-METB_527860_EIMOR_Dodecanoic acid, n- (1TMS)	1,27	E14	A1	. . . . .	– . – – –	-0,06	-0,31	-0,15	-0,08	-0,48	-0,78	-0,62	-1,41	-1,22	-1,57
5253fa36_767	2036	M000249_A290012-101_METB_959360_EIFIEHN_	1,49	D7	A6	. . . . +	+ – – – –	0,08	-0,01	0,10	0,13	0,63	0,07	-1,14	-0,92	-0,85	-0,86
5253fa36_768	3446	M000799_A327001-101_METB_1051900_EIFIEHN_Ergosterol (1TMS)	1,08	D7	A2	. . . . .	– – – – –	0,29	0,06	-0,08	0,23	0,41	-0,13	-0,57	-0,63	-0,78	-0,67
5253fa36_769	2036	M000249_A290012-101_METB_959360_EIFIEHN_	1,19	D7	B11	. . . . +	– – – – .	-0,27	-0,04	-0,05	0,02	0,95	-0,34	-0,99	-0,97	-0,84	-0,24
5253fa36_770	3447	M000799_A327001-101_METB_1051900_EITTMS_Ergosterol (1TMS)	1,43	D7	A2	. . . . +	– . – . –	0,34	0,01	0,09	0,17	0,63	-0,81	-0,46	-0,89	-0,63	-0,79
5253fa36_771	3447	M000799_A327001-101_METB_1051900_EITTMS_Ergosterol (1TMS)	1,39	A4	A4	– – – – –	– – – – –	-1,27	-1,36	-2,64	-3,38	-3,23	-1,15	-1,63	-2,79	-4,25	-4,62
5253fa36_772	1883	M000158_A332001-101_METB_1114100_EITTBS_Stigmasterol (1TMS)	1,74	D7	B16	. + + + +	– – – . .	0,28	0,61	0,37	1,08	1,91	-0,39	-0,92	-0,75	-0,18	0,17
5253fa36_774	1889	M000158_A332001-101_METB_1114100_EIFIEHN_Stigmasterol (1TMS)	1,07	00	00	– + + + +	– – – – –	LOD	0,31	0,34	0,19	0,09	-4,63	-0,64	-0,73	-0,51	-0,53
5253fa36_780	3060	M000623_A291001-101_METB_998140_EINS_Tocopherol, delta- (1TMS)	1,08	D7	A2	. . . . .	– – – – –	0,34	0,06	-0,06	0,26	0,37	-0,23	-0,57	-0,67	-0,76	-0,72
5253fa36_781	2041	M000249_A290009-101_METB_969530_EIFIEHN_Gibberellic acid A3 (3TMS)	1,11	E15	A1	. . – . .	– – – – –	0,11	-0,24	-0,32	-0,12	-0,37	-0,65	-0,66	-1,37	-1,08	-1,48
5253fa36_784	1889	M000158_A332001-101_METB_1114100_EIFIEHN_Stigmasterol (1TMS)	1,23	D7	B13	. . + + +	– – – – –	-0,06	0,12	0,32	0,30	0,74	-0,69	-0,97	-0,49	-0,36	-0,49
5253fa36_785	3447	M000799_A327001-101_METB_1051900_EITTMS_Ergosterol (1TMS)	1,55	A2	A4	– – – – –	– – – – –	-1,18	-1,44	-2,45	-3,15	-2,11	-1,07	-1,33	-2,61	-3,82	-3,66
5253fa36_787	1883	M000158_A332001-101_METB_1114100_EITTBS_Stigmasterol (1TMS)	1,15	C8	A1	. + – – .	– – – – –	0,03	0,39	-0,27	-0,26	-0,52	-0,53	-0,28	-1,42	-1,15	-1,51

Analyte ID[a]	Hit ID[b]	Metabolite/ Best Library Hit[c]	Profile dissimilarity[d]	Response profile assignment[e]		Direction of change in analyte level[g]		Analyte level[h] (log2 ratio) for									
								CC-1690					sac1				
				CC-1690	*sac1*	CC-1690	*sac1*	+2h	-2h	-5h	-10h	-24 h	+2h	-2h	-5h	-10h	-24 h
5253fa36_789	1889	M000158_A332001-101_METB_1114100_EIFIEHN_Stigmasterol (1TMS)	1,52	D12	A4	. . . . .	– . – – –	-0,21	-0,37	-0,39	-0,62	0,49	-1,16	-0,30	-0,94	-1,20	-1,03
5253fa36_790	1742	M000107_A287001-101_METB_909948_EINS_Isomaltose (1MEOX) (8TMS)	1,74	D7	A6	+	+ – – – –	0,62	0,48	0,08	0,40	0,73	0,30	-1,15	-1,24	-0,99	-1,01
5253fa36_791	2071	M000296_A283011-101_METB_926665_EINS_Gentiobiose (1MEOX) (8TMS)	1,30	A2	A1	. – – – –	– – – – –	0,12	-0,26	-0,50	-0,23	-0,26	-0,25	-0,69	-1,48	-1,28	-1,56
5253fa36_792	2071	M000296_A283011-101_METB_926665_EINS_Gentiobiose (1MEOX) (8TMS)	1,51	E21	A6	. . + + .	– – – – –	0,61	0,02	0,33	0,29	0,14	-0,53	-1,32	-1,00	-1,22	-1,10
5253fa36_793	2039	M000249_A290010-101_METB_951560_EIFIEHN_Gibberellic acid A3 (3TMS)	1,21	E15	A1	. . . . .	– – – – –	0,17	-0,19	-0,22	-0,03	-0,25	-0,51	-0,77	-1,39	-1,08	-1,46
5253fa36_794	1889	M000158_A332001-101_METB_1114100_EIFIEHN_Stigmasterol (1TMS)	1,19	D7	E14	. . + . +	– – – – –	-0,05	0,07	0,32	0,11	0,72	-0,58	-0,88	-0,23	-0,40	-0,47
5253fa36_795	1889	M000158_A332001-101_METB_1114100_EIFIEHN_Stigmasterol (1TMS)	0,61	A2	A4	– – – – –	– – – – –	-1,27	-0,99	-1,93	-2,46	-1,88	-0,63	-0,58	-1,94	-2,87	-2,50
5253fa36_796	2071	M000296_A283011-101_METB_926665_EINS_Gentiobiose (1MEOX) (8TMS)	1,61	A4	A1	. . . . .	– – – – –	0,42	-0,03	-0,05	-0,16	-0,07	-0,21	-0,81	-1,12	-1,13	-1,69
5253fa36_797	22	M000000_AE050823-101_MST_908080_EICAT_fatty acid-457	1,60	D12	B5	. . . . +	– – – – .	0,04	-0,18	-0,42	-0,10	1,40	-0,25	-0,72	-1,76	-1,53	-0,21
5253fa36_798	2039	M000249_A290010-101_METB_951560_EIFIEHN_Gibberellic acid A3 (3TMS)	1,22	B16	A2	. – . . .	– – – – –	0,09	-0,36	-0,16	-0,11	0,06	-0,30	-0,65	-1,07	-1,05	-1,16
5253fa36_799	6	M000000_AE050823-101_MST_1077300_EICAT_cholesterol-D(RI marker)-505	1,67	C10	A1	. + . . .	– – – – –	0,02	0,26	-0,01	0,13	-0,09	-0,33	-0,92	-1,49	-1,30	-1,76
5253fa36_800	1889	M000158_A332001-101_METB_1114100_EIFIEHN_Stigmasterol (1TMS)	8,69	A4	A4	+ . – – –	– + – – –	0,62	0,23	-1,92	LOD	LOD	-0,55	0,68	-1,19	-2,07	-3,29
5253fa36_803	3210	M000663_A283001-101_METB_979380_EIFIEHN_Squalene, all-trans-	2,05	E18	00	+ . + . +	– . – – –	1,21	0,27	0,32	-0,06	0,61	-4,63	0,20	-1,73	-0,35	-0,83
5253fa36_805	1883	M000158_A332001-101_METB_1114100_EITTBS_Stigmasterol (1TMS)	1,53	D12	A2	. . – . +	+ . – – –	0,08	0,18	-0,32	-0,05	0,96	0,06	0,11	-1,19	-1,20	-0,57
5253fa36_812	3446	M000799_A327001-101_METB_1051900_EIFIEHN_Ergosterol (1TMS)	1,23	A2	A1	+	– – – – –	0,35	-0,05	-0,27	-0,18	-0,23	-0,50	-0,52	-1,29	-0,98	-1,46

[a] Spectrum and additional peak information are deposited in the ChlamyLib spectra library.
[b] Indicates the library entry ID of the best library hit in the EINST_MSRI_136 spectra library for all unidentified metabolites.
[c] Knowns: The metabolite represented by the respective analyte derivate; Unknowns: Best library hit in EINST_MSRI_136.
[d] The dissimilarity between the analyte profile recorded for the mutant and the parental strain measured by the Chebychev metric, i.e. the maximum absolute difference at any time point.
[e] Indicates the assignment of the individual profiles to the pattern groups and clusters. 00 indicates that the profile was not used in HCA.
[g] Difference in analyte abundance (+ or –; a dot indicates no statistically significant change) relative to controls (24 h sulfur replete conditions). The five symbols represent 2h (sulfur replete conditions), 2, 5, 10, 24 h (sulfur deplete conditions).
[h] LOD indicates analyte levels below the limit of detection. This corresponds to the value –10.76 in cluster analysis plots. Values in italics indicate that analyte levels for the +24 h control were below LOD. The values given are based on the imputation of ⅛ of the overall minimum response measured for each of these analyte